

# Mechanistic Studies of Reversible Addition-Fragmentation chain Transfer Mediated Polymerization

by

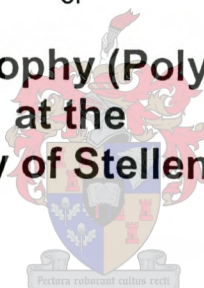
**Francois Malan Calitz**

Dissertation presented for the degree  
of

**Doctor of Philosophy (Polymer Science)**

at the

**University of Stellenbosch**



Promoter:

Prof. R.D. Sanderson

Mentor:

Dr. M.P. Tonge

Stellenbosch

April 2004

## **DECLARATION**

I, the undersigned, hereby declare that the work contained in this dissertation is my own original work and has not in its entirety, or in part, been submitted at any university as a degree.

Malan Calitz

# Abstract

To comply with the ever growing demands for materials with better properties and complex architectures, polymer chemistry has resorted to the use of living free radical polymerization techniques. Despite the structural control some of these techniques offer, major disadvantages do exist. For example, most require ultra-pure reagents, hence only a small fraction of the monomers used in industry can be polymerized in this way. This rendered these new living techniques less advantageous from a commercial point of view. Recently, a revolutionary new living free radical process, namely the reversible addition-fragmentation chain transfer process, or RAFT process, was developed that combines the control over the polymer produced with the robustness and versatility of a free radical process.

However, the RAFT process is not without its problems. In some dithioester mediated polymerizations, significant inhibition and rate retardation effects have been observed. Two main opposing opinions have been proposed in recent literature to explain these phenomena observed. The main point of difference between these two groups is the fate of the formed intermediate RAFT radicals, i.e., slow fragmentation of the formed intermediate radicals together with possible reversible intermediate RAFT radical termination, or fast fragmentation of the formed intermediate radicals together with possible irreversible intermediate RAFT radical termination. Between these opposing two groups, there is a difference of six orders of magnitude for the rate of fragmentation of the formed intermediate RAFT radicals.

The work presented in this thesis is an attempt to clarify some of the mysteries, i.e., inhibition and rate retardation observed in some RAFT polymerizations. Experimental evidence to support or contradict the theories of the above mentioned two opposing groups was investigated.

The concentration-time evolution of the intermediate radical concentration ( $c_Y$ ), for styrene and butyl acrylate polymerizations mediated by cumyl dithiobenzoate (CDB) at 70 °C and 90 °C, was followed via *in situ* electron spin resonance spectroscopy (ESR). The concentration-time evolution profiles observed were ascribed to the formation of very short chains during the early stages of the reaction. It was also found that the RAFT process is not particularly sensitive to oxygen. The intermediate and propagating radical ( $c_P$ ) concentrations (and their ratio) for the cumyl dithiobenzoate mediated styrene polymerizations were examined by ESR spectroscopy and kinetics. The system showed strong chain length effects in kinetics, assuming all chains were of similar number average molar mass ( $\bar{M}_n$ ). However, unusual behavior with respect to existing mechanistic knowledge was observed in other aspects of the system. The central equilibrium "constant" ( $K_{eq}$ ) was found to be dependent on both temperature and initial reactant concentrations. The observed intermediate radical concentrations were not consistent with predictions based on existing literature models. It was also found that the time dependence of the intermediate radical concentration varies significantly with the type of RAFT agent used. Unexpectedly,

intermediate radicals were detected at very long reaction times in the virtual absence of initiator, enhancing the belief of possible reversible termination reactions involving the intermediate radicals. An extra radical (non-propagating or intermediate) species was observed (via ESR spectroscopy) to form during some reactions. Its concentration increased with time.

The combination of data from several analytical techniques provided evidence for the formation of dead chains by the termination of intermediate radicals in the free radical polymerization of styrene, mediated by a cumyl dithiobenzoate RAFT agent, at 84 °C. Experiments done focused on the early stages of the reactions, targeting very low final number average molar mass values, with high initiator concentrations. The formation of these terminated chains did not occur to a significant extent until a large fraction of the chains reached a degree of polymerization greater than unity. This corresponded to the occurrence of a maximum in intermediate radical concentration.

*In situ*  $^1\text{H}$  nuclear magnetic resonance (NMR) and electron spin resonance spectroscopy was used to directly investigate the processes that occur during the early stages (typically the first few monomer addition steps) of an AIBN-initiated reversible addition fragmentation chain transfer polymerization of styrene, in the presence of a cyanoisopropyl dithiobenzoate and cumyl dithiobenzoate RAFT agent, at 70 °C and 84 °C respectively.  $^1\text{H}$  NMR spectroscopy allowed the investigation of the change in concentration of important dithiobenzoate species as a function of time. Identification and concentrations of the radicals present in the system could be inferred from corresponding ESR spectroscopy data. An apparent "inhibition" effect was observed in both the cyanoisopropyl and cumyl dithiobenzoate mediated polymerizations. This effect could be reduced by increasing the reaction temperature to 84 °C. However, the use of cumyl dithiobenzoate as RAFT agent prolonged this effect. This apparent "inhibition" effect was attributed to selective fragmentation of the formed intermediate radicals during the early stages of the reaction, and to different propagation rate coefficients ( $k_p$ ) of the resulting (different) radicals. A change in the equilibrium coefficient for the systems investigated was ascribed to possible progressively decreasing addition and fragmentation rate coefficients of propagating and intermediate radicals formed during the reaction. The increase in intermediate radical concentration, and thus possible intermediate radical termination, was shown to also be a probable cause of the rate retardation observed in the RAFT mediated systems investigated.

To conclude, probable causes of the observed inhibition and rate retardation in some dithiobenzoate mediated systems were investigated. It was found that intermediate RAFT radical termination does occur, albeit reversibly or irreversibly. A maximum in the intermediate radical concentration, and thus possible intermediate radical termination, was seen to occur during the observed rate retardation. An apparent inhibition effect observed was ascribed to a possible change in termination kinetics, the formation of terminated intermediate radical products and a rapidly changing  $k_p$  of the propagating radicals.

# Opsomming

Om te voldoen aan die ewig groeiende aanvraag vir materiale met beter eienskappe en komplekse samestellings, is in die polimeerchemie lewende vry-radikaal polimerisasietegnieke ontwikkel. Ten spyte van die feit dat party van die polimerisasie tegnieke die struktuur van die gevormde polimere kan beheer, bestaan daar tog nadele. Die meeste polimerisasie tegnieke benodig ultra suiwer reagense, dus kan net 'n klein fraksie van die monomere wat deur die industrie gebruik word op so 'n manier gepolimeriseer word. Dus, vanuit 'n komersiële oogpunt, is die nuwe lewende polimerisasietegnieke minder voordelig. Onlangs is 'n revolusionere nuwe lewende vry-radikaal polimerisasieproses, naamlik die RAFT-(*eng.* reversible addition-fragmentation chain transfer process) proses ontwikkel, wat die beheer oor die geproduseerde polimere, kombineer met die robuustheid en veelsydigheid van 'n vry-radikaalproses.

Die RAFT proses is egter nie sonder probleme nie. Beduidende inhibisie en vertraging van die polimerisasie tempo is in sommige dithioester-bemiddelde polimerisasies opgemerk. Daar is hoofsaaklik twee opponerende opinies oor die redes vir die inhibisie en vertragingseffekte. Die grootste verskil tussen die twee groepe lê in die lot van die gevormde intermediêre radikaal, m.a.w. stadige fragmentasie van die gevormde intermediêre radikale tesame met moontlike onveranderlike intermediêre radikaalterminasie, of vinnige fragmentasie tesame met moontlike omkeerbare intermediêre radikaalterminasie. Tussen die twee groepe, is daar 'n verskil van ses ordegrades vir die grootte van die tempo van fragmentasie van die gevormde intermediêre radikaal.

Die werk wat in die tesis weergegee word, is 'n poging om sommige van die geheime van die RAFT proses, m.a.w. inhibisie en vertraging van die polimerisasietempo, op te los. Die ondersoek was gerig op eksperimentele bewyse om die teorieë van die twee opponerende groepe of te bevestig of teen te spreek.

Die konsentrasie tyd-verandering van die intermediêre radikaal konsentrasie vir stireen- en butielakrilaatpolimerisasie, bemiddel deur CDB (*eng.* cumyl dithiobenzoate) by 70 °C and 90 °C, is gevolg deur middel van *in situ* (*lat.* vir in die oorspronklike plek, m.a.w. binne-in die ESR masjien) elektronspin-resonans (ESR) spektroskopie. Die vorm van die konsentrasie tyd-profiel is toegeskryf aan die vorming van baie kort polimeerkettings gedurende die vroeë reaksietye. Dit is ook bepaal dat die RAFT-proses nie besonder sensitief was vir suurstof nie. Die intermediêre en die propagerende radikaalkonsentrasie (en hulle verhouding) vir die CDB bemiddelde stireen polimerisasies, is bepaal deur middel van elektronspin-resonans spektroskopie en die kinetika van die sisteem. Die kinetika van die sisteem toon 'n sterk afhanklikheid teenoor die lengte van die polimeerkettings, as aanvaar word dat al die kettings dieselfde numeriese gemiddelde molêre massa het. Desnieteenstaande, is egter onverwagte gedrag in ander aspekte van die sisteem opgemerk. Dit was ook gevind dat die sentrale ewewigs-"konstante" ( $K_{eq}$ ) afhanklik was van die temperatuur en die oorspronklike reaktant konsentrasie. Die bepaalde intermediêre radikaalkonsentrasie het verskil van voorspelde waardes gebaseer op

literatuur modelle. Dit is ook gevind dat die intermediêre radikaalkonsentrasie afhanklik is van die tipe RAFT agent wat in die polimerisasie reaksies gebruik word. Intermediêre radikale is onverwags gevind na baie lang reaksietye, wanner vermag is dat die konsentrasie van die afsetter, en dus ook die intermediêre radikale, baie klein sou wees. Dit het die verwagting dat omkeerbare intermediêre radikaalterminasie kan plaasvind, versterk. 'n Ekstra radikale spesie, wat gedurende die reaksie vorm en waarvan die konsentrasie groter word met tyd, is ook deur ESR-spektroskopie geïdentifiseer.

'n Kombinasie van verskillende skeikundige tegnieke is gebruik om bewyse te kry vir die vorming van dooie kettings wat ontstaan deur middel van intermediêre radikale terminasiereaksies, in die vry-radikaalpolimerisasie van stireen, wat deur 'n CDB RAFT-agent bemiddel word by 84 °C. Eksperimente is gedoen om die reaksie tydens vroeë reaksietye te ondersoek. Baie hoë afsetter konsentrasies is ook gebruik, wat tot uiters lae numeriese gemiddelde molêre massas van die polimeerkettinge gelei het. Beduidende konsentrasies van die dooie kettings is eers gevind nadat 'n graad van polimerisasie van groter as een bereik is. Dit het ooreengestem met 'n maksimum in die konsentrasie van die intermediêre radikale.

*In situ*  $^1\text{H}$  kern magnetiese-resonans (KMR) en elektronspin-resonans spektroskopie was gebruik om 'n RAFT proses, wat gedurende die vroeë reaksie tye (tipies gedurende die eerste paar monomeer toevoegingstappe) te bestudeer, wat deur AIBN (*eng* azo bis(isobutyronitrile)) afgeset word en bestaan uit stireen en CIDB (*eng* cyanoisopropyl dithiobenzoate) en CDB RAFT agente onderskeidelik, en by 70 °C and 84 °C reageer.  $^1\text{H}$  KMR-spektroskopie was gebruik om die veranderinge in die konsentrasie van die belangrike spesies te bepaal. Die identifikasie en konsentrasie van die radikale kon bepaal word deur middel van ESR data. 'n Skynbare 'inhibisie-effek' is waargeneem in die reaksies wat bemiddel word deur CIDB en CDB. Die effek is verminder toe die reaksietemperatuur verhoog is na 84 °C. Die gebruik van CDB as RAFT agent het egter die effek vergroot. Die skynbare 'inhibisie effek' was toegeskryf aan die selektiewe fragmentasie van die intermediêre radikale gedurende die vroeë reaksietye, en aan verskillende propagasie tempokoëffisiënte ( $k_p$ ) van die verskillende radikale. Die veranderlike sentrale ewewigskoëffisiënte is toegeskryf aan die toevoegings en fragmentasie tempokoëffisiënte van die propagerende en intermediêre radikale wat toenemend afneem. Die is ook getoon dat die toename in die konsentrasie van die intermediêre radikale en dus moontlike intermediêre radikale terminasie, 'n oorsaak kan wees van die vertraging van die polimerisasietempo in die RAFT-bemiddelde reaksies.

Ter samevatting, die waarskynlike oorsake vir inhibisie en die polimerisasietempo vertraging opgemerk in sekere dithiobenzoaat-bemiddelde sisteme, is ondersoek. Dit was gevind dat intermediêre radikaalterminasie wel kan gebeur, of dit nou omkeerbaar of onveranderlik gebeur. 'n Maksimum in die konsentrasie van die intermediêre radikale, en dus moontlike intermediêre radikaalterminasie, het voorgekom tesame met 'n vertraging in die polimerisasietempo. Die skynbare inhibisie-effek wat opgemerk was kan toegeskryf word aan 'n moontlike

verandering in die terminasie kinetika, die formasie van getermineerde intermediêre radikale en 'n vinnig veranderende propagasie tempokoëffisiënt.

# Acknowledgements

During the 4 years of my PhD study, my path has crossed with a variety of persons. Even though some stayed just acquaintances, while others developed to become my best friends, all have influenced my life to a certain extent. Thus, to acknowledge all the people whom have helped me on the PhD path, which eventually came together as this thesis, becomes a rather difficult exercise. Then there is also the fear of forgetting to acknowledge someone. So, as a start, to all whom for some or the other reason have not been mentioned, thank you!

The first group of people to acknowledge is the students and staff at the KCPC (Key Centre for Polymer Colloids), University of Sydney, Australia. To the director of the KCPC, Prof Robert Gilbert, or just plain Bob as he prefers it, my deepest gratitude for all the sponsored visits to the KCPC. Thank you for fueling my scientific fire with all the fruitful discussions, challenges and opportunities. Being able to share my two greatest passions in life, surfing and science, with you was an experience that will always be remembered. Also, thank you for the opportunity to travel to various conferences around the world and to mingle with the best of the best in the field of polymer science. To the guys and girls from the KCPC zoo: Chris, Hank, Duc, Rob, Paul, Stuart, Shane, Dave, Joost, Ali, Gavin, Thomas, Herb, Bradford, Franc, Antoine, Dave (Sangster), Laurance, Thorsten, Scotty; the people from the fish tank: Jeff, Chislane, Gaza; the other staff; Monty, Brian and Chris, a special thanks to all of you. You guys made the three visits to the KCPC an absolute unforgettable experience and introduced me to the fantastic world of spicy oriental food. Keith Fisher at the University of Sydney is also thanked for giving me endless time on the ESR equipment and for the running of my ES-MS samples.

The second group of people to acknowledge is the friends, work colleagues and staff at the Institute for Polymer Science, University of Stellenbosch. The staff consisting of Aneli, Erinda, Johan, Margie and Calvin, is sincerely thanked for all their help and willing assistance. The Free Radical group is also thanked for the fantastic experience of sharing an office and closely working together with all of you. Arguably, the two most important persons to thank are my promoter Prof. Ron Sanderson, and my mentor Dr. Matthew Tonge. Prof. Sanderson, thank you for the opportunity to do a PhD degree at the Polymer Institute, for all the ideas and guidance, and also for the organization of funds, not only for this PhD, but also for the numerous travels to various Polymer Institutes and international conferences. Matthew, without your knowledge and keen interest, this thesis would not have been possible. All the help, ideas and guidance, especially in writing this thesis, is dearly appreciated.

The third group of people I would like to thank is Prof Bert Klumperman and Marion van Staden from the Dutch Polymer Institute, University of Eindhoven, The Netherlands. Bert provided helpful information regarding the nuclear magnetic resonance data and the interpretation thereof. Marion did MALDI-TOF analysis on a seeming endless number of RAFT samples. Thanks to both of you for all the help.

On a different note, to all the surfers from the Strand area, Rudolph, Pieter, Juan, Palmie, Lee, Xaver, Francois, Pottie, Le Roux and my twin brother Coenie, thanks for all the surf trips and shared experiences. Thanks to you guys, my passion for surfing is still alive and well.

A special mention must go to my various flatmates Ruth, Laura, Ashley, Bridget, Isobel and Corlene. They kept me sane throughout the four years of my PhD study and showed me the finer arts of student living.

Closer to the heart, I would like to thank all my friends, especially those whom I have closely worked with during my PhD. Never have I seen such an energetic, intelligent and fun group of people before. There was never a dull moment. Ewan, Andre, Sven, Jerrie, Valerie, Peter, Martina, Jaco, Desi and Patrice all made it possible to deem the 4 years of PhD study as truly the best years of my life. A special mention must also go to James McLeary (Mother) with whom I worked closely together for the last 2 years of my study. Together we slaved, discussed and argued the RAFT mechanism. Thanks, those were really fantastic and exiting times.

To my mom and dad, many thanks in providing me with the opportunity to do this PhD, and for all the support and guidance. And last, but not the least, a special thanks to my girlfriend Dani. She configured and corrected all the spectra and RAFT agent molecules given in the Appendix during the last chaotic week of thesis writing, and was always ready with answers for language related questions from the English impaired Afrikaans boy. Thank you for keeping me motivated through the rough times of my PhD, and for the endless love and support.

# Life and Science, Science and Life

Life and science, more specifically, scientific ideas that evolve into a dissertation such as this one are, in various ways, very similar. A scientific idea, like life, is conceived from the ideas and actions of a previous generation, whether it is by careful planning or by pure accident. Once an idea has been conceived it multiplies and grows into a new concept. Initially the concept is a matter of hushed conversation, but as it grows the wonder of being outweighs the secrecy of the concept until, one day, the concept is realized in the competitive world.

At this stage, the concept is very much like a new born baby; it is joyfully accepted into the world with congratulations all round, very similar to a young scientist presenting his ideas for a thesis to his supervisor for the first time. In the time following, the concept grows rapidly, nourished by ideas from literature and visions of future industrial applications. After months of rapid growth, the novelty of the concept starts waning and the reality of sleepless nights and worries of what is to become of the frail concept starts seeping in. Nights are spent working on the concept, improving, reshaping and modifying it. This is normally the stage where the creator wonders if this concept was such a good idea after all! He sees all the other failed concepts and their disgruntled scientists, and it makes him wonder. However, through ages and ages of creators before him, that left the imprint of their perseverance on their DNA that now also flows in his veins, the creator manages to nurture the concept into a respectable proposal.

The proposal gets presented and accepted and then enters the competitive world of science. It has now become a scientific project. Once the project is on its feet, new fields are explored and discoveries are made daily. This is a wonderful carefree time, during which the sun is always brighter and the stars always more beautiful than the day before. Soon, however, the reality of the cruel work sets in as the project experiences its first setback, one of many to come. But life goes on and the project soon gets back on track.

As time goes by, the project and its creator progresses through a variety of stages, some good and some not so good. Discoveries are made, not by "eureka!" but by "this is strange?". Traveling the globe together, they realize that the world is indeed a small place. They travel south to discover new scientific methods; they meet new people, experience new and strange things. Some they will remember, some they will not, but all have influenced their lives, have shaped their beings. The creator gains knowledge he never knew even existed and files it away in his memory banks. The project has now evolved from just another project, to become a labor of love.

Daily the project goes from strength to strength, but like all good things in life, all has to come to an end. The creator soon realizes that time has run out; another project will take this one's place and the whole process of

creation will start all over again. So he sets to work feverishly to finish all the experiments, compile all the data and formulate all the conclusions. Everything gets crammed together on a file of paper and is eventually (after much blood, sweat and tears) sent out to world, to proclaim: "This is the work of the creator, his contribution to life".

This is the story of this thesis.

# Table of Contents

---

<b>Glossary</b>	<b>V</b>
<b>List of Figures</b>	<b>IX</b>
<b>List of Schemes</b>	<b>XIV</b>
<b>List of Tables</b>	<b>XVI</b>

## CHAPTER 1

---

### Introduction

1.1 Free Radical Polymerization	1
1.2 Living/Controlled Radical Polymerization	1
1.3 Reversible Addition-Fragmentation chain Transfer Polymerization	2
1.4 Humble Beginnings	3
1.4.1 Polymeric Surfactants	4
1.4.2 Electron Spin Resonance Spectroscopy	5
1.4.3 RAFT Agent Degradation	6
1.4.4 MALDI-TOF and GPC Subtraction	6
1.4.5 <i>In situ</i> $^{13}\text{C}$ NMR Spectroscopy with a $^{13}\text{C}$ -enriched RAFT Agent	7
1.4.6 Electrospray - Mass Spectrometry	7
1.4.7 <i>In situ</i> $^1\text{H}$ -NMR Spectroscopy	8
1.4.8 Electron Spin Resonance Revisited	8
1.5 Objectives and Thesis outlay	8
References	10

---

**CHAPTER 2**

---

**Living Radical Polymerization: A Brief Overview**

Summary	12
2.1 Overview of Living Radical Polymerization	13
2.2 Reversible Addition-Fragmentation chain Transfer Polymerization	15
2.2.1 The RAFT Mechanism	16
2.2.2 What Controls the Activity of RAFT Agents?	19
2.3 Anomalities in RAFT Polymerization	21
2.3.1 Inhibition	22
2.3.2 Rate Retardation	23
2.4 Conclusions	27
References	28

---

**CHAPTER 3**

---

**Electron Spin Resonance Spectroscopy Investigations**

Summary	31
3.1 Electron Spin Resonance Spectroscopy	32
3.1.1 Basic ESR Principles	32
3.1.2 The g-value	36
3.1.3 Hyperfine Coupling	36
3.1.4 Instrumental Factors Influencing the ESR Spectrum	36
3.1.5 Quantitative ESR Spectroscopy	38
3.1.6 ESR Applications to RAFT Polymerization	39
3.2 Experimental	43
3.2.1 Sample Preparation	43
3.2.2 ESR Equipment	43
3.2.3 ESR Parameters	44
3.2.4 ESR Calibration	45
3.2.5 SEC Analysis	45
3.3 Initial ESR Spectroscopy Investigations of the Intermediate RAFT Radical	47
3.3.1 Intermediate Radical Signals of Different RAFT Agents	54
3.3.2 Intermediate Radical Concentrations at Long Reaction Times	56
3.3.3 Oxygen Sensitivity	59
3.3.4 Extra Signals	60

3.4 Conclusions	62
References	62

---

## CHAPTER 4

---

### Evidence for Termination of Intermediate Radical Species in RAFT-Mediated Polymerization

Summary	65
4.1 Inhibition and Rate Retardation	66
4.1.1 Experimental planning	67
4.2 Experimental	68
4.2.1 Chemicals	68
4.2.2 Sample Preparation	68
4.2.3 Spectroscopic Instruments	69
4.2.4 Instrumental Parameters	69
4.2.5 ESR Calibration	70
4.3 $^{13}\text{C}$ NMR and ESR Spectroscopy Investigations Into the Fate of the Intermediate RAFT Radicals	71
4.3.1 $^{13}\text{C}$ NMR Spectroscopy Investigations: <i>In Situ</i> Reactions	71
4.3.2 <i>Ex Situ</i> Reactions	76
4.3.3 <i>In Situ</i> ESR Spectroscopy Reactions	76
4.4 Conclusions	79
References	81

---

## CHAPTER 5

---

### Beyond Inhibition: A $^1\text{H}$ NMR and ESR Investigation of the Early Kinetics of RAFT Mediated Polymerization

Summary	83
Introduction to <i>in situ</i> $^1\text{H}$ NMR spectroscopy	84
5.1 Experimental	86
5.1.1 Chemicals	86
5.1.2 Sample Preparation	86
5.1.3 Spectroscopic Instruments	88
5.1.4 Instrumental Parameters	88

---

5.1.5 ESR Calibration	89
RAFT Mediated Polymerization with the Same Initiating and Leaving Groups.	90
5.2 Reactions Mediated by Cyanoisopropyl Dithiobenzoate	90
5.2.1 Temperature effects	101
5.2.2 Monomer Consumption	101
5.2.3 The Apparent Equilibrium "constant", $K_{eq}$	105
5.2.4 Radical Generation and Termination Products	112
5.2.5 Beyond Initialization	114
5.2.6 Conclusions	114
RAFT Mediated Polymerization with Different Initiating and Leaving Groups.	116
5.3 Reactions Mediated by Cumyl Dithiobenzoate	116
5.3.1 ESR Observations and Implications on the RAFT Mechanism	122
5.3.2 Temperature effects	127
5.3.3 Monomer Consumption	128
5.3.4 The Apparent Equilibrium "constant", $K_{eq}$	136
5.3.5 Radical Generation and Termination Products	140
5.3.6 Beyond Initialization	144
5.3.7 Conclusions	144
5.4 Overall Conclusions	145
References	147

## CHAPTER 6

---

### Epilogue

Summary	149
6.1 Conclusions	150
6.2 Recommendations	152
References	154

## APPENDIX

---

A.1 Additional $^{13}\text{C}$ NMR Spectra	155
A.2 Possible Intermediate Radical Termination Products	157
A.3 $^{13}\text{C}$ NMR Shift Predictions	165
A.4 ESR simulations: Theory and parameters	166
References	167

# Glossary

## Abbreviations

$^{13}\text{C}$ NMR	carbon thirteen nuclear magnetic resonance
$^1\text{H}$ NMR	proton nuclear magnetic resonance
1-MEDB	1-methoxycarbonyl ethyl dithiobenzoate
1-PEDB	1-phenylethyl dithiobenzoate
AIBN	2,2'-azo bis(isobutyronitrile)
AR	analytical grade
ATRP	atom transfer radical polymerization
C	carbon atom
$\text{C}_6\text{D}_6$	deuterated benzene
CDB	cumyl dithiobenzoate
$\text{CDB-}^{13}\text{C}$	carbon thirteen labeled cumyl dithiobenzoate
CIPD	cyanoisopropyl dithiobenzoate
CPDA	cumyl phenyl dithioacetate
D	dithiobenzoate
DEPT	distortionless enhancement by polarization transfer
DIBTC	S-1-Dodecyl-S'-(R,R'-dimethyl-R-acetic acid) trithiocarbonate
EPR	electron paramagnetic resonance
ES-MS	electro spray mass spectrometry
ESR	electron spin resonance
Et	ethyl
G	gauss
GC-MS	gas chromatography – mass spectrometry
GPC	gradient permeation chromatography
HPLC-MS	gradient high-performance liquid chromatography – mass spectrometry
iniferter	initiator-transfer agent-terminator
IR-grade	infra red grade
KOH	potassium hydroxide
M	molar ( $\text{mol}/\text{dm}^{-3}$ )
MA	methyl acrylate
MALDI-TOF	matrix assisted laser desorption ionization – time of flight
mW	milli watts
N	nitrogen atom
NMR	nuclear magnetic resonance
O	oxygen atom

PDI	polydispersity index
Ph	phenyl ring
ppm	parts per million
PSt	polystyrene
RAFT	reversible addition-fragmentation chain transfer
S	sulfur atom
SEC	size exclusion chromatography
St	styrene
TEMPO	2,2,6,6-tetramethylpiperidinyl-1-oxy
THF	tetrahydrofuran
UV	ultra violet

## Notations

$\mu_B$	Bohr magneton
$P_{1/2}$	half saturation power
$P$	microwave power
$\frac{dE}{dt}$	rate of microwave energy absorption
$H_1$	applied field strength
$\bar{n}$	average number of radicals per particle
$\Delta E$	energy difference between the states
$B_{loc}$	local magnetic field
$\bar{M}_n$	number average molecular weight
$n_0$	population difference between the electron's spin states at thermal equilibrium
$T_1$	spin-lattice relaxation time
$\bar{M}_w$	weight average molecular weight
$\sigma$	dimensionless shielding constant
$\nu$	frequency of electromagnetic radiation
$\gamma$	gamma radiation
$\gamma$	magnetogyric ratio
$[I]$	initiator concentration
$[I]_0$	initial initiator concentration
$[P-X]$	number of dithiobenzoate end-capped chains
$\langle k_t \rangle$	average termination rate coefficient
$A^\bullet$	cyanoisopropyl radical
AA	tetramethyl succinonitrile

AB	degenerative transfer agent
AD	cyanoisopropyl dithiobenzoate
AR <sub><i>i</i></sub>	polymer molecule of length <i>i</i> terminated by a degenerative transfer fragment
AR <sub><i>j</i></sub>	polymer molecule of length <i>j</i> terminated by a degenerative transfer fragment
AS <sup>•</sup>	cyanoisopropyl styryl radical
AS <sub>2</sub> <sup>•</sup>	cyanoisopropyl styryl styryl radical
AS <sub>2</sub> D	cyanoisopropyl styryl styryl dithiobenzoate
ASD	cyanoisopropyl styryl dithiobenzoate
B	magnetic field of strength
B <sup>•</sup>	radical generated from degenerative transfer agent
C <sup>•</sup>	cumyl radical
CC	termination product of two cumyl radicals
CD	cumyl dithiobenzoate RAFT agent
C <sub>P</sub>	propagating radical concentration
CS <sup>•</sup>	cumyl styryl radical
CS <sub>2</sub> <sup>•</sup>	cumyl styryl styryl radical
CS <sub>2</sub> D	cumyl styryl styryl dithiobenzoate
CSD	cumyl styryl dithiobenzoate
C <sub>tr</sub>	chain transfer constant
C <sub>Y</sub>	intermediate radical concentration
D <sub><i>i</i></sub>	dead polymer molecule of chain length <i>i</i>
D <sub><i>i+j</i></sub>	dead polymer molecule of chain length <i>i + j</i>
<i>f</i>	initiating efficiency factor
<i>g</i> ( $\omega$ )	general lineshape function
<i>g</i> <sub>e</sub>	<i>g</i> -factor of an electron (= 2.0023)
<i>h</i>	Planck constant
I	initiator
<i>k</i> <sub><math>\beta</math></sub>	addition rate coefficient
<i>k</i> <sub>-<math>\beta</math></sub>	fragmentation rate coefficient
<i>k</i> <sub>add</sub>	addition rate coefficient
<i>k</i> <sub>-add</sub>	fragmentation rate coefficient
<i>k</i> <sub>d</sub>	the rate coefficient for initiator decomposition
<i>K</i> <sub>eq</sub>	equilibrium coefficient
<i>k</i> <sub><i>i</i></sub>	rate coefficient for re-initiation
<i>k</i> <sub>p</sub>	propagation rate coefficient
<i>k</i> <sub>t</sub>	rate coefficient of conventional radical termination
<i>k</i> ' <sub>t</sub>	rate coefficient of intermediate radical termination
<i>k</i> <sub>tr</sub>	transfer rate coefficient
M	monomer
M <sub>1</sub> <sup>•</sup>	1-mer radical generated by thermal initiation

---

$M_2\bullet$	dimer radical generated by thermal initiation
$m_s$	orientation of the electron's spin angular momentum
$Mt^n/\text{ligand}$	transition metal complex for atom transfer reaction, without the halide
$P$	transition probability per spin
$P_1(\omega)$	first-order transition probability
$P_{i+1}\bullet$	polymer radical of chain length $i + 1$
$P_i\bullet$	polymer radical of chain length $i$
$P_j\bullet$	polymer radical of chain length $j$
$P_n$	polymeric chain of $n$ -degree of polymerization
$P_n\bullet$	propagating radical of $n$ -degree of polymerization
$R$	RAFT agent leaving group
$R\bullet$	RAFT agent leaving group radical
$R_i$	rate of initiation
$T\bullet$	nitroxide radical
$TH$	hydroxylamine
$TR_i$	polymer molecule of chain length $i$ capped by a nitroxide radical
$X-Mt^{n+1}/\text{ligand}$	transition metal complex for atom transfer reaction with the halide
$XR_i$	alkyl halide of chain length $i$
$Y\bullet$	intermediate RAFT radical
$Z$	RAFT agent stabilizing group

# List of Figures

		Page
<b>Chapter 3</b>		
Figure 3.1	Schematic representation of the electron spin levels in a magnetic field.	33
Figure 3.2	The basic layout of a continuous wave ESR spectrometer.	34
Figure 3.3	ESR spectrum of the intermediate radical.	35
Figure 3.4	The observed ESR absorption signal and the first derivative thereof.	35
Figure 3.5	Idealized plot of relative signal intensity versus square root of microwave power.	38
Figure 3.6	Plot indicating the differences in reaction rates of typical RAFT mediated reactions and their respective control reactions.	41
Figure 3.7	Plot of relative signal intensity (due to intermediate radicals) versus square root of microwave power for the duplicate reactions carried out at 70 °C.	45
Figure 3.8	ESR spectrum of the intermediate radical observed in the polymerization of styrene with CDB and AIBN in benzene at 90 °C.	48
Figure 3.9	Intermediate radical concentration-time profile for the <i>in situ</i> reaction of solution 1 at 90 °C.	49
Figure 3.10	Intermediate radical concentration-time profile for the <i>in situ</i> reaction of solution 5 at 90 °C.	49
Figure 3.11	Intermediate radical concentration-time profile for the <i>in situ</i> reaction of solution 1 at 70 °C.	50
Figure 3.12	Intermediate radical concentration-time profile for the <i>in situ</i> reaction of solution 5 at 70 °C.	50
Figure 3.13	Intermediate radical concentration-time profiles for the styrene polymerization in the presence of CDB.	51
Figure 3.14	Semi-logarithmic plot of the monomer consumption for the styrene polymerization in the presence of CDB.	51
Figure 3.15	Calculated equilibrium coefficient as a function of time for styrene polymerization in the presence of CDB.	52
Figure 3.16	Calculated equilibrium coefficient as a function of $\overline{M}_n$ for styrene polymerization in the presence of CDB.	52
Figure 3.17	Time evolution of $c_V$ for the <i>in situ</i> polymerization of solution 10 at 90 °C.	53
Figure 3.18	Comparison between the intermediate radical concentrations observed and that calculated by assuming the rate coefficients of Barner-Kowollik <i>et al.</i>	54
Figure 3.19	(a) Cumyl phenyl dithioacetate and (b) dibenzyl trithiocarbonate RAFT agents.	55
Figure 3.20	(a) ESR signal detected in the early reaction time for the <i>in situ</i> polymerization of solution 7 at 90 °C. (b) ESR signal due to the butyl acrylate propagating radical.	55

Figure 3.21	ESR signal detected in the early reaction time for the <i>in situ</i> polymerization of solution 8 at 90 °C.	56
Figure 3.22	ESR signal detected in the early reaction time for the <i>in situ</i> polymerization of solution 9 at 90 °C.	56
Figure 3.23	Time evolution of $c_{\gamma}$ indicating detectable concentrations of the intermediate radicals after 19 h reaction time at 90 °C.	57
Figure 3.24	Concentrations of intermediate radicals, propagating radicals, and remaining initiator after reaction of solution 4 at 90 °C for 19 h.	57
Figure 3.25	ESR signals observed for the intermediate radicals at long reaction times for: (a) styrene, CDB and AIBN in benzene; (b) butyl acrylate, CDB and AIBN in benzene; (c) the "extra signal" at a different g-value than the intermediate radical signal; (d) usually observed ESR signal due to intermediate RAFT radicals.	59
Figure 3.26	Effect of exposure to oxygen on the time evolution of $c_{\gamma}$ .	60
Figure 3.27	(a) "Extra" signal observed in most reactions with styrene and CDB. (b) Signal at low (2 mW) and (c) higher (8 mW) microwave power.	61

## Chapter 4

Figure 4.1	$^{13}\text{C}$ NMR spectra in the 50 - 80 ppm region of the solution polymerization of styrene in the presence of CDB- $^{13}\text{C}$ at 84 °C, using AIBN as initiator.	72
Figure 4.2	Comparison of the $^{13}\text{C}$ spectrum recorded at 181 min to the corresponding DEPT spectra.	73
Figure 4.3	Examples of possible structures and predicted chemical shifts of the quaternary dithioester carbon in species formed by the termination reactions of intermediate radicals.	74
Figure 4.4	Spectra of the CDB- $^{13}\text{C}$ reaction after 331 min reaction time at (a) 84 °C, 256 scans; (b) room temperature, 256 scans; (c) room temperature, 17 144 scans.	75
Figure 4.5	(a) Spectrum of the CDB- $^{13}\text{C}$ reaction at 84 °C after 181 min, 256 scans; (b) Spectrum of the unlabeled CDB reaction at room temperature, 181 min, 17144 scans.	76
Figure 4.6	Intermediate radical concentration evolution for the <i>in situ</i> ESR solution polymerization of styrene in the presence of CDB at 84 °C, using AIBN as initiator.	77
Figure 4.7	Successive $^{13}\text{C}$ spectra of the <i>in situ</i> polymerization mediated by CDB- $^{13}\text{C}$ used to follow the time evolution of the species in the reaction.	77
Figure 4.8	The structures of the observed dithiobenzoate species in the reaction mixture.	78
Figure 4.9	Intermediate radical concentration, CD, CSD, CS <sub>2</sub> D -time profiles for the solution polymerization of styrene in the presence of CDB at 84 °C, using AIBN as initiator.	79

---

**Chapter 5**

---

Figure 5.1	Predominant non-radical species of interest for the investigation of the early period of the free radical polymerization of styrene in the presence of cyanoisopropyl dithiobenzoate, using AIBN as an initiator.	91
Figure 5.2	Typical $^1\text{H}$ NMR spectrum between 2.5 and 0.5 ppm, directly after initialization.	91
Figure 5.3	Relative concentrations of methyl protons of the dithiobenzoate species versus time in the free radical polymerization of styrene in the presence of cyanoisopropyl dithiobenzoate using AIBN as an initiator, polymerized <i>in situ</i> at 70 °C.	92
Figure 5.4	Time evolution of $c_{\gamma}$ and the corresponding rate of initiator decomposition for solution 1 <i>in situ</i> ESR polymerization at 70 °C.	93
Figure 5.5	Overlay of the $c_{\gamma}$ and the relative concentrations of the methyl protons of dithiobenzoate species versus time in the <i>in situ</i> NMR polymerization of styrene in the presence of CIDB using AIBN as an initiator at 70 °C.	93
Figure 5.6	Time evolution of the intermediate radical concentration and the corresponding rate of initiator decomposition for solution 1, polymerized <i>in situ</i> at 84 °C.	101
Figure 5.7	Overlay of the intermediate radical concentration and the relative concentrations of the methyl protons of dithiobenzoate species versus time in the polymerization of styrene in the presence of CIDB using AIBN as an initiator, polymerized <i>in situ</i> at 84 °C.	101
Figure 5.8	Semi-logarithmic plot of fractional conversion versus time in the reactions of cyanoisopropyl dithiobenzoate with AIBN and styrene in deuterated benzene at 84 and 70 °C.	102
Figure 5.9	Effect of $k_p/k_{p,1}$ on the rate of monomer consumption during the two phases of the reaction.	104
Figure 5.10	Semi-logarithmic plot of fractional conversion versus time in the reactions of CIDB with AIBN and styrene in deuterated benzene at 70 and 84 °C.	106
Figure 5.11	Residuals from the fit of an exponential curve to the monomer consumption data for the reaction at (a) 70 °C and (b) 84 °C.	106
Figure 5.12	Calculated propagation radical concentration time evolution for the CIDB mediated reactions with AIBN and styrene in deuterated benzene at 70 and 84 °C.	107
Figure 5.13	Decrease in concentration of species AD as observed by <i>in situ</i> $^1\text{H}$ NMR spectroscopy at 70 °C.	107
Figure 5.14	The time evolution for the calculated apparent equilibrium constant for the CIDB mediated reactions at 70 and 84 °C.	109
Figure 5.15	The time evolution for the intermediate to propagating radical concentration for the CIDB mediated reactions at 70 and 84 °C.	109
Figure 5.16	The concentrations of AIBN and AA of reactions 2 and 4 carried out in deuterated	

	benzene at 84 °C.	113
Figure 5.17	The concentrations of AIBN and AA of reactions 1 and 3 carried out in deuterated benzene at 70 °C.	113
Figure 5.18	The cycle by which cyanoisopropyl radicals are rapidly regenerated by addition-fragmentation through a dithioester mediating species, during the early stages of the cyanoisopropyl dithiobenzoate-mediated polymerization of styrene.	113
Figure 5.19	The species of interest for the investigation of initialization in the free radical polymerization of styrene in the presence of cumyl dithiobenzoate, using AIBN as an initiator.	117
Figure 5.20	Typical $^1\text{H}$ NMR spectrum between 1.9 and 0.5 ppm taken during initialization.	117
Figure 5.21	Relative concentrations of methyl protons of the dithiobenzoate species versus time, overlaid with the intermediate radical concentration evolution in the free radical polymerization of styrene in the presence of cumyl dithiobenzoate using AIBN as an initiator, polymerized <i>in situ</i> at 70 °C.	119
Figure 5.22	The observed ESR signals at 4, 113 and 240 minutes for the <i>in situ</i> ESR polymerization reaction at 70 °C.	123
Figure 5.23	The observed ESR signals at 9, 37 and 65 minutes for the <i>in situ</i> ESR polymerization reaction at 84 °C.	123
Figure 5.24	(a) ESR signal detected when 8 scans were accumulated for an ESR spectrum during the reaction of cumyl dithiobenzoate and AIBN in benzene at 84 °C. Detected signal consisted of the signals due to (b) cyanoisopropyl radicals, (c) intermediate radicals, and (d) cumyl radicals.	125
Figure 5.25	Relative concentrations of the methyl protons of the dithiobenzoate species versus time in the polymerization of styrene in the presence of cumyl dithiobenzoate using AIBN as an initiator, polymerized <i>in situ</i> at 84 °C.	128
Figure 5.26	The consumption of the AD species in the reaction at 84 °C is enlarged for clarity.	128
Figure 5.27	Semi-logarithmic plot of fractional conversion versus time in the reactions of CDB with AIBN and styrene in deuterated benzene at 70 and 84 °C.	128
Figure 5.28	Residuals from the fit of an exponential curve to the monomer consumption data for the reactions at (a) 70 and (b) 84 °C.	129
Figure 5.29	The calculated $k_{pCp}$ time evolution for the CDB mediated reactions with AIBN and styrene in deuterated benzene at 70 and 84 °C.	131
Figure 5.30	The calculated $k_{pCp}$ (corrected for square root of radical flux) time evolution for the CDB mediated reactions with AIBN and styrene in deuterated benzene at 70 and 84 °C.	132
Figure 5.31	Semi-logarithmic plot of fractional conversion versus time in the reactions of CDB and CIDB with AIBN and styrene in deuterated benzene at 70 and 84 °C.	134
Figure 5.32	The calculated $k_{pCp}$ (corrected for square root of radical flux) time evolution for the CIDB and CDB mediated reactions with AIBN and styrene in deuterated benzene at 70 and 84 °C.	134

---

Figure 5.33	Calculated propagation radical concentration time evolution for the CDB mediated reactions with AIBN and styrene in deuterated benzene at 70 and 84 °C.	137
Figure 5.34	The determined and estimated intermediate radical concentration time evolution for the CDB mediated reactions with AIBN and styrene in deuterated benzene at 84 °C.	137
Figure 5.35	The decrease in concentration of species CD as observed by <i>in situ</i> <sup>1</sup> H NMR spectroscopy at 70 °C and 84 °C.	138
Figure 5.36	The time evolution for the calculated apparent equilibrium constant for the CDB mediated reactions at 70 and 84 °C.	138
Figure 5.37	Plot of the cumulative integrated end-groups of the dithiobenzoate species in the polymerization of styrene, in the presence of CDB, using AIBN as initiator in deuterated benzene at 70 °C.	140
Figure 5.38	Plot of the cumulative integrated end-groups of the dithiobenzoate species in the polymerization of styrene, in the presence of CDB, using AIBN as initiator in deuterated benzene at 84 °C.	141
Figure 5.39	The concentrations evolution of the termination products formed and initiator decomposition in the reaction of styrene and AIBN with and without CDB in deuterated benzene at 84 °C.	142
Figure 5.40	The concentrations evolution of the termination products formed in the reaction of styrene and AIBN with and without CDB in deuterated benzene at 70 °C.	143

## Appendix

---

Figure A.1	<sup>13</sup> C NMR spectra in the 50 – 80 ppm region of the solution polymerization of styrene in the presence of CDB- <sup>13</sup> C at 84 °C, using AIBN as initiator. 0-136 minutes	155
Figure A.2	<sup>13</sup> C NMR spectra in the 50 – 80 ppm region of the solution polymerization of styrene in the presence of CDB- <sup>13</sup> C at 84 °C, using AIBN as initiator. 136-331 minutes	156
Figure A.3	Potential terminated intermediate radical species.	164

# List of Schemes

Page

## Chapter 1

---

Scheme 1.1	The circle of events that comprised this investigation of the RAFT mechanism.	4
------------	---	---

## Chapter 2

---

Scheme 2.1	Stable free radical polymerization.	13
Scheme 2.2	Atom transfer radical polymerization.	13
Scheme 2.3	Degenerative transfer.	14
Scheme 2.4	The reversible addition fragmentation chain transfer process using methacrylic macromonomers as transfer agents.	15
Scheme 2.5	The reversible addition fragmentation chain transfer (RAFT) mechanism.	16
Scheme 2.6	Canonical forms of xanthates and dithiocarbamates.	21
Scheme 2.7	Possible additional (reversible and irreversible) termination reactions involving the intermediate radical, to generate new species.	25

## Chapter 3

---

Scheme 3.1	The central equilibrium of the reversible addition fragmentation chain transfer process.	39
Scheme 3.2	Schematic representation of considering the RAFT process as a degenerative transfer process.	40
Scheme 3.3	Possible reversible and irreversible termination reactions involving the intermediate radical to generate non-radical species.	58

## Chapter 4

---

Scheme 4.1	The currently accepted elementary steps for the central equilibrium in the RAFT process.	66
Scheme 4.2	Possible termination process involving termination of the intermediate radical.	71

---

**Chapter 5**

---

Scheme 5.1	The central equilibrium of the reversible addition fragmentation chain transfer process.	84
Scheme 5.2	The steps involved in the initialization period of the RAFT reaction of cyanoisopropyl dithiobenzoate, styrene monomer and AIBN initiator.	95
Scheme 5.3	The main steps involved in the early part of the initialization period of the RAFT reaction of cumyl dithiobenzoate, styrene monomer and AIBN initiator at the beginning of initialization.	120
Scheme 5.4	The additional steps involved in the initialization period of the RAFT reaction of cumyl dithiobenzoate, styrene monomer and AIBN initiator during initialization.	121
Scheme 5.5	The additional steps involved at the end of initialization in the RAFT reaction of cumyl dithiobenzoate, styrene monomer and AIBN initiator.	122
Scheme 5.6	The possible reaction steps involved in the <i>in situ</i> reaction of cumyl dithiobenzoate with AIBN initiator in benzene at 84 °C.	124

# List of Tables

Page

---

## Chapter 2

Table 2.1	The apparent transfer constants for the dithiobenzoate derivatives $S=C(Ph)-S-R$ in methyl methacrylate polymerization at 60 °C.	20
Table 2.2	The apparent transfer constants for benzyl thiocarbonylthio compounds $S=C(Z)-SCH_2Ph$ in styrene polymerization at 110 °C.	21

---

## Chapter 3

Table 3.1	Composition of reaction mixtures used for <i>in situ</i> ESR analysis.	44
-----------	--	----

---

## Chapter 5

Table 5.1	Composition of reaction mixtures used for the <i>in situ</i> ESR polymerizations.	87
Table 5.2	Composition of reaction mixtures used for the <i>in situ</i> NMR experiments.	87
Table 5.3	$^1H$ NMR chemical shifts of the integrated species followed during the <i>in situ</i> $^1H$ NMR reaction at 70 °C.	92
Table 5.4	$^1H$ NMR chemical shifts of the integrated species relevant to the investigation of cumyl dithiobenzoate mediated reactions.	116

---

## Appendix

Table A.1	$^{13}C$ NMR shift predictions of the possible terminated intermediate radical species.	165
-----------	---	-----

*Any old saying looks a lot more profound when written in italics*  
- Jesse Stevens

# Chapter 1

## Introduction

### 1.1 Free Radical Polymerization

Free radical polymerization is one of the most convenient ways to prepare polymers on a large industrial scale. The versatility of this technique stems from its tolerance towards all kind of impurities, be it stabilizers, water or trace amounts of oxygen.<sup>1</sup> Free radical polymerization in aqueous media, more specifically emulsion polymerization, is a truly unique way to produce a variety of polymers. It offers many benefits, as is evident in the field of all polymerizations, by the large proportion of free radical polymerizations (40 – 50% of the total) that are conducted in this way.<sup>2</sup> Moreover, an added benefit is the wide range of monomers than can be polymerized by radical means. Unfortunately, the process is not without its shortcomings, as control over the produced polymer architecture is difficult to attain; molecular weight distributions are generally broad, but can however be controlled to some extent by transfer agents and the careful selection of initiator concentrations. This lack of control confines the overall versatility of the free radical process.

To comply with the demands for materials with better properties and complex architectures of an ever growing polymer industry, polymer chemistry has resorted to the use of living free radical polymerization techniques, such as anionic and group transfer polymerization and several others, to make such materials. Despite the structural control some of these techniques offer, major disadvantages do exist. Most require ultra-pure reagents and hence only a small fraction of the monomers used in industry can be polymerized in this way. This rendered these new living techniques less advantageous from a commercial point of view. Clearly, a process is required that combines the control over polymer produced with the robustness and versatility of a free radical process.

### 1.2 Living/Controlled Radical Polymerization

The first discoveries of living polymerizations were made by Szwarc,<sup>3,4</sup> who defined a range of criteria from which a polymerization process can be considered as “living”. These criteria were the following:

- I. The number of polymer chains in the polymerization remains constant.
- II. The polydispersity of the molecular weight distribution is low.
- III. The number average molecular weight is linearly dependent on conversion.
- IV. The molecular weight can be controlled via the reaction stoichiometry.
- V. The polymerization proceeds to full conversion. Upon further addition of monomer the polymerization will continue.

- VI. Quantitative chain-end functionalized polymers can be obtained.
- VII. The number of active end groups in radical polymerization should be two, one for each chain end.

Therefore, living polymerizations should allow the preparation of complex architectures in a controlled manner. The degree of polymerization can be tuned by the appropriate choice of reactant concentrations. Traditionally, controlled/living processes were limited to anionic polymerizations. Although excellent living character and control over the polymerization process was achieved, its application to commercial processes was restricted by the stringent requirements of reaction conditions and limited choice of monomers that can be polymerized.

During the past few decades, living radical polymerization underwent a complete revival. Usually, living radical polymerization would be written within quotation marks, as these types of polymerizations were not considered as animate as anionic polymerizations. The onset of this revival is attributed mainly to the earlier work of Otsu,<sup>5</sup> who discovered that the mere addition of certain compounds (e.g. dithiocarbamates and disulfides) to a radical polymerization resulted in the polymerization exhibiting some living characteristics. Although his *iniferter* polymerization technique was prone to side reactions and unable to yield low polydispersity material, some interesting results were obtained. Furthermore, and more importantly, insight was gained into the requirements needed for living radical polymerization. This resulted in the formation of a fundamental model, based on reversible termination, which formed the basis for living radical polymerizations. Several other polymerization techniques were later developed, based on the reversible termination model of Otsu.<sup>5</sup> Among these was the reversible addition-fragmentation chain transfer (RAFT) process, which is the subject of this thesis.

The essential feature in the mechanism of living radical polymerization is the reversible deactivation process, which mimics the anionic polymerization process by ensuring that all of the chains grow throughout the duration of the polymerization process. Although not all chains grow at every instant, equilibrium between active and dormant states guarantees that macroscopic variations in the reaction conditions are translated into intermolecular variations rather than large differences between the individual chains, resulting in a homogeneous and well-defined product.

### 1.3 The Reversible Addition-Fragmentation chain Transfer Process

Rizzardo *et al.*<sup>6,7</sup> patented and published a revolutionary new living free radical process, namely the reversible addition-fragmentation chain transfer process or RAFT process. The main feature of this process is the reversible addition-fragmentation process (see Scheme 2.5, Chapter 2) by which chain activity is transferred from one chain to another, to bestow living characteristics to the polymerization system.<sup>6-15</sup> The more effective RAFT agents are certain thiocarbonylthio compounds ( $\mathbf{R-SC(Z)=S}$ ), where  $\mathbf{Z}$  is the group that modifies the reactivity of the thiocarbonyl group toward free radical addition and  $\mathbf{R}$  is the free radical leaving group.<sup>7,10,11</sup> The main advantage of this process over other living free radical polymerization techniques is

the wide variety of monomers that can be polymerized, and the wide range of reaction conditions under which the systems could be polymerized, to still exhibit controlled behavior and to yield polymers with narrow polydispersities. Another advantage of the RAFT technique is that existing polymer chains, i.e. dithiobenzoate end-capped chains, can be re-activated for chain extensions or used as precursors to block formation by the addition of further monomer(s).<sup>10,11,13,14,16-18</sup> RAFT polymerization also provides a route to other exotic architectures, e.g. stars, grafts and brushes.<sup>11,14,19-21</sup>

However, the RAFT process is not without its problems. In some dithioester-mediated polymerizations, significant inhibition and rate retardation effects have been observed.<sup>14,17,22-26</sup> Two main opposing opinions have been proposed to explain this phenomena observed (this will be discussed in detail in Chapter 2).<sup>24,27</sup> The main point of difference between these two groups is the fate of a formed intermediate RAFT radical. Between these opposing two groups, there is a difference of six orders of magnitude for the rate of fragmentation of the formed intermediate RAFT radical.

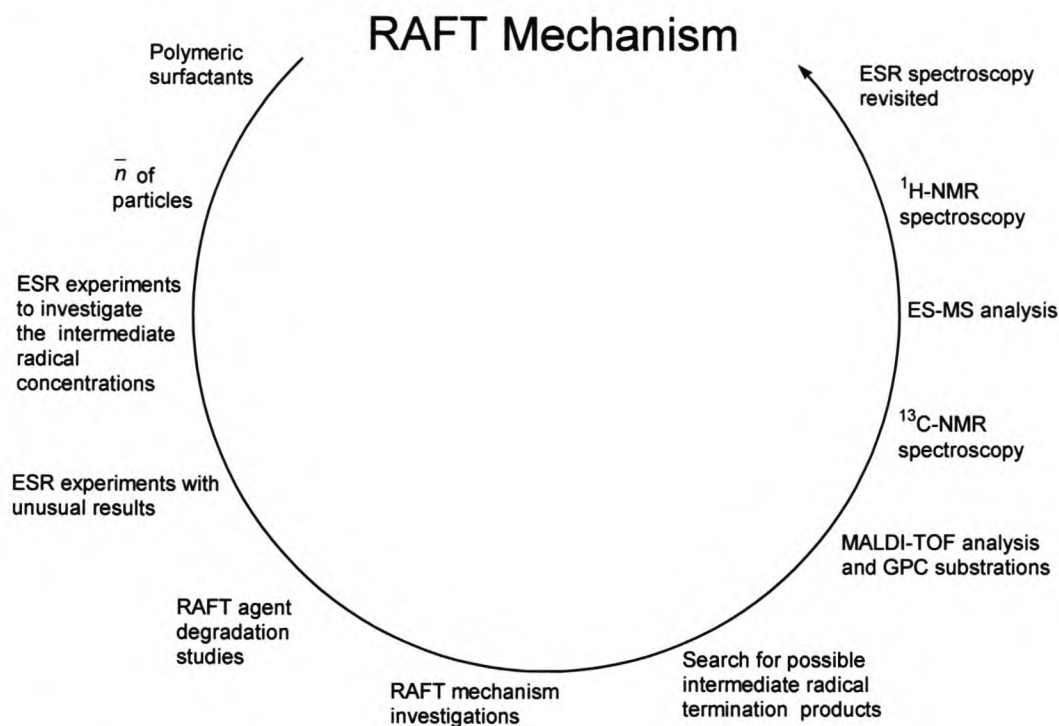
The work presented in this thesis is an attempt to clarify some of the mysteries, i.e. inhibition and rate retardation, observed in some RAFT polymerizations. Experimental evidence to support or contradict the theories of the two opposing groups was sought. Similar to most PhD projects, the study given in this thesis evolved from an initial subject to another throughout the course of the study, i.e. from ways to implement RAFT into emulsion systems, to investigations into the mechanism governing the RAFT process.

## 1.4 Humble Beginnings

This section is a walk through the development process of what was eventually to be this dissertation. It is a description of ideas, experiments, results and discoveries that lead us to some of the secrets of the RAFT mechanism (Scheme 1.1).

The original project was based on the problems experienced when employing RAFT mediated polymerization in emulsion systems.<sup>28,29</sup> The original aims of the project involved polymeric surfactants as “carriers” of RAFT agents in water-borne systems. During mathematical modelling of this system, doubts about the average number of propagating radicals per particle<sup>2</sup> ( $\bar{n}$ ) for these RAFT systems led to the investigation of the intermediate radical concentrations via electron spin resonance (ESR) spectroscopy (Chapter 3). Unusual ESR results and the observation of some unexpected behaviour of the RAFT systems investigated, prompted RAFT agent degradation investigations as well as the start of the search for possible terminated intermediate RAFT radicals, which was deemed a probable explanation for the observed anomalous behaviour. Consecutive GPC trace subtraction, MALDI-TOF and ES-MS characterization were employed to find evidence for terminated intermediate RAFT radicals. This approached lead however to more questions than answers. *In situ* <sup>13</sup>C NMR spectroscopy, with a <sup>13</sup>C labeled RAFT agent (Chapter 4), provided the first evidence for possible terminated intermediate radical species. *In situ* <sup>1</sup>H NMR spectroscopy was also found to be an excellent way to follow the time evolution of the species involved in

the RAFT reactions (Chapter 5). The *in situ*  $^1\text{H}$  NMR spectroscopy together with follow-up ESR investigations (Chapter 5) provided most of the final missing pieces to the RAFT mechanism puzzle and some answers to anomalies observed in some RAFT systems.



**Scheme 1.1** The circle of events that comprised this investigation of the RAFT mechanism.

### 1.4.1 Polymeric Surfactants

The original project was to investigate the role of chemically modified polymeric surfactants as emulsifiers in living polymerization. Having just completed an MSc. project on polymeric surfactants, and at the same time living/controlled free radical polymerization, and especially RAFT polymerization, being the topic of hot discussion in most polymer journals, it was therefore not surprising that this project was born out of the problems experienced by mostly Hans de Brouwer and his co-promoter, Michael Monteiro while working on RAFT systems.<sup>17,18,25,28-32</sup>

As RAFT polymerization had already been used as a living/controlled free radical process in homogeneous media, *De Brouwer et al.*<sup>28</sup> set out to incorporate the RAFT system in water-borne systems. Their efforts resulted in a lack of molecular weight control and broad polydispersities of the polymer produced, latex instability and the unexplained occurrence of inhibition and retardation of reaction rates during certain experiments. *De Brouwer et al.*<sup>28</sup> ascribed these observations to: 1) An increased rate of exit of short radicals species from micelles, leading to a slower polymerization; 2) the RAFT agent being surface-active, therefore facilitating exit from the particles and; 3) possible termination of the intermediate RAFT radicals. It was proposed that RAFT agents attached to polymeric surfactants should be used in designed experiments

to explain the above mentioned unusual observations and to test the explanations given for these observed behavior. It was originally proposed (for this project) to attach RAFT agents (in various concentrations) to a styrene-maleic anhydride alternating copolymer (polymeric surfactant) of various molecular weights. The RAFT agent would be attached in such a way that: 1) The attached RAFT agent would remain attached to its polymeric surfactant backbone throughout the reaction and; 2) the attached RAFT agent would be liberated from its polymeric backbone when undergoing the first fragmentation step, therefore rendering it free to move around in the reaction medium. The reasoning behind this was to test the exit of short radicals and surface-active theory; a non-fixed RAFT agent will be able to exit a particle, whereas a fixed RAFT agent will be "trapped" inside the particle. It was also proposed to use spacers of different lengths between the attached RAFT agent and the polymeric surfactant backbone, to determine if a non-fixed RAFT agent will still be able to exit when a long spacer is used, i.e. when an attached RAFT agent is "released" deep inside a particle.

Preliminary mini-emulsion reactions were done with these attached RAFT agent polymeric surfactants. During the mathematical modeling of these reactions, the question arose as to the value for  $\bar{n}$ , as there are now two types of radical present, i.e. propagating and intermediate RAFT radicals. One way to determine the value was to investigate the ratio of intermediate to propagating radical concentrations. One of the best ways to investigate radical concentrations was with ESR spectroscopy.

It should be noted that, during some preliminary miniemulsion reactions, severe color loss was observed during the reaction with a consequent loss in "control" of the system, which resulted in broad polydispersities. It was suspected that this effect was due to degradation of the RAFT agent, which might, during the degradation mechanism, form radicals that can interfere with the reaction kinetics.

#### 1.4.2 Electron Spin Resonance Spectroscopy

To investigate the type of radicals and the concentration of radicals present in the RAFT system, electron spin resonance spectroscopy (ESR) was employed. *In situ* ESR reactions were performed to determine the time evolution of the intermediate radical concentration ( $c_i$ ). In all reactions mediated by cumyl dithiobenzoate, an unexpected concentration-time profile for  $c_i$  was observed. The ratio of the intermediate to propagating radical concentrations ( $c_i/c_p$ ) was determined by combining ESR and rate data, in an attempt to explain the observed unusual  $c_i$  profile. The variation in  $c_i/c_p$  observed was inconsistent with the standard RAFT model. A simple explanation was proposed, which included chain-length dependent addition and fragmentation rate coefficients. Other possibilities include reactions that consume intermediate radicals, such as reversible or irreversible termination reactions involving the intermediate. Even though the idea of intermediate radical termination was not a new concept, it was felt that it might be a probable explanation for the observed behavior. Thus, the search for the terminated intermediate radical species began.

It was suspected that the origin of the observed unusual  $c_{\gamma}$  profile might also be due to RAFT agent degradation occurring in the reactions. Therefore, research into the RAFT agent degradation was begun.

The nature of the reactions performed was such that very sensitive ESR instrumentation was required. This was not expected, given examination of related recent literature,<sup>22</sup> which predicted quite different behavior from that observed. Thus, work had to be done near the ESR instrument sensitivity limits, which for some reactions led to scatter in the results and possibly ambiguous interpretations. Thus, upgrades in ESR sensitivity were needed to attain more accurate results.

### 1.4.3 RAFT Agent Degradation

Preliminary degradation experiments of cumyl dithiobenzoate in benzene indicated that degradation of RAFT agents does occur at elevated temperatures. It was also observed by mini-emulsion experiments that RAFT agent degradation was also occurring in water borne systems.<sup>33</sup> The degradation of cumyl dithiobenzoate in water at elevated temperatures was therefore investigated. The resulting degradation products were first analyzed via gas chromatography linked to a mass spectrometer (GC-MS). It was found that the elevated temperatures by which the GC operates, induced further degradation of the resulting degradation products, leading to inaccurate degradation product identification. A softer analysis technique, gradient high performance liquid chromatography coupled to mass spectrometry (HPLC-MS) was therefore employed. The various degradation species could be separated via HPLC, but due to the constantly changing composition of the eluent used in the HPLC, identification of the eluted products via MS was problematic. It was however clear from this investigation that a wide variety of degradation products formed when cumyl dithiobenzoate in water was exposed to elevated temperatures. This investigation did not allow us to determine whether radicals were formed during the degradation process that might interfere with the reaction kinetics.

### 1.4.4 MALDI-TOF and GPC Subtraction

By this stage of the investigation it was determined that intermediate RAFT radical termination was indeed probable, but no experimental proof of its occurrence existed. It was therefore decided to find evidence for these intermediate radical termination products by doing consecutive GPC trace subtraction.<sup>34</sup> Results from this were inconclusive as terminated chains formed throughout the reaction, thus masking the presence of intermediate radical terminated chains.

MALDI-TOF is a very powerful analysis technique to investigate the average molecular weight and molecular weight distributions of polymerization reactions, as it gives a peak for every single chain in the sample mixture.<sup>2</sup> This is theoretically true, as in reality peaks only represent chains that are able to “fly”. To maximize the amount of possible intermediate radical termination products, high RAFT agent concentrations were used to target short chains at full conversion. High initiator concentrations were therefore used, to maximize

the concentration of radical species in the reaction mixture, and thus also the amount of termination that can occur in the system. This did however also lead to the formation of a large number of species in the reaction mixture, which made identification of the peaks in the MALDI-TOF spectra virtually impossible. It was also suspected that the laser used in the MALDI-TOF instrumentation might cleave the dithiobenzoate endgroups from the polystyrene chains. These might then recombine with other chains or cleaved groups, to form species not present in the original reaction mixture.

#### 1.4.5 *In situ* $^{13}\text{C}$ NMR Spectroscopy with a $^{13}\text{C}$ -enriched RAFT Agent

Currently, there is a heated debate in literature as to the fate of the intermediate radicals, and the rate coefficients associated therewith. (This will be discussed in detail in Chapter 2.) Using the rate coefficients of Monteiro *et al.*<sup>25</sup> and Barner-Kowollik *et al.*<sup>22</sup> in a developed mathematical model to simulate the RAFT process, it was found that the model could not predict the low intermediate radical concentrations observed by ESR spectroscopy. It was suspected that some "other" process must be in operation to decrease the amount of intermediate radicals present in the system. It was proposed by some authors that (irreversible) termination of intermediate radicals were possible.<sup>25,26</sup> It was therefore decided to use  $^{13}\text{C}$  NMR spectroscopy to find these proposed intermediate radical termination products. As it was expected that only minute quantities of the terminated intermediate RAFT radicals would form, it was decided to embark upon using a  $^{13}\text{C}$  labeled RAFT agent. It was also discovered through analysis of the  $^{13}\text{C}$  spectra that the RAFT reaction was extremely selective in the addition of a single monomer unit to all growing chains before further additions occurred, during the early stages of the reaction. This discovery led to the belief that the RAFT reactions could be followed by *in situ*  $^1\text{H}$  NMR. Thus, it was decided to perform *in situ*  $^1\text{H}$  NMR experiments to follow the concentration-time evolution of the various species present in the reactions.

#### 1.4.6 Electrospray - Mass Spectrometry

Electrospray mass spectrometry (ES-MS) was done on the *in situ*  $^{13}\text{C}$  NMR reaction samples after the reaction was completed. ES-MS analysis was however not ideal for this styrenic system, as it is not quantitative and numerous scans were needed to detect the suspected very small amount of terminated intermediate RAFT radicals. To ionize the styrenic chains in the sample a high cone voltage was needed. This might cause the dithiobenzoate end-capped species inside the ES-MS to fragment, which will lead to inaccurate analysis of the samples. Peaks in the ES-MS spectra were identified as possible intermediate terminated radicals. Again, in the process to identify (via  $^1\text{H}$  NMR) the terminated intermediate radical species that might be present after a specific reaction time, it was found that the RAFT process is extremely selective and can possibly be followed by *in situ*  $^1\text{H}$  NMR.

### 1.4.7 *In situ* $^1\text{H}$ -NMR Spectroscopy

During  $^{13}\text{C}$  NMR and ES-MS analysis it was discovered that the RAFT reactions could be followed via *in situ*  $^1\text{H}$  NMR. *In situ* NMR reactions were used to follow the concentration-time evolutions of various species in the reaction mixture. From these observations, a RAFT reaction scheme for the specific reactions could be proposed, based on the reaction selectivity observed.<sup>35</sup>

### 1.4.8 Electron Spin Resonance Revisited

The second round of ESR experiments (on new high sensitivity ESR equipment) involved investigating the time evolution of the intermediate radical concentrations of the systems used for the *in situ*  $^1\text{H}$  NMR experiments, in an attempt to explain the observed concentration-time evolutions of the various species in the reaction mixtures.

The combined results obtained from the above-mentioned analytical techniques were used to evaluate the currently accepted RAFT mechanism<sup>6</sup> and to make amendments to the mechanism to explain unusual observations and behavior.

## 1.5 Objectives and Thesis Outlay

The prospects of a RAFT mediated system is appealing, as the addition of a “*magic*” ingredient, a RAFT agent, to existing polymerization recipes utilizing existing techniques should, in principle, render total control over the properties of the end-product without influencing the radical concentration or the polymerization rate. The fact that over a hundred publications on the applications of RAFT and anomalies observed in certain RAFT systems have appeared in the last 4 years, should serve as an indication that the RAFT process is more complicated than is to be expected at first sight. It is therefore imperative to understand the mechanism by which the RAFT process functions and the possible occurrence of side reactions influencing the RAFT mechanism and thus also the reaction kinetics. The investigations in this thesis are thus aimed at gaining a more thorough understanding of the RAFT mechanism and the important reactions therein. Experiments done were designed specifically to investigate the probable causes for inhibition and rate retardation observed in some RAFT mediated polymerization systems.

Chapter 2 presents a brief overview of living radical polymerization, highlighting the similarities and differences of the various living polymerization techniques compared to the RAFT-mediated polymerizations. Several characteristic kinetic and mechanistic aspects of the RAFT system are discussed, together with a literature review on the anomalies observed in certain RAFT systems. The two main streams of thought behind the reasons of these anomalies are discussed and the implications on the RAFT mechanism compared.

Chapter 3 describes the initial *in situ* ESR spectroscopy experiments. A short overview on ESR spectroscopy techniques is first given, after which the unexpected concentration-time profiles of the intermediate radicals are discussed. Possible causes for these profiles are given and the implications on the RAFT mechanism explained. Several anomalies observed in the ESR experiments are given and probable solutions explained in the light of a modified RAFT mechanism.

In Chapter 4, evidence for the formation of possible intermediate RAFT termination products is given. Identification of these species was done by means of *in situ* and *ex situ*  $^{13}\text{C}$  NMR polymerizations. Through the use of unusually high RAFT agent and initiator concentrations, the extremely selective behavior (as inferred from the  $^{13}\text{C}$  spectra) of the RAFT process could be seen.

Chapter 5 is dedicated to *in situ*  $^1\text{H}$  NMR reactions and their corresponding *in situ* ESR polymerizations. The extremely selective behavior of the RAFT process observed is explained in the light of a proposed RAFT mechanism. The intermediate radical concentration-time profile, as determined by ESR spectroscopy, is used to determine the stability of the intermediate radicals formed, in accordance to the proposed RAFT mechanism. The apparent equilibrium constants for the reactions are calculated from rate and ESR data, and interpreted in terms of the (ratio of the) rate coefficients for addition and fragmentation of the formed intermediate radicals. The similarities and differences in the reaction mechanisms of cyanoisopropyl dithiobenzoate and cumyl dithiobenzoate RAFT agents are discussed.

Chapter 6 is an epilogue in which the conclusions of all of the previous chapters are summarized. Recommendations for future research to further elucidate the mysteries surrounding the RAFT process are also made.

## References

1. Moad, G.; Solomon, D. H. *The Chemistry of Free Radical Polymerization*; First ed.; Elsevier Science Ltd, **1995**.
2. Gilbert, R. G. *Emulsion Polymerization: A Mechanistic Approach*; Academic Press: London, **1995**.
3. Szwarc, M.; Levy, M.; Milkovich, R. M. *J. Am. Chem. Soc.* **1956**, *78*, 2656.
4. Szwarc, M. *Nature* **1956**, *178*, 1168.
5. Otsu, T.; Yoshida, M.; Tazaki, T. *Makromol. Chem., Rapid Commun.* **1982**, *3*, 133.
6. Le, T. P.; Moad, G.; Rizzardo, E.; Thang, S. H., *PCT Int. Appl.*, **1998**, wo98/01478.
7. Chiefari, J.; Chong, Y. K. B.; Ercole, F.; Krstina, J.; Jeffery, J.; Le, T. P. T.; Mayadunne, R. T. A.; Meijs, G. F.; Moad, C. L.; Moad, G.; Rizzardo, E.; Thang, S. H. *Macromolecules* **1998**, *31*, 5559.
8. Krstina, J.; Moad, G.; Rizzardo, E.; Winzor, C. L.; Berge, C. T.; Fryd, M. *Macromolecules* **1995**, *28*, 5381.
9. Krstina, J.; Moad, C. L.; Moad, G.; Rizzardo, E.; Berge, C. T.; Fryd, M. *Macromol. Symp.* **1996**, *111*, 13.
10. Chong, B. Y. K.; Le, T. P. T.; Moad, G.; Rizzardo, E.; Thang, S. H. *Macromolecules* **1999**, *32*, 2071.
11. Rizzardo, E.; Chiefari, J.; Chong, Y. K.; Ercole, F.; Krstina, J.; Jeffery, J.; Le, T. P. T.; Mayadunne, R. T. A.; Meijs, G. F.; Moad, G.; Moad, C. L.; Thang, S. H. *Macromol. Symp.* **1999**, *143*, 291.
12. Mayadunne, R. T. A.; Rizzardo, E.; Chiefari, J.; Chong, Y. K.; Moad, G.; Thang, S. H. *Macromolecules* **1999**, *32*, 6877.
13. Mayadunne, R. T. A.; Rizzardo, E.; Chiefari, J.; Krstina, J.; Moad, G.; Postma, A.; Thang, S. H. *Macromolecules* **2000**, *33*, 243.
14. Moad, G.; Chiefari, J.; Chong, Y. K.; Krstina, J.; Mayadunne, R. T. A.; Postma, A.; Rizzardo, E.; Thang, S. H. *Polym. Int.* **2000**, *49*, 993.
15. Rizzardo, E.; Chiefari, J.; Mayadunne, R. T. A.; Moad, G.; Thang, S. H., in *ACS Symp. Ser.*; ACS: Washington DC, **2000**; Vol. 768, p 278.
16. Mitsukami, Y.; Donovan, M. S.; Lowe, A. B.; McCormick, C. L. *Macromolecules* **2001**, *34*, 2248.
17. De Brouwer, H.; Schellekens, M. A. J.; Klumperman, B.; Monteiro, M. J.; German, A. L. *J. Polym. Sci., Part A: Polym. Chem.* **2000**, *38*, 3596.
18. Monteiro, M. J.; Sjoberg, M.; Van Der Vlist, J.; Gottgens, C. M. *J. Polym. Sci., Part A: Polym. Chem.* **2000**, *38*, 4206.
19. Stenzel-Rosenbaum, M.; Davis, T. P.; Chen, V.; Fane, A. G. *J. Polym. Sci., Part A: Polym. Chem.* **2001**, *39*, 2777.
20. Tsujii, Y.; Ejaz, M.; Sato, K.; Goto, A.; Fukuda, T. *Macromolecules* **2001**.
21. Baum, M.; Brittain, W. J. *Macromolecules* **2001**.
22. Barner-Kowollik, C.; Quinn, J. F.; Morsley, D. R.; Davis, T. P. *J. Polym. Sci., Part A: Polym. Chem.* **2001**, *39*, 1353.
23. Barner-Kowollik, C.; Quinn, J. F.; Nguyen, T. L. U.; Heuts, J. P. A.; Davis, T. P. *Macromolecules* **2001**, *34*, 7849.

24. Barner-Kowollik, C.; Coote, M. L.; Davis, T. P.; Radom, L.; Vana, P. *J. Polym. Sci., Part A: Polym. Chem.* **2003**, *41*, 2828.
25. Monteiro, M. J.; de Brouwer, H. *Macromolecules* **2001**, *34*, 349.
26. Kwak, Y.; Goto, A.; Tsujii, Y.; Murata, Y.; Komatsu, K.; Fukuda, T. *Macromolecules* **2002**, *35*, 3026.
27. Wang, A. R.; Zhu, S.; Kwak, Y.; Goto, A.; Fukuda, T.; Monteiro, M. J. *J. Polym. Sci., Part A: Polym. Chem.* **2003**, *41*, 2833.
28. De Brouwer, H., **2001**, Thesis, Technical University of Eindhoven, The Netherlands.
29. Monteiro, M. J.; Hodgson, M.; de Brouwer, H. *J. Polym. Sci., Part A: Polym. Chem.* **2000**, *38*, 3864.
30. De Brouwer, H.; Tsavalas, J. G.; Schork, F. J.; Monteiro, M. J. *Macromolecules* **2000**, *33*, 9239.
31. Monteiro, M. J.; de Barbeyrac, J. *Macromolecules* **2001**, *34*, 4416.
32. Tsavalas, J. G.; Schork, F. J.; de Brouwer, H.; Monteiro, M. J. *Macromolecules* **2001**, *34*, 3938.
33. McLeary, J. B.; Calitz, F. M. *Unpublished results*.
34. Clay, P. A.; Christie, D. I.; Gilbert, R. G., in *Advances in Free-Radical Polymerization*; Matyjaszewski, K., Ed. ACS: Washington DC, **1998**; Vol. 685, p 104.
35. McLeary, J. B.; Calitz, F. M.; McKenzie, J. M.; Tonge, M. P.; Sanderson, R. D.; Klumperman, B. *Macromolecules* **2003**, *Submitted*.

# Chapter 2

## Living Radical Polymerization: A Brief Overview

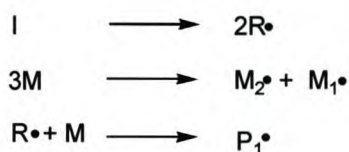
### Summary

*The mechanisms, by which different living/controlled free radical processes exert control over the polymerization process, are reviewed and compared. Various kinetic and mechanistic aspects of the RAFT process are also discussed. Prerequisites for an efficient RAFT transfer agent are discussed in the contexts of the RAFT mechanism and the intermediate radicals formed. The anomalies of inhibition and rate retardation observed in some RAFT systems are described. The two (opposing) main schools of thought for the possible rationale for these anomalies are reviewed, and the implications on the RAFT mechanism explained.*

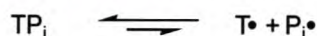
## 2.1 Overview of Living Radical Polymerization

Living radical polymerization can be classified as having polymer chain growth controlled by either reversible termination or reversible transfer.<sup>1</sup> Reversible termination mechanisms, such as nitroxide-mediated polymerizations<sup>2</sup> (stable free radical polymerization) (Scheme 2.1) and atom transfer radical polymerization (ATRP)<sup>3</sup> (Scheme 2.2) use a controlling agent that reacts reversibly with a propagating radical to yield a dormant chain. The equilibrium is shifted strongly towards the dormant species so that the active radical concentration is lower than in conventional radical polymerizations. Because the rate of propagation has a first order dependence on propagating radical concentration, while irreversible bi-radical termination is second order, the lower radical concentration results in a significantly reduced termination rate that preserves the living character of the chains. Inevitably, some bi-radical irreversible termination occurs, leading to dead chains and a broadening of the molecular weight distribution. In addition, the irreversible termination also leads to an increase in controlling agent concentration, driving the equilibrium toward the dormant state, thereby lowering the radical concentration and reaction rate even further.

### Initiation



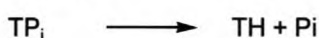
### Reversible Termination



### Propagation

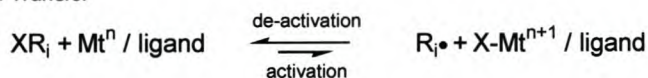


### Termination



**Scheme 2.1** Stable free radical polymerization. I is the initiator,  $R^\bullet$  an initiator derived radical, M a monomer,  $M_1^\bullet$  and  $M_2^\bullet$  an 1-mer and dimer generated by thermal initiation,  $P_i^\bullet$ , where ( $i = 1, 2, 3, \dots, j$ ), a polymer radical of length  $i$ ,  $T^\bullet$  a nitroxide radical,  $TP_i$  a polymer of length  $i$  capped by a nitroxide radical, TH a hydroxylamine and  $P_{i+j}$  a polymer of chain length  $i+j$ .

### Atom Transfer



### Propagation



### Termination



**Scheme 2.2** Atom transfer radical polymerization.  $XR_i$  is an alkyl halide of chain length  $i$ ,  $Mt^n / \text{ligand}$  the transition metal complex without the halide,  $X-Mt^{n+1} / \text{ligand}$  the transition metal complex with the halide.

Reversible transfer mechanisms such as degenerative transfer and reversible addition-fragmentation chain transfer (RAFT)<sup>4</sup> employ a chain transfer agent to transfer activity between propagating radicals. The reversible reaction is between a dormant chain and an active (propagating) radical, in which the end group originating from the initial transfer agent is exchanged between the two chains, thereby transferring chain activity from one polymer chain to another. In degenerative transfer (Scheme 2.3), there is a direct exchange

involving, for example, an iodine atom.<sup>5</sup> With RAFT, an addition fragmentation process is used to exchange a moiety such as a dithioester between two chains. With reversible transfer mechanisms, a conventional initiator is used to initiate the chains. The initial transfer agent is consumed by the radicals originating from the initiator decomposition. To maximize livingness, there should be a large excess of transfer agent to initiator. A highly active initial transfer agent is rapidly consumed (within a few percent monomer conversion), while a less active transfer agent may take most of the polymerization to be consumed. If consumption is rapid, there will be few dead chains, resulting in a narrow molecular weight distribution. If initial transfer agent consumption is slow, a broader distribution and more dead chains result. Because a conventional initiator is used, new chains are created as long as initiator remains. As with reversible termination mechanisms, some irreversible termination inevitably occurs, leading to a broadening of the molecular weight distribution. However, unlike reversible termination, the rate is not consequently suppressed. Because the reversible step is transfer, and not termination, the concentration of radicals is not affected, as would be the case in a conventional free radical polymerization.

*Initiation**Degenerative Transfer**Propagation**Termination*

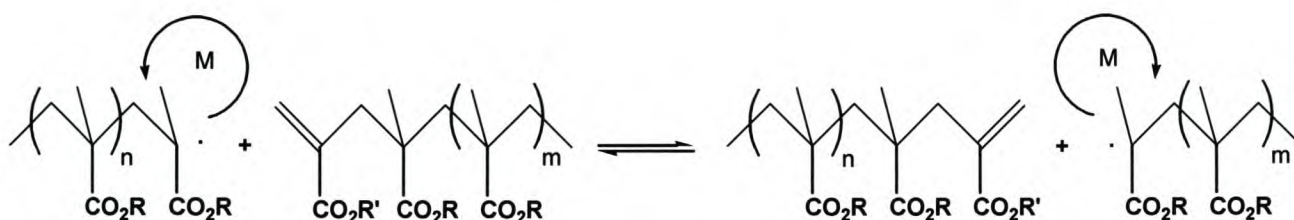
**Scheme 2.3** Degenerative transfer. AB is a degenerative transfer agent, AP<sub>i</sub> a polymer molecule of length i terminated by a degenerative transfer agent, AP<sub>j</sub> a polymer molecule of length j terminated by a degenerative transfer agent, and B<sup>•</sup> the radical generated from the degenerative transfer agent.

The fundamental difference between the two controlling mechanisms for living radical polymerization, i.e. reversible termination and reversible transfer, involves the total (propagating) radical concentration in the systems. With reversible termination, the propagating radical concentration is lower than in reversible transfer mechanisms. In addition, the deactivation step of a growing radical is very fast (close to diffusion controlled) and is therefore comparable to termination rate coefficients. However, the higher concentration of deactivating species compared to radicals means deactivation strongly dominates over irreversible termination. In reversible transfer, the radical concentration is (theoretically) not affected. When highly reactive transfer agents are used, transfer is preferred over propagation, leading to chain activity being transferred between growing polymer chains resulting in equal opportunities of all chains to grow throughout the length of the reaction.

Although a linear relationship between  $\overline{M}_n$  and conversion is often interpreted as evidence that a system is living, all it really requires is that the total number of chains remains unchanged and that some of the chains are living. Plots of  $\overline{M}_n$  versus conversion should be examined together with the polydispersity of the molecular weight distribution, although polydispersity is not very sensitive to the formation of small numbers of dead chains.

## 2.2 Reversible Addition-Fragmentation chain Transfer Polymerization

Methacrylate monomers were the first species used as RAFT agents. The discovery of cobalt complexes that acted as catalytic chain transfer agents<sup>6</sup> allowed the facile preparation of methacrylate oligomers with terminal double bonds.<sup>7</sup> It was found that these macromonomers could be applied as transfer agents that operate through a so-called addition-fragmentation process.<sup>8,9</sup> When these macromonomers were used in the polymerization of methacrylate monomer, the addition-fragmentation process was reversible (Scheme 2.4).



**Scheme 2.4** The reversible addition-fragmentation chain transfer process using methacrylic macromonomers as transfer agents. A single methacrylic unit is exchanged in the process. R and R' can be the same or different.

However, due to the low reactivity of these macromonomers,<sup>10</sup> transfer could not compete with propagation when high monomer concentrations were used, leading to uncontrolled behavior. When these reactions were conducted under monomer-starved conditions, living radical characteristics could be observed. The reversible character disappeared however when monomers other than methacrylates were used, as polystyryl and -acryl chains form poor leaving groups, resulting in a loss of living character. For such a process to be generally applicable in polymerization reactions, transfer agents with higher reactivity are required. These were found in the form of dithioesters,<sup>4,11</sup> selected dithiocarbamates,<sup>12,13</sup> xanthates<sup>12</sup> and trithiocarbonates.<sup>12,14</sup> These transfer agents are remarkably similar to the original iniferters discovered by Otsu *et al.*,<sup>15</sup> but were optimized for more efficient transfer reactions. The patent by Le *et al.*<sup>11</sup> gives detailed applications of these transfer agents in both homogeneous and heterogeneous systems, using many different monomers and functional groups. The reaction mechanisms of these species are similar in many respects to those of the macromonomers. In this dissertation, the polymerization systems investigated, using these specific dithiocarbonyl compounds as transfer agents, will be described using the RAFT mechanism.

## 2.2.1 The RAFT Mechanism

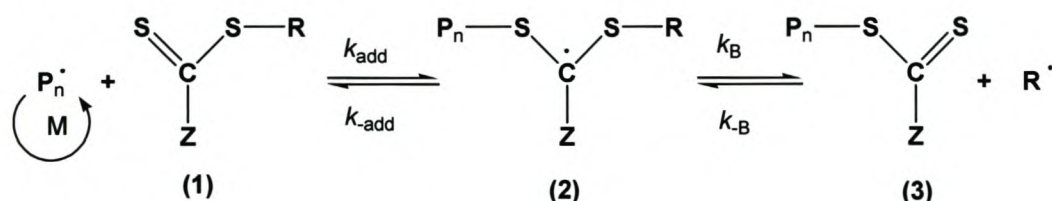
Understanding the RAFT mechanism is the key to understanding the intricacies involved in RAFT polymerization reactions. As all of the reactions in this study were designed to investigate a specific aspect of the RAFT mechanism, the RAFT mechanism will be discussed in detail, as will be the factors influencing the effectiveness of the RAFT agents and anomalies (and possible explanations) seen in some RAFT systems.

The generally accepted RAFT scheme<sup>11</sup> is given below.

### Initiation



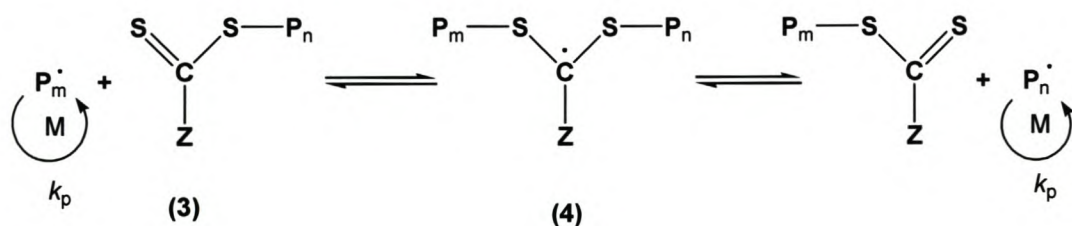
### Pre-equilibrium



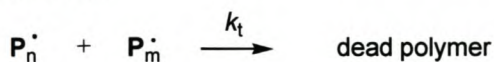
### Re-initiation



### Chain equilibrium



### Termination



**Scheme 2.5** The currently accepted elementary steps of the reversible addition fragmentation chain transfer (RAFT) mechanism.

Radicals generated by initiator decomposition (or by  $\gamma$  – or UV radiation) can propagate by the addition of monomer (the number of monomer units added will depend on the concentration of the RAFT agent to

monomer used), to form propagating radicals, which in turn can add to the carbon-sulfur double bond of the RAFT agent (1). The initiator-derived radicals can also directly add to the RAFT agent without first undergoing propagation. The probability of the two processes occurring will depend on the ratio of monomer to RAFT agent concentration used in the polymerization. A high ratio will favor propagation over addition to the RAFT agent.

The labile intermediate radical (2) that is formed fragments to regenerate the starting materials (1) or to form a temporarily deactivated dormant species (3), together with a radical ( $R^*$ ) derived from the original RAFT agent. The selection of the correct initiator, type of RAFT agent and monomer is crucial for this first fragmentation step. This will be discussed in section 2.2.2.

The expelled radical ( $R^*$ ) should then add to monomer, thereby re-initiating polymerization. An essential feature in the RAFT mechanism is the fact that the dithiocarbonate moiety ( $-S-C(Z)-S-$ ), present in the initial RAFT agent (1), is retained in the polymer products (3). Because of this, the dormant polymer chains can act as transfer agents themselves.

The propagating radical can then add to the polymeric RAFT agent (3) to form a (less labile) intermediate radical (4) that fragments to form another polymeric RAFT agent and expel a polymeric radical. Through this reaction, the propagating radical ( $P_m$ ) ( $m$  is a variable) is transformed into a dormant polymer, while the polymer chain from the polymeric RAFT agent ( $P_n$ ) is released as a radical which is capable of further growth. Again, the dithiocarbonate moiety is retained and the newly formed dormant species can be reactivated.

Inevitably, some termination between propagating radicals will occur to produce "dead" polymer of molecular weight equivalent to that of the two terminating chains combined (assuming termination by combination).

The reactions in Scheme 2.5 infer that the concentration of propagating radicals is in principle unaffected by the transfer reactions. This is only true as a first approximation. As transfer agents influence the radical chain length distribution, the chain length dependent termination rate coefficient will also be affected, and with it the equilibrium between initiation and termination. Furthermore, it will be illustrated in Chapter 4 that side termination reactions with the intermediate radicals can occur. These decrease the propagating radical concentration and in the process also "destroy" a dithiocarbonate moiety. This means that the (pseudo steady state) radical concentration is determined by the equilibrium between initiation and termination. In a *typical* RAFT polymerization the propagating radical concentrations will be in the order of  $10^{-9}$  -  $10^{-8}$  M, while the concentration of the RAFT agent (initial and polymeric) will be approximately  $10^{-4}$  -  $10^{-2}$  M (assuming that no or very little dithiocarbonate moieties are destroyed during the polymerization reaction). This indicates that a very small number of radicals are distributed between a large number of polymer chains at any given time. Contrary to previous belief<sup>11</sup> (and to complicate matters), the existence and concentration of the intermediate species will have a significant effect on the control obtained in RAFT polymerization.

It should be mentioned here that the experiments done in this study were designed to investigate a very specific aspect (intermediate radical termination) of the RAFT mechanism. The propagating and intermediate radical concentrations in the reactions investigated are thus far from those expected in typical RAFT mediated polymerizations.

To obey the rules of living polymerization, the RAFT process has to meet a few requirements:

- I. A fast exchange reaction.
- II. A good homolytic leaving group ( $R^*$ ), capable of rapid re-initiation.
- III. A constant number of growing chains during the polymerization.

I. The addition fragmentation reaction should be rapid compared to propagation. If this condition holds then the radical reactivity will be exchanged rapidly among the chains, giving all chains an equal chance to add to monomer and grow at the same rate.

II. For the final molar mass distribution to have a low polydispersity, it is important that all the chains start growing at the same time. Therefore, the transformation of the initial RAFT agent to dormant polymer species (pre-equilibrium, Scheme 2.5) has to be fast. In this reaction, the formed intermediate species (**2**) is not symmetrical and the R group will need to be chosen in such a way that it is a better homolytic leaving group than the (oligomeric) polymer chain. In general, the leaving group character is better for substituted alkyls and can be increased by substitution with groups that stabilize the expelled radical through resonance. This will be discussed in detail in section 2.2.2.

III. The number of growing chains throughout the reaction is important as both the chains that cease to grow and those that start growing later during the polymerization will have chain lengths that are different to those of the bulk material. The concentration of chains at the end of the reaction is given by equation 2-1, assuming termination by disproportionation:

$$[chains] = [RAFT] + 2f([I] - [I]_0) \quad (2-1)$$

in which  $[RAFT]$  is the concentration of the dormant chains, which is equal to the initial RAFT agent concentration, assuming rapid transformation of the RAFT agent into dormant polymer chains. The second term ( $2f([I] - [I]_0)$ ) represents the number of chains formed by initiator decomposition,  $f$  being the efficiency factor, and  $[I]$  the initiator and  $[I]_0$  the initial initiator concentrations. For the number of chains to be constant during a reaction, the second term has to be negligibly small compared to the first term. This shows that the instantaneous, as well as the cumulative, concentration of radicals must be small compared to that of the RAFT agent/dormant species.

## 2.2.2 What Controls the Activity of RAFT Agents?

As for conventional chain transfer, the effective chain transfer constant ( $C_{tr}$ ) is given by the ratio of the rate constant for transfer to that for propagation  $k_{tr}/k_p$ .<sup>16</sup> However, in the case of reagents that react by an addition-fragmentation process,  $k_{tr}$  is a composite term which depends on the rate constant for addition to the thiocarbonyl group (of a RAFT agent)  $k_{add}$  and the partitioning of the intermediate radical (**2**) formed between starting materials and products, and is described in equation 2-2.<sup>17</sup>

$$k_{tr} = k_{add} \frac{k_{\beta}}{k_{-add} + k_{\beta}} \quad (2-2)$$

Here  $k_{add}$  is the rate constant for addition of a propagating radical to a RAFT agent to form an intermediate radical (**2**),  $k_{-add}$  the rate constant for fragmentation of the formed intermediate radical to liberate a propagating radical and a RAFT agent,  $k_{\beta}$  is the rate constant for fragmentation of an intermediate radical to liberate the original RAFT agent end group radical ( $R^*$ ).

Depending on the R and Z groups used, the RAFT agent can have transfer constants spanning more than five orders of magnitude ( $< 0.01 - 1\ 000 >$ ). Theory suggests that to yield narrow polydispersities ( $< 1.5$ ) in a batch polymerization, the transfer constants should be greater than two.<sup>18-20</sup>

On the basis of the proposed elementary reactions of the RAFT mechanism (Scheme 2.5), at least four factors can be seen to influence the effectiveness of the dithiobenzoate species (**1**) as RAFT agents: (a) The rate constant of reaction of (**1**) with the propagating radicals ( $k_{add}$ ); (b) partitioning of the intermediate radical (**2**) between products and starting materials (determined by the magnitude of  $k_{add}$  and  $k_{\beta}$ ); (c) the rate constants for fragmentation of the intermediate radicals (**2**) and (**4**); (d) the ability of the expelled radicals,  $R^*$ , to re-initiate polymerization.

### Role of the free-radical leaving group (R)

The magnitude of the transfer coefficient of (**1**) should directly reflect factors (a) and (b) mentioned above. Factor (c) is not directly influenced by the transfer coefficient, however, if fragmentation is slow (i.e. both  $k_{add}$  and  $k_{\beta}$  are small) or re-initiation is slow compared to propagation, then retardation of the polymerization reaction may result and the likelihood of (intermediate) radicals (**3**) and/or  $R^*$  to undergo side reactions leading to possible inhibition is increased.

R should be a good free radical leaving group both in absolute terms and relative to the propagating species derived from the monomer being polymerized. The effect of the R group can be gauged by determining the apparent transfer constants of a series of dithiobenzoate derivatives in a methyl methacrylate polymerization (Table 2.1).<sup>16,21</sup> Based on the (reasonable) assumption that the R group does not dramatically affect the rate

of addition to a RAFT agent, the magnitudes of the transfer constants should reflect the partitioning of the intermediate radical (**2**) between starting materials and products, and the relative leaving group ability of R.

**Table 2.1** The apparent transfer constants ( $C_{tr}$ ) for the dithiobenzoate derivatives  $S=C(Ph)-S-R$  in methyl methacrylate polymerization at 60 °C.<sup>16,21</sup>

RAFT agent	$C_{tr}$	RAFT agent	$C_{tr}$
<b>1a</b> , R = C(CH <sub>3</sub> ) <sub>2</sub> CN	13	<b>1d</b> , R = C(CH <sub>3</sub> ) <sub>2</sub> CH <sub>2</sub> C(CH <sub>3</sub> ) <sub>3</sub>	0.4
<b>1b</b> , R = C(CH <sub>3</sub> ) <sub>2</sub> Ph	10	<b>1e</b> , R = CH(CH <sub>3</sub> )Ph	0.16
<b>1c</b> , R = C(CH <sub>3</sub> ) <sub>2</sub> CO <sub>2</sub> Et	2	<b>1f</b> , R = C(CH <sub>3</sub> ) <sub>3</sub>	0.03
		<b>1g</b> , R = CH <sub>2</sub> Ph	0.03

The comparatively low transfer constants of benzyl (**1g**) and 1-phenylethyl (**1e**) dithiobenzoates indicate that steric factors may be more important than radical stability in determining leaving group ability. The importance of steric factors is also indicated by the finding that 2,4,4-trimethylpent-2-yl dithiobenzoate (**1d**) has a much higher transfer constant than *tert*-butyl dithiobenzoate (**1f**). The finding that cyanoisopropyl dithiobenzoate (**1a**) appears to have a higher transfer constant than cumyl dithiobenzoate (**1b**) may suggest that polar factors are also important in determining the transfer constant. However, the 'transfer constant' for more active compounds, which were determined by comparing the rate of RAFT agent consumption as a function of conversion, decreased with the concentration of RAFT agent.<sup>21</sup> In general, the demands on the R group are dependent on the monomer being polymerized and decrease in the order methacrylates > styrenes > acrylates.

For the RAFT agent to be effective, R\*, besides being a good homolytic leaving group with respect to the propagating radical, must also be efficient in re-initiating the polymerization. The rate of re-initiation should be equal to or greater than the rate of propagation to avoid retardation (see section 2.3). It is also necessary to consider the rate of re-initiation in relation to the rate of reaction of R\* with the polymeric RAFT agent. If the rate of re-initiation is small, the rate of initial RAFT agent consumption will be reduced and this may cause the transfer coefficient to be dependent on the RAFT agent concentration and conversion, as is the case for cyanoisopropyl (**1a**) and cumyl (**1b**) dithiobenzoate polymerization.

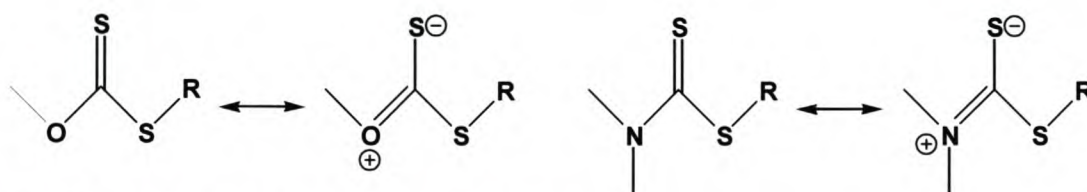
#### Effect of the activating group (Z)

To assess the effect of the Z group on the activity of the RAFT agents, the transfer constants of a series of benzyl thiocarbonylthio compounds of general structure  $S=C(Z)-S-CH_2Ph$  are compared (Table 2.2).<sup>16</sup> This was done by following the relative rates of transfer agent and monomer consumption.<sup>22</sup> Because the R group is common, the differences in transfer constants can be largely attributed to the differences in reactivity of the C=S bond due to the different Z groups.

**Table 2.2** Apparent transfer constants ( $C_{tr}$ ) for benzyl thiocarbonylthio compounds  $S=C(Z)-SCH_2Ph$  in styrene polymerization at 110 °C.<sup>16</sup>

RAFT agent	$C_{tr}$	RAFT agent	$C_{tr}$
<b>1h</b> , Z = Ph	26	<b>1l</b> , Z = OC <sub>6</sub> F <sub>5</sub>	2.3
<b>1i</b> , Z = SCH <sub>2</sub> Ph	18	<b>1m</b> , Z = lactam	1.6
<b>1j</b> , Z = CH <sub>3</sub>	10	<b>1n</b> , Z = OPh	0.72
<b>1k</b> , Z = pyrrole	9	<b>1o</b> , R = NEt <sub>2</sub>	0.1

The transfer constants decrease in the series where Z is aryl > alkyl  $\approx$  alkylthio  $\approx$  pyrrole > aryloxy > amido > alkoxy > dialkylamino. More generally, transfer constants decrease in the series dithiobenzoates > trithiocarbonates > dithioalkanoates > dithiocarbonates (xanthates) > dithiocarbamates. Electron withdrawing substituents on Z can enhance the activity of RAFT agents to modify the above order. The low activity of xanthates and dithiocarbamate derivatives can be qualitatively understood in terms of the importance of the zwitterionic canonical forms (Scheme 2.6), which serve to reduce the C=S double bond character.

**Scheme 2.6** Canonical forms of xanthates and dithiocarbamates.

Thus, the trend in relative effectiveness of the RAFT agents can be rationalized in terms of interaction of the Z group with the C=S double bond to activate or deactivate the group towards free radical addition.

### 2.3 Anomalies in RAFT Polymerization

Ideally, the RAFT process should be fast, and the intermediate RAFT adduct radical (**2** and **4**) should therefore be short-lived. In this way, the rapid transfer of the growing radicals between their active and corresponding dormant (**1** and **3**) forms minimizes unwanted termination processes without significantly reducing the propagation and hence the rate of polymerization. The stability (and fate) of the intermediate radicals (**2** and **4**) has in recent literature attracted considerable controversy. It is documented that the RAFT agents cumyl and 1-phenylethyl dithiobenzoate (Z = phenyl, R = C(CH<sub>3</sub>)<sub>2</sub>C<sub>6</sub>H<sub>5</sub> or CH(CH<sub>3</sub>)C<sub>6</sub>H<sub>5</sub>) significantly retard the polymerization rate for styrene,<sup>16,23-26</sup> methyl methacrylate,<sup>27</sup> butyl acrylate,<sup>16</sup> and methyl acrylate.<sup>25,28,29</sup> This retardation effect can be relieved through either a reduction in the RAFT agent concentration, an increase in polymerization temperature, or the use of RAFT agents containing a benzyl

(rather than phenyl) group in the Z-position.<sup>16,28,29</sup> The effect of the R group on retardation is more variable. Changing the R group to cyanoisopropyl was found to relieve rate retardation in styrene<sup>16</sup> and methyl methacrylate<sup>27</sup> polymerization and, while it did not relieve the retardation in methyl acrylate polymerization, it was found that the initial inhibition period was relieved.<sup>29</sup>

The main point of controversy concerns the interpretation of the above results. Based on the RAFT mechanism shown in Scheme 2.5, several explanations for retardation and inhibition may be envisaged.<sup>16</sup> These include the following:

- a) Slow fragmentation of the intermediate radical (**2**) to liberate the initial RAFT leaving group ( $R^*$ ).
- b) Slow fragmentation of the polymeric intermediate radical (**4**).
- c) Slow initiation by the expelled radical ( $R^*$ ).
- d) Consumption of intermediate radicals (**2**) and (**4**) in side reactions – e.g. reversible or irreversible termination reactions.
- e) Specificity for  $R^*$  to add to RAFT agent rather than monomer.
- f) Specificity for the propagating radical ( $P_n^*$ ) to add to RAFT agent rather than monomer (i.e. transfer constant too high).

Some workers<sup>16,25-30</sup> argue that the rate retardation is due to the slow fragmentation of the intermediate radical when the highly stabilizing phenyl substituent is attached to the radical center. Others<sup>23,24,31,32</sup> suggest that termination reactions involving the intermediate radical must be responsible, as the fragmentation rate of the intermediate radical is not slow enough to account for the retardation in the polymerization rates. Due to the intricacies involved, the fragmentation rate cannot be measured directly and must instead be inferred from an assumed kinetic model, based on values obtained from the overall rate of polymerization, the total radical concentration or the molecular weight distribution of the resulting polymer. Depending on the method used, estimates of the fragmentation rate coefficient of the intermediate radicals in a cumyl dithiobenzoate/styrene polymerization at 60 °C range from  $10^4$  to  $10^{-2} \text{ s}^{-1}$ , a difference of 6 orders of magnitude.<sup>23,24,30,31</sup> This enormous discrepancy reflects the difficulty in using conventional kinetic experiments to study the rates of the individual steps in the RAFT process.

### 2.3.1 Inhibition

The occurrence of an inhibition period, i.e. the experimental observation that upon releasing radicals from a given source (e.g. a thermally decaying initiator or  $\gamma$ -radiation) a monomer/RAFT agent mixture shows no polymerization reactivity, in RAFT systems has been extensively investigated by various authors.<sup>16,26,29,30,33,34</sup>

Some authors<sup>29,35</sup> have attributed the inhibition period to either slow re-initiation of the  $R^*$  group or slow fragmentation of the formed intermediate radicals. In an attempt to distinguish between the two effects, Perrier *et al.*<sup>29</sup> conducted a set of experiments in which the pre-equilibrium was effectively circumvented by using a polymeric RAFT agent ( $\bar{M}_n = 8\,000 \text{ g mol}^{-1}$ , PDI = 1.1) as the  $R^*$  group was already a polymeric

species. No inhibition period was observed. They concluded that the inhibition period was therefore not caused by (or reactions associated with) the key equilibrium of the RAFT process. When cyanoisopropyl dithiobenzoate (CIDB) was used instead of 1-phenylethyl dithiobenzoate (1-PEDB) as a RAFT agent in a bulk reaction of methyl acrylate (MA) with AIBN as initiator, a marked decrease in the length of the inhibition period was observed. However, when a 1-methoxycarbonyl ethyl dithiobenzoate (1-MEDB) RAFT agent was used, which has a faster addition rate to an acrylate monomer than a poly(acrylate) propagating species,<sup>36-40</sup> it should display less inhibition as observed by the poly(methyl acrylate) RAFT agent mentioned above. This was not the case. They concluded that the inhibition period was thus not likely to be due to slow re-initiation, but most likely due to the variation in stability of the intermediate radical (**2**) formed in the pre-equilibrium process, induced by the changing of the structure of the R<sup>\*</sup> group. These conclusions were confirmed via high level *ab initio* molecular orbital calculations by Coote *et al.*,<sup>41</sup> who predicted that in MA polymerization using CIDB as RAFT agent it is fragmentation of the polymeric intermediate radical rather than the initial agent that is retarded.

Vana *et al.*,<sup>35</sup> through simulations based on styrene/CDB/AIBN reactions, showed that  $k_i$  (the rate coefficient for re-initiation) has to be close to approximately  $10 \text{ M s}^{-1}$  to produce the inhibition observed in the reactions. Another unexpected simulation result was that slow re-initiation induces rate retardation throughout the whole polymerization. Based on the simulations, they concluded that inhibition phenomena in RAFT polymerizations may be attributed to slow fragmentation of the intermediate radicals in the pre-equilibrium or, kinetically similarly, their reversible storage in a non-radical sink.<sup>25,30,42</sup>

Moad *et al.*<sup>16</sup> observed an inhibition period lasting up to 1 h during which the RAFT agent is only slowly consumed for the styrene polymerization mediated by CDB. For longer reaction times, when the initial RAFT agent is converted to polymeric species, the polymerization rate increased. They attributed this to the cumyl radical being relatively slow to initiate styrene polymerization (i.e. (c) or (d) above), as cumyl is anticipated to be a good free radical leaving group. They also found that the use of CIDB as a RAFT agent alleviated the observed inhibition.

For the RAFT systems presented in this study, it will indeed be shown that the initial polymerization period during which no apparent polymerization occurs, reported as an observed inhibition period, is erroneous, as polymerization indeed occurs. This "inhibition" period is due to the extreme selectivity of the RAFT process to add one monomer unit to all initial RAFT agents before the addition of a second monomer unit. This also explains the observation of increased inhibition periods when higher initial RAFT agent concentrations are used.

### 2.3.2 Rate Retardation

There has been an ongoing debate regarding the mechanism that causes rate retardation phenomena observed in some RAFT polymerization systems. Some attributed the retardation to slow fragmentation of the intermediate radicals,<sup>16,26,29,30,33,34</sup> others attributed it to fast fragmentation coupled with cross-termination

between propagating and intermediate radicals.<sup>23,24,31,32,43</sup> As mentioned before, a difference of six orders of magnitude ( $10^{-2}$  versus  $10^4 \text{ s}^{-1}$ ) in the reported values of the fragmentation rate constant for virtually similar RAFT systems.

The reason for the huge discrepancies in  $k_{\text{add}}$  can be explained in the light of equation 2-3, where the propagating radical concentration ( $c_P$ ) or the rate of polymerization is given by<sup>44</sup>

$$c_P = \left( \frac{R_i}{k_t} \right)^{1/2} \left( 1 + K \left( \frac{k_t'}{k_t} \right) [P-X] \right)^{-1/2} \quad (2-3)$$

where  $R_i$  is the rate of initiation,  $k_t$  and  $k_t'$  the rates of conventional and intermediate radical termination respectively,  $K$  the equilibrium coefficient ( $= k_{\text{add}}/k_{-\text{add}}$ ) and  $[P-X]$  the number of dithiobenzoate end-capped chains, which can be approximated by the initial RAFT agent concentration. The rate of

polymerization is determined by the group of rate constants  $\left( \frac{k_{\text{add}}}{k_{-\text{add}}} \right) \left( \frac{k_t'}{k_t} \right)$ . Therefore, the combination of a

large  $k_{\text{add}}$  and a large  $k_t'$  or a small  $k_{\text{add}}$  and a small  $k_t'$ , for example, have the same effect on the

polymerization rate, insofar as the ratio  $\left( \frac{k_t'}{k_{-\text{add}}} \right)$  remains constant. Without any other data but the rate, there

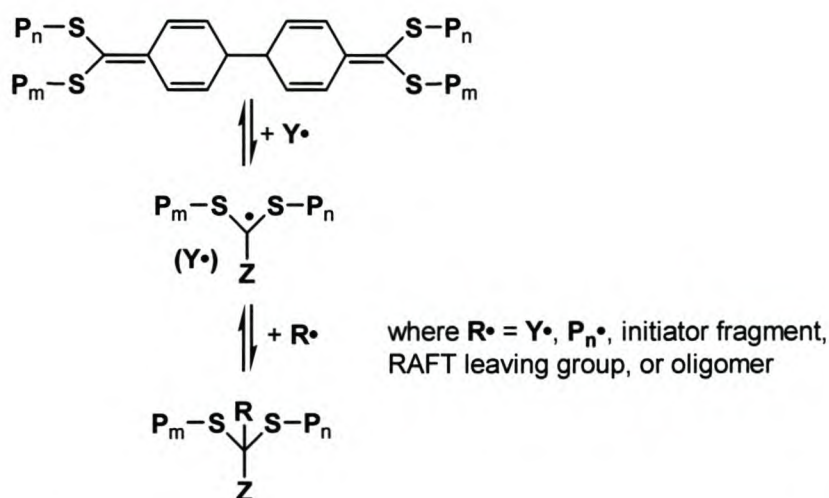
obviously is no unique answer.

#### Slow fragmentation (and reversible intermediate radical termination)

Barner-Kowollik and coworkers<sup>16,26,29,30,33,34</sup> attributed the retardation to the slow fragmentation of intermediate radicals. They suggested that intermediate radicals are rather stable and have long lifetimes. Using a commercial software simulation package (PREDICI) to correlate monomer conversion and molecular weight data of the bulk polymerization of styrene at 60 °C, initiated by AIBN and mediated by CDB, they reported a fragmentation rate constant of  $k_{\text{add}} \approx 3 \times 10^{-2} \text{ s}^{-1}$ . Changing the RAFT agent to cumyl phenyl dithioacetate (CPDA) resulted in  $k_{\text{add}} \approx 2.7 \times 10^{-1} \text{ s}^{-1}$ . The intermediate radical lifetimes ( $1/k_{\text{add}}$ ) were estimated to be approximately 100 s and 10 s respectively. It was commented by Wang *et al.*<sup>44</sup> that utilizing molecular weight and rate data is not adequate for the estimation of rate constants, but that radical concentration data must be included. They also commented on the adaptation of the existing PREDICI model to be useful in correlating data, but not optimal for estimations of rate constants.

Barner-Kowollik *et al.*<sup>25</sup> and Barner *et al.*<sup>45</sup> designed experiments that demonstrated that the intermediate radical (and species that could be reversibly made from it, Scheme 2.7) could remain dormant for up to an hour at room temperature and then, upon heating, release radicals to show significant polymerization. A mixture of CDB and styrene was subjected to an initiation source ( $\gamma$ -radiation) for 18 h at room temperature. Subsequently the reaction mixture was left untouched for a given period of time at ambient temperature and

then raised to an elevated temperature (60 °C) for 22 h. Significant polymerization activity was only observed during the heating period, indicating free radical storage during the irradiation sequence. To exclude the possibility of radical formation by thermal initiation of styrene, the same reaction procedure was repeated with MA. After irradiation of an MA/CDB mixture for 18 h at room temperature, the mixture was left for 20 min at room temperature and then heated for 4 h at 80 °C. Again, no polymerization could be detected after the initiation and waiting periods, but only after the subsequent heating period (11% conversion). They concluded that radicals can only survive if the intermediate radicals are sufficiently stabilized or reversibly stored (top half of Scheme 2.7) in sufficient quantities to allow for the polymerization to proceed after a waiting period.



**Scheme 2.7** Possible additional (reversible and irreversible) termination reactions involving the intermediate radical to generate new species.<sup>42</sup>

Using specially designed experiments to enhance termination of the intermediate radical, Vana *et al.*<sup>46</sup> could not identify any intermediate termination products, which seemed to underpin Barner-Kowollik *et al.*'s notion of the presence of relative stable intermediate radicals.

Coote and Radom<sup>41</sup> recently used high-level *ab initio* molecular orbital calculations to directly study the fragmentation of intermediate radicals of the form  $\text{CH}_3\text{-S-C(Z)-S-R}$ , where  $\text{Z} = \text{CH}_3$ , benzyl and phenyl and  $\text{R} = \text{CH}_3$ ,  $\text{CH}_2\text{COOCH}_3$ , and  $\text{C}(\text{CH}_3)_2\text{CN}$ . Using this approach, Coote and Radom found that when  $\text{Z}$  is phenyl, the fragmentation rate is approximately  $1.3 \times 10^{-1} \text{ s}^{-1}$  at 60 °C and  $9.8 \text{ s}^{-1}$  when  $\text{Z}$  is benzyl. This result seemed to support the idea that rate retardation is caused by slow fragmentation of the intermediate radicals.

#### Fast fragmentation and intermediate radical termination

Monteiro and coworkers<sup>23,24,31,32,43</sup> suggested an amendment to the RAFT mechanism to include termination between propagating and intermediate radicals (bottom half, Scheme 2.7). An experimental observation of products with tripled molecular weight formed during the UV-radiation of poly(styryl) dithiobenzoate in the

absence of a monomer provided some support for this mechanism. Using a computer simulation, they estimated  $k_{\text{add}}$  to be  $10^5 \text{ s}^{-1}$ . They also found that without the intermediate termination being taken into consideration, the rate retardation phenomenon could not be explained by varying  $k_{\text{add}}$  except when a (unrealistic) value of  $k_{\text{add}} = 0.1 \text{ s}^{-1}$  was used. This implied that the intermediate radical concentration was approximately an order of magnitude greater than the propagating radical concentration. Consequently, the value calculated for the intermediate radical concentration agrees well with that observed by ESR experiments.<sup>47-51</sup> The probability of intermediate radical termination will therefore be far greater than conventional termination.

A recent experiment by Kwak *et al.*<sup>24</sup> that combined conversion data (obtained by dilatometry) with the intermediate radical concentration obtained by electron spin resonance (ESR) spectroscopy gave an estimate of  $k_{\text{add}} = 7 \times 10^4 \text{ s}^{-1}$  for a system of bulk styrene initiated by AIBN and mediated by a poly(styryl) dithiobenzoate RAFT agent ( $\bar{M}_n = 1100$ ,  $\bar{M}_w/\bar{M}_n = 1.08$ ) at  $60 \text{ }^\circ\text{C}$ . A model experiment was also carried out to confirm the formation of a three-arm polymer product caused by intermediate radical termination, thus causing retardation in the rate of polymerization. The rate of intermediate termination was estimated to be similar to conventional termination in order of magnitude. The significance of these discoveries by Kwak *et al.*<sup>24</sup> can be explained in the light of equation 2-3; the obtained ESR data permitted the determination of

$\left(\frac{k_{\text{add}}}{k_{\text{-add}}}\right)$  and therefore  $k_{\text{add}}$  to be  $7 \times 10^4 \text{ s}^{-1}$  from a known value of  $k_{\text{add}}$  and, subsequently, the

determination of  $\left(\frac{k'_t}{k_t}\right)$  to be 0.8 with the already known retarded polymerization rate.

Barner-Kowollik *et al.*<sup>52</sup> cast doubt on the accuracy of the ESR data, particularly the use of 2,2,6,6-tetramethyl-1-piperidinyloxy (TEMPO) for calibrating the ESR spectra. The ESR technique has been well established in identifying radical types and quantifying radical concentrations in radical polymerizations.<sup>53,54</sup> There are rather exceptional cases in which the integration becomes unreliable, but an error of three orders of magnitude ( $<10^{-6} \text{ M}$  (observed via ESR spectroscopy)<sup>24,31,32,48-51</sup> vs.  $10^{-3} \text{ M}$  predicted by Barner-Kowollik<sup>26</sup>) is most unlikely.

Recently, Wang and Zhu<sup>32</sup> developed a RAFT kinetics simulation based on the method of moments. The object of the work was to use the model to simulate the effects of a chemical recipe and various reaction rate constants on the RAFT process. A set of rate constants was used as reference. Centered on this, each rate constant was varied over many orders of magnitude to examine its effects. Originally, a  $k_{\text{add}}$  of  $10^{-2} \text{ s}^{-1}$  was used, as estimated by Barner-Kowollik and coworkers,<sup>26,30</sup> which predicted a very high level of intermediate radical concentrations at  $10^{-4} \sim 10^{-3} \text{ M}$ . However, all ESR experiments report many orders of magnitude lower radical concentrations at  $< 10^{-6} \text{ M}$ ,<sup>24,31,32,48-51</sup> which corresponded to the results of using a  $k_{\text{add}}$  of  $10^{-4} \text{ s}^{-1}$  in Wang and Zhu's model.<sup>32</sup> This result seems to agree with the proposed theory of Monteiro and coworkers on the cause for rate retardation in RAFT systems.

As a final comment it should be noted that the anomalies discussed above may not be generic to all RAFT systems. Different RAFT agents and different monomers may (and indeed do) show quite different behavior.

## 2.4 Conclusions

In the last 4 years, more than 100 papers were published on the RAFT process and the applications thereof, elevating the RAFT process to a “hot topic” in the field of free radical polymerization research. As evident from this brief overview, the matter of inhibition and rate retardation observed in certain RAFT systems are also far from resolved. This thesis is thus but a small cog in the research machine driving to elucidate the mysteries surrounding the RAFT process. In particular, the work done in this thesis is a step in the process to investigate the anomalies observed in certain RAFT systems. With the use of a variety of analytical techniques, possible explanations for the observed anomalies are given in the light of a modified RAFT mechanism, to include reversible and/or irreversible termination reactions of the intermediate RAFT radical.

## References

1. Cunningham, M. F. *Prog. Polym. Sci.* **2002**, *27*, 1039.
2. Georges, M. K.; Veregin, R. P. N.; Kazmaier, P. M.; Hamer, G. K. *Macromolecules* **1993**, *26*, 2987.
3. Wang, J.-S.; Matyjaszewski, K. *J. Am. Chem. Soc.* **1995**, *117*, 5614.
4. Chiefari, J.; Chong, Y. K. B.; Ercole, F.; Krstina, J.; Jeffery, J.; Le, T. P. T.; Mayadunne, R. T. A.; Meijs, G. F.; Moad, C. L.; Moad, G.; Rizzardo, E.; Thang, S. H. *Macromolecules* **1998**, *31*, 5559.
5. Lansalot, M.; Farcet, C.; Charleux, B.; Vairon, J.-P. *Macromolecules* **1999**, *32*, 7354.
6. Ernikolopyan, N. S.; Smirnov, B. R.; Ponomarev, G. V.; Beklgoovskii, I. M. *J. Polym. Sci., Polym. Chem. Ed.* **1981**, *19*, 879.
7. Cacioli, P.; Hawthorne, D. G.; Laslett, R. L.; Rizzardo, E.; Solomon, D. H. *J. Macromol. Sci. - Chem.* **1986**, *A23*, 839.
8. Krstina, J.; Moad, G.; Rizzardo, E.; Winzor, C. L.; Berge, C. T.; Fryd, M. *Macromolecules* **1995**, *28*, 5381.
9. Krstina, J.; Moad, C. L.; Moad, G.; Rizzardo, E.; Berge, C. T.; Fryd, M. *Macromol. Symp.* **1996**, *111*, 13.
10. Moad, C. L.; Moad, G.; Rizzardo, E.; Thang, S. H. *Macromolecules* **1996**, *29*, 7717.
11. Le, T. P.; Moad, G.; Rizzardo, E.; Thang, S. H., *PCT Int Appl*, **1998**, wo98/01478.
12. Chiefari, J.; Mayadunne, R. T.; Moad, G.; Rizzardo, E.; Thang, S. H., *PCT Int. Appl.*, **1999**,
13. Mayadunne, R. T. A.; Rizzardo, E.; Chiefari, J.; Chong, Y. K.; Moad, G.; Thang, S. H. *Macromolecules* **1999**, *32*, 6877.
14. Mayadunne, R. T. A.; Rizzardo, E.; Chiefari, J.; Krstina, J.; Moad, G.; Postma, A.; Thang, S. H. *Macromolecules* **2000**, *33*, 243.
15. Otsu, T.; Yoshida, M.; Tazaki, T. *Makromol. Chem., Rapid Commun.* **1982**, *3*, 133.
16. Moad, G.; Chiefari, J.; Chong, Y. K.; Krstina, J.; Mayadunne, R. T. A.; Postma, A.; Rizzardo, E.; Thang, S. H. *Polym. Int.* **2000**, *49*, 993.
17. Moad, C. L.; Moad, G.; Rizzardo, E.; Thang, S. H. *Macromolecules* **1996**, *29*, 7717.
18. Moad, G.; Solomon, D. H. *The Chemistry of Free Radical Polymerization*; First ed.; Elsevier Science Ltd, **1995**.
19. Müller, A. H. E.; Zhuang, R. G.; Yan, D. Y.; Litvinenko, G. *Macromolecules* **1995**, *28*, 4326.
20. Muller, A. H. E.; Litvenko, G. *Macomolecules* **1997**, *30*, 1253.
21. Chong, Y. K. B.; Krstina, J.; Le, T. P. T.; Moad, G.; Postma, A.; Rizzardo, E.; Thang, S. H. *Macromolecules* **2003**, *36*, 2256.
22. Chiefari, J.; Mayadunne, R. T. A.; Moad, C. L.; Moad, G.; Rizzardo, E.; Postma, A.; Skidmore, M. A.; Thang, S. H. *Macromolecules* **2003**, *36*, 2273.
23. Monteiro, M. J.; de Brouwer, H. *Macromolecules* **2001**, *34*, 349.
24. Kwak, Y.; Goto, A.; Tsujii, Y.; Murata, Y.; Komatsu, K.; Fukuda, T. *Macromolecules* **2002**, *35*, 3026.
25. Barner-Kowollik, C.; Vana, P.; Quinn, J. F.; Davis, T. P. *J. Polym. Sci., Part A: Polym. Chem.* **2002**, *40*, 1058.

26. Barner-Kowollik, C.; Quinn, J. F.; Morsley, D. R.; Davis, T. P. *J. Polym. Sci., Part A: Polym. Chem.* **2001**, *39*, 1353.
27. Moad, G.; Chiefari, J.; Mayadunne, R. T. A.; Moad, C. L.; Postma, A.; Rizzardo, E.; Thang, S. H. *Macromol. Symp.* **2002**, *182*, 65.
28. Quinn, J. F.; Rizzardo, E.; Davis, T. P. *Chem. Comm.* **2001**, 1044.
29. Perrier, S.; Barner-Kowollik, C.; Quinn, J. F.; Vana, P.; Davis, T. P. *Macromolecules* **2002**, *35*, 8300.
30. Barner-Kowollik, C.; Quinn, J. F.; Nguyen, T. L. U.; Heuts, J. P. A.; Davis, T. P. *Macromolecules* **2001**, *34*, 7849.
31. Kwak, Y.; Goto, A.; Fukuda, T. *Macromolecules* **2003**, *Submitted*.
32. Wang, A. R.; Zhu, S. *J. Polym. Sci., Part A: Polym. Chem.* **2003**, *41*, 1553.
33. McLeary, J. B.; Calitz, F. M.; McKenzie, J. M.; Tonge, M. P.; Sanderson, R. D.; Klumperman, B. *Macromolecules*, *Submitted*.
34. Calitz, F. M.; McLeary, J. B.; McKenzie, J. M.; Klumperman, B.; Sanderson, R. D.; Tonge, M. P. *Manuscript in preparation*.
35. Vana, P.; Davis, T. P.; Barner-Kowollik, C. *Macromolecular theory and simulations* **2002**, *11*, 823.
36. Buback, M.; Kurz, C. H.; Schmaltz, C. *Macromol. Chem. Phys.* **1998**, *199*, 1721.
37. Heuts, J. P. A.; Gilbert, R. G.; Radom, L. *Macromolecules* **1995**, *28*, 8771.
38. Deady, M.; Mau, A. W. H.; Moad, G.; Spurling, T. H. *Makromol. Chem.* **1993**, *194*, 1691.
39. Gridnev, A. A.; Ittel, S. D. *Macromolecules* **1996**, *29*, 5864.
40. Olaj, O. F.; Vana, P.; Zoder, M.; Kornherr, A.; Zifferer, G. *Macromol. Rapid Commun.* **2000**, *21*, 913.
41. Coote, M. L.; Radom, L. *J. Am. Chem. Soc.* **2003**, *125*, 1490.
42. Barner-Kowollik, C.; Davis, T. P.; Heuts, J. P. A.; Stenzel, M. H.; Vana, P.; Whittaker, M. *J. Polym. Sci., Part A: Polym. Chem.* **2002**, *41*, 365.
43. De Brouwer, H.; Schellekens, M. A. J.; Klumperman, B.; Monteiro, M. J.; German, A. L. *J. Polym. Sci., Part A: Polym. Chem.* **2000**, *38*, 3596.
44. Wang, A. R.; Zhu, S.; Kwak, Y.; Goto, A.; Fukuda, T.; Monteiro, M. J. *J. Polym. Sci., Part A: Polym. Chem.* **2003**, *41*, 2833.
45. Barner, L.; Quinn, J. F.; Barner-Kowollik, C.; Vana, P.; Davis, T. P. *Eur. Polym. J.* **2003**, *39*, 449.
46. Vana, P.; Albertin, L.; Barner, L.; Davis, T. P.; Barner-Kowollik, C. *J. Polym. Sci., Part A: Polym. Chem.* **2002**, *40*, 4032.
47. Alberti, A.; Benaglia, M.; Laus, M.; Macciantelli, D.; Sparnacci, K. *Macromolecules* **2002**, *36*, 736.
48. Calitz, F. M.; Tonge, M. P.; Sanderson, R. D. *Macromolecules* **2003**, *36*, 5.
49. Hawthorne, D. G.; Moad, G.; Rizzardo, E.; Thang, S. H. *Macromolecules* **1999**, *32*, 5457.
50. Du, F. S.; Zhu, M. Q.; Guo, H. Q.; Li, Z. C.; Li, F. M.; Kamachi, M.; Kajiwara, A. *Macromolecules* **2002**, *35*, 6739.
51. Laus, M.; Papa, R.; Sparnacci, K.; Alberti, A.; Benaglia, M.; Macciantelli, D. *Macromolecules* **2001**, *34*, 7269.
52. Barner-Kowollik, C.; Coote, M. L.; Davis, T. P.; Radom, L.; Vana, P. *J. Polym. Sci., Part A: Polym. Chem.* **2003**, *41*, 2828.
53. Tonge, M. P.; Kajiwara, A.; Kamachi, M.; Gilbert, R. G. *Polymer* **1998**, *39*, 2305.

54. Yamada, B.; Westmoreland, D. G.; Kobatake, S.; Konosu, O. *Prog. Polymer Sci.* **1999**, *24*, 565.

# Chapter 3

## Electron Spin Resonance Spectroscopy Investigations

### Summary

*In this chapter, the concentration-time evolution of the intermediate radical concentration ( $c_Y$ ) for cumyl dithiobenzoate mediated styrene and butyl acrylate in situ ESR polymerizations at 70 and 90 °C was followed. The concentration-time evolution profiles observed were ascribed to the formation of very short chains during the early stages of the reaction. It was also found that the RAFT process is not particularly sensitive to oxygen. The intermediate and propagating radical concentrations (and their ratio) were examined by ESR spectroscopy and kinetics for the cumyl dithiobenzoate mediated styrene polymerizations. The system showed strong chain length effects in kinetics, assuming all chains were of mass  $\bar{M}_n$ . However, unusual behavior with respect to existing mechanistic knowledge was observed in other aspects of the system. The central equilibrium "constant" ( $K_{eq}$ ) was found to be dependent on both temperature and initial reactant concentrations. The observed intermediate radical concentrations were not consistent with the predictions based on existing literature models. It was also found that the time dependence of the intermediate radical concentration varied significantly with the type of RAFT agent used. Unexpectedly, intermediate radicals were detected at very long reaction times in the virtual absence of initiator, enhancing the belief of possible reversible termination reactions involving the intermediate radicals. An extra radical (non-propagating or intermediate) species was observed to form during reaction; its concentration increased with time.*

---

This chapter is an adapted version of the following paper:

**Kinetic and Electron Spin Resonance Analysis of RAFT Polymerization of Styrene;** F. M. Calitz, M. P. Tonge, R. D. Sanderson, *Macromolecules*, **2003**, 36, 5-8.

## 3.1 Electron Spin Resonance Spectroscopy

Section 3.1 (and subsections) provides a brief description of the basic principles and methodology of the performed ESR experiments. For a more complete introduction to the quantum and mathematical background behind ESR experiments, the reader is referred to Carrington and McLachlan<sup>1</sup> or Weil and Wertz.<sup>2</sup>

Electron Spin Resonance (ESR) spectroscopy is used to detect species that contain unpaired electrons, e.g. free radicals. ESR spectroscopy is particularly useful for the study of free radical polymerizations, since in principle the structure and concentration of the radical species can be observed and determined through careful calibration.<sup>3</sup>

The hyperfine structure of the ESR spectrum is a valuable source of information. Magnetic nuclei, especially protons, which are close to the unpaired electron, will couple to the electron's spin states. This leads to splitting of energy levels, leading to hyperfine couplings. The hyperfine couplings provide information regarding the positions, orientations, and dynamics of the magnetic nuclei with respect to the unpaired electron, which can often be used to infer the local structure of the paramagnetic species. This will be further discussed in section 3.1.3.

### 3.1.1 Basic ESR Principles

ESR spectroscopy works by the coupling of microwave radiation with the spin of the unpaired electron in an applied magnetic field. Typically, a magnetic field is applied to a sample, which splits the energy levels of the unpaired electron. This splitting allows microwave radiation to be absorbed at a resonant frequency. Coupling of the electron's spin to nearby magnetic nuclei further splits the energy levels (hyperfine coupling), causing several distinct resonant frequencies, resulting in a number of resonance lines being observed in the ESR spectrum. The number, relative positions, and widths of these lines yield valuable information regarding the paramagnetic species.

The energy levels of an electron in a magnetic field of strength,  $B$ , (Figure 3.1) are given by

$$E_{m_s} = g_e \mu_B m_s B \quad m_s = \pm \frac{1}{2} \quad (3-1)$$

where  $g_e = 2.0023$  (the  $g$ -factor of an electron),  $\mu_B$  the Bohr magneton and  $m_s$  the orientation of the electron's spin angular momentum. This equation shows that the energy of an electron in the  $\alpha$  state ( $m_s = +\frac{1}{2}$ ) increases and the energy of an electron in the  $\beta$  state ( $m_s = -\frac{1}{2}$ ) decreases as the field is increased, and that the separation of the levels is

$$\Delta E = E_{\alpha} - E_{\beta} = g_e \mu_B m_s B \quad (3-2)$$

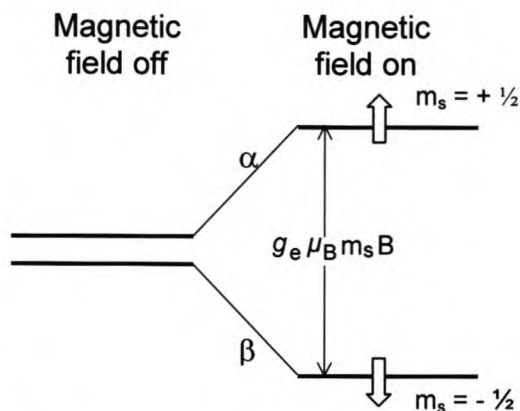


**Figure 3.1** Electron spin levels in a magnetic field. Note that  $\alpha$  and  $\beta$  are the excited and ground states of the electron respectively. Resonance is achieved when the frequency of the incident radiation matches the frequency corresponding to the energy separation.

When the sample is exposed to electromagnetic radiation of frequency  $\nu$ , the resonant absorption occurs when the resonance condition

$$h\nu = g_e \mu_B B \quad (3-3)$$

is met. Here  $h$  is the Planck constant. In ESR spectroscopy, the molecules containing unpaired electrons are detected by observing the magnetic fields at which they resonate with monochromatic (typically microwave frequency) radiation. A magnetic field of about 0.3 T (the value used for most X-band ESR spectrometers) corresponds to resonance with an electromagnetic field of frequency 10 GHz ( $10^{10}$  Hz) and wavelength 3 cm. Because 3 cm radiation falls in the X-band of the microwave region of the electromagnetic spectrum, ESR is a microwave technique.

Thus, the ESR experiment detects species containing unpaired electrons. When the resonance condition is met (equation 3-3), a transition occurs, with a characteristic  $g$ -value. The resonance line may be further split due to hyperfine interactions with nearby magnetic nuclei. Many of the underlying principles are common to both NMR and ESR spectroscopy, since these are both different manifestations of magnetic resonance. Thus, an understanding of NMR spectroscopy forms a basis for an understanding of the principles behind ESR spectroscopy. Some of the useful information that may be obtained from the interpretation of ESR spectra will be discussed in the following sections, after a discussion of the basics of the ESR instrument.

The layout of a typical ESR spectrometer is shown in Figure 3.2. The main features are a microwave source (a klystron), a cavity into which the sample is inserted in a quartz tube, a microwave detector, and an electromagnet with a field that can be varied in the region of 0.3 T (for the X-band region). The magnet produces the oscillating magnetic field responsible for inducing the transitions in the electron's spin state. During the ESR experiment, a sample is placed inside the cavity, and a strong magnetic field is applied in

the z-direction. An oscillating field in the microwave region is applied to the sample in the x-direction, which induces transitions between the allowed spin states when the resonance condition is met.

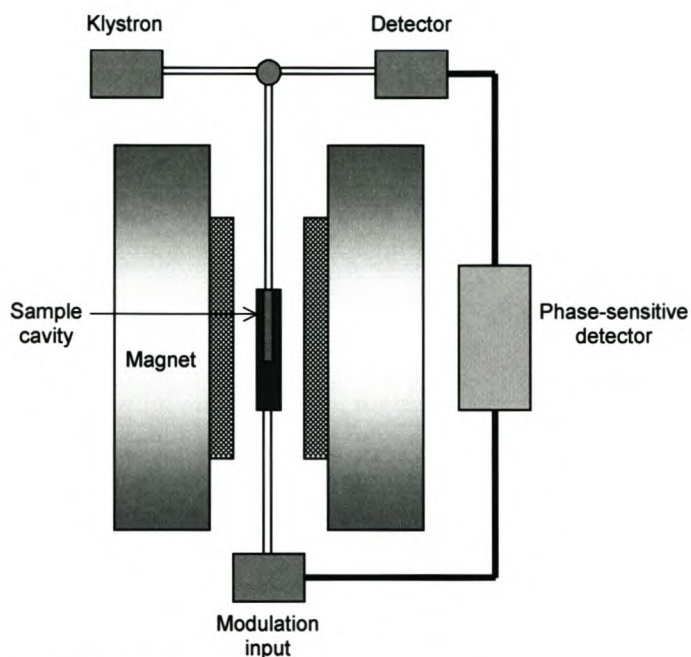


**Figure 3.2** The basic layout of a continuous wave ESR spectrometer.

The applied magnetic field is varied between the minimum to maximum value across the sweep width at a constant rate, and the absorption of microwave power is observed as a function of magnetic field strength. A typical spectrum of an intermediate RAFT radical (observed in these studies) is given in Figure 3.3.

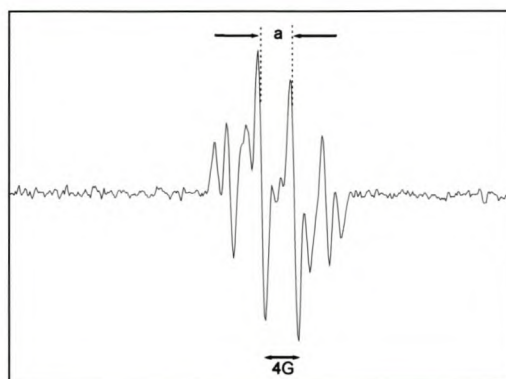


**Figure 3.3** The ESR spectrum of the RAFT intermediate radical observed in this study. *a* is one of the hyperfine splittings of the spectrum; the center of the spectrum is determined by the *g*-value of the radical.

The peculiar appearance of the spectrum, which is in fact the first derivative of the absorption, arises from the detection technique, which is sensitive to the slope of the absorption curve (Figure 3.4) when a low modulation amplitude is used.

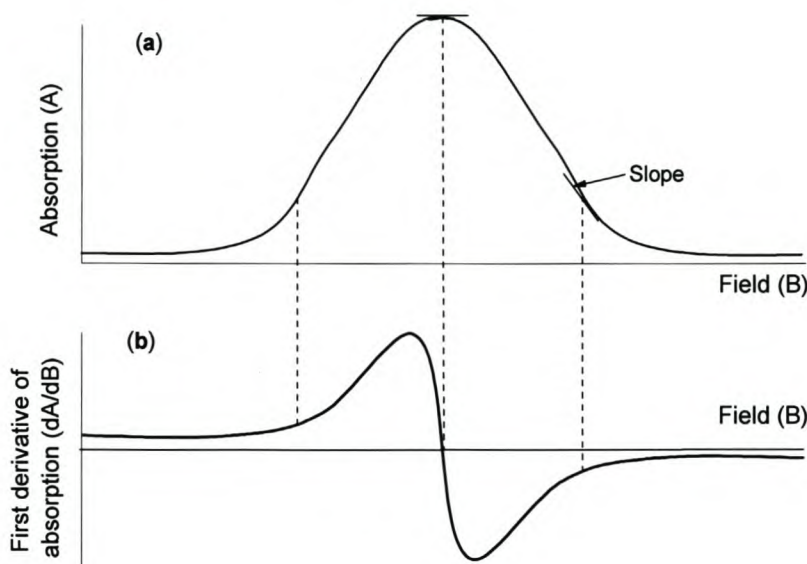


**Figure 3.4** When phase-sensitive detection is used, the signal is the first derivative of the absorption intensity. (a) The absorption; (b) the signal, the slope of the absorption signal at each point.

Many factors may affect the observed signal intensity, some of which are discussed in sections 3.2.4 and 3.2.5. Other instrumental factors may also affect the response of the detector. The most important of these are the absorption of microwave power by parts of the sample (or the cavity) other than the radical species of interest, and the inherent sensitivity of the cavity. The absorption of microwave radiation in the cavity may lead to a reduction in overall signal intensity, or to spurious signals (possibly due to contamination in the cavity). Both of these factors can be eliminated or their effects reduced by subtraction of background spectra (recorded with an empty sample tube) from the standard and unknown spectra.

The absorption of microwave radiation by other parts of the sample might be due to the solvent. This can be allowed for by calibration with standards in the same solvent as the unknown (when aqueous systems are used this step is essential). The material from which the ESR tubes are constructed is chosen such that minimal absorption of microwave radiation occurs. However, spurious signals due to impurities in the tubes are sometimes observed, and it is generally recommended that ESR spectra to be used for comparison (and appropriate backgrounds/standards) should be recorded in the same tubes whenever possible.

The final consideration here is the inherent sensitivity of the cavity. The sensitivity of the cavity (Q-factor) is mostly dependent on the size and geometry. Cavities with high Q-factors are usually preferable for quantitative studies of free radical polymerizations, since the propagating radical concentrations are often very small.

### 3.1.2 The $g$ -value

As in NMR, the spin magnetic moment interacts with the local magnetic field, so the resonance condition can be written

$$h\nu = g_e \mu_B B_{loc} = g_e \mu_B (1 - \sigma) B \quad (3-4)$$

where  $B_{loc}$  is the local magnetic field and  $\sigma$  the dimensionless shielding constant. However, in ESR it is conventional to write  $g = (1 - \sigma)g_e$ , where  $g$  is the  $g$ -value of the radical or complex. Then the resonance condition is

$$h\nu = g \mu_B B \quad (3-5)$$

The deviation of  $g$  from  $g_e = 2.0023$  depends on the ability of the applied field to induce local electron currents in the radical, and therefore its value gives some information about electronic structure. However, because  $g$ -values differ very little from  $g_e$  in many radicals, its main use in chemical applications is to aid in the identification of the species in the sample.

### 3.1.3 Hyperfine Coupling

Most radical species also contain nearby magnetic nuclei (those with non-zero spin, such as the proton). The nearby magnetic nuclei perturb the electron's magnetic dipole. This leads to the phenomenon known as hyperfine coupling, which is the interaction between the electron's spin and the spins of the nearby magnetic nuclei (usually protons). This coupling is responsible for most of the structure observed in ESR spectra, since each magnetic nucleus' spin may have more than one orientation with respect to the electron's spin. This causes a splitting of the electron's energy levels, leading to a splitting of the ESR signal. The hyperfine coupling constants are an important source of structural information in the vicinity of the unpaired electron. The hyperfine couplings can give information regarding the electron spin density at the nuclei, the number and nature of nearby magnetic nuclei, and the orientation of the nuclei with respect to the unpaired spin.

### 3.1.4 Instrumental Factors Influencing the ESR Spectrum

The intensity and appearance of an ESR spectrum can be affected by several factors. The most obvious of these is the structure of the radical species itself. However, other factors such as the environment of the species, the temperature, relaxation rates, and instrumental factors may also have an effect on the appearance of the spectrum. The following discussion is to illustrate the importance of choosing the correct instrumental variables when qualitative, and especially quantitative, ESR work is done.

The ESR signal observed during an ESR experiment is due to microwave-induced transitions and subsequent relaxations. There are a number of mechanisms by which relaxation can occur. The spin-lattice relaxation mechanism has the strongest effect on the signal intensity. The ESR signal is strongly dependent on the transition probability

$$\frac{dE}{dt} = n_0 \Delta E \frac{P}{1 + 2PT_1} \quad (3-6)$$

where  $\frac{dE}{dt}$  is the rate of microwave energy absorption,  $n_0$  the population difference between the electron's spin states at thermal equilibrium,  $\Delta E$  the energy difference between the states,  $T_1$  the spin-lattice relaxation time and  $P$  the transition probability per spin. The transition probability is proportional to the square of the amplitude of the microwave field, so in the unsaturated regime, the rate of absorption of microwave energy is proportional to the square of the amplitude of the microwave field strength.

At low microwave powers, the transition probabilities are proportional to  $H_1^2$  (the applied field strength) and to the corresponding microwave power, since the microwave power is proportional to the square of the applied field:

$$P_1(\omega) = \frac{1}{2} \pi \gamma^2 H_1^2 g(\omega) \quad (3-7)$$

where  $P_1(\omega)$  is the first-order transition probability (note that  $P_1$  and  $P$  can be interchanged here, since second-order transition contributions to the transition probability are usually negligible),  $\gamma$  is the magnetogyric ratio,  $H_1$  the applied magnetic field, and  $g(\omega)$  is the general lineshape function. Saturation results at higher microwave powers (where  $2PT_1$  is comparable to unity) as the rate of absorption of microwave energy is no longer proportional to the applied microwave power. An expression, in terms of half saturation power for the integrated signal intensity, can be derived:<sup>4</sup>

$$\text{signal} \propto \frac{\sqrt{P}}{(1 + P/P_{1/2})^{1/2}} \quad (3-8)$$

where  $P_{1/2}$  is the half saturation power, and  $P$  is the microwave power.

Usually, experiments are carried out at low microwave powers, to avoid saturation, since the response is then no longer linear with the square root of applied power. This region can be determined experimentally by plotting the intensity of the transition versus the square root of microwave power (see Figure 3.5). Experiments are usually carried out in the linear region of this plot, once this region has been experimentally determined.

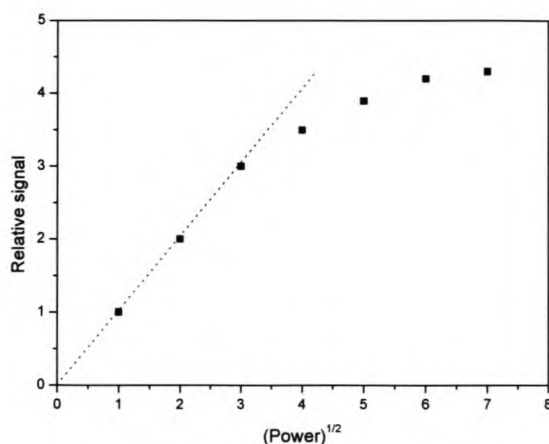


**Figure 3.5** Idealised plot of relative signal intensity versus square root microwave power. The dashed line (----) indicates the approximately linear region at low powers.

Another factor resulting from power saturation is the possible distortion of the lineshape. In qualitative studies, this might lead to possible misinterpretation of the spectra.

### 3.1.5 Quantitative ESR Spectroscopy

ESR spectroscopy was used to determine the concentration of the intermediate RAFT radicals. In this study this was done by taking the double integral (the observed ESR spectrum is usually a first derivative of the absorption spectrum) of the signals for an experimental spectrum of unknown radical concentration and comparing the value obtained to that of a standard of known concentration. Unfortunately, quantitative measurements of radical concentrations via ESR spectroscopy are quite prone to error.<sup>3</sup> The most important of these are discussed below.

An ESR spectrum is a representation of all of the radical species present in a sample. Therefore, care should be taken when integrating over a specific region that there are no other signals other than that due to the species of interest. Integration of signals due to species other than those of interest will lead to incorrect apparent concentrations.

When measuring the standard and unknown spectra, the experimental conditions should be identical. This includes instrumental factors such as microwave power level, modulation amplitude and the cavity temperature. To avoid systematic errors, the spectra of the unknowns and the standards should both be recorded in the unsaturated regime. Selection and preparation of standards for ESR spectroscopy is also important. The standard species should be prepared in a similar way and under a similar environment to that of the unknown species. The concentrations should be in a similar range, and should be measured in a similar (or better, the same) solvent, such that relaxation rates and dielectric signal loss due to solvent is essentially the same.

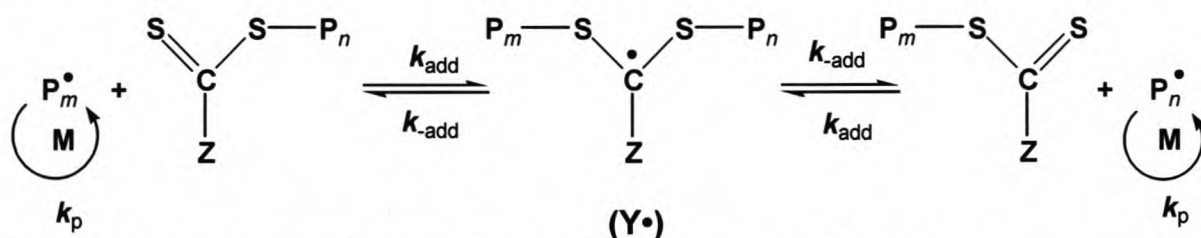
In order to use the obtained spectra in accurate qualitative measurements, the spectra of both the unknown and standard species should have appropriate background spectra (recorded under the same instrumental and experimental parameters) subtracted before use in quantitative work. This is particularly important when possible impurities exist in the cavity or the ESR tube, where the double integral of the background across the unknown spectrum's width may yield a significant apparent concentration. This could lead to significant errors in the determination of the concentration of the unknown species. The background-corrected spectra should be checked to see that the corrected background is indeed flat. Sometimes, the baseline may appear to be sloping or curved, and the integration process will then yield incorrect results. This can usually be checked by inspection of the first integral of the baseline-corrected spectrum. The integral should appear as a clearly-defined absorption spectrum, with no part dropping below the baseline. If the ESR spectrum appears to be symmetrical, the height above the baseline of the baseline-corrected first integral should be symmetrical.

To conclude, the correct calibration of the ESR instrument is essential for use in quantitative work, or substantial errors may occur. However, if appropriate precautions are taken, it is possible to use ESR spectroscopy to accurately measure the concentrations of radicals.

### 3.1.6 ESR Applications to RAFT Polymerization

Electron spin resonance (ESR or EPR) spectroscopy provides valuable information regarding the structure and close environment of free radicals, which is extremely useful in free radical polymerization reactions.<sup>5-12</sup> Careful calibration enables measurement of accurate concentrations of all detectable radical species present, including the propagating radical. This technique has been used to obtain propagation rate coefficients for free radical polymerizations of some monomers that are in excellent agreement with IUPAC-accepted values,<sup>3,13</sup> thus establishing the quantitative reliability of measuring free radical concentrations via ESR spectroscopy. However, some researchers,<sup>14-16</sup> when utilizing ESR spectroscopy to determine propagation rate coefficients, have not obtained such agreement because of technique problems and unwarranted assumptions. Thus, to avoid such problems in this study, the guidelines given by Tonge *et al.*,<sup>3</sup> were strictly followed.

The core reactions in RAFT polymerization are in the addition-fragmentation equilibrium process (Scheme 3.1).<sup>17</sup> This process allows the rapid redistribution of radical activity between growing chains, and thus control of their molar mass.



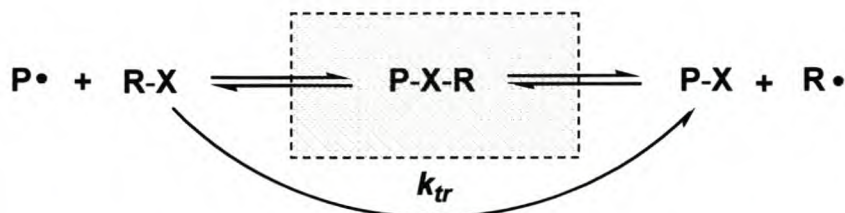
**Scheme 3.1** The central equilibrium of the reversible addition-fragmentation chain transfer (RAFT) process.

According to Scheme 3.1, the RAFT process involves a propagating radical  $P_m^\bullet$  that undergoes addition (with rate constant  $k_{\text{add}}$ ) to a dormant species  $P_n\text{-X}$  to form an intermediate radical ( $Y^\bullet$ ) followed by the fragmentation (with rate constant  $k_{\text{add}}$ ) to form another propagating radical  $P_n^\bullet$  and a dormant species  $P_m\text{-X}$ .

At first glance, the RAFT process would appear to be an ideal candidate for ESR studies, since the propagating radical concentration ( $c_P$ ) is usually very low, and the intermediate radical concentration ( $c_Y$ ) is expected to be high, according to simulations done by Barner-Kowollik *et al.*<sup>15</sup> Few studies to date have carefully examined the RAFT process by ESR spectroscopy. Hawthorne *et al.*<sup>16</sup> was the first to prove the existence of the intermediate radical species, thereby confirming the RAFT mechanism proposed by Rizzardo *et al.*<sup>17</sup> Systems containing cumyl dithiobenzoate with n-butyl acrylate, styrene and n-butyl methacrylate were investigated. Signals corresponding to the intermediate radicals of the first two monomers could be detected, and estimations could be made for their concentrations. No ESR signals could be detected for the system with n-butyl methacrylate as monomer. This was attributed to a fast rate of fragmentation of the intermediate radicals for this monomer. In all cases propagating radicals could not be detected, implying that  $c_P$  is much lower than  $c_Y$ . Laus *et al.*<sup>18</sup> and Du *et al.*<sup>19</sup> also used ESR spectroscopy to detect and identify the intermediate radical species in systems with novel RAFT agents. A benzyl (diethoxyphosphoryl) dithioformate RAFT agent enabled Alberti *et al.*<sup>20</sup> to detect (via ESR spectroscopy) several radical species corresponding to various different intermediate radicals formed during the early stages of the polymerization reaction. Utilizing ESR simulations based on a Monte Carlo minimization procedure, Alberti *et al.*<sup>20</sup> made estimations of the various intermediate radicals' concentrations. Their findings were in agreement with the generally accepted mechanism of the RAFT process.

According to the original RAFT mechanism proposed by Rizzardo *et al.*<sup>21</sup> (see Chapter 1, Scheme 1.5) the RAFT mechanism does not influence the propagating radical concentration. Thus, the rate of polymerization should be similar to a system that is not mediated by an added RAFT agent.

Therefore, as a first approximation, the RAFT mechanism can be treated as a degenerate transfer reaction, to which classical polymerization kinetics apply (Scheme 3.2). A macroradical ( $P^\bullet$ ), reacts with a chain transfer agent  $R\text{-X}$ , during which the end group originating from the transfer agent ( $X$ ) is exchanged between the two chains. A new transfer agent ( $P\text{-X}$ ) is formed and a propagating radical ( $R^\bullet$ ) liberated.



**Scheme 3.2** Schematic representation of considering the RAFT process as a degenerative transfer process. The formation of intermediate radicals (inside dotted box) is effectively ignored by this approach.

This treatment does not consider the addition-fragmentation transfer process or the formation of intermediate radicals. If it is assumed that all chains are of equal length (often not a bad assumption for controlled radical polymerization processes), then “classical” kinetics can be used to predict the propagating radical concentration and the rates of reaction from the rate of initiator decomposition and average termination rate coefficients. The differential equation describing the propagating radical concentration would then be given by:

$$\frac{dc_P}{dt} = 2fk_d c_I - \langle k_t \rangle c_P^2 \quad (3-9)$$

where  $c_I$  and  $c_P$  are the initiator and propagating radical concentrations,  $f$  the initiator efficiency,  $k_d$  the rate coefficient for initiator decomposition, and  $\langle k_t \rangle$  the average termination rate coefficient. If steady state in  $c_P$  is assumed and the resulting quadratic equation solved,  $c_P$  is given by:

$$c_P = \sqrt{\frac{2fk_d c_I}{\langle k_t \rangle}} \quad (3-10)$$

According to equation 3-10, the propagating radical concentration, and thus the rate of polymerization, is only dependent on the rate of initiator decomposition and the average termination rate coefficients. One of the problems of this approach is that it is unable to explain inhibition and rate retardation phenomena observed in cumyl dithiobenzoate RAFT agent mediated systems (see Figure 3.6).

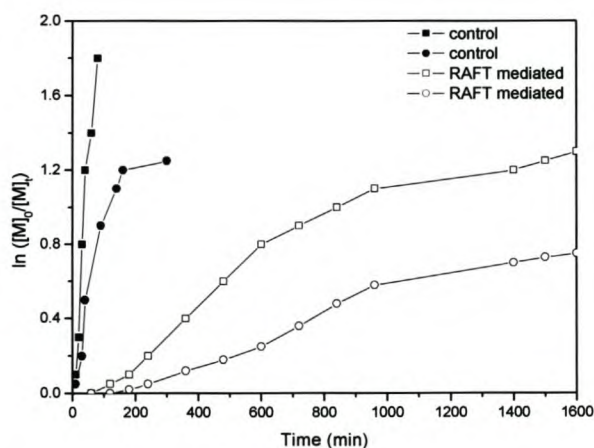


**Figure 3.6** Plot indicating the differences in reaction rates of typical RAFT mediated reactions (○:  $4.11 \times 10^{-3}$  M AIBN, 4.30 M styrene, 5.68 M benzene,  $9.17 \times 10^{-3}$  M cumyl dithiobenzoate; □:  $2.13 \times 10^{-3}$  M AIBN, 4.56 M styrene, 4.73 M benzene,  $9.87 \times 10^{-3}$  M cumyl dithiobenzoate) and their respective control reactions, (●:  $4.01 \times 10^{-3}$  M AIBN, 4.45 M styrene, 5.03 M benzene; ■:  $2.16 \times 10^{-3}$  M AIBN, 4.64 M styrene, 4.78 M benzene) polymerized at 70 °C. Data was obtained through gravimetry.

These phenomena are inconsistent with the “classical” proposed RAFT mechanism. Obviously, some amendments to the original proposed RAFT mechanism are needed, to explain the observed unusual

phenomena. Perhaps, the biggest question is whether the intermediate radicals undergo termination (or other) reactions, and if so, how frequently this occurs.

There is currently debate in the literature regarding the fate of the intermediate radicals ( $Y^*$ ), and the equilibrium between propagating ( $P^*$ ) and intermediate radicals.<sup>15,22-28</sup> Currently, there are two main schools of thought on the fate of the intermediate RAFT radical and thus the cause of observed rate retardation and inhibition in certain RAFT systems. Barner-Kowollik and coworkers<sup>15,29-33</sup> has put evidence forward for a relatively long lifetime of the intermediate radicals in cases in which a high stabilization of such radicals is possible (i.e. lifetime in the order of seconds) and for a possible reversible cross-termination reaction of the intermediate radicals with themselves or with propagating chains.<sup>34,35</sup> Monteiro and coworkers<sup>26,27,36</sup> argue that the lifetimes of the intermediate radicals are actually short and that cross termination reactions occur irreversibly and are the cause for the observed rate retardation. The resulting estimations of the rate coefficients for the addition and fragmentation processes for the same RAFT agent and monomer combinations differ greatly as a consequence.<sup>25,26,30,36,37</sup> Understanding of this equilibrium between propagating and intermediate radicals is key to understanding the possibilities and limitations of the RAFT process.

To date, there has been only one ESR spectroscopy study to investigate the fate of the intermediate radicals and the equilibrium between propagating and intermediate radicals. Kwak *et al.*<sup>26</sup> carefully examined RAFT polymerization by ESR spectroscopy, utilizing both the intermediate radical concentration and kinetic data to model the process. Results based on the developed model indicated that fragmentation of the intermediate radical is a fast process and that intermediate radicals undergo cross-termination to form 3-arm star chains, thus causing rate retardation. The rate constant for the cross termination reaction was also estimated. Kwak *et al.* also showed the formation of the 3-arm star termination product to occur by means of an independent model experiment.

In this chapter, the concentration of the intermediate radicals and the time evolution of the intermediate radical concentration have been investigated. This was done in an attempt to gain an understanding of the equilibrium between propagating and intermediate radicals and to pose possible explanations for the fate of the observed intermediate radicals.

## 3.2 Experimental

### 3.2.1 Chemicals

#### Chemicals used

Styrene and butyl acrylate monomer (Plascon Research Centre, University of Stellenbosch, estimated purity for both monomers ~99%  $^1\text{H}$  NMR) was washed with 0.3 M KOH, and distilled under vacuum prior to use, to remove inhibitor and polymer. Azo bis(isobutyronitrile) (AIBN, Riedel De Haen), was recrystallized from AR grade methanol and found to be ~99% pure by  $^1\text{H}$  NMR. Benzene (AR grade, Sigma-Aldrich) was used as received.

#### Synthesis of transfer agents

The synthesis of cumyl dithiobenzoate (CDB) was carried out according to the method of Le *et al.*<sup>21</sup> The RAFT agent was purified by successive liquid chromatography on silica and alumina using hexane as eluent. The product crystallized after vacuum removal of solvent and storage below  $-10\text{ }^\circ\text{C}$ . The purity was estimated by  $^1\text{H}$  NMR to be  $> 98\%$ . Cumyl phenyl dithioacetate (CPDA) was prepared according to the method of Quinn *et al.*<sup>38</sup> The product obtained was concentrated and crystallized from cold methanol.  $^1\text{H}$  NMR purity was estimated to be at 99%. S-1-Dodecyl-S'-(R,R'-dimethyl-R-acetic acid) trithiocarbonate (DIBTC) was prepared by James McLeary (University of Stellenbosch) according to the method of Lai *et al.*<sup>39</sup> The purity was estimated by  $^1\text{H}$  NMR to be  $> 99\%$ .

### 3.2.2 Sample Preparation

The compositions of the solutions used for ESR analysis are given in Table 3.1. A typical ESR spectrometry reaction mixture was prepared as follows. The RAFT agent and AIBN were dissolved in a benzene and monomer solution. An aliquot (0.2 g) of the solution was transferred to an ESR tube and oxygen removed by flushing with ultra-high purity nitrogen for 10 min. For solutions 6 to 10 (Table 3.1) oxygen was removed by multiple freeze-thaw cycles. The tube was sealed and transferred to the ESR cavity, which had been pre-heated to the reaction temperature.

**Table 3.1** Composition of reaction mixtures for in situ ESR analysis. (AIBN = 2,2' (azobis(isobutyronitrile), St = styrene, BA = butyl acrylate, CDB = cumyl dithiobenzoate, CPDA = cumyl phenyl dithioacetate, DIBTC = dibenzyl trithiocarbonate, concentrations are given in mol/L.)

No	Solvent	Initiator	Monomer		RAFT agent		[M] <sub>0</sub> / [R] <sub>0</sub>	[R] <sub>0</sub> / 2[I] <sub>0</sub>
	(Benzene)	(AIBN)	Type	Conc	Type	Conc ( $\times 10^2$ )		
	Conc	Conc ( $\times 10^2$ )						
1	5.68	4.11	St	4.30	CDB	9.17	4.69	11.2
2	5.67	8.00	St	4.31	CDB	18.2	2.37	11.4
3	5.71	16.2	St	4.28	CDB	36.3	1.18	11.2
4	5.74	40.5	St	4.25	CDB	90.6	0.47	11.2
5	5.65	4.02	BA	4.25	CDB	9.10	4.67	11.3
6	5.70	4.30	St	4.29	CPDA	9.17	4.67	10.7
7	5.68	4.09	BA	4.24	CPDA	9.08	4.67	11.1
8	5.70	4.13	St	4.29	DIBTC	9.24	4.64	11.2
9	5.66	4.06	BA	4.25	DIBTC	9.05	4.70	11.2
10	5.64	0.375	BA	4.26	CDB	1.01	42.02	13.5

### 3.2.3 ESR Equipment

Two types of ESR equipment were used to record the ESR spectra. The first was a Bruker EMX spectrometer with an ER4102 cavity. The second (after an equipment upgrade) was a Bruker ELEXSYS E 500 EPR spectrometer equipped with a microwave bridge with super X feature and frequency counter, controlled by a LINUX based workstation. The cavity used was a Bruker ER4122SHQ super high Q X-band cavity. For both cases, the cavity temperature was controlled by a modified Bruker B-VT 1000 temperature controller with a 100 K to 373 K range. This was achieved by heated nitrogen (from the temperature controller) flowing into the ESR cavity, the flow being regulated by the temperature controller and the temperature by a thermocouple situated at the bottom of the heated cavity. The temperature controller and thermocouple were calibrated by measuring the temperature of the cavity (at the sample tube position) with a digital thermometer. With both spectrometers the spectra were recorded in the X-band region, with the cavity pre-heated to the reaction temperature.

In situ experiments of solutions 1 - 5 and 10 were run on the older Bruker EMX spectrometer, while solutions 6 - 9 were run on the upgraded Bruker ELEXSYS E 500 EPR spectrometer.

### 3.2.4 ESR Parameters

The magnetic field was modulated at 100 kHz, with amplitude between 1 and 5 G. Experiments were carried out at low microwave powers, to avoid saturation, since the response is then no longer linear with the square root of applied power (see section 3.1.4, equation 3-8). This region was experimentally determined by plotting the value of the double integral of the obtained ESR spectrum of the intermediate radical, in benzene as solvent under reaction conditions, versus the square root of microwave power (see Figure 3.7). Duplicate reactions were carried out at both 70 and 90 °C, with the result of the 70 °C experiments given in Figure 3.7. Experiments were carried out with a microwave power of 2 mW (well below saturation) that falls within the linear region of this plot.

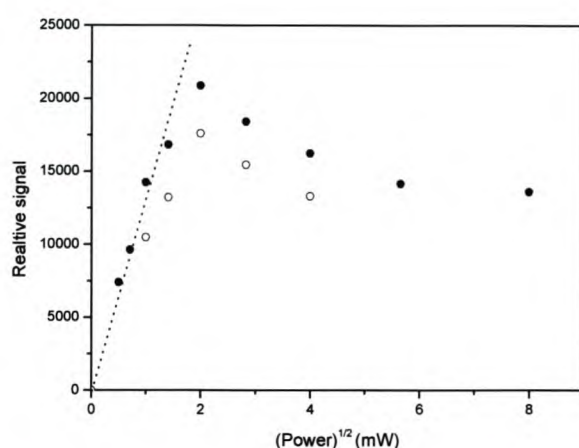


**Figure 3.7** Plot of relative signal intensity (due to intermediate radicals) versus square root microwave power for the duplicate reactions (● and ○) carried out at 70 °C. The first set of experiments (●) was performed after 5 min equilibration at 70 °C, the second set (○) after equilibrating for 30 min at 70 °C. A magnetic field of 100 kHz was used, together with a modulation amplitude of 1G, with a 81.92 ms time constant and 83.89 s sweep time. The dotted line (---) indicates the linear region for the first set of experiments (●).

For the time evolution studies of the intermediate radical concentration, spectra were recorded as single 1 min scans (with conversion time constants of 81.92 ms, sweep time of 83.89 s and modulation amplitude of 1 G) every 3 minutes for the first hour and then every 5 minutes for the remainder of the time. Spectra were adjusted by subtraction of cavity scans under identical conditions. To detect the propagating radicals in some reactions, the modulation amplitude was increased to 2 G, and 4 or 16 single scans (with sweep time of 83.89 s) accumulated for each spectrum. Concentrations were obtained by double integrals of the ESR signal and compared with a range of 2,2,6,6-tetramethylpiperidinyl-1-oxy (TEMPO) standards recorded under similar reaction conditions.

### 3.2.5 ESR Calibration

The ESR system was calibrated with a series of TEMPO standards ( $10^{-5}$  –  $10^{-8}$  M) in benzene, under the reaction conditions at 70 and 90 °C. The concentration range for the TEMPO standards was selected to be similar to that expected for the intermediate RAFT radical concentrations. Careful integration of the obtained

radical spectra, by means of techniques of a previous quantitative ESR study<sup>3</sup> (see section 3.1.5), was used to calculate the intermediate radical concentrations. The background spectra, obtained from recording ESR spectra of an empty ESR tube under reaction conditions, were subtracted from the obtained ESR spectra of the TEMPO standards. The baselines of the background-corrected spectra were then corrected, to yield a flat baseline. The resulting spectra were then subjected to double integration to obtain the concentrations of the TEMPO standards.

### 3.2.6 SEC Analysis

Molar masses were determined using size-exclusion chromatography (SEC). The SEC instrument consisted of a Waters 717 plus auto sampler, Waters 600E System Controller (run by Millennium 32 V3.05 software) and a Waters 610 fluid unit. A Waters 410 differential refractometer was used at 30 °C as detector. Tetrahydrofuran (THF, HPLC-grade) sparged with IR-grade helium was used as eluent at a flow rate of 1 mL min<sup>-1</sup>. Sample acquisition time was 30 minutes per sample. The column oven was kept at 30 °C and the injection volume was 100 µL. Two PL gel mixed C columns were used in series. The system was calibrated using 10 polystyrene narrow molar mass standards in the range of 580 – 2 000 000 g mol<sup>-1</sup>. All molar masses are reported as polystyrene equivalents.

### 3.3 Initial ESR Spectroscopy Investigations of the Intermediate RAFT Radical

As mentioned in section 3.1.6, the rate coefficient for fragmentation of the formed intermediate radicals (i.e. intermediate radical lifetimes) and the fate of the intermediate radicals are currently under debate.<sup>18,25,27,29</sup> The resulting estimations for the rate coefficients for fragmentation by the various groups for the same RAFT and monomer combinations consequently differ by six orders of magnitude.<sup>29,33,39</sup> Understanding of this equilibrium between propagating and intermediate radicals is key to understanding the possibilities and limitations of the RAFT process.

The central exchange reactions in Scheme 3.1 imply equilibrium between intermediate and propagating radicals, with an equilibrium coefficient ( $K_{\text{eq}}$ ) determined by the relative rates of addition of propagating radicals to RAFT-capped chains and fragmentation of the formed intermediate radicals.<sup>29</sup>

$$K_{\text{eq}} = \left( \frac{c_Y}{c_P c_{PX}} \right) = \left( \frac{k_{\text{add}}}{k_{-\text{add}}} \right) \quad (3-11)$$

Here  $k_{\text{add}}$  and  $k_{-\text{add}}$  are the rate coefficients for addition of a propagating radical to a RAFT agent and fragmentation of the formed intermediate radical;  $c_Y$  and  $c_P$  are the concentrations of the intermediate and propagating radicals respectively; and  $c_{PX}$  is the concentration of RAFT-capped chains.  $c_{PX}$  may be approximated by the initial RAFT agent concentration, since  $c_Y$  is negligibly small ( $\sim 10^{-7}$  M) compared to the initial RAFT agent concentration ( $9 \times 10^{-2}$  M). According to equation (3-11),  $K_{\text{eq}}$  should be constant for a particular RAFT agent and monomer combination at a particular temperature, and independent of other conditions.

To find the value for  $K_{\text{eq}}$  and to test the validity of the above statements,  $c_Y$  and  $c_P$  (and their ratio) were examined by ESR spectroscopy and solution polymerization of an AIBN initiated system, containing styrene as monomer and cumyl dithiobenzoate (CDB) as RAFT agent, in benzene at 70 and 90 °C.

ESR measurements were performed on sealed ESR tubes containing degassed solutions 1, 2, 3 and 4 (Table 3.1). The sample preparation, ESR reaction procedures, reaction parameters and calibration of the observed ESR signals are described in section 3.2. Reactions were run *in situ* at 70 and 90 °C for solutions with progressively lower monomer to RAFT agent concentrations, while keeping the ratio of RAFT agent to initiator concentrations (= 0.56) constant. To maximize the ESR signal intensities, high initiator (and RAFT agent) concentrations were used, resulting in chains with low  $\overline{M}_n$  (typically < 2 000). ESR spectra were recorded at 3 min intervals. The concentration of the intermediate radical (which includes the contribution due to the signal of any underlying propagating radicals in this region) was measured by double integration of the background-corrected ESR signal of the intermediate radical, and comparison with the TEMPO

calibration. Corresponding kinetic reactions were run for the *in situ* ESR reactions. Solutions, with similar compositions to those used in the ESR experiments, were prepared, degassed by bubbling N<sub>2</sub> through for 10 min, and transferred to glass aliquots under a N<sub>2</sub> atmosphere. The aliquots were sealed and reacted in an oil bath at the different temperatures. At specified time intervals, the aliquots were taken out of the oil bath, quenched in ice and dried at 40 °C under vacuum for 12 h. The samples were used for gravimetric (conversion) and SEC analysis ( $\overline{M}_n$ ).

The observed ESR signal was similar to those observed in previous studies,<sup>16,26</sup> with the same *g*-factor and hyperfine splittings as those reported by Hawthorne *et al.*<sup>16</sup>

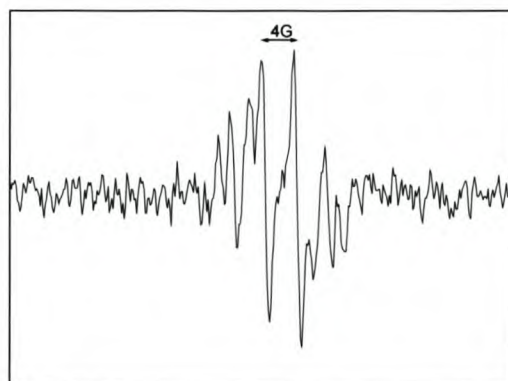


**Figure 3.8** ESR spectrum of the intermediate radical observed in the polymerization of styrene with CDB, and AIBN in benzene at 90 °C. A magnetic field of 100 kHz was used, together with a modulation amplitude of 1G, with a 81.92 ms time constant and 83.89 s sweep time.

A typical concentration-time profile of the intermediate radicals for solution 1 ( $4.11 \times 10^{-2}$  M AIBN, 4.30 M styrene, 5.68 M benzene and  $9.17 \times 10^{-2}$  M cumyl dithiobenzoate) at 90 °C is shown in Figure 3.9. In all of the reactions,  $c_Y$  was initially too low for direct observation in the ESR spectra, but could be detected when examining the first integrals of the spectra in the appropriate region. This initial period in which no  $c_Y$  could be detected, varied in length depending on the cavity temperature and concentrations of the reactants used. This will be discussed to some extent in this chapter, but an in depth discussion will be given in Chapter 5. The  $c_Y$  increased (to observable concentrations) with time to a maximum ( $\sim 10^{-6}$  M), followed by a very slow decrease corresponding to the relative decrease in square root of radical flux (initiator decomposition). The observed decrease in  $c_Y$  corresponding to the decrease in square root radical flux can be explained by at least two possible rationales. If, after a maximum in  $c_Y$  is reached, and the RAFT system is in a steady state equilibrium, the intermediate radical concentration ( $c_Y$ ) and the propagating radical concentration ( $c_P$ ) will be in rapid equilibrium with each other according to equation 3-11. As  $K_{eq}$  is a constant at steady state,<sup>26</sup> and  $c_{PX}$  (the concentration of the chains with RAFT end groups) is constant, the ratio of  $c_Y$  to  $c_P$  must be constant. As  $c_P$  is proportional to the square root of initiator decomposition (equation 3-10), so will  $c_Y$  be.

Thus, a decrease in square root of radical flux will be seen as a decrease in  $c_p$  and thus also a proportional decrease in  $c_Y$ .

A possible second explanation is that the RAFT system has not yet attained steady state equilibrium after a maximum in  $c_Y$  is reached. The decrease in  $c_Y$  will thus correspond to an increase in the average degree of polymerization of the system. The rate of increase of the average degree of polymerization is proportional to the rate of polymerization, which in turn is proportional to the square root of initiator decomposition. Again, a decrease in square root radical flux will be seen as a proportional decrease in  $c_Y$ .

The propagating radical concentration under all tested conditions was too low to be directly observed with the Bruker EMX spectrometer. Wider sweeps (up to 200 G width) at a wide range of modulation amplitudes and power levels showed no significant broad or narrow signals other than the observed intermediate radical. However, in reactions performed on the (more sensitive) Bruker ELEXSYS E 500 spectrometer, using higher modulation amplitudes (2 G) and accumulating at least 4 scans for each spectrum, signals due to propagating radicals could be observed (see Figure 5.22). This will be discussed in more detail in Chapter 5, section 5.3.1. In both cases, when a modulation amplitude of 1G and single scans were used, (conditions that were used for following the time evolution of the intermediate radicals), no (clear) evidence could be found for the presence of propagating radicals, indicating that their concentrations must be very low ( $< 10^{-7}$  M, the concentration lower limit than can be detected under the specific ESR spectrometer conditions) in the systems used.

As evident from Figure 3.10, similar behavior was observed when *n*-butyl acrylate (instead of styrene) was used as monomer (solution 5, Table 3.1).

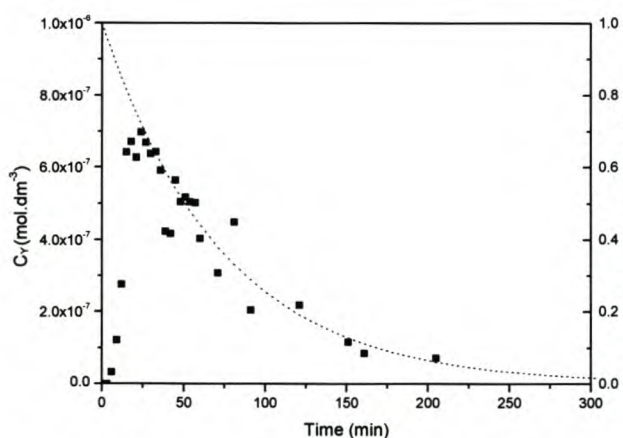


**Figure 3.9** The intermediate radical concentration–time profile for the *in situ* reaction of solution 1 ( $4.11 \times 10^{-2}$  M AIBN, 4.30 M styrene, 5.68 M benzene,  $9.17 \times 10^{-2}$  M cumyl dithiobenzoate) at 90 °C. The dotted line (---) indicates the square root of initiator decomposition in the system.

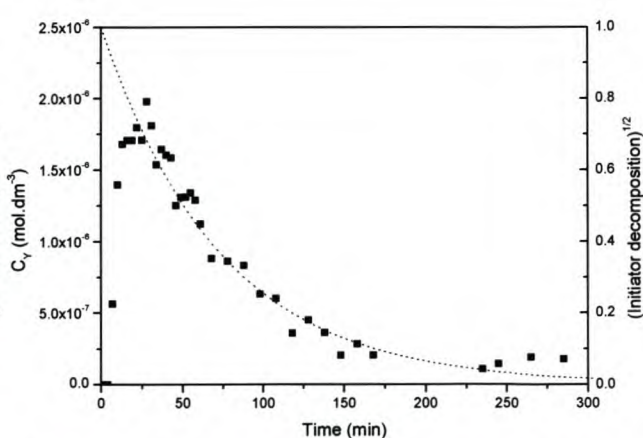


**Figure 3.10** The intermediate radical concentration–time profile for the *in situ* reaction of solution 5 ( $4.02 \times 10^{-2}$  M AIBN, 4.25 M butyl acrylate, 5.65 M benzene,  $9.11 \times 10^{-2}$  M cumyl dithiobenzoate) at 90 °C. The dotted line (---) indicates the square root of initiator decomposition in the system.

The reaction in which butyl acrylate was used as monomer, showed a significantly higher maximum intermediate radical concentration (ca.  $2 \times 10^{-6}$  M compared to  $7 \times 10^{-7}$  M for the styrene systems).

According to equation 3-7, the intermediate radical concentration will be dependant on  $c_{PX}$  (the initial RAFT agent concentration),  $c_P$  (the propagating radical concentration), and the rate coefficients for addition and fragmentation of the intermediate radical, according to equation 3-12.

$$c_Y = \frac{k_{add}}{k_{-add}} c_P c_{PX} \quad (3-12)$$

The same type of RAFT agent and similar initial RAFT agent, monomer and initiator concentrations were used in the reaction in which styrene and butyl acrylate were used as monomers. The reactions were also run under identical experimental conditions. The difference in  $c_Y$  for the two reactions is therefore likely to be either due to a different ratio of the addition rate coefficient (for addition of a propagating radical to a RAFT agent) to the fragmentation rate coefficient (of the formed intermediate radical), or a difference in the termination kinetics of the two systems, which would lead to a lower average termination rate coefficient for the butyl acrylate system, would give rise to a higher  $c_P$  value for the butyl acrylate system, and consequently a higher  $c_Y$  value.

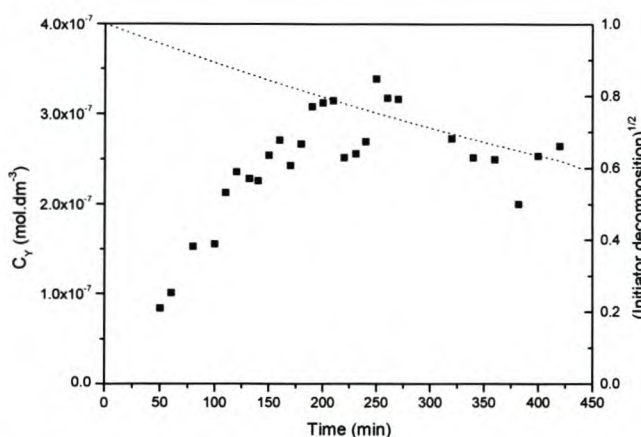


**Figure 3.11** The intermediate radical concentration–time profile for the *in situ* reaction of solution 1 ( $4.11 \times 10^{-2}$  M AIBN, 4.30 M styrene, 5.68 M benzene,  $9.17 \times 10^{-2}$  M cumyl dithiobenzoate) at 70 °C. The dotted line (—) indicates the square root of initiator decomposition (normalised to initial rate) in the system.

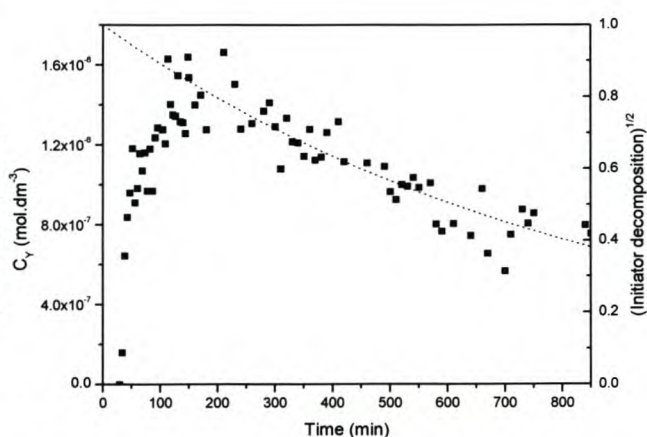


**Figure 3.12** The intermediate radical concentration–time profile for the *in situ* reaction of solution 5 ( $4.02 \times 10^{-2}$  M AIBN, 4.25 M butyl acrylate, 5.65 M benzene,  $9.11 \times 10^{-2}$  M cumyl dithiobenzoate) at 70 °C. The dotted line (—) indicates the square root of initiator decomposition (normalised to initial rate) in the system.

The same reactant solutions as discussed above (solutions 1 and 5, Table 3.1) were polymerized *in situ* at 70 °C. From Figures 3.11 and 3.12, the slow increase in  $c_Y$  became a lot more evident. No intermediate radicals could be detected up to 50 and 38 minutes (compared to 9 and 7 minutes at 90 °C) for the styrene and butyl acrylate cases respectively, after which  $c_Y$  slowly increased to a broad maximum after 210 and 150 minutes (compared to 23 and 21 minutes at 90 °C), and then decreased corresponding to the decrease in square root radical flux. This initial period of low  $c_Y$  in the styrene and butyl acrylate systems was first attributed to incomplete oxygen removal from the ESR samples. However, no difference in  $c_Y$  with time was observed when oxygen was rigorously removed by multiple freeze-pump-thaw cycles (rather than the

usual nitrogen flushing). This will be discussed in more detail in section 3.3.4. Thus, the slower than expected increase of  $c_Y$  early (i.e. much slower relative rate of increase than that of the reaction rate) in the reaction was unlikely to be due to dissolved oxygen. Unknown at the time, this initial period of no (or very little)  $c_Y$  was due to the initialization period<sup>40</sup> (see Chapter 3 and section 5.3.7.2) observed in the RAFT systems with high concentrations of initiator and RAFT agent. It should also be noted here that no sharp maximum in  $c_Y$  was observed as in the case of the reactions polymerized at 90 °C.

The lower values of  $c_Y$  observed for both the styrene and butyl acrylate systems at 70 °C (compared to the  $c_Y$  values observed at 90 °C) are suspected to be due to significantly lower  $c_P$  values in the 70 °C polymerizations than those of the polymerizations performed at 90 °C. Due to the slower rate of initiator decomposition at 70 °C, the radical flux and thus, according to equation 3-10,  $c_P$  will be significantly lower in the reactions performed at 70 °C. If it is assumed that  $c_Y$  and  $c_P$  are in rapid equilibrium with each other, the lower  $c_P$  value will be seen as a lower  $c_Y$  value throughout the reaction time (equation 3-12).

It was suspected that one of the reasons for the systems showing the slow increase in  $c_Y$  might be due to the fact that the systems had not yet attained steady state equilibrium. To determine this,  $K_{eq}$  for the systems, as given by equation 3-11, was investigated, as a constant value for  $K_{eq}$  would be indicative that steady state equilibrium has been attained.<sup>26</sup> As mentioned before,  $K_{eq}$  should be a constant for a specific RAFT agent/monomer combination at a specific temperature, and independent of all other factors. To test this,  $K_{eq}$  was determined for RAFT mediated systems with similar RAFT agent to initiator concentrations, but varying monomer to RAFT agent concentrations (solutions 2, 3 and 4, Table 3.1). Solution 4 was also run at 70 °C, to test the effects of temperature on the value of  $K_{eq}$ . The ratio of the intermediate to propagating radical concentrations ( $c_Y / c_P$ ) was determined by combining ESR and rate data. The time evolutions of the intermediate radical concentrations for the systems investigated are given in Figure 3.13.

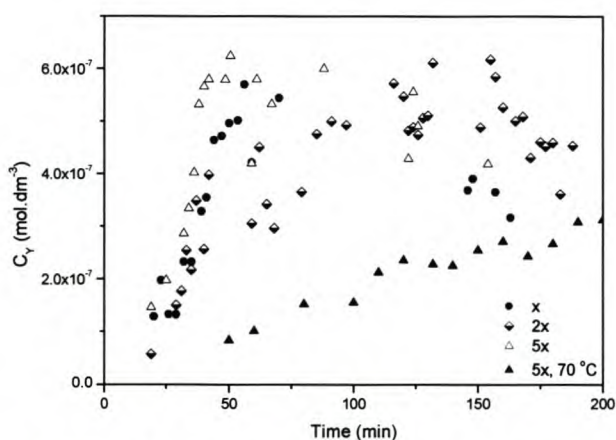


**Figure 3.13** The intermediate radical concentration–time profiles for the styrene polymerization in the presence of CDB. ●: 90 °C,  $C_{RAFT} = 0.182$  M; ◆: 90 °C,  $C_{RAFT} = 0.363$  M; △: 90 °C,  $C_{RAFT} = 0.906$  M; ▲: 70 °C,  $C_{RAFT} = 0.906$  M.

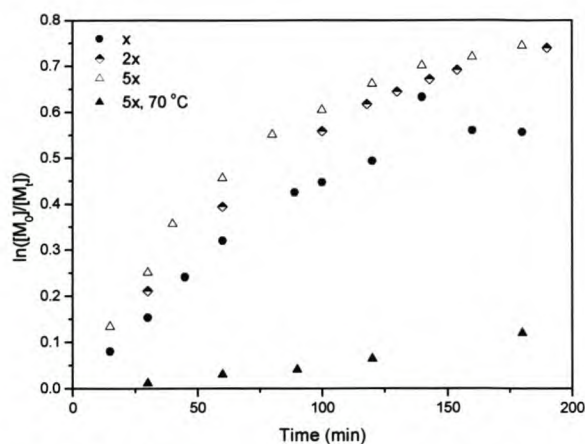


**Figure 3.14** The semi-logarithmic plot of the monomer consumption for the styrene polymerization in the presence of CDB. ●: 90 °C,  $C_{RAFT} = 0.182$  M; ◆: 90 °C,  $C_{RAFT} = 0.363$  M; △: 90 °C,  $C_{RAFT} = 0.906$  M; ▲: 70 °C,  $C_{RAFT} = 0.906$  M.

The corresponding semi-logarithmic plot of the monomer consumption (as determined by gravimetry) for the reactions is given in Figure 3.14.

The value for  $c_p$  was calculated by taking the time-derivative of the monomer consumption data, and using a value of  $480 \text{ M}^{-1}\text{s}^{-1}$  and  $898 \text{ M}^{-1}\text{s}^{-1}$  for  $k_p$  in the reactions at 70 and 90 °C respectively.<sup>44</sup> The value of  $c_{PX}$  was taken at the initial RAFT agent concentration. The calculated  $K_{eq}$  (see Figure 3.15) always started very low and increased with time, showing initial correlations with  $\overline{M}_n$  (Figure 3.16).

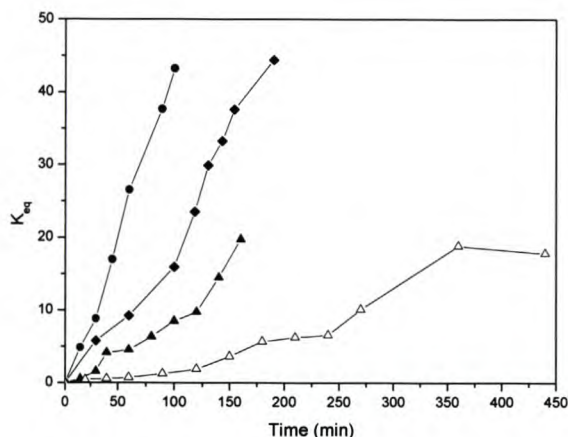


**Figure 3.15** The calculated equilibrium coefficient ( $K_{eq}$ ) as a function of time for styrene polymerization in the presence of CDB. ●: 90 °C,  $C_{RAFT} = 0.182 \text{ M}$ ; ◆: 90 °C,  $C_{RAFT} = 0.363 \text{ M}$ ; ▲: 90 °C,  $C_{RAFT} = 0.906 \text{ M}$ ; △: 70 °C,  $C_{RAFT} = 0.906 \text{ M}$ .

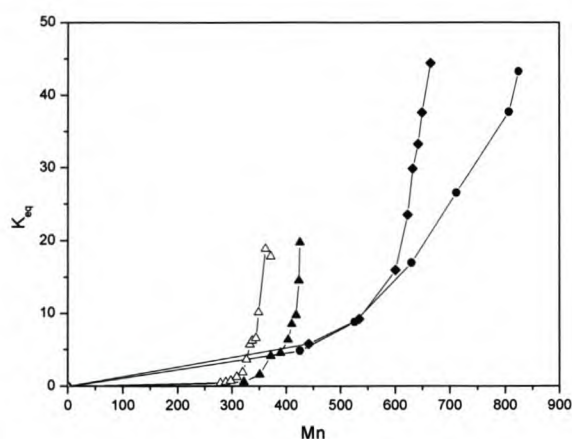


**Figure 3.16** The calculated equilibrium coefficient ( $K_{eq}$ ) as a function of  $\overline{M}_n$  for styrene polymerization in the presence of CDB. ●: 90 °C,  $C_{RAFT} = 0.182 \text{ M}$ ; ◆: 90 °C,  $C_{RAFT} = 0.363 \text{ M}$ ; ▲: 90 °C,  $C_{RAFT} = 0.906 \text{ M}$ ; △: 70 °C,  $C_{RAFT} = 0.906 \text{ M}$ .

The variation in  $K_{eq}$  with time and/or  $\overline{M}_n$  is inconsistent with both the standard RAFT model and the data of Kwak *et al.*<sup>29</sup> The very short chains in the systems studied (usually  $\overline{M}_n < 2000$ ), and the time-dependence of  $K_{eq}$  suggests that both initiator concentration and chain lengths play important roles here.

Without inferring major changes to the RAFT mechanism, a simple explanation for the variation in  $K_{eq}$  is that both  $k_{add}$  and  $k_{-add}$  are chain-length dependent for very short chains, as exist in the current systems. This is consistent with observations of the chain length dependence of the propagation reaction.<sup>45,46</sup> Moreover, an inverse relationship exists between the “goodness” of a leaving group (fragmentation ability) and its subsequent rate of radical addition, such that reduction in  $k_{add}$  may give a corresponding increase in  $k_{-add}$ , leading to enhanced  $k_{add}$  to  $k_{-add}$  ratio changes. Other possible explanations include reactions that consume intermediate radicals, either reversibly or irreversibly. The most likely reactions of the intermediate radical would be with primary radicals or other short-chain species, due to increasing steric congestion at the radical site with increasing chain lengths of nearby ( $P_n$ ,  $P_m$ , or  $Z$ ) or approaching chains. Either case will show a strong correlation with time and  $\overline{M}_n$ . In subsequent  $^{13}\text{C}$  NMR spectroscopy (with a labeled RAFT agent) and corresponding ESR spectroscopy experiments on the same solutions and under similar conditions, it was discovered that the probability of intermediate radical termination (either reversibly or irreversibly) increases with reaction time, as the concentrations of the initially formed intermediate radicals are too low to allow

significant amounts of cross-termination. This will be discussed in detail Chapter 4. The approximately constant  $K_{\text{eq}}$  ( $\approx 55 \text{ M}^{-1}$ ) observed by Kwak *et al.*<sup>26</sup> (starting with macro-RAFT agent,  $\overline{M}_n = 2000$ ) suggests that the  $K_{\text{eq}}$  in the current system might eventually reach a “pseudo-plateau” at sufficiently long chain lengths and times, to approach a constant value.

It was thought that a probable cause for the observed slow increase in  $c_Y$  might be due to the fact that all of the chains are short during the initial stages of the reactions (for the systems investigated). To test this hypothesis, a solution containing 5.64 M benzene,  $0.375 \times 10^{-2} \text{ M}$  AIBN, 4.26 M butyl acrylate and  $1.01 \times 10^{-2} \text{ M}$  CDB (solution 10, Table 3.1) was polymerized *in situ* in an ESR spectrometer at 90 °C. The reactant concentrations in this solution were chosen such that longer chain lengths were targeted at full conversion, due to a ten times higher ratio of monomer to RAFT agent concentration used, while the RAFT agent to initiator concentration ratio (= 13.5) was kept similar to that used in the previous experiments ( $\sim 11$ ).

The time evolution of the intermediate radical concentration for the *in situ* polymerization of solution 10 at 90 °C is given in Figure 3.17.

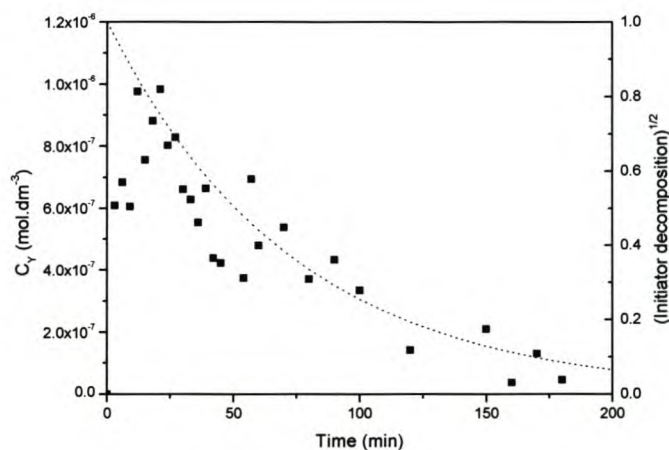


**Figure 3.17** The time evolution of  $c_Y$  for the *in situ* polymerization of solution 10 ( $0.375 \times 10^{-2} \text{ M}$  AIBN, 4.26 M butyl acrylate, 5.64 M benzene,  $1.01 \times 10^{-2} \text{ M}$  cumyl dithiobenzoate) at 90 °C. The dotted line (---) indicates the square root of initiator decomposition in the system.

In contradiction to the previous intermediate radical concentration-time evolutions observed, a nearly instant increase in intermediate radical concentration was observed during the *in situ* polymerization of solution 10 (see Figure 3.17).  $c_Y$  reached a maximum within 12 minutes, whereafter it declined steadily according to the decrease in square root initiator decomposition. This result confirmed the suspicion that the slow increase in  $c_Y$  was mainly due to extremely short chains being present during early stages of the reactions, which resulted from using very high RAFT agent and monomer concentrations (compared to reactant concentrations used in literature) in the systems investigated.

The  $c_Y / c_P$  ratios (at longer reaction times) calculated above, were roughly consistent with those of Kwak *et al.*<sup>29</sup> The ratio of  $c_Y / c_P$  predicted by the addition and fragmentation rate coefficients proposed by Barner-Kowollik *et al.*<sup>18</sup> give predicted  $c_Y$  (from the observed  $c_P$ ) values that are much higher (several orders of magnitude) than observed (Figure 3.18). Hence, those rate coefficients are clearly not applicable to the current systems. It should be noted here that the predictions for  $c_Y$  are above the maximum possible concentrations that could be formed in the current case, since  $c_{PX}$  is too low to allow that concentration of intermediate radicals to form.

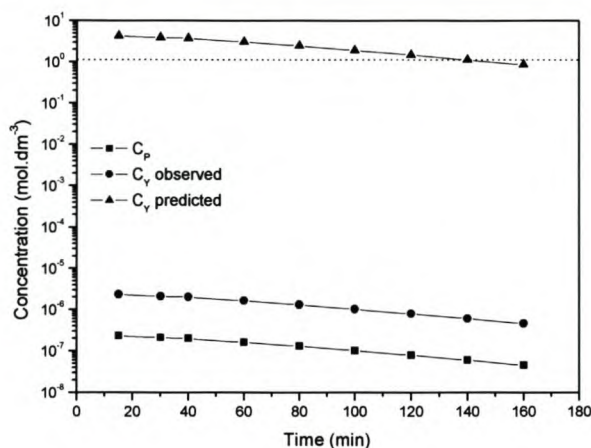


**Figure 3.18** A comparison between the intermediate radical concentrations observed (■) and that calculated by assuming the rate coefficients of Barner-Kowollik *et al.*<sup>18</sup> (▲). The dotted line indicates the maximum value for  $c_Y$  if all the RAFT agents were converted to intermediate radical species.

To conclude, preliminary indications suggested that the slow increase in  $c_Y$  observed for the investigated reactions are due to the varying  $k_{add}$  and  $k_{-add}$  values for the very short chains present in the reaction mixture during that period. Dissolved oxygen is unlikely to be the cause of this slow increase. The decrease in  $c_Y$  followed the decrease in square root of initiator decomposition, indicating that  $c_Y$  and  $c_P$  are (probably) in rapid equilibrium with each other. For all reactions investigated, steady state equilibrium had not been reached in the time investigated.

### 3.3.1 Intermediate Radical Signals of Different RAFT Agents

Similar *in situ* ESR experiments to those mentioned above were attempted with two other RAFT agents: cumyl phenyl dithioacetate (CPDA) and dibenzyl trithiocarbonate (DIBTC), shown in Figure 3.19.

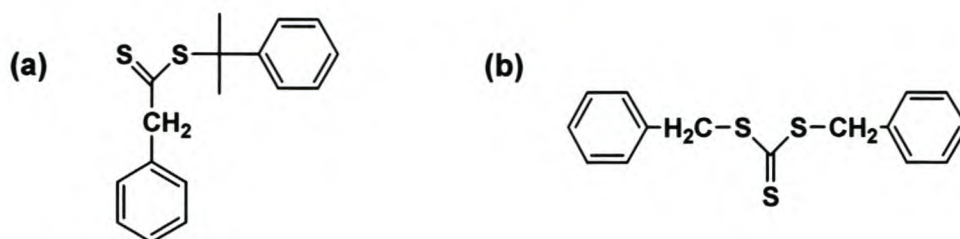


Figure 3.19 (a) Cumyl phenyl dithioacetate and (b) dibenzyl trithiocarbonate RAFT agents.

A solution containing  $4.30 \times 10^{-2}$  M AIBN, 4.29 M styrene, 5.70 M benzene and  $9.17 \times 10^{-2}$  M CPDA (solution 6, Table 3.1) was polymerized *in situ* in a Bruker ELEXSYS E 500 EPR spectrometer at 90 °C. The intermediate radical concentration was undetectable for the CPDA/styrene system. This is in sharp contrast with the CDB/styrene system, presumably due to a lower  $c_Y/c_P$  ratio of the CPDA/styrene system.<sup>30</sup> The non-stabilizing benzyl (Z)-group of the CPDA RAFT agent is unable to stabilize the formed intermediate radical, leading to a fast fragmentation and thus very low observed concentrations of intermediate radicals. However, when a solution containing butyl acrylate as monomer instead of styrene (solution 7, Table 3.1) ( $4.09 \times 10^{-2}$  M AIBN, 4.24 M butyl acrylate, 5.67 M benzene and  $9.08 \times 10^{-2}$  M CPDA) was used, an ESR signal could almost immediately be seen (Figure 3.20 (a)). This observed ESR signal was at a maximum during the initial stages of the reaction and progressively decreased with reaction time. This observed ESR signal corresponded mostly to the butyl acrylate propagating radical (Figure 3.20 (b)) and to a small concentration of intermediate radicals. The butyl acrylate propagating signal (Figure 3.20 (b)) was obtained by polymerizing a solution containing 4.39 M butyl acrylate,  $8.75 \times 10^{-2}$  M AIBN in 5.60 M benzene *in situ* at 90 °C.

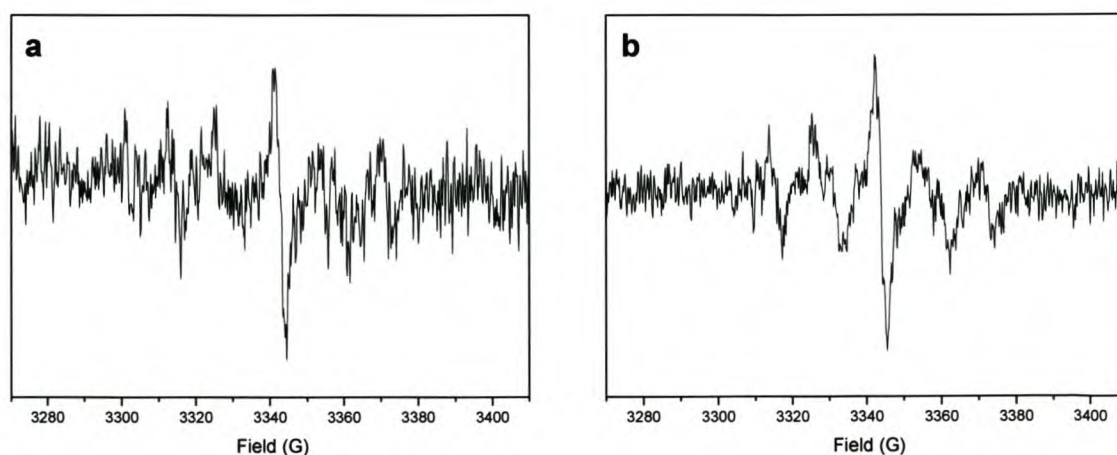
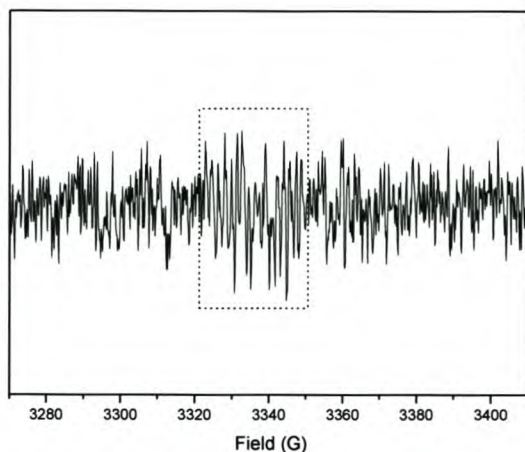


Figure 3.20 (a) The ESR signal detected in the early reaction time for the *in situ* polymerization of solution 7 at 90 °C. (b) The ESR signal due to the butyl acrylate propagating radical.

This result validates the idea that the  $c_Y/c_P$  ratio is lower for systems mediated by a phenyl dithiobenzoate RAFT agent (compared to a dithiobenzoate RAFT agent), leading to a faster reaction rate than that observed in the cumyl dithiobenzoate RAFT agent systems.<sup>30,43,44</sup>

For the *in situ* solution polymerization mediated by the dibenzyl trithiocarbonate RAFT agent (solution 8, Table 3.1, containing  $4.23 \times 10^{-2}$  M AIBN, 4.29 M styrene, 5.70 M benzene and  $9.24 \times 10^{-2}$  M DIBTC) at 90 °C, the ESR signal was too low for reliable integration, but  $c_Y$  could be (by examination) seen to show an immediate maximum, followed by a rapidly decreased, presumably in accordance with the rapidly decreasing initiator concentration, without the complicating factors observed for the CDB system. The effectively immediate maximum  $c_Y$  supports the hypothesis that the slow increase in  $c_Y$  for the CDB system is not due to dissolved oxygen. Several hyperfine splittings (see Figure 3.21), probably due to couplings with the nearby protons during the formation of the intermediate radicals, could also be observed.



**Figure 3.21** The ESR signal detected during the early reaction time for the *in situ* polymerization of solution 8 at 90 °C. The dotted box indicates the central hyperfine splittings observed due to the formed intermediate radicals.

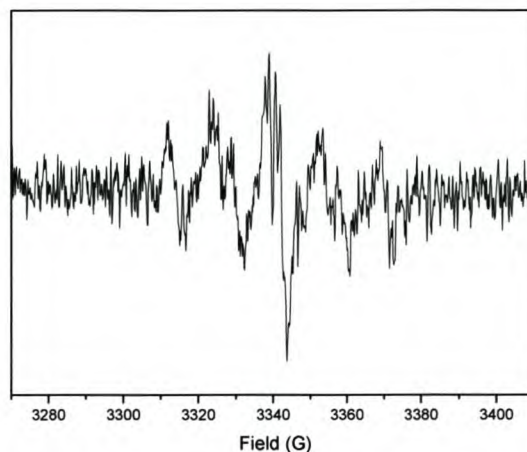


**Figure 3.22** The ESR signal detected during the early reaction time for the *in situ* polymerization of solution 9 at 90 °C.

When a similar DIBTC mediated system, containing  $4.06 \times 10^{-2}$  M AIBN, 4.25 M butyl acrylate, 5.66 M benzene and  $9.05 \times 10^{-2}$  M DIBTC (solution 9, Table 3.1) was polymerized *in situ* at 90 °C, hyperfine splittings (similar to those seen in the styrene case), superimposed on a strong signal due to butyl acrylate propagating (and mid-chain) radicals, could be seen. This is shown in Figure 3.22.

### 3.3.2 Intermediate Radical Concentrations at Long Reaction Times

An unexpected observation was that detectable concentrations of intermediate RAFT radical species were still present after very long reaction times at 90 °C. A sample containing  $4.05 \times 10^{-1}$  M AIBN, 4.25 M styrene, 5.74 M benzene and  $9.06 \times 10^{-1}$  M cumyl dithiobenzoate (solution 4, Table 3.1) was run *in situ* in the ESR spectrometer at 90 °C for 150 min during which ESR spectra were recorded. The sample was then removed from the ESR cavity and heated for another 16 h at 90 ( $\pm 0.5$ ) °C in an oil bath, after which it was cooled to room temperature and ESR scans recorded (at room temperature) once more. No evidence of *any* radical species could be found in the ESR spectra. Accumulating spectra for extensive periods (5 scans with a sweep time of 327.68 s each) and increasing the modulation amplitude (from 1 G to 5 G) in an attempt to

increase the signal to noise ratio, also did not yield any evidence of radicals being present in the systems. The ESR cavity (with sample) was then heated to 90 °C and scans recorded once more. In this case, a signal corresponding to the intermediate RAFT radicals was seen (Figure 3.25 (a)), and was estimated to be slightly less than  $10^{-7}$  M (Figure 3.23). Given the literature values of  $k_d$ ,<sup>45</sup> almost no initiator would be expected to remain, and the predicted  $c_Y$  by the classical model (using rate coefficients as given by Kwak *et al.*<sup>26</sup>) would therefore be below  $10^{-12}$  M (undetectable) (Figure 3.24). This huge discrepancy could not be explained by experimental uncertainties in reaction temperature or concentrations.

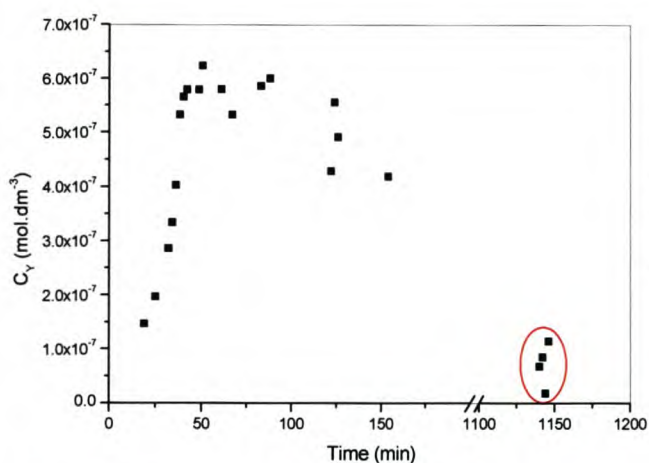


**Figure 3.23** The time evolution of  $c_Y$  indicating detectable concentrations of the intermediate radicals after 19 h reaction time at 90 °C.

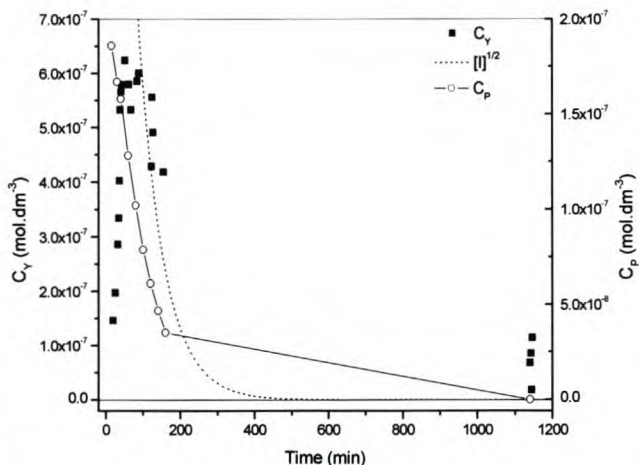


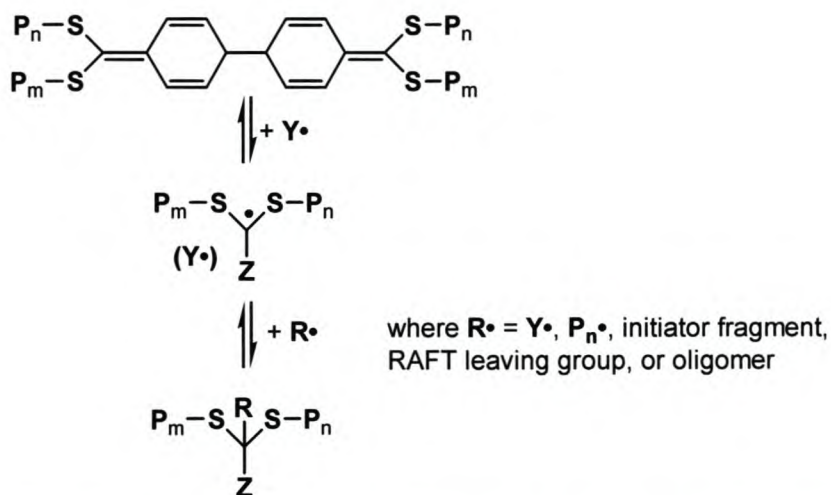
**Figure 3.24** The concentrations of intermediate radicals (from ESR data), propagating radicals (from rate data) and remaining initiator after reaction of solution 4 at 90 °C for 19 h.

Assuming that there is no large change (at least 3 orders of magnitude being necessary) in the equilibrium between propagating and intermediate radicals at long reaction times (as implied by the data of Kwak *et al.*<sup>26</sup>), the detectable intermediate concentration implies the presence of propagating radicals. This is consistent with observations of significant polymerization occurring in a RAFT system at 60 °C containing no initiator, after removal from a gamma ray source.<sup>22</sup> The propagating radical concentrations required to produce the observed signal using the observed maximum  $c_Y/c_P$  ratio is between  $5 \times 10^{-9}$  and  $10^{-8}$  M. Using the observed rates of thermal polymerization of Barner-Kowollik *et al.*<sup>22</sup> give an average  $c_P$  of significantly less than  $5 \times 10^{-10}$  M at 60 °C. Thermal radical production in the current system is expected to be much slower due to the very low monomer concentration at the nearly terminal conversions (the rate of thermal initiation being dependent on the third power of the monomer concentration<sup>41</sup>) under such conditions, and is incapable of producing sufficient radicals to give the observed intermediate radical concentration. Note that radical trapping due to vitrification cannot produce the observed radical signal (since final  $w_p = 0.65$ ), as in analogous reactions, samples were heated to 90 °C in the ESR cavity and when the temperature suddenly decreased to room temperature, the signal was observed to decrease very rapidly following the decrease in cavity temperature.

The same experimental and analysis procedure was repeated with butyl acrylate as monomer instead of styrene (reaction 5, Table 3.1). As in the styrene case, no signal due to intermediate radicals could be

detected at room temperature. However, upon heating the sample to 90 °C, the presence of intermediate RAFT radicals was detected (Figure 3.25 (b)) in higher concentrations than in the styrene case. As butyl acrylate does not readily undergo thermal initiation, the most likely explanation is that a RAFT-originated radical source was present in the reaction after long reaction times.

The presence of radicals in the virtual absence of initiator and their disappearance upon cooling implies very long-lived (non-intermediate radical) species that may act as a thermally-activated radical source. This is consistent with a significant fraction of radicals being “protected” from termination events, possibly through reversible coupling mechanisms (see Scheme 3.3). This is also consistent with the observation by Kwak *et al.*<sup>28</sup> who observed that 3-arm star chains, formed by termination of intermediate radicals, could possibly “degrade” at elevated temperatures to form the RAFT agent (PSt-S-C(Ph)=S) and polystyrene (PSt) radicals again. Evidence for the presence of such terminated intermediate radical species has been detected, and will be discussed in Chapter 4.



**Scheme 3.3** Possible reversible and irreversible termination reactions involving the intermediate radical to generate non-radical species.

The above-mentioned experimental procedure (reaction of the sample at 90 °C in an oil bath for 16 h) was again repeated for a sample containing  $4.11 \times 10^{-2}$  M AIBN, 4.30 M styrene, 5.68 M benzene and  $9.17 \times 10^{-2}$  M cumyl dithiobenzoate (reaction 1, Table 3.1). No signal could be detected via ESR spectroscopy after the sample was cooled to room temperature. When the ESR cavity with sample was heated to 90 °C, a signal due to radicals present in the reaction could be detected. However, on close inspection it was seen that the signal had a different line shape and appeared (Figure 3.25 (c)) at a different g-value than the expected intermediate RAFT radical signal (g-value = 2.0043). This observed signal did however exactly correspond to the “extra signal” observed in certain RAFT reactions, and was attributed to possible RAFT agent degradation.<sup>50</sup> The significance and possible origin of this signal will be discussed in section 3.3.5.

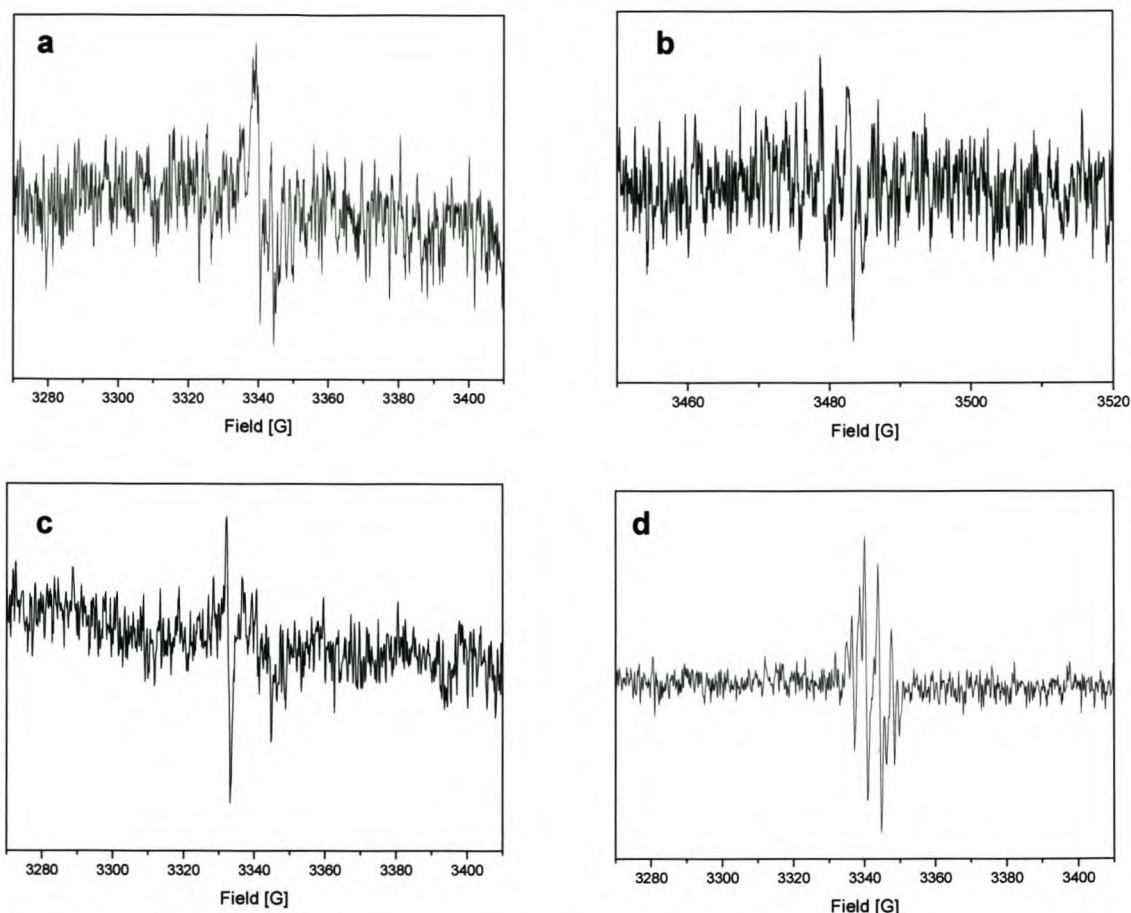


**Figure 3.25** The ESR signals observed for the intermediate radicals at long reaction times for: (a) styrene, CDB and AIBN in benzene (solution 1); (b) butyl acrylate, CDB and AIBN in benzene (solution 5); (c) the “extra signal” at a different  $g$ -value than the intermediate radical signal, (d) usually observed ESR signal due to intermediate RAFT radicals (early in the reaction).

The apparent anomalous long time concentration of intermediate RAFT radicals cannot be explained by alternative models for radical fates. Any irreversible termination of intermediate species would further decrease the propagating and intermediate radical concentrations. Even if intermediate-intermediate radical termination is impossible, the intermediate species will still be in equilibrium with the propagating radicals, which can still undergo termination. Thus, any assumed model based on mechanisms including only irreversible termination predicted that no (or extremely little) intermediate or propagating radical species would remain. The observed intermediate radical concentration thus implies that additional events are occurring either to protect radicals from irreversible termination, or that there is a thermally activated radical source in the system.

### 3.3.3 Oxygen Sensitivity

Another example of unusual behavior was the apparently low sensitivity of the cumyl dithiobenzoate RAFT systems to oxygen. It was first thought that the long delay in the observation of the intermediate radicals was due to inhibition caused by dissolved oxygen in the sample. To test this hypothesis, some samples

were vigorously degassed by consecutive freeze-pump-thaw cycles. However, no difference in the time evolution of  $c_Y$  was observed when oxygen was rigorously removed by multiple freeze-pump-thaw cycles (rather than the usual nitrogen flushing for 10 min). Thus, the slower than expected increase of  $c_Y$  early (i.e. much slower relative rate of increase that of than  $c_P$ ) in the reaction was unlikely to be due to dissolved oxygen.

During an *in situ* ESR experiment (solution 3, Table 3.1), the deliberate exposure of the reaction mixture to the atmosphere for more than 30 minutes at 90 °C (Figure 3.26) showed little change in rate, concentration, or nature of radicals present, although a small amount of an underlying peroxy peak may have been present. The lack of retardation was probably due to the extremely high radical flux in this specifically chosen system, as similar results were observed for an analogous reaction in which no RAFT agent was included. This, and the apparent insensitivity of the observed time evolution of  $c_Y$  to degassing procedures, indicated that the RAFT agent and process were not particularly sensitive to oxygen up to 90 °C, and implies that handling in the presence of oxygen, even at elevated temperatures, would not be extremely detrimental to RAFT performance.

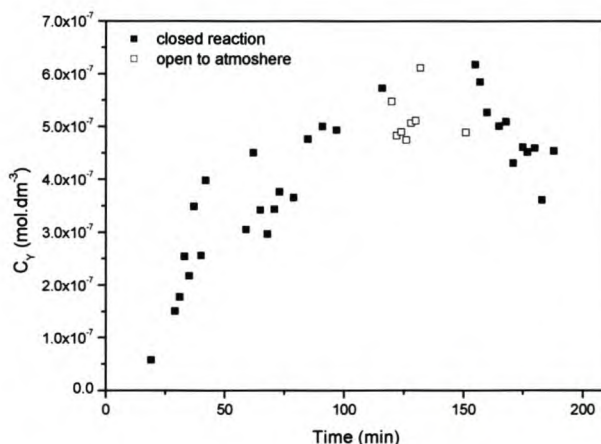


**Figure 3.26** The effect of exposure to oxygen on the time evolution of  $c_Y$  for solution 3 (Table 3.1) at 90 °C.

It should be mentioned here that this apparent insensitivity of the RAFT systems towards oxygen is very specific for the cumyl dithiobenzoate RAFT systems investigated. When using trithiocarbonates as RAFT agents, incomplete initial oxygen removal or oxygen that is introduced into the system by sampling, can cause severe rate retardation effects.<sup>47</sup>

### 3.3.4 Extra Signals

An extra signal, neither corresponding to intermediate nor propagating radicals, (Figure 3.27 (a)) appeared at intermediate conversions during most styrene reactions using CDB. This signal always appeared after  $c_Y$  reached a maximum, and was never seen to appear in reactions at lower temperatures (70 °C). The

intensity of the signal increased with reaction time, but its concentration was independent of  $c_Y$ . RAFT color intensity decreased as this signal increased, suggesting that this signal may be due to a RAFT degradation product. In an attempt to identify the origin of the “extra” signal, the microwave power used for the ESR scans was increased from 2 mW to 8 mW (Figure 3.27 (b) and (c)). A corresponding increase of the intensity of the “extra” signal, while saturating the intermediate and propagating radical signals (decrease in signal intensities and loss in fine structure), was observed.

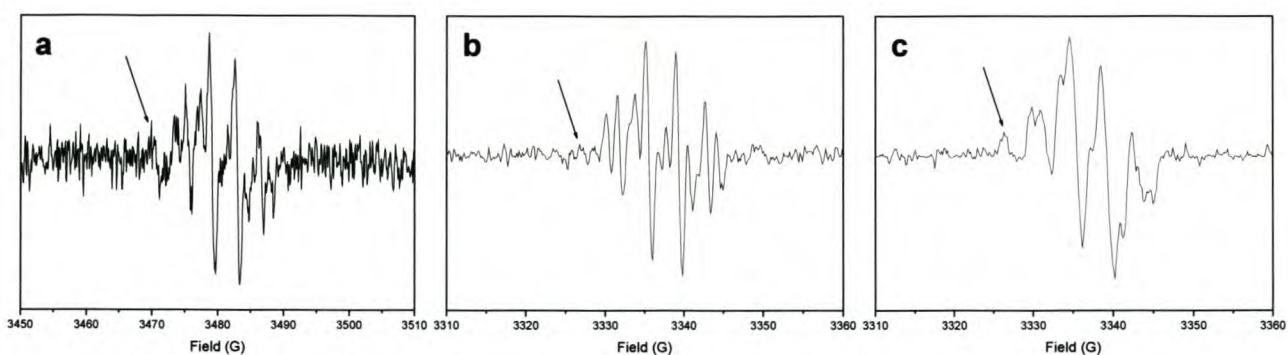


**Figure 3.27** (a) The “extra” signal (indicated by arrow) observed in most reactions with styrene and CDB. A magnetic field of 100 kHz and microwave power of 1 mW was used, together with a modulation amplitude of 1G, with a 81.92 ms time constant and 83.89 s sweep time. (b) The signal at low (2 mW) and (c) higher (8 mW) microwave power.

According to equation 3-8, a corresponding increase in signal intensity with the increase in microwave power is indicative of species that is still unsaturated, as it can relax fast enough to give a signal increase. As the carbon centered intermediate (and propagating) radical signal decreases with a power increase from 2 mW to 8 mW, the extra signal has therefore clearly different relaxation behavior, indicating that it is probably a different species to the intermediate radicals, and suggesting that it might not be a carbon centered radical. The higher  $g$ -value (compared to that of the intermediate radicals) and lack of hyperfine splittings suggests a significant amount of spin density on a heteroatom.

In section 3.2.3 it was stated that a signal was observed at long reaction times that did not correspond to the intermediate RAFT radicals signal. This signal had the same  $g$ -value as that of the “extra signal” observed at intermediate reaction times in some CDB reactions. It was also stated that even though no signal was observed at room temperature, a prominent signal was clearly observed at elevated temperatures for the same sample. The origin of this signal is therefore likely to be due to radicals forming from non-radical species that are stable at low temperatures, but fragment at elevated temperatures to form detectable concentrations of radicals. It was shown by Kwak *et al.*<sup>25</sup> that intermediate radical termination can occur and that the intermediate termination products probably degrade at elevated temperatures. As the “extra signal” was never observed in styrene CDB reactions at lower temperatures, it is therefore suspected that these signals might be due to radicals forming from fragmenting (at the C-S bond) intermediate terminated products at elevated temperatures. These products could be sulfur-centered radicals, which have little coupling with the nearby protons (leading to little or no hyperfine splitting), and can relax faster than carbon-centered radicals, leading to a consequent increase in signal intensity with an increasing in power.

In summary, the “extra signal” appeared in most styrene CDB reactions. It appeared in significant concentrations only after the intermediate radical concentrations reached their maximum, corresponding with possible intermediate radical terminated products that might form (see Chapter 3). These radicals are likely to be sulfur-centered, which will lead to an increase in signal intensity with a microwave power increase. These sulfur-centered radicals are likely to have formed from the degradation (at elevated temperatures) of intermediate radical termination products, as shown by Kwak *et al.*<sup>25</sup>

### 3.4 Conclusions

The time evolution of  $c_Y$  was examined for cumyl dithiobenzoate mediated styrene and butyl acrylate polymerizations. A characteristic  $c_Y$ -time profile, which consisted of: an initial period of no  $c_Y$ , followed by a rapid increase to a maximum, whereafter  $c_Y$  decreased according to the decrease in square root initiator decomposition, was observed for all reactions. This profile was attributed to the formation of, and properties inferred from, short chains that formed during the early stages of the reaction. The  $K_{eq}$  values calculated for the systems by means of rate and ESR data always started very low, but increased with time, showing initial correlations with  $\overline{M}_n$ . This was attributed to varying  $k_{add}$  and  $k_{-add}$  values for the very short chains present in the reaction mixture during that period. For all reactions investigated, steady state equilibrium had not been reached in the time investigated.  $K_{eq}$  calculated was also dependent on both temperature and starting reactant concentrations.

The intermediate radical concentrations observed were not consistent with the predictions based on existing rate coefficients of Barner-Kowollik *et al.*,<sup>15</sup> but were similar to those observed by Kwak *et al.*<sup>26</sup> The time dependence of the intermediate radical concentration varied significantly with the type of RAFT agent used. Intermediate radicals were also detected at long reaction times in the virtual absence of initiator. This was explained in the light of a possible reversible intermediate radical termination mechanism.

The CDB/styrene system used is not particularly sensitive to oxygen. This was however not true for systems mediated by trithiocarbonates as RAFT agents. An extra signal, not corresponding to the propagating or intermediate radicals, was observed. It is suspected that the origin of the signal might be RAFT degradation products or possible (reversibly) terminated intermediate products.

## References

1. Carrington, A.; McLachlan, A. D. *Introduction to Magnetic Resonance*; Harper and Row: New York, **1967**.
2. Weil, J. A.; Wertz, J. E.; Bolton, J. R. *Electron Paramagnetic Resonance: Elementary Theory and Practical Applications*; Wiley-Interscience: New York, **1994**.
3. Tonge, M. P.; Kajiwara, A.; Kamachi, M.; Gilbert, R. G. *Polymer* **1998**, *39*, 2305.
4. Pople, J. A. S.; Bernstein, H. J. *High-resolution Nuclear Magnetic Resonance*; McGraw-Hill: New York, Toronto, London, **1959**.
5. Kamachi, M. *J. Polym. Sci., Part A: Polym. Chem.* **2002**, *40*, 269.
6. Kamachi, M.; Kajiwara, A. *Macromolecules* **1996**, *29*, 2378.
7. Kamachi, M.; Kohno, M.; Kuwae, Y.; Nozakura, S. *Polymer J.* **1982**, *14*, 749.
8. Yamada, B.; Kageoga, M.; Otsu, T. *Macromolecules* **1991**, *24*, 5234.
9. Yamada, B.; Kageoka, M.; Otsu, T. *Polym. Bull.* **1992**, *29*, 385.
10. Yamada, B.; Westmoreland, D. G.; Kobatake, S.; Konosu, O. *Prog. Polymer Sci.* **1999**, *24*, 565.
11. Yamada, B.; Kageoka, M.; Otsu, T. *Macromolecules* **1992**, *25*, 4828.
12. Rånby, B.; Rabek, J. F. *ESR Spectroscopy in Polymer Research*; Springer-Verlag: Berlin, **1977**.
13. Buback, M.; Kowollik, C.; Kamachi, M.; Kajiwara, A. *Macromolecules* **1998**, *31*, 7208.
14. Lau, W.; Westmoreland, D. G.; Novak, R. W. *Macromolecules* **1987**, *20*, 457.
15. Zhu, S.; Tian, Y.; Hamielec, A. E.; Eaton, D. R. *Macromolecules* **1990**, *23*, 1144.
16. Yamada, B.; Kageoka, M.; Otsu, T. *Polym. Bull.* **1992**, *28*, 75.
17. Chiefari, J.; Chong, Y. K. B.; Ercole, F.; Krstina, J.; Jeffery, J.; Le, T. P. T.; Mayadunne, R. T. A.; Meijs, G. F.; Moad, C. L.; Moad, G.; Rizzardo, E.; Thang, S. H. *Macromolecules* **1998**, *31*, 5559.
18. Barner-Kowollik, C.; Quinn, J. F.; Morsley, D. R.; Davis, T. P. *J. Polym. Sci., Part A: Polym. Chem.* **2001**, *39*, 1353.
19. Hawthorne, D. G.; Moad, G.; Rizzardo, E.; Thang, S. H. *Macromolecules* **1999**, *32*, 5457.
20. Chiefari, J.; Mayadunne, R. T.; Moad, G.; Rizzardo, E.; Thang, S. H., *PCT Int. Appl.*, **1999**, wo/9931144.
21. Laus, M.; Papa, R.; Sparnacci, K.; Alberti, A.; Benaglia, M.; Macciantelli, D. *Macromolecules* **2001**, *34*, 7269.
22. Du, F. S.; Zhu, M. Q.; Guo, H. Q.; Li, Z. C.; Li, F. M.; Kamachi, M.; Kajiwara, A. *Macromolecules* **2002**, *35*, 6739.
23. Alberti, A.; Benaglia, M.; Laus, M.; Macciantelli, D.; Sparnacci, K. *Macromolecules* **2002**, *36*, 736.
24. Le, T. P.; Moad, G.; Rizzardo, E.; Thang, S. H., *PCT Int. Appl.*, **1998**, wo98/01478.
25. Barner-Kowollik, C.; Vana, P.; Quinn, J. F.; Davis, T. P. *J. Polym. Sci., Part A: Polym. Chem.* **2002**, *40*, 1058.
26. Barner-Kowollik, C.; Coote, M. L.; Davis, T. P.; Radom, L.; Vana, P. *J. Polym. Sci., Part A: Polym. Chem.* **2003**, *41*, 2828.
27. Prescott, S. W.; Ballard, M. J.; Rizzardo, E.; Gilbert, R. G. *Aust. J. Chem.* **2002**, *55*, 415.
28. Kwak, Y.; Goto, A.; Fukuda, T. *Macromolecules* **2003**, Submitted.

29. Kwak, Y.; Goto, A.; Tsujii, Y.; Murata, Y.; Komatsu, K.; Fukuda, T. *Macromolecules* **2002**, *35*, 3026.
30. Wang, A. R.; Zhu, S.; Kwak, Y.; Goto, A.; Fukuda, T.; Monteiro, M. J. *J. Polym. Sci., Part A: Polym. Chem.* **2003**, *41*, 2833.
31. Calitz, F. M.; McLeary, J. B.; McKenzie, J. M.; Klumperman, B.; Sanderson, R. D.; Tonge, M. P. *Manuscript in preparation*.
32. Barner-Kowollik, C.; Davis, T. P.; Heuts, J. P. A.; Stenzel, M. H.; Vana, P.; Whittaker, M. J. *Polym. Sci., Part A: Polym. Chem.* **2002**, *41*, 365.
33. Barner-Kowollik, C.; Quinn, J. F.; Nguyen, T. L. U.; Heuts, J. P. A.; Davis, T. P. *Macromolecules* **2001**, *34*, 7849.
34. Vana, P.; Davis, T. P.; Barner-Kowollik, C. *Macromolecular theory and simulations* **2002**, *11*, 823.
35. Perrier, S.; Barner-Kowollik, C.; Quinn, J. F.; Vana, P.; Davis, T. P. *Macromolecules* **2002**, *35*, 8300.
36. Coote, M. L.; Radom, L. *J. Am. Chem. Soc.* **2003**, *125*, 1490.
37. Vana, P.; Quinn, J. F.; Davis, T. P.; Barner-Kowollik, C. *Aust. J. Chem.* **2002**, *55*, 425.
38. Monteiro, J. M.; Bussels, R.; Beuermann, S.; Buback, M. *Aust. J. Chem.* **2002**, 433.
39. Monteiro, M. J.; de Brouwer, H. *Macromolecules* **2001**, *34*, 349.
40. Wang, A. R.; Zhu, S. *J. Polym. Sci., Part A: Polym. Chem.* **2003**, *41*, 1553.
41. Quinn, J. F.; Rizzardo, E.; Davis, T. P. *Chem. Comm.* **2001**, 1044.
42. Lai, J. T.; Filla, D.; Shea, R. *Macromolecules* **2002**, *35*, 6754.
43. McLeary, J. B.; Calitz, F. M.; McKenzie, J. M.; Tonge, M. P.; Sanderson, R. D.; Klumperman, B. *Macromolecules* **2003**, *Submitted*.
44. Buback, M.; Gilbert, R. G.; Hutchinson, R. A.; Klumperman, B.; Kuchta, F.-D.; Manders, B. G.; O'Driscoll, K. F.; Russell, G. T.; Schweer, J. *Macromol. Chem. Phys.* **1995**, *196*, 3267.
45. Moad, G.; Solomon, D. H. *The Chemistry of Free Radical Polymerization*; First ed.; Elsevier Science Ltd, **1995**.
46. Heuts, J. P. A.; Gilbert, R. G.; Radom, L. *Macromolecules* **1995**, *28*, 8771.
47. Barner-Kowollik, C. *Aust. J. Chem.* **2001**, *54*, 343.
48. Prescott, S. W.; Ballard, M. J.; Rizzardo, E.; Gilbert, R. G. *Macromolecules* **2002**, *35*, 5417.
49. Billmeyer, F. W. *Textbook of Polymer Science*; Wiley-Interscience: New York, **1962**.
50. Calitz, F. M.; Tonge, M. P.; Sanderson, R. D. *Macromolecules* **2003**, *36*, 5.
51. Hawket, B. H.; Ferguson, C. J., Personal Communication, **2003**.

# Chapter 4

## Evidence for Termination of Intermediate Radical Species in RAFT-Mediated Polymerization

### Summary

*The combination of data from several analytical techniques has provided evidence for the formation of dead chains by the termination of intermediate radicals in the free radical polymerization of styrene, mediated by the RAFT agent cumyl dithiobenzoate, at 84 °C. Experiments done focused on the early stages of the reactions, targeting very low final  $\overline{M}_n$  values, using high initiator concentrations. The formation of these terminated chains did not occur to a significant extent until a large fraction of the chains reached a degree of polymerization greater than unity. This corresponded to the occurrence of a maximum in intermediate radical concentration.*

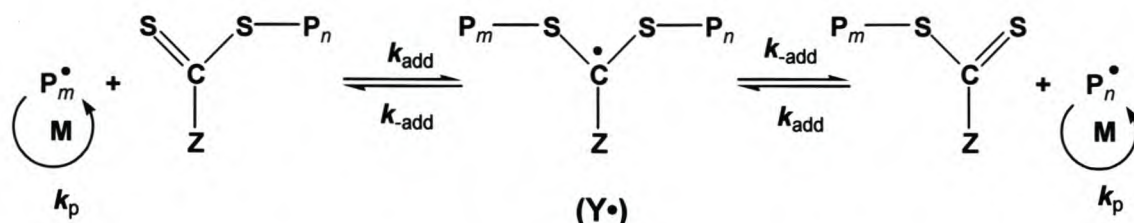
---

The  $^{13}\text{C}$  NMR work in this chapter was partly done in collaboration with James McLeary. This chapter forms part of a paper:

**Evidence for Termination of Intermediate Radical Species in RAFT-Mediated Polymerization;** F.M. Calitz, J. B. McLeary, J. M. McKenzie, M. P. Tonge, R. D. Sanderson, B. Klumperman; *Macromolecules*, **2003**, 36, 9687-9690.

## 4.1 Inhibition and Rate Retardation

The foundations of the RAFT process rest in the rapid central addition-fragmentation equilibrium process between chain activity and dormancy shown in Scheme 4.1. An important species in the equilibrium is the relatively stable intermediate RAFT radical that is sometimes formed in quantities that are detectable by electron spin resonance (ESR) spectroscopy.<sup>1-7</sup> The concentrations of the species involved in this equilibrium are dependent on the relative rate coefficients for addition ( $k_{\text{add}}$ ) of a propagating radical ( $P_m^\bullet$ ) to the RAFT agent and fragmentation ( $k_{\text{-add}}$ ) of a propagating radical ( $P_n^\bullet$ ) from the formed intermediate radical ( $Y^\bullet$ ). This equilibrium only strictly holds for polymeric chains ( $P_m^\bullet$  and  $P_n^\bullet$ ), which are only present in significant concentrations after an initialization period,<sup>3</sup> during which mainly shorter chains are present. This will be discussed in detail in Chapter 5.



**Scheme 4.1** The currently accepted elementary steps for the central equilibrium in the RAFT process.

Two anomalies that have been observed in RAFT mediated polymerization reactions are inhibition<sup>8,9</sup> and rate retardation phenomena.<sup>1,10-14</sup> Rate retardation is observed as a reduction in the rate of polymerization in a reaction in the presence of a RAFT agent, compared with an equivalent reaction where the RAFT agent is absent. Cases exhibiting both of these phenomena have been observed in dithiobenzoate mediated polymerization reactions.<sup>1,12,15</sup> The two phenomena have sometimes been linked,<sup>8</sup> but recent studies have shown that the reasons for these phenomena appear to be independent for the dithiobenzoate systems studied.<sup>3</sup> Since Scheme 4.1 contains no reaction that affects the propagating radical concentration, and thus, the rate of reaction, neither inhibition nor retardation is explicitly predicted for systems mediated by RAFT agents. Models attempting to explain these phenomena differ significantly, which has led to much debate recently, especially regarding explanation for the observed rate retardation.<sup>1,10,14-19</sup> The two main models propose either slow fragmentation of intermediate radicals, leading to a lower propagating radical concentration,<sup>8,12,14,17,20-23</sup> or termination of intermediate RAFT radicals.<sup>1,15,19</sup>

To determine whether the intermediate radicals undergo side reactions, several authors have used model systems to conclusively prove that these reactions can and do occur.<sup>1,15</sup> The reactions in those studies were performed in the absence of monomer, and thus their frequency or importance for a RAFT mediated polymerization was not determined. On the other hand, recent high level *ab initio* quantum chemical calculations<sup>24</sup> suggest that slow fragmentation of the intermediate radical might occur in some cases. ESR studies of the RAFT process<sup>1,2,5</sup> appear to show that the concentration of intermediate radicals is far too low

to support the very slow fragmentation required to cause rate retardation, as predicted by Barner-Kowollik *et al.*<sup>12</sup>

To date, there has been no direct experimental evidence for either mechanism, thus the debate has not yet been resolved to the satisfaction of all researchers in the field. In this chapter, direct evidence will be provided to support the formation of intermediate radical terminated products.

### 4.1.1 Experimental planning

#### What was known?

The time evolution of the intermediate radical concentration ( $c_Y$ ), as determined by the initial ESR spectroscopy investigations, exhibited a particular and unexpected profile (section 3.3 Chapter 3). In all cases examined, the time evolution of  $c_Y$  showed an initial period (of varying length) of no or very small intermediate radicals, followed by a sudden increase in  $c_Y$  to a maximum, after which  $c_Y$  decreased according to the decrease in radical flux in the system. Dissolved oxygen was discarded as a cause for the observed initial period of little or no intermediate radicals (section 3.3.4). It was proposed in the literature<sup>1,10-14</sup> that termination of the intermediate radicals might be the cause of the observed rate retardation for some RAFT mediated systems and thus also for the initial period in the observed  $c_Y$  profile. Reversible intermediate radical termination, in which the terminated products can act as a radical source, might also be an explanation for the ESR observation of radical signals at long reaction times, when it is predicted that very little initiator would remain.

#### Experiments to be done

After failing to detect the intermediate terminated products through GPC subtractions and MALDI-TOF analysis, it was thought that the best way of detecting intermediated terminated products would be by <sup>13</sup>C NMR spectroscopy, as it was expected that only small amounts of intermediate radical termination products would form. By combining ESR and <sup>13</sup>C NMR spectroscopy data, it was sought to explain the  $c_Y$  profile observed in the light of the possible formation of intermediate terminated products. A carbon thirteen labeled cumyl dithiobenzoate RAFT agent (at the dithioester carbon) was also synthesized to aid in the search for the possible terminated products. This was done in an attempt to increase the signal to noise ratio of the recorded spectra.

## 4.2 Experimental

### 4.2.1 Chemicals

#### Chemicals used

Styrene monomer (Plascon Research Centre, University of Stellenbosch, estimated purity ~99%  $^1\text{H}$  NMR) was washed with 0.3 M KOH and distilled under vacuum prior to use, to remove inhibitor and polymer. Azo bis(isobutyronitrile) (AIBN, Riedel De Haen), was recrystallized from AR grade methanol and found to be ~99% pure by  $^1\text{H}$  NMR. Deuterated benzene ( $\text{C}_6\text{D}_6$  99.6%, 0.1% TMS, Sigma-Aldrich) and benzene (AR grade, Sigma-Aldrich) were used as received.

#### Synthesis of transfer agents

The synthesis of cumyl dithiobenzoate (CDB) was carried out according to the method of Le *et al.*<sup>25</sup> and purified by liquid chromatography on a silica column, using hexane as eluent. The product was dried under vacuum to provide the compound with a  $^1\text{H}$  NMR purity estimated at ~ 98%.  $^{13}\text{C}$  enriched cumyl dithiobenzoate (CDB- $^{13}\text{C}$ ), labeled at the dithioester carbon, from  $^{13}\text{CS}_2$  (99%, Cambridge Isotope Laboratories) instead of the normally unlabeled  $\text{CS}_2$  used, was synthesized (purity,  $^1\text{H}$  NMR > 95%) by standard procedures in a similar fashion to unlabeled cumyl dithiobenzoate.<sup>25</sup>

### 4.2.2 Sample Preparation

#### ESR spectroscopy

A typical reaction mixture was prepared as follows: The RAFT agent CDB (0.400 g,  $8.35 \times 10^{-1}$  M) and AIBN (0.0407 g,  $1.14 \times 10^{-1}$  M) were dissolved in a benzene (1.00 g, 5.49 M) and styrene (1.01 g, 4.48 M) solution. An aliquot (~ 0.2 g) of the solution was transferred to an ESR tube and oxygen removed by multiple freeze-thaw cycles. The tube was sealed and transferred to the ESR cavity, which had been pre-heated to the reaction temperature.

#### NMR spectroscopy

For the *in situ* experiment, 0.0980 g ( $8.35 \times 10^{-1}$  M) CDB- $^{13}\text{C}$  RAFT agent and 0.0098g ( $1.13 \times 10^{-1}$  M) AIBN were dissolved in a 0.246 g (4.46 M) styrene and 0.246 g (5.51 M) deuterated benzene solution in a NMR tube. A stock solution containing 0.405 g ( $8.44 \times 10^{-1}$  M) CDB, 0.0397 g ( $1.12 \times 10^{-1}$  M) AIBN, 1.01 g (4.48 M) styrene and 1.00 g (5.49 M) deuterated benzene was prepared for the *ex situ* experiments. Samples were transferred to NMR tubes. In both cases the samples were flushed with ultra-high purity nitrogen for 10 min and the tube sealed. The *ex situ* reactions were run for various times at 84 °C in an oil bath, after which they were stopped by rapid freezing in liquid  $\text{N}_2$ .

## 4.2.3 Spectroscopic Instruments

### ESR instrument

The ESR equipment used was a Bruker ELEXSYS E 500 EPR spectrometer, equipped with a super X microwave bridge and frequency counter, controlled by a LINUX based workstation. The cavity used was an ER4122SHQ super high Q X-band cavity. The cavity temperature was controlled by a modified Bruker B-VT 1 000 temperature controller with a 100 K to 373 K range. This was achieved by heated nitrogen (from the temperature controller) flowing into the ESR cavity, the flow being regulated by the temperature controller and the temperature by a thermocouple situated at the bottom of the heated cavity. The temperature controller and thermocouple were calibrated by measuring the temperature of the cavity (at the sample tube position) with a digital thermometer. The cavity was pre-heated to the reaction temperature prior to reaction. Spectra were recorded in the X-band region.

### NMR instrument

Polymerization experiments were observed/monitored at 84 °C using a 600 MHz Varian <sup>Unity</sup>Inova NMR spectrometer operating at 150 MHz for the <sup>13</sup>C spectra. A 5 mm inverse detection PFG probe was used for the experiments. The probe temperature was calibrated using an ethylene glycol sample in the manner suggested by the manufacturer, using the method of Van Geet.<sup>26</sup>

## 4.2.4 Instrumental Parameters

### ESR spectrometer parameters

The magnetic field was modulated at 100 kHz, with amplitude between 0.1 and 0.5 G. Experiments were carried out at low microwave powers (2 mW), to avoid saturation. This region was experimentally determined by plotting the intensity of the transition versus the square root of microwave power (see Chapter 3, section 3.2.4).

Spectra were recorded as single 1 min scans (with time constants of 81.92 ms, sweep time of 83.89 s and modulation amplitude of 1 G) every 5 minutes for the first 4 hours of the reaction. Spectra were adjusted by subtraction of cavity scans under identical conditions. Concentrations were obtained by double integration of the ESR signal and compared with a range of TEMPO standards recorded under similar reaction conditions and in a similar concentration range to the propagating and intermediate radicals.

### NMR spectrometer parameters

During the *in situ* experiments, 128 transients (for the first 9 spectra) and 256 transients (for the last 16 spectra) with a 6  $\mu$ s ( $43^\circ$ ) pulse width, a 1.3 sec acquisition time and a 1 sec pulse delay were accumulated for each  $^{13}\text{C}$  spectrum, while 124 transients were accumulated for each DEPT spectrum. The DEPT spectra were collected using a modified DEPT sequence in which a final  $^1\text{H}$  decoupler pulse of  $45^\circ$  was used. The resultant DEPT spectra, which only contain peaks belonging to protonated carbons, were used to identify quaternary carbons peaks in the  $^{13}\text{C}$  spectra. For the *in situ* NMR experiments, the sample was inserted into the magnet at 25  $^\circ\text{C}$  and the magnet fully shimmed on the sample. A spectrum was collected at 25  $^\circ\text{C}$  to serve as a reference. The sample was then removed from the magnet and the cavity of the magnet was raised to 84  $^\circ\text{C}$ . Once the magnet cavity had stabilized at the required temperature, the sample was re-inserted and allowed to equilibrate for approximately 5 minutes. Additional shimming was then carried out to fully optimize the system and the experiments started approximately 10 min after the sample was inserted into the magnet, the exact time being noted.

The  $^{13}\text{C}$  NMR and DEPT spectra for the *ex situ* samples were obtained, at room temperature, by accumulating transients for 11 h and 5 h respectively.

Integration of spectra was carried out both manually and automatically to allow identification of species during formation. Automated integration was carried out using ACD labs 7.0  $^1\text{H}$  processor®.

### 4.2.5 ESR Calibration

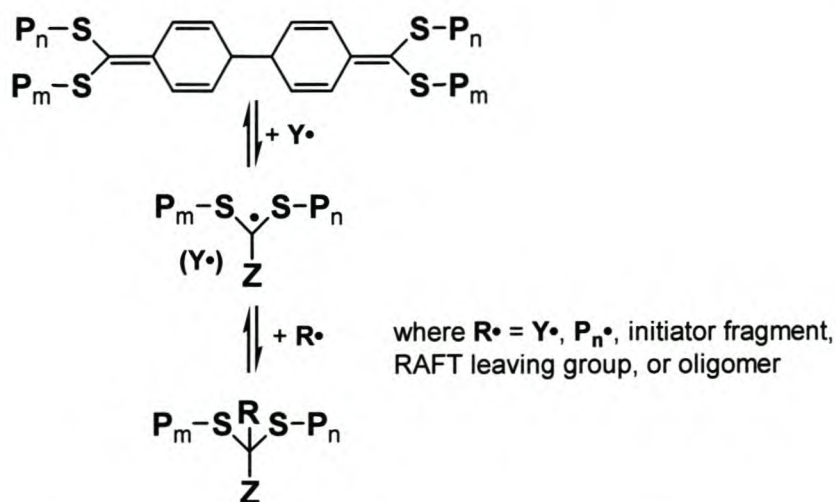
The ESR system was calibrated with a series of 2,2,6,6-tetramethylpiperidiny-1-oxyl (TEMPO) standards ( $10^{-5}$  –  $10^{-8}$  M) in benzene, under the reaction conditions at 70 and 90  $^\circ\text{C}$ . Careful integration of the intermediate radical spectra, using the techniques of a previous quantitative ESR study,<sup>27</sup> was used to calculate the intermediate radical concentrations. For the reaction at 84  $^\circ\text{C}$ , calibration parameters of the standards done at 90  $^\circ\text{C}$  were taken, as the variation in calibration parameters at 70 and 90  $^\circ\text{C}$  was less than 7 %.

## 4.3 $^{13}\text{C}$ NMR and ESR Spectroscopy Investigations Into the Fate of the Intermediate RAFT Radicals

### 4.3.1 $^{13}\text{C}$ NMR Spectroscopy Investigations: *In Situ* Reactions

The reactions of short chain species in the cumyl dithiobenzoate (CDB) mediated polymerizations of styrene were investigated at 84 °C. High initiator and CDB concentrations were chosen such that very short chains were targeted at nearly complete conversion, and high radical concentrations were present. The high radical and RAFT agent concentrations allowed the detailed examination of the nature and concentrations of both radical and non-radical species during the reaction. The probability of side reactions, such as termination of intermediate radicals, was enhanced, due to the high concentrations of the potential reactants that were present.

Reactions were run under identical conditions for each of the experimental techniques. The most likely site of termination reactions of intermediate radicals (by either propagating or intermediate radicals) is at the dithioester carbon, although it has been suggested that bonding through the delocalized ring system may also be possible (Scheme 4.2).<sup>28</sup> To investigate the formation of possible non-radical intermediate RAFT termination products, a series of  $^{13}\text{C}$  NMR experiments was conducted by employing a  $^{13}\text{C}$  enriched cumyl dithiobenzoate (CDB- $^{13}\text{C}$ ) RAFT agent (the dithioester carbon being labeled). Preliminary *in situ*  $^{13}\text{C}$  NMR reactions indicated that due to the fast reaction rates of these reactions at 84 °C, the acquisition period of successive transients that can be accumulated for each  $^{13}\text{C}$  NMR spectrum, has to be short. However, this would result in a very low signal to noise ratio for each recorded  $^{13}\text{C}$  NMR spectrum. By employing a 97-99%  $^{13}\text{C}$  enriched CDB RAFT agent an approximate 88-fold enhancement in signal to noise (the natural abundance of  $^{13}\text{C}$  is approximately 1%) is obtained for the peaks. This should enable the observation of any possible terminated (reversible or irreversible) intermediate products that might form during the course of the reaction. Analogous reactions were run with the unlabeled CDB RAFT agent to aid in peak assignment.



**Scheme 4.2** Possible termination process involving termination of the intermediate radical.

From Scheme 4.2, it can be seen that products of termination of intermediate RAFT radicals will result in the formation of a (labeled) *quaternary* dithioester carbon. Identification of these labeled quaternary carbons in a  $^{13}\text{C}$  NMR spectrum was done by comparison to the corresponding DEPT (distortionless enhancement by polarization transfer) spectrum, as only peaks corresponding to protonated carbons appear in DEPT spectra. According to theoretical  $^{13}\text{C}$  NMR predictions (ACD labs 7.0  $^{13}\text{C}$  NMR Predictor®) of quaternary carbons of any reversible or irreversible intermediate terminated products that might form during the reaction, will result in peaks appearing between 60 and 80 ppm in a typical  $^{13}\text{C}$  spectrum. Thus, the 50 - 80 ppm regions of the  $^{13}\text{C}$  NMR spectra were targeted.

A solution containing  $8.35 \times 10^{-1}$  M CDB- $^{13}\text{C}$  and  $1.13 \times 10^{-1}$  M AIBN was dissolved in 4.46 M styrene and 5.51 M deuterated benzene in a NMR tube. The solution was polymerized *in situ* in a NMR spectrometer at 84 °C. 128 transients were collected for each of the first 9  $^{13}\text{C}$ -spectra, while 124 transients were recorded for each of the corresponding DEPT spectra. For the remaining  $^{13}\text{C}$  (and corresponding DEPT) spectra, 256 and 124 transients were recorded for each spectrum respectively. The  $^{13}\text{C}$  spectra for the *in situ* NMR reaction mediated by CDB- $^{13}\text{C}$  at 84 °C are given in Figure 4.1.

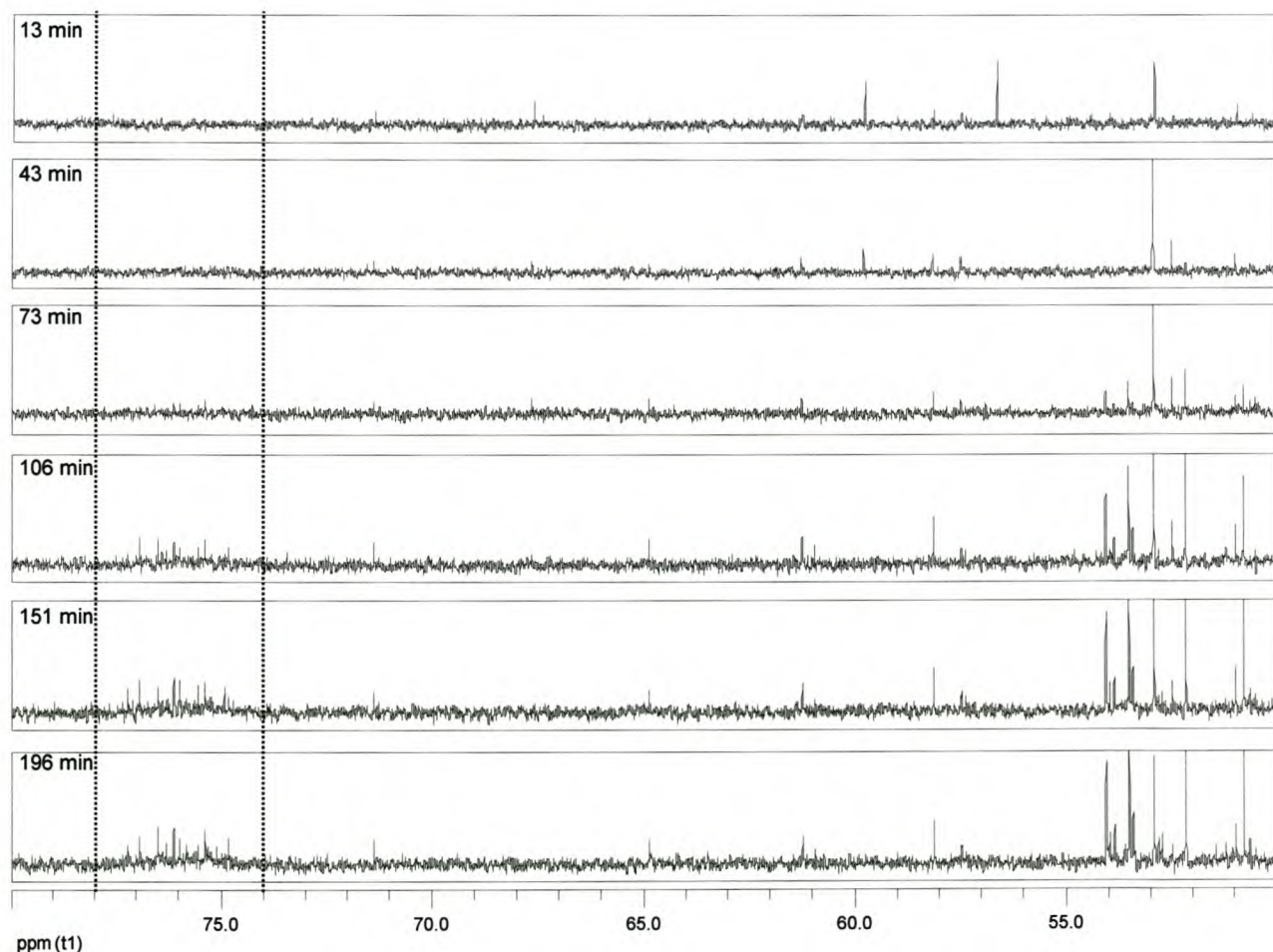


**Figure 4.1**  $^{13}\text{C}$  NMR spectra in the 50 – 80 ppm region of the solution (50 wt% in  $\text{C}_6\text{D}_6$ ) polymerization of styrene in the presence of CDB- $^{13}\text{C}$  at 84 °C, using AIBN as initiator. Spectra given were recorded at 13, 43, 73, 106, 151 and 196 min time intervals. The area between the dotted lines indicates the specific area of interest.

The spectra given were recorded at 13, 43, 73, 106, 151 and 196 min time intervals. For all the  $^{13}\text{C}$  spectra recorded during the reaction, the reader is referred to the Appendix. Several peaks due to quaternary carbons were detected in the 74 – 78 ppm region at intermediate to long reaction times, which were suspected to be due to intermediate radical terminated products. They were identified as quaternary peaks by comparison to the corresponding DEPT spectra (Figure 4.2). The peak intensities (and implied concentrations) of the potential terminated species were extremely low.

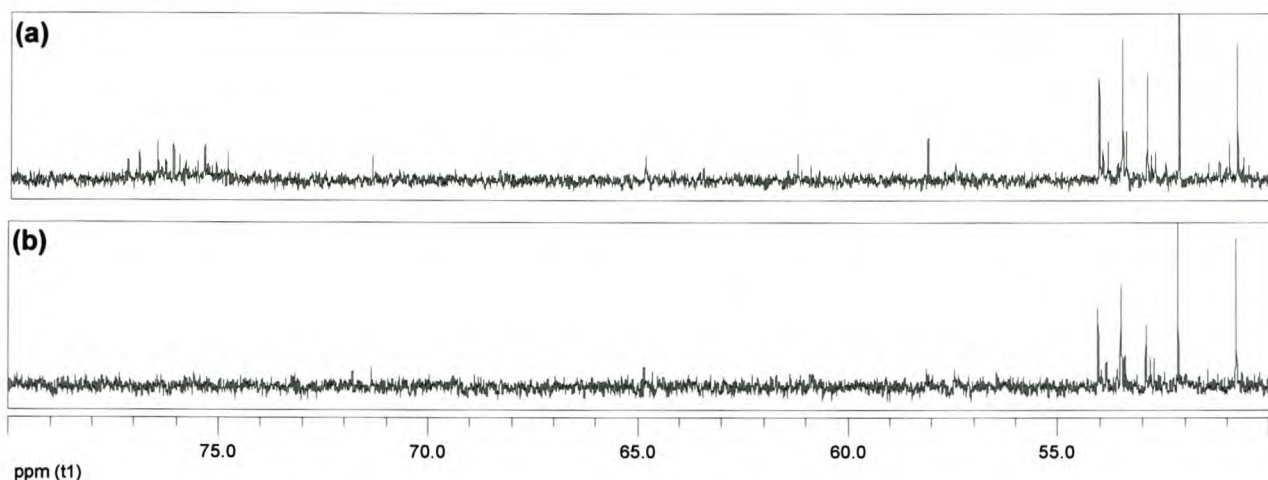


**Figure 4.2** Comparison of the  $^{13}\text{C}$  spectrum recorded at 181 min, to the corresponding DEPT spectra. (a)  $^{13}\text{C}$  spectrum, 181 min, 256 scans; (b)  $^{13}\text{C}$  DEPT spectrum, 191 min, 124 scans.

Very low concentrations of labeled impurities, that were only detectable due to the  $^{13}\text{C}$  enrichment, were present in the initial synthesized CDB- $^{13}\text{C}$  RAFT agent. Some of these impurities participated in the reaction, but their low concentration made it extremely unlikely that any quaternary carbons generated by radical addition (termination) to these centers would be detectable. There was no time correlation between the disappearance of the impurity peaks and the appearance of peaks in the region from 74 – 78 ppm.

The observed quaternary carbon peaks exhibited chemical shifts that corresponded well (within uncertainties) with predictions (ACD labs 7.0  $^{13}\text{C}$  NMR Predictor®) for the signal due to the dithioester carbon of dithiobenzoate species formed by termination of intermediate radicals. Examples of species that could give these signals are shown in Figure 4.3. The selection of potential terminated species given in Figure 4.3 were all but random, but instead based on  $^1\text{H}$  NMR data obtained from *in situ*  $^1\text{H}$  NMR experiments done with the same stock solution under similar reaction conditions (Chapter 5). This is explained below. Through further analysis of the obtained  $^{13}\text{C}$  spectra, it was suspected that the RAFT mediated reactions might show extreme selectivity and control during the time of reaction. This prompted the use of  $^1\text{H}$  NMR spectroscopy to investigate these RAFT systems. This will be discussed in section 4.3.3 and Chapter 5. At this stage, it will suffice to mention that from these  $^1\text{H}$  NMR experiments, the dithiobenzoate species present in the reaction could be identified and their concentration evolution with reaction time followed. By observing the type and concentration of species present at a specific time, educated guesses could be made about the most probable intermediate terminated species that might form

at a specific time. The  $^1\text{H}$  NMR experiments will be discussed in detail in Chapter 5. Quaternary  $^{13}\text{C}$ -peaks, corresponding to other species that are also expected to be present in these RAFT reactions, were predicted not to occur near the 74 - 78 ppm region under investigation. A list of all the species considered and the predicted chemical shifts for their respective quaternary dithioester carbons are given in the Appendix.

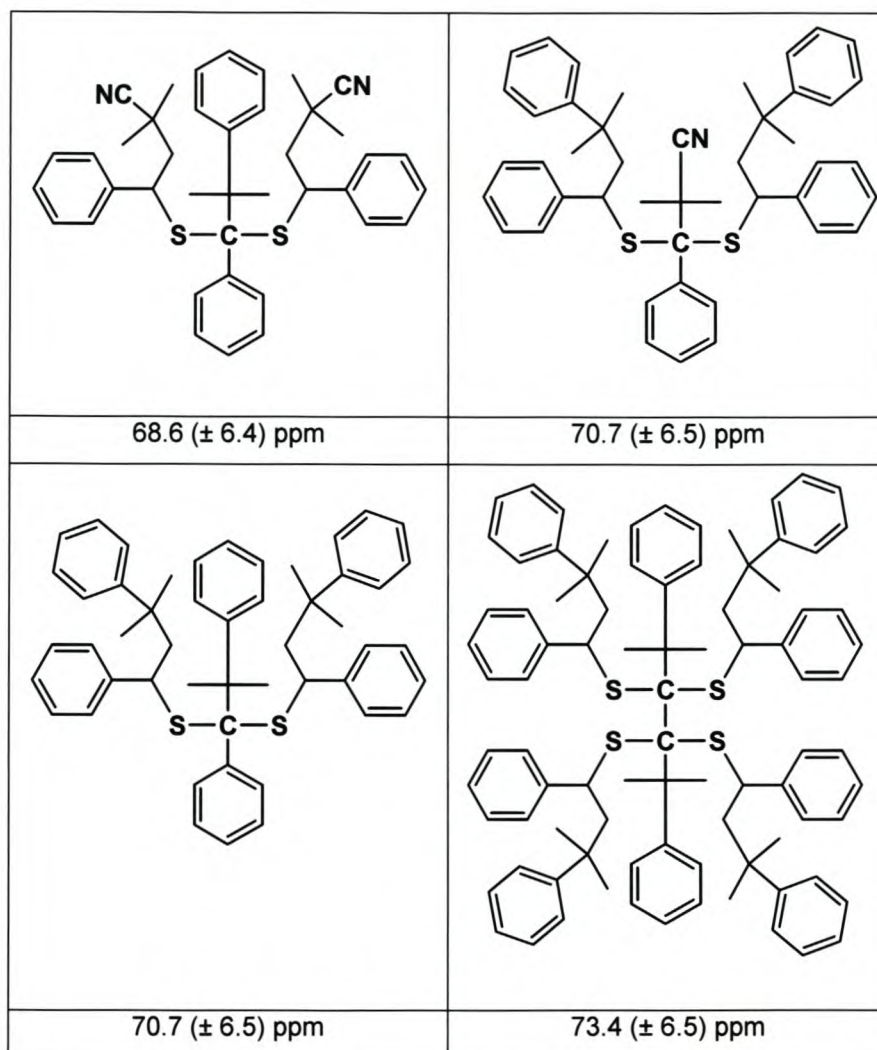


**Figure 4.3** Examples of possible structures, predicted chemical shifts (and uncertainties) of the quaternary dithioester carbon in species formed by the termination reactions of intermediate radicals, corresponding to the observed peaks in the 74 – 78 ppm region of the  $^{13}\text{C}$  NMR spectra of the reaction mediated by CDB- $^{13}\text{C}$ .

The abovementioned *in situ* reaction mixture mediated by CDB- $^{13}\text{C}$  was then left to cool down to room temperature and 256 transients again collected via  $^{13}\text{C}$  NMR spectroscopy. From comparison with the last *in situ* spectrum collected at 84 °C (Figure 4.4), conclusions about the stability of the (potential intermediate terminated) species that give rise to the peaks observed in the 78 - 74 ppm region, can be made. Peaks appearing in the 78 - 74 ppm region of the  $^{13}\text{C}$  spectrum collected at room temperature will be from quaternary carbon-containing species that are stable at room temperature. Peaks that appear in the spectrum obtained during the *in situ* reaction at 84 °C are suspected to be due to terminated intermediate species as well as transient species being present in the reaction mixture at 84 °C.

The comparison given in Figure 4.4 indicates that there seems to be some transient terminated species present in the reaction mixture at 84 °C. The low signal to noise ratio of the spectrum given in Figure 4.4 (b) made the identification and assignment of peaks very difficult. To increase the low signal to noise ratio of the spectra,  $^{13}\text{C}$  transients were collected for 11 h (17 144 transients) at room temperature on the “cooled down” reaction mixture. As the signal to noise ratio has a square root dependence on the number of transients collected for each spectrum, and increase from 256 to 17 144 of transients collected for each spectrum (Figure 4.4 (b) and (c) respectively), will have a ca. 8 fold increase in signal to noise ratio. With a ca. 8 fold increase in signal to noise ratio (Figure 4.4 (c)), it can be seen that a variety of potential terminated species are present and stable at 25 °C.

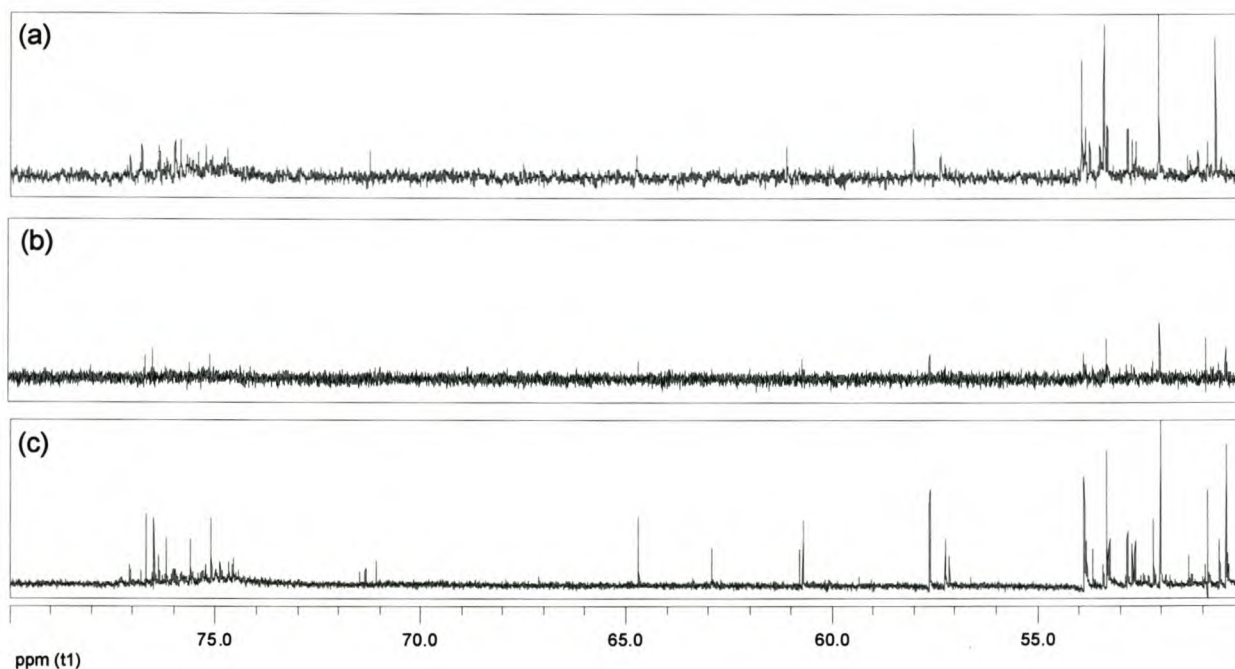


**Figure 4.4** Spectra of the CDB- $^{13}\text{C}$  reaction after 331 min reaction time at (a) 84 °C, 256 scans; (b) room temperature, 256 scans; (c) room temperature, 17144 scans.

A duplicate *in situ*  $^{13}\text{C}$  NMR reaction was run with unlabeled CDB ( $8.44 \times 10^{-8}$  M), AIBN ( $1.11 \times 10^{-1}$  M), styrene (4.44 M) and deuterated benzene (5.54 M) under similar reaction conditions as mentioned above.  $^{13}\text{C}$  NMR and DEPT spectra were again recorded alternatively throughout the reaction, in a similar manner as described for the  $^{13}\text{C}$ -labeled reaction above. No peaks in the 74 – 78 ppm region corresponding to those seen in the CDB- $^{13}\text{C}$  *in situ* reaction could be detected. This confirms the assignment of the  $^{13}\text{C}$  peaks observed in the 74 – 78 ppm region of the reaction mediated by CDB- $^{13}\text{C}$ , to labeled quaternary carbons.

In an attempt to increase the low signal to noise ratio of the *in situ* reactions polymerized with unlabeled CDB, *ex situ* reactions were performed. The reactions were stopped by snap freezing at specific times and  $^{13}\text{C}$  transients accumulated for long periods of time.

### 4.3.2 *Ex Situ* Reactions

A duplicate reaction, with the same reactant concentrations as mention above, was run with unlabeled CDB in an oil bath heated to 84 °C. The reaction was stopped at 181 min by rapid freezing in liquid nitrogen.  $^{13}\text{C}$  spectra of the reaction mixture were recorded for much longer (17144 scans, versus 128 scans for the enriched spectra), at room temperature, resulting in a significantly higher signal to noise ratio for the unlabeled CDB reaction spectra than that of the enriched CDB reaction spectra (Figure 4.5). However, there were no detectable peaks in the 74 – 78 ppm region for the unlabeled CDB spectra, again indicating that the quaternary peaks detected at the same reaction time in this region, using labeled CDB, were due to the enriched dithioester carbon, and supports the assignment of terminated intermediate RAFT species. Further evidence for this assignment is now discussed, in terms of both  $^1\text{H}$  NMR and ESR spectroscopic observations of the reaction.

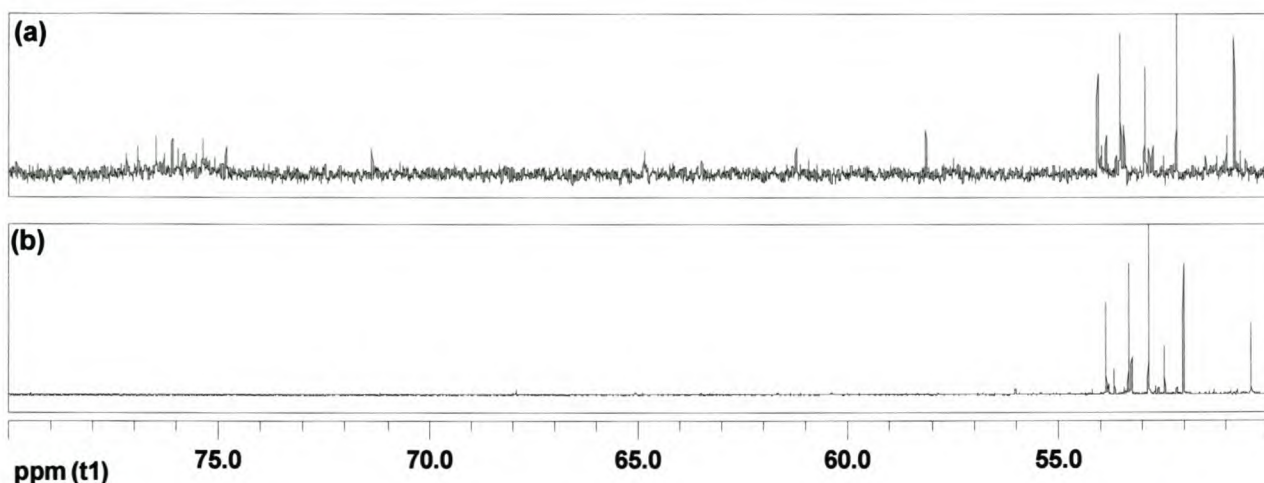


**Figure 4.5** (a) Spectrum of the CDB- $^{13}\text{C}$  reaction at 84 °C after 181 min, 256 scans; (b) spectrum of the unlabeled CDB at room temperature, 181 min, 17144 scans.

### 4.3.3 *In Situ* ESR Spectroscopy Reactions

To investigate the time evolution profile of the intermediate radical concentration ( $c_Y$ ) for the *in situ*  $^{13}\text{C}$  NMR reactions discussed above, an *in situ* ESR reaction was done (at 84 °C) on a sample containing a similar reaction mixture as used in the labeled *in situ*  $^{13}\text{C}$  NMR reaction ( $8.35 \times 10^{-1}$  M CDB RAFT agent,  $1.14 \times 10^{-1}$  M AIBN, 5.49 M benzene and 4.48 M styrene). The characteristic  $c_Y$  profile (Figure 4.6), exhibiting an initial period of no or very little signal (60 min), followed by a rapid increase (around 70 min) to a maximum (at ca. 110 min), whereafter  $c_Y$  decreases with radical flux, was observed.

The peaks appearing in the 74 – 78 ppm region of the labeled  $^{13}\text{C}$  NMR reaction were not present during the initial stages of the *in situ* reaction, but formed and increased in intensity after about 70 min, when the

intermediate radical concentration was rapidly increasing (Figure 4.6). The implication of this observed behavior will be discussed below.

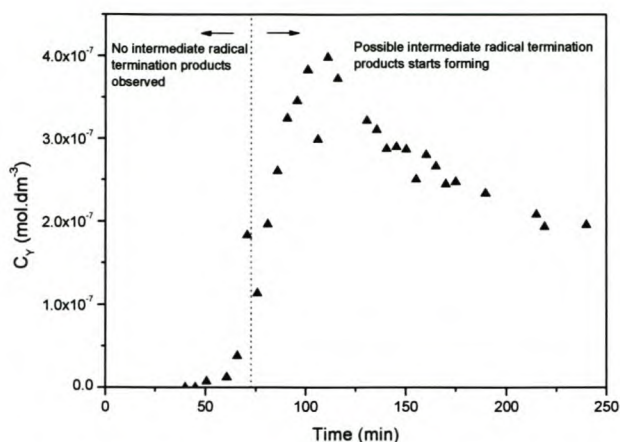


**Figure 4.6** Intermediate radical concentration evolution for the *in situ* ESR solution polymerization of styrene in the presence of CDB at 84 °C, using AIBN as initiator.

It was found by analysis of subsequent  $^{13}\text{C}$  spectra recorded for the labeled CDB *in situ* reaction that the relative concentrations of the dithiobenzoate species, formed during the early stages of the reaction, could be followed with time (Figure 4.7). This discovery led to the subsequent investigations of these reactions via  $^1\text{H}$  NMR spectroscopy, which will be discussed in Chapter 5. The species that could be identified during the early stages of the reactions were the original labeled cumyl dithiobenzoate RAFT agent (CD), the cumyl (C) endcapped dithiobenzoate (D) species with one added monomer unit (CSD), and the cumyl endcapped dithiobenzoate species with two added monomer units ( $\text{CS}_2\text{D}$ ). The structures of the species are given in Figure 4.8.

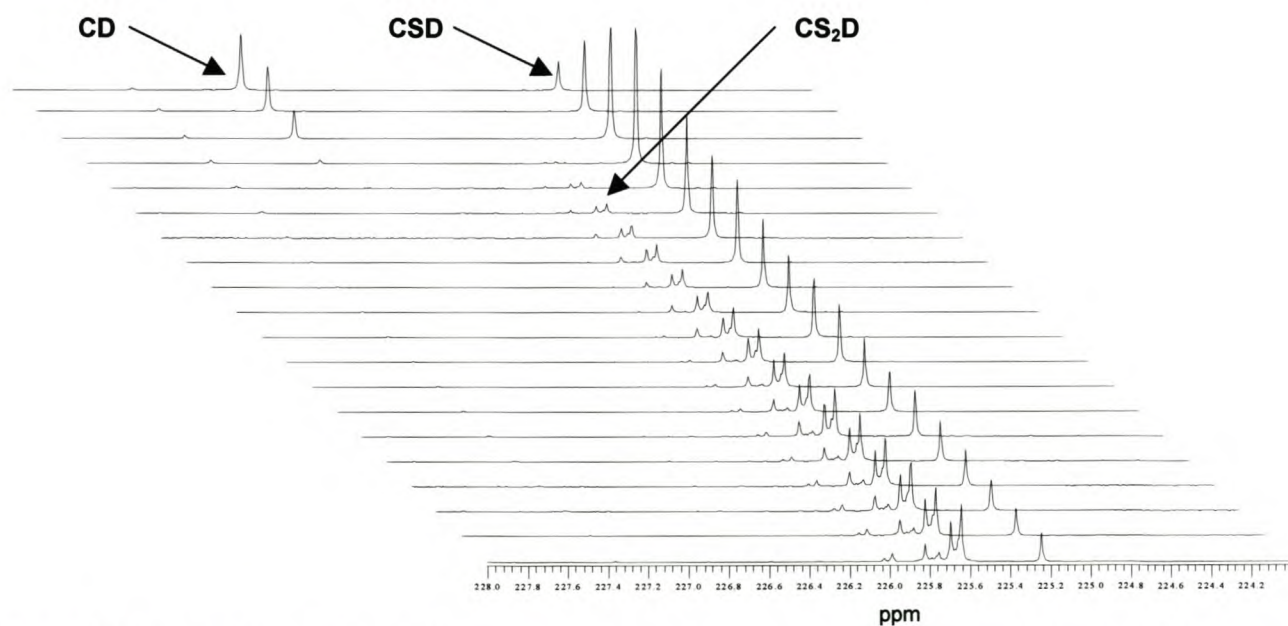


**Figure 4.7** Successive  $^{13}\text{C}$  spectra (in the 228 - 224 ppm region) of the *in situ* polymerization mediated by CDB- $^{13}\text{C}$  used to follow the time evolution of the species in the reaction of a solution containing,  $8.35 \times 10^{-1}$  M CDB- $^{13}\text{C}$ ,  $1.13 \times 10^{-1}$  M AIBN, 4.46 M styrene and 5.51 M deuterated benzene at 84 °C.

The time dependencies of the concentrations of the dithiobenzoate species were determined by integration of relevant peaks, relative to the solvent (benzene) peaks, which was assumed to be of constant concentration during the reaction. Even though the concentrations of the species in the reaction mixture are not directly related to the integrals of their corresponding peaks in  $^{13}\text{C}$  spectra, their integrals could be used as a first approximation of the relative concentrations of the various species during the reaction. From this  $^{13}\text{C}$  data, and particularly from the  $^1\text{H}$  NMR experiments done afterwards, it was seen that the early reaction is extremely selective, particularly with respect to fragmentation. This means that almost no chains reach a degree of polymerization greater than unity until all of the initial RAFT agent adds a single monomer unit. Only after all of the initial RAFT agent has been consumed (after approximately 50 min), will another styrene unit add. Thus all of the initial RAFT agent, species CD, will add a single monomer unit to form species CSD, before adding another monomer unit, thus forming species  $\text{CS}_2\text{D}$ .

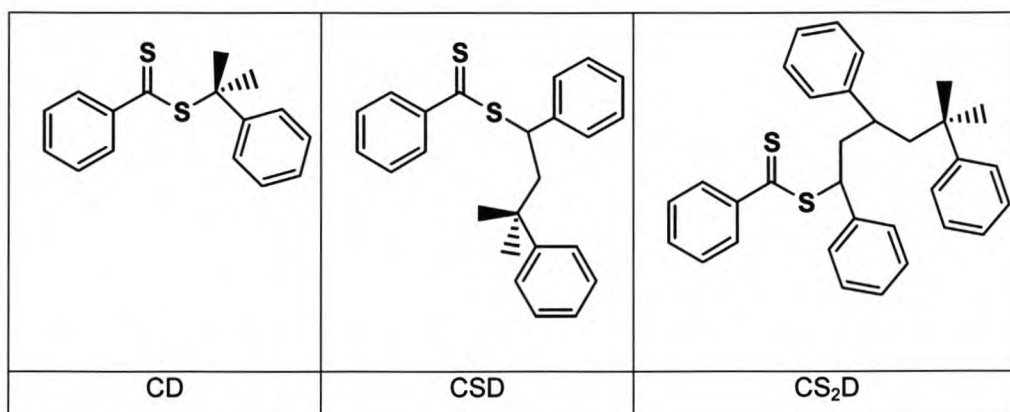


**Figure 4.8** The structures of the observed dithiobenzoate species in the reaction mixture.

The observed selectivity is directly related to the addition and fragmentation rate coefficients of the species involved in the early reaction (the “initialization” period, before all of the initial RAFT is consumed), and is discussed in detail in Chapter 5. The selectivity results in the successive formation of intermediate radicals with progressively higher radical stabilities. During the initialization period (0 – 55 min), intermediate radicals of the type C-D-C, CS-D-C and CS-D-SC will be present. These intermediate radicals are not stable enough to produce detectable ESR signals. After the initialization period, as another styrene unit adds to the growing chains, intermediate radicals of the type  $\text{CS}_2\text{-D-SC}$  and  $\text{CS}_2\text{-D-S}_2\text{D}$  form. Such radicals are stable enough to be detected by ESR spectroscopy, and are responsible for the sudden increase in detected intermediate radical concentration. This was confirmed by *in situ* ESR spectra of the system. The intermediate radical concentrations were very low early in the reaction (0 – 60 min), increased rapidly (60 – 110 min), and reached a maximum (at 110 min) some time after the initialization period was complete. The maximum concentration occurred when *both* growing chains attached to the dithiobenzoate moiety contain at least one monomer unit. The time evolution of the intermediate radical and species CD, CSD and  $\text{CS}_2\text{D}$  concentrations determined from ESR and  $^{13}\text{H}$  NMR data respectively are shown in Figure 4.9.

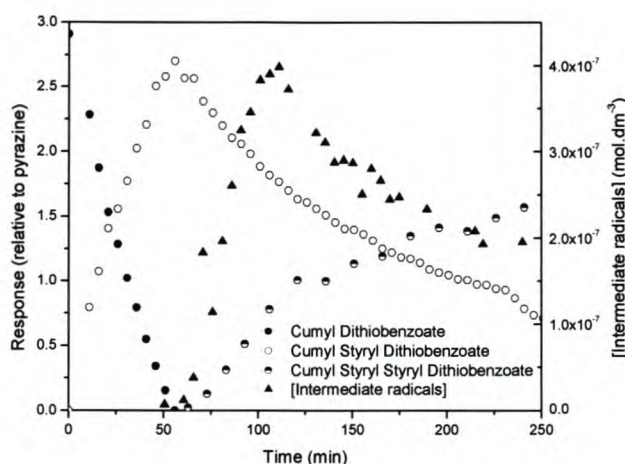


**Figure 4.9** Intermediate radical concentration (by ESR), CD, CSD and CS<sub>2</sub>D (<sup>13</sup>C NMR)-time profiles for the solution (50 wt% in benzene or C<sub>6</sub>D<sub>6</sub>) polymerization of styrene in the presence of CDB at 84 °C, using AIBN as initiator.

Since the intermediate radical concentration is negligible during the early stages of the reaction, i.e. during the “initialization” period, little termination of these species in this period is expected. This is consistent with the lack of observed peaks in the 74 – 78 ppm region in the <sup>13</sup>C spectra during this period. The rate of termination of intermediate radicals would be expected to be much higher once significant concentrations of intermediate radicals have formed, which occurred after about 60 minutes, reaching a maximum at 110 minutes, when most of these species will consist of two cumylstyryl chains attached to the dithiobenzoate group (CS<sub>2</sub>D). It is near this time that the peaks in the 74 – 78 ppm region in the <sup>13</sup>C spectra appear to increase in concentration most rapidly. The correlation between intermediate radical concentration and the formation of these peaks strongly supports the hypothesis that these peaks correspond to the termination product of reactions of intermediate radicals.

At this stage, it is thought that some explanation should be given as to why species resulting from termination of intermediate radicals have been found in this study, and not in others, as this topic has been extensively investigated. The concentrations of the termination products are normally extremely low with respect to other chains in a “typical” RAFT reaction, making detection difficult. Very high initiator and RAFT agent concentrations were used to increase the (propagating and intermediate) radical concentrations, thereby enhancing the concentrations of products of termination reactions of both propagating and intermediate radicals. This study used a <sup>13</sup>C-labeled dithioester at the carbon where the reaction of intermediate radicals is expected to occur, leading to a signal enhancement by a factor of about 88 times. Even then, the observed signals are very weak. Target chain lengths were very low, allowing both viscosity and the number of different species formed to be kept low, which lead to narrow, well-defined NMR signals.

## 4.4 Conclusions

*In situ* <sup>13</sup>C NMR spectroscopy observations of the termination products of the intermediate radicals have been made. The observed intermediate radical termination products occurred at a time that corresponds to

an observed maximum in the intermediate radical concentration, as determined ESR spectroscopy. The reaction is very specific during these initial stages, showing a very strong preference to add a single monomer unit to all of the initial RAFT agent, before adding a second monomer unit. The *in situ* observation of the formation of species by termination of intermediate radicals in CDB mediated free radical polymerization of styrene implies that extra termination events are occurring in these reactions, other than the normal combination of propagating radicals. Rate retardation will thus occur compared with an analogous conventional free radical polymerization. The possibility exists that a large fraction of the intermediate radical termination products might be due to termination by initiator fragments or other short chain radicals, due both to steric constraints and the selectivity of the fragmentation step towards producing high concentrations of the shorter, tertiary, propagating radicals, as seen by both  $^{13}\text{C}$  and  $^1\text{H}$  NMR (to be discussed in Chapter 5). Precise assignments of these terminated species (and whether the reactions that form these are reversible), and the relative frequency of these termination events (and the resulting degree of retardation) still needs to be investigated.

Although it has been shown that this reaction will lead to radical loss events and therefore rate retardation, it might not be the only such cause. The cause(s) of rate retardation can only reliably be proven by quantitative analysis of rate retardation and corresponding amounts of termination products. However, the occurrence of this intermediate radical termination reaction does mean that reactions that define the original accepted RAFT mechanism should be amended to include intermediate radical termination reactions. It also indicates that the theory of Monteiro *et al.*,<sup>1,11,19</sup> which cites intermediate radical termination as a probable cause for rate retardation, is likely to be true. This does however not discount the theory of a slow rate coefficient for fragmentation of the intermediate radical as a cause for rate retardation, as proposed by Barner-Kowollik *et al.*,<sup>8,12,14,17,20-23</sup> but significantly complicates investigations aimed at resolving the values for the rate coefficients for the addition and fragmentation of the intermediate radical.

## References

1. Kwak, Y.; Goto, A.; Tsujii, Y.; Murata, Y.; Komatsu, K.; Fukuda, T. *Macromolecules* **2002**, *35*, 3026.
2. Calitz, F. M.; Tonge, M. P.; Sanderson, R. D. *Macromolecules* **2003**, *36*, 5.
3. McLeary, J. B.; Calitz, F. M.; McKenzie, J. M.; Tonge, M. P.; Sanderson, R. D.; Klumperman, B. *Macromolecules* **2003**, *Submitted*.
4. Hawthorne, D. G.; Moad, G.; Rizzardo, E.; Thang, S. H. *Macromolecules* **1999**, *32*, 5457.
5. Alberti, A.; Benaglia, M.; Laus, M.; Macciantelli, D.; Sparnacci, K. *Macromolecules* **2003**, *36*, 736.
6. Du, F. S.; Zhu, M. Q.; Guo, H. Q.; Li, Z. C.; Li, F. M.; Kamachi, M.; Kajiwara, A. *Macromolecules* **2002**, *35*, 6739.
7. Laus, M.; Papa, R.; Sparnacci, K.; Alberti, A.; Benaglia, M.; Macciantelli, D. *Macromolecules* **2001**, *34*, 7269.
8. Perrier, S.; Barner-Kowollik, C.; Quinn, J. F.; Vana, P.; Davis, T. P. *Macromolecules* **2002**, *35*, 8300.
9. Vana, P.; Davis, T. P.; Barner-Kowollik, C. *Macromolecular theory and simulations* **2002**, *11*, 823.
10. Goto, A.; Sato, K.; Tsujii, Y.; Fukuda, T.; Moad, G.; Rizzardo, E.; Thang, S. H. *Macromolecules* **2000**, *34*, 402.
11. Monteiro, M. J.; de Brouwer, H. *Macromolecules* **2001**, *34*, 349.
12. Barner-Kowollik, C.; Quinn, J. F.; Morsley, D. R.; Davis, T. P. *J. Polym. Sci., Part A: Polym. Chem.* **2001**, *39*, 1353.
13. Barner-Kowollik, C.; Davis, T. P.; Heuts, J. P. A.; Stenzel, M. H.; Vana, P.; Whittaker, M. *J. Polym. Sci., Part A: Polym. Chem.* **2002**, *41*, 365.
14. Barner-Kowollik, C.; Coote, M. L.; Davis, T. P.; Radom, L.; Vana, P. *J. Polym. Sci., Part A: Polym. Chem.* **2003**, *41*, 2828.
15. Monteiro, M. J.; de Brouwer, H. *Macromolecules* **2000**, *34*, 349.
16. Vana, P.; Quinn, J. F.; Davis, T. P.; Barner-Kowollik, C. *Aust. J. Chem.* **2002**, *55*, 425.
17. Barner-Kowollik, C.; Quinn, J. F.; Nguyen, T. L. U.; Heuts, J. P. A.; Davis, T. P. *Macromolecules* **2001**, *34*, 7849.
18. Barner-Kowollik, C.; Davis, T. P.; Heuts, J. P. A.; Stenzel, M. H.; Vana, P.; Whittaker, M. *Journal of Polymer Science: Part A: Polymer Chemistry* **2003**, *41*, 365.
19. Wang, A. R.; Zhu, S.; Kwak, Y.; Goto, A.; Fukuda, T.; Monteiro, M. J. *J. Polym. Sci., Part A: Polym. Chem.* **2003**, *41*, 2833.
20. Moad, G.; Chiefari, J.; Chong, Y. K.; Krstina, J.; Mayadunne, R. T. A.; Postma, A.; Rizzardo, E.; Thang, S. H. *Polym. Int.* **2000**, *49*, 993.
21. Barner-Kowollik, C.; Vana, P.; Quinn, J. F.; Davis, T. P. *J. Polym. Sci., Part A: Polym. Chem.* **2002**, *40*, 1058.
22. Moad, G.; Chiefari, J.; Mayadunne, R. T. A.; Moad, C. L.; Postma, A.; Rizzardo, E.; Thang, S. H. *Macromol. Symp.* **2002**, *182*, 65.
23. Quinn, J. F.; Rizzardo, E.; Davis, T. P. *Chem. Comm.* **2001**, 1044.
24. Coote, M. L.; Radom, L. *J. Am. Chem. Soc.* **2003**, *125*, 1490.
25. Le, T. P.; Moad, G.; Rizzardo, E.; Thang, S. H., *PCT Int. Appl.*, **1998**, wo98/01478.

26. Van Geet, A. L. *Anal. Chem.* **1968**, *40*, 2227.
27. Tonge, M. P.; Kajiwara, A.; Kamachi, M.; Gilbert, R. G. *Polymer* **1998**, *39*, 2305.
28. Barner, L.; Quinn, J. F.; Barner-Kowollik, C.; Vana, P.; Davis, T. P. *European Polymer Journal* **2003**, *39*, 449.

# Chapter 5

## Beyond Inhibition: A $^1\text{H}$ NMR and ESR Investigation of the Early Kinetics of RAFT Mediated Polymerization

### Summary

*In situ*  $^1\text{H}$  nuclear magnetic resonance (NMR) and electron spin resonance (ESR) spectroscopy have been used to directly investigate the processes that occur during the early stages (typically the first few monomer addition steps) of an AIBN-initiated reversible addition fragmentation chain transfer polymerization of styrene in the presence of a cyanoisopropyl dithiobenzoate and cumyl dithiobenzoate RAFT agent, at 70 and 84 °C respectively.  $^1\text{H}$  NMR spectroscopy allowed the investigation of the change in concentration of important dithiobenzoate species as a function of time. Identification and concentrations of the radicals present in the system could be inferred from corresponding ESR spectroscopy data. An “inhibition” effect was observed in the cyanoisopropyl dithiobenzoate mediated polymerizations. This effect was enhanced by increasing the reaction temperature to 84 °C. However, the use of cumyl dithiobenzoate as RAFT agent prolonged this effect. This “inhibition” effect was attributed to the extreme selectivity exhibited in the RAFT process during the early stages of the reaction, which led to a difference in  $k_p$  values of resulting (different) radicals. This extreme selectivity was ascribed to progressively decreasing addition and fragmentation rate coefficients of propagating and intermediate radicals formed during the early periods of the reaction. The increase in intermediate radical concentration, and thus possible intermediate radical termination, was shown to be a probable cause for the rate retardation observed in the RAFT mediated systems investigated.

---

The  $^1\text{H}$  NMR work in this chapter was done in collaboration with James McLeary. This chapter is a slightly modified version of two papers:

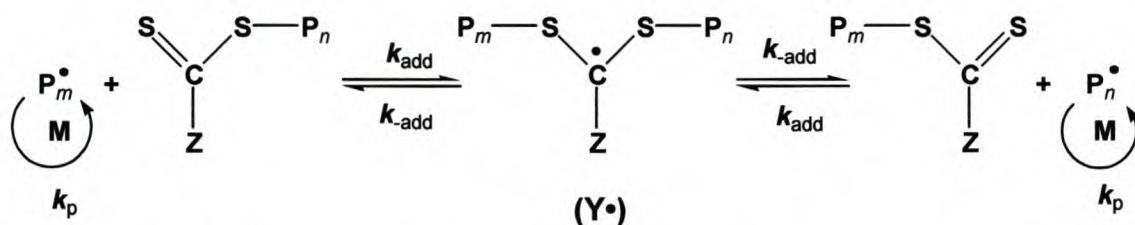
- 1) **Beyond inhibition: A  $^1\text{H}$  NMR investigation of the early kinetics of RAFT mediated polymerization with the same initiating and leaving groups**; J. B. McLeary, F. M. Calitz, J. M. McKenzie, M. P. Tonge, R. D. Sanderson, B. Klumperman; *Macromolecules*, Submitted.
- 2) **A  $^1\text{H}$  NMR investigation of the RAFT polymerization kinetics and mechanism: part two; beyond inhibition with different initiating and leaving groups**; F. M. Calitz, J. B. McLeary, J. M. McKenzie, M. P. Tonge, R. D. Sanderson, B. Klumperman; *Macromolecules*, to be submitted.

## Introduction to *in situ* $^1\text{H}$ NMR Spectroscopy

*In situ* NMR is an elegant way to investigate the kinetics of free radical polymerization reactions. Some pioneering work has been carried out,<sup>1-3</sup> but the limitations of kinetic experiments usually lie with the complexity of the system to be investigated.

*In situ* NMR investigation of radical polymerization is normally extremely complicated due to the nature of free radical polymerization. High molecular weight polymer forms very rapidly, resulting in peak broadening (two factors often contribute to this: overlap of peaks of many slightly different species, and high system viscosities) and difficulty in identifying and examining specific species (usually for the same reasons and also the very low concentrations of polymer end groups being below the detection limit of the NMR equipment). In living radical polymerization this situation is significantly different as the molecular weight increases linearly with monomer conversion and consequently does not usually involve the formation of high molecular weight polymer early in the reaction.

In Scheme 5.1 the elementary reactions for the central exchange process of the RAFT mechanism are depicted (the main focus of this chapter will be on the reactions preceding the central RAFT exchange process, but the central exchange process is used to demonstrate the importance of considering the transfer reactions as bimolecular processes). The process requires the interaction of two species, namely the incoming radical ( $P_m^\bullet$ , a propagating radical of degree of polymerization  $m$ ), which adds the thiocarbonyl thio compound, i.e., the RAFT agent.



**Scheme 5.1** The central equilibrium of the reversible addition fragmentation chain transfer process.

The relatively stable intermediate radical ( $Y^\bullet$ ) that is formed by the addition process, can fragment to release one of two radical species: the original incoming radical species ( $P_m^\bullet$ ), or the homolytic leaving group ( $P_n^\bullet$ ) that was part of the initial RAFT agent. Once the central equilibrium has set in, it is expected that the value for  $k_{\text{add}}$  will be in the order of  $10^6 \text{ s}^{-1}$  for dithiobenzoates at these temperatures.<sup>4</sup> There is currently a heated debate about the value for  $k_{\text{add}}$ ; consequently, literature values for  $k_{\text{add}}$  range from  $10^{-2}$  to  $10^4 \text{ s}^{-1}$ .<sup>5-10</sup>

There are currently a number of mysteries regarding the details of the mechanism of the RAFT process. If the central exchange process is all that controls the RAFT mediated polymerization reaction, then there are some common observations that cannot easily be explicitly explained by this mechanism. The most significant anomalies in RAFT systems are the inhibition and retardation phenomena that occur in many

polymerizations.<sup>5,8,11</sup> These anomalous phenomena have been investigated by a number of authors, and most investigations have concerned the fate of the intermediate radical species and its effects on polymerization kinetics. In this chapter the issue of an apparent “inhibition” period is addressed directly, with focus on the cause and length of the observed “inhibition” period with reference to the reaction temperature. In the first part of this chapter, the system in which both the initial RAFT agent leaving group and the initiator derived radicals are the same will be considered. In the second part of this chapter, the system in which the initial RAFT agent leaving group and the radicals resulting from initiator decomposition are different is described. Similarities and differences between these two afore-mentioned systems will also be given.

To understand the mechanism of the RAFT process, especially during the early stages of polymerization, it is important to examine the nature of the radical species in each reaction. Radical reactivities for addition and radical leaving group stabilities are very important factors that, together with reactant concentrations, determine the rates of polymerization in the RAFT mediated polymerizations investigated. The reader is referred to the review by Moad and Solomon<sup>12</sup> for an in dept discussion of this subject. At this stage, it will suffice to note that within a series, tertiary radicals are typically more stable and less reactive than secondary radicals, and that primary radicals are more reactive than secondary radicals. Substituents, as well as steric and electronic effects may also all play important roles to determine rates of reactions of these radicals with specific molecules.<sup>13,14</sup>

## 5.1 Experimental

### 5.1.1 Chemicals

#### Chemicals used

Styrene monomer (Plascon Research Centre, University of Stellenbosch, estimated purity ~99%  $^1\text{H}$  NMR) was washed with 0.3 M KOH and distilled under vacuum prior to use, to remove inhibitor and polymer. Azo bis(isobutyronitrile) (AIBN, Riedel De Haen) was recrystallized from AR grade methanol and found to be ~99% pure by  $^1\text{H}$  NMR. Deuterated benzene ( $\text{C}_6\text{D}_6$  99.6%, 0.1% TMS, Sigma-Aldrich) and benzene (AR grade, Sigma-Aldrich) were used as received.

#### Synthesis of transfer agents

The synthesis of cyanoisopropyl dithiobenzoate was carried out according to the method of Le *et al.*<sup>15</sup> and purified by liquid chromatography on a silica column using a 4.5:4.5:1 ratio of pentane: heptane: diethyl ether. The product was dried under vacuum to provide the compound with a  $^1\text{H}$  NMR purity estimated at ~98%. The synthesis of cumyl dithiobenzoate (CDB) was carried out according to the method of Le *et al.*<sup>15</sup> The RAFT agent was purified by successive liquid chromatography on silica and alumina using hexane as eluent. The product crystallized after vacuum removal of solvent and storage below  $-10\text{ }^\circ\text{C}$ . The purity was estimated by  $^1\text{H}$  NMR to be > 95%. Impurities were identified during the  $^1\text{H}$  NMR integration process and found to be unreactive on the timescale of the reaction.

### 5.1.2 Sample Preparation

#### ESR spectroscopy

A typical reaction mixture was prepared as follows. The RAFT agent and AIBN were dissolved in a benzene and monomer solution. An aliquot (0.2 g) of the solution was transferred to an ESR tube, and oxygen removed by multiple freeze-thaw cycles. The tube was sealed and transferred to the ESR cavity, which had been pre-heated to the reaction temperature. The compositions of the solutions used for ESR analysis are given in Table 5.1. In the text below the stock solutions given in Table 5.1 will be referred to as (ESR) *solutions* 1-4.

The solvent used was benzene, and the initiator used was AIBN (2,2'-(azobis(isobutyronitrile))). The monomer used was styrene (St). The RAFT agents were cyanoisopropyl dithiobenzoate (CIDB) and cumyl dithiobenzoate (CDB). All concentrations are given in mol/L.

**Table 5.1** Composition of reaction mixtures used for the *in situ* ESR polymerizations.

No	Solvent	Initiator	Monomer		RAFT agent		[M] <sub>0</sub> / [R] <sub>0</sub>	[R] <sub>0</sub> / 2[I] <sub>0</sub>
	(Benzene)	(AIBN)	Type	Conc	Type	Conc ( $\times 10^{-1}$ )		
	Conc	Conc ( $\times 10^{-1}$ )						
1	5.73	1.12	St	4.26	CIDB	8.06	5.29	36.13
2	5.68	1.10	St	4.30	CDB	6.48	6.64	29.51
3	11.2	5.31						
4	11.2	5.28			CDB	6.45	0.00	6.11

### NMR spectroscopy

Samples were prepared by dissolving the initiator and RAFT agent in a deuterated benzene and monomer solution according to the concentrations given in Table 5.2. The samples were then transferred to NMR tubes. The tubes were flushed with ultra-high purity nitrogen for 10 minutes. At that point a sealed glass tube containing the integration reference standard (pyrazine) was inserted and the NMR tubes were sealed. The use of the reference standard was solely for integration purposes. In the text below the reactant mixtures given in Table 5.2 will be referred to as (NMR) *reactions* 1-8.

The solvent used was deuterated benzene (C<sub>6</sub>D<sub>6</sub>, 99.6%), and the initiator used was AIBN. The RAFT agents were cyanoisopropyl dithiobenzoate (CIDB) and cumyl dithiobenzoate (CDB). Reactions 1, 3, 5 and 7 were polymerized at 70 °C and reactions 2, 4, 6 and 8 were polymerized at 84 °C.

**Table 5.2** Composition of reaction mixtures used for *in situ* NMR experiments.

No	Solvent	Initiator	Monomer		RAFT agent		[M] <sub>0</sub> / [R] <sub>0</sub>	[R] <sub>0</sub> / 2[I] <sub>0</sub>
	(C6D6)	(AIBN)	Type	Conc	Type	Conc ( $\times 10^{-1}$ )		
	Conc	Conc ( $\times 10^{-1}$ )						
1	6.03	1.03	St	4.06	CIDB	8.17	4.97	39.71
2	6.14	1.05	St	3.98	CIDB	7.78	5.11	37.10
3	5.40	0.834	St	4.55	CIDB	0.00	0.00	0.00
4	4.85	0.829	St	4.98	CIDB	0.00	0.00	0.00
5	5.40	1.11	St	4.55	CDB	6.67	6.82	30.09
6	5.40	1.11	St	4.55	CDB	6.67	6.82	30.09
7	5.40	0.834	St	4.55	CDB	0.00	0.00	0.00
8	4.85	0.829	St	4.97	CDB	0.00	0.00	0.00

### 5.1.3 Spectroscopic Instruments

#### ESR instrument

A Bruker ELEXSYS E 500 EPR spectrometer equipped with a super X microwave bridge and frequency counter, controlled by a LINUX-based workstation, was used. The cavity used was an ER4122SHQ super high Q X-band cavity. The cavity temperature was controlled by a modified Bruker B-VT 1000 temperature controller with a 100 K to 373 K range. This was achieved by heated nitrogen (from the temperature controller) flowing into the ESR cavity, the flow being regulated by the temperature controller and the temperature by a thermocouple situated at the bottom of the heated cavity. The temperature controller and thermocouple were calibrated by measuring the temperature of the cavity (at the sample tube position) with a digital thermometer. Spectra were recorded in the X-band region, with the cavity pre-heated to the reaction temperature.

#### NMR instrument

NMR spectra were collected on a 600 MHz Varian <sup>Unity</sup>Inova spectrometer. A 5 mm inverse detection PFG probe was used for the experiments and the probe temperature was calibrated using an ethylene glycol sample in the manner suggested by the manufacturer, using the method of Van Geet.<sup>16</sup>

### 5.1.4 Instrumental Parameters

#### ESR spectrometer parameters

The magnetic field was modulated at 100 kHz, with a modulation amplitude of 1 G. Experiments were carried out at low microwave powers (2mW), to avoid saturation. (The choice of microwave power used was described in section 3.2, Chapter 3.)

For the time evolution studies of the intermediate radical concentration, spectra were recorded as single 1 min scans (with time constants of 81.92 ms, sweep time of 83.89 s (1024 points) and modulation amplitude of 1 G) every 3 minutes for the first hour and then every 5 minutes for the remainder of the time. Spectra were adjusted by subtraction of cavity scans under identical conditions. To detect the propagating radicals in some reactions, the modulation amplitude was increased to 2 G, and 4 or 16 single scans (with sweep time of 83.89 s) accumulated for each spectrum. Concentrations were obtained by double integration of the ESR signal, and compared with those of a range of TEMPO standards, recorded under similar reaction conditions (i.e. the same solvent, temperatures and ESR parameters).

### NMR spectrometer parameters

$^1\text{H}$  spectra were acquired with a  $3\ \mu\text{s}$  ( $40^\circ$ ) pulse width and a 4 sec acquisition time. For the  $^1\text{H}$  kinetic experiments, samples were inserted into the magnet at  $25\ ^\circ\text{C}$  and the magnet fully shimmed on the sample. A spectrum was collected at  $25\ ^\circ\text{C}$  to serve as a reference. The sample was then removed from the magnet and the cavity of the magnet was raised to the required temperature ( $70\ ^\circ\text{C}$  or  $84\ ^\circ\text{C}$ ). Once the magnet cavity had stabilized at the required temperature, the sample was re-inserted (time zero) and allowed to equilibrate for approximately 5 minutes. Additional shimming was then carried out to fully optimize the system and the first spectra were recorded approximately 10 min after the sample was inserted into the magnet.

Integration of spectra was carried out both manually and automatically to allow identification of species during formation. Automated integration was carried out using ACD labs 7.0  $^1\text{H}$  processor®.

#### 5.1.5 ESR Calibration

The ESR system was calibrated with a series of 2,2,6,6-tetramethylpiperidiny-1-oxy (TEMPO) standards ( $10^{-5}$  –  $10^{-8}$  M) in benzene, under the reaction conditions at  $70$  and  $90\ ^\circ\text{C}$ . Careful integration of the ESR spectra, based on techniques of a previous quantitative ESR study,<sup>17</sup> was used to calculate the radical concentrations. For the reactions at  $84\ ^\circ\text{C}$ , calibration parameters of the standards measured at  $90\ ^\circ\text{C}$  were used, as the variation in calibration parameters at  $70$  and  $90\ ^\circ\text{C}$  was found to be less than 7 %. The reason for the difference in one calibration temperature ( $90\ ^\circ\text{C}$ ) and polymerization temperature used ( $84\ ^\circ\text{C}$ ), was that a long period of instrument failure occurred after calibrations could be run at  $70\ ^\circ\text{C}$ , but before calibrations at  $84\ ^\circ\text{C}$  could be run.

## RAFT Mediated Polymerization with the Same Initiating and Leaving Groups.

After obtaining unexpected and unusual results from the initial *in situ* ESR spectroscopy experiments (Chapter 3), *in situ*  $^1\text{H}$  NMR and ESR spectroscopy experiments were performed on similar solutions and under the same experimental conditions. This was done in an attempt to confirm, contradict or clarify some of the conclusions and observations made during the initial ESR spectroscopy experiments. From the  $^1\text{H}$  NMR spectroscopy data, an indication of the types of species present in the solution at a specific time interval could be determined. Together with the ESR spectroscopy data, conclusions could be made about the types and stabilities of the radicals present, and therefore predictions about the addition and fragmentation rates of the various radicals could be made. The results obtained will be discussed in light of a proposed reaction mechanism for the specific reactions. A possible explanation for the anomalous behavior observed in certain RAFT systems will also be given.

The use of cyanoisopropyl dithiobenzoate as a RAFT agent together with styrene monomer and AIBN as initiator, results in a single active tertiary radical species in the system. This system is far less complex than the case in which two different tertiary radical species are present,<sup>18</sup> as is the case when cumyl dithiobenzoate is used as RAFT agent together with AIBN. It should be noted that the choice of styrene as a monomer means that the vast majority of radicals formed from propagation reactions should be secondary radicals.

Temperature plays an important role in the rate of reactions in a RAFT mediated polymerization. For that reason two different temperatures (70 °C and 84 °C) were used to determine the validity of the results obtained and the conclusions thus drawn.

### 5.2 Reactions Mediated by Cyanoisopropyl Dithiobenzoate

An *in situ*  $^1\text{H}$  NMR experiment was carried out for a period of 4 hours at 70 °C with a reaction mixture containing styrene monomer (4.06 M), cyanoisopropyl dithiobenzoate ( $8.17 \times 10^{-1}$  M) and AIBN initiator ( $1.03 \times 10^{-1}$  M) in benzene (6.03 M) (reaction 1, Table 5.2). A corresponding solution with cyanoisopropyl dithiobenzoate ( $8.06 \times 10^{-1}$  M), styrene (4.26 M) and AIBN ( $1.12 \times 10^{-1}$  M) in benzene (5.73 M) (solution 1, Table 5.1) was polymerized *in situ* in an ESR spectrometer at 70 °C.

Very high initiator and RAFT agent concentrations were used to target short chains at nearly full conversion. This was done to emphasize reactions that occur during the early stages of the reaction and to maximize the occurrence of possible side reactions, as termination of intermediate RAFT radicals (Chapter 4). It also limited the number of species present in the reaction mixtures, but at the same time increased the concentrations and thereby the detectability of the species present.

The  $^1\text{H}$  NMR data so obtained provides instantaneous concentrations of non-radical species in the RAFT reactions. The effect of chemically induced nuclear polarization on the apparent concentrations of the observed NMR signals in the experiments was found to be minimal under the conditions used.

Figure 5.1 shows the chemical structures of the species of interest in this study. The following naming convention will be used. Species AD is the initial RAFT agent containing the dithiobenzoate species (D) and the initial cyanoisopropyl leaving group (A), ASD is the dithiobenzoate species formed by a single styrene (S) adduct of a cyanoisopropyl radical ( $\text{A}^*$ ), while  $\text{AS}_2\text{D}$  species are formed by the second styrene adduct of the cyanoisopropyl radicals. In the various  $^1\text{H}$  NMR spectra, the peaks representing the methyl protons on the AIBN initiator and on the cyanoisopropyl endgroups of the various dithiobenzoate species were used for integration purposes. Where peak overlap made integration of the methyl peaks difficult, the peaks representing the ortho-protons on the dithiobenzoate ring of the various dithiobenzoate species were used. The AA species is formed by mutual termination of two cyanoisopropyl radicals and from geminate recombination (cage product) due to AIBN decomposition.

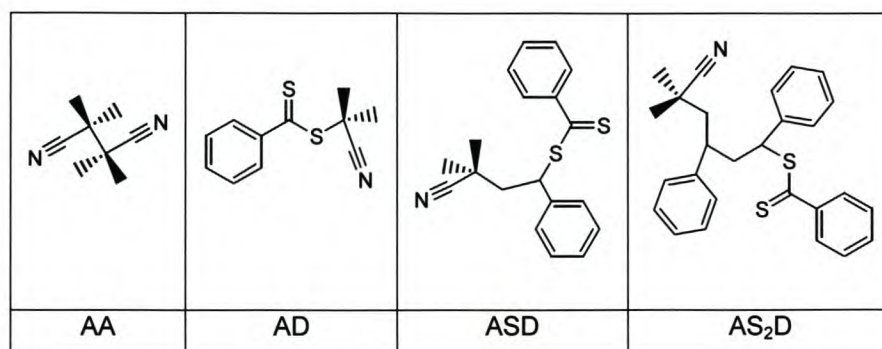


**Figure 5.1** The predominant non-radical species of interest for the investigation of the early period of the free radical polymerization of styrene in the presence of cyanoisopropyl dithiobenzoate, using AIBN as an initiator.

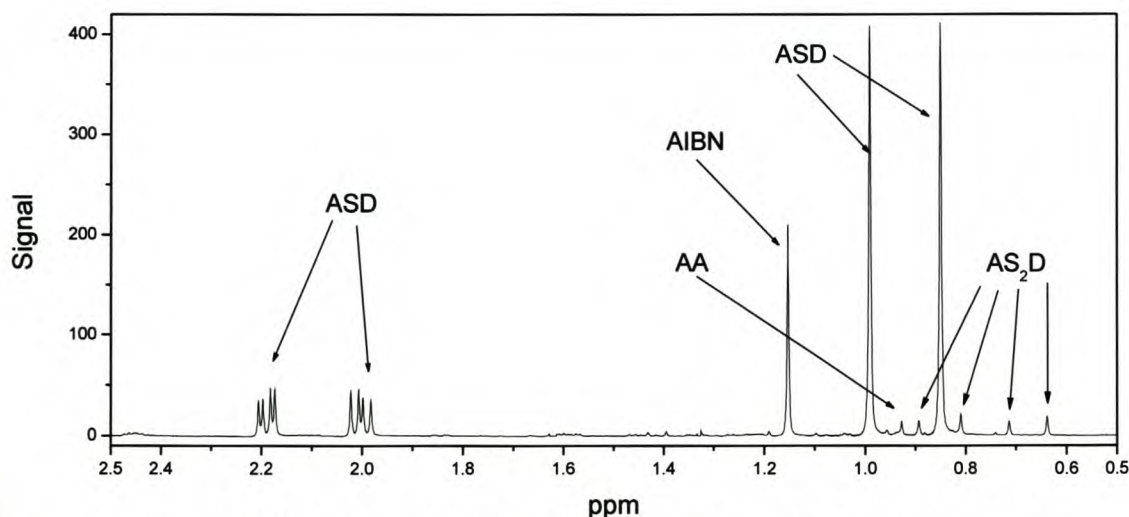


**Figure 5.2:** A typical  $^1\text{H}$  NMR spectrum between 2.5 and 0.5 ppm, directly after initialization, showing the peaks corresponding to several of the important species studied here. ASD and  $\text{AS}_2\text{D}$  are the peaks for the methyl protons of the first and second styrene adducts of the cyanoisopropyl dithiobenzoate respectively, AA the product of the termination reaction between two cyanoisopropyl radicals, and AIBN the initiator.

In Figure 5.2 a typical  $^1\text{H}$  NMR spectrum of the *in situ* reaction at 70 °C is shown, indicating the most important peaks used in this investigation. Where two peaks are indicated, diastereotopic groups were present. The  $^1\text{H}$  NMR chemical shifts of the peaks of these protons that represent the species followed in this study can be found in Table 5.3.

**Table 5.3**  $^1\text{H}$  NMR chemical shifts of the integrated species followed during the *in situ*  $^1\text{H}$  NMR reaction at 70 °C.

Methyl protons of R group $\delta$ (ppm)	Ortho protons of corresponding dithiobenzoate ring $\delta$ (ppm)	Species
Singlet 0.93	N/A	AA
Singlet 1.45	Doublet 7.71	AD
Two peaks 1.01, 0.87	Doublet 7.85	ASD
Two peaks 0.81, 0.65	Doublet 7.90	AS <sub>2</sub> D
Two peaks 0.89, 0.72	Doublet 7.79	AS <sub>2</sub> D

Figure 5.3 shows the concentration-time dependence of the dithiobenzoate species during the *in situ*  $^1\text{H}$  NMR reaction at 70 °C. A rapid decrease in concentration of the species AD and a buildup of the species ASD until the cyanoisopropyl dithiobenzoate had been completely consumed (after 50 min), was observed. At this point the concentration of species ASD reached a maximum. The nearly linear decrease of [AD] with reaction time is indicative of a pseudo-zero order reaction in [AD]. Once all of the cyanoisopropyl dithiobenzoate had been converted to ASD, the second and third monomer additions to the radical species began to increase in frequency (species AS<sub>2</sub>D and AS<sub>3</sub>D). Note that almost no formation of these species occurred before this stage, i.e. the reaction is extremely (although not completely) selective. This will be explained below.

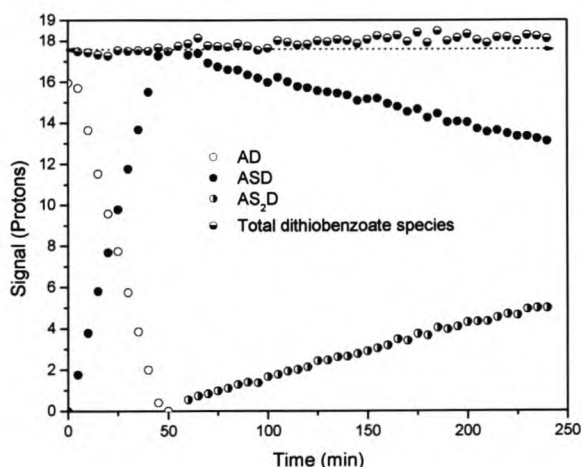


**Figure 5.3** Relative concentrations of methyl protons of the dithiobenzoate species versus time in the free radical polymerization of styrene in the presence of cyanoisopropyl dithiobenzoate, using AIBN as an initiator, polymerized *in situ* at 70 °C (Table 5.2, reaction 1).

There are several important points to note here. The first is that the conversion of the species AD to ASD is complete, with no detectable “loss” of dithiobenzoate groups to side reactions. Termination products, resulting from intermediate radical termination reactions, could not be detected during the course of the reaction (or were below the detection limits of the instrument used), implying that the concentrations of such species were below approximately  $10^{-3}$  M (the approximate detection limit) during this reaction. The same was observed for all of the  $^1\text{H}$  NMR reactions. The second point to note is that the reaction is extremely selective during the early stages of the polymerization. Only one type of radical addition (to monomer) reaction appeared to occur to any significant extent during this initial period (before 50 min), i.e., the propagation of cyanoisopropyl radicals. Very little propagation of longer chain radicals occurred until after this initial period. This also implies that the concentration of these other propagating radicals (i.e.  $\text{AS}_2^*$ , etc.) and the corresponding dithiobenzoate dormant chains ( $\text{AS}_2\text{D}$ , etc.) were very low during this period.

To facilitate further discussion, the following terms are defined:

- *Initialization* is the process by which the starting RAFT agent is consumed.
- *Initialization period* is the period in which the starting RAFT agent is consumed.
- *Initialization time* is the time required for the starting RAFT agent to be completely consumed (converted to other forms).

In Figure 5.4 the time evolution of the intermediate radical concentration ( $c_Y$ ) for the *in situ* ESR spectroscopy reaction at 70 °C is given. A comparison with the concentration-time evolution of the various dithiobenzoate species as determined by the corresponding *in situ*  $^1\text{H}$  NMR reaction is given in Figure 5.5. In the time evolution of  $c_Y$  given in Figure 5.4, an initial period up to at least 20 minutes of no (or undetectably small) intermediate radical concentrations is seen, followed by a rapid increase to a maximum after approximately 54 minutes. After reaching a maximum,  $c_Y$  decreased according to the square root of radical flux from initiator decomposition, as the concentration of initiator declined.

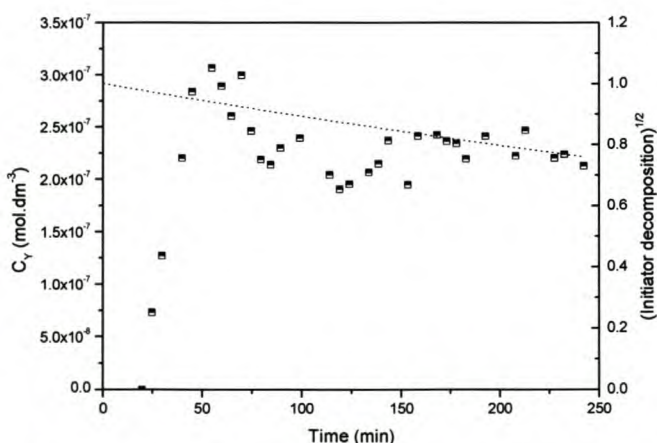


**Figure 5.4** The time evolution of  $c_Y$  (■) and the corresponding rate of initiator decomposition (···) for solution 1, Table 5.1 *in situ* ESR polymerization at 70 °C.

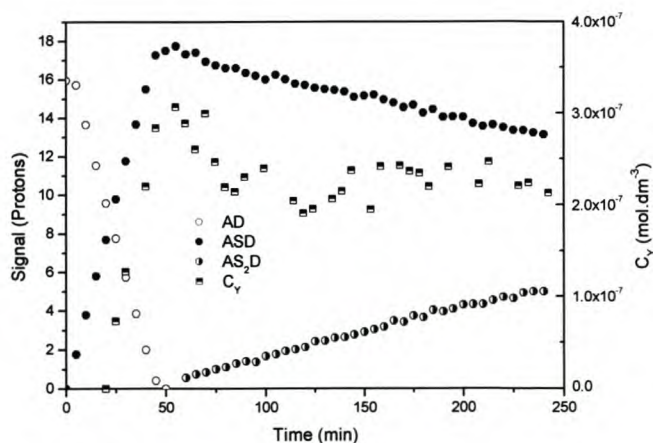


**Figure 5.5** Overlay of  $c_Y$  and the relative concentrations of the methyl protons of dithiobenzoate species versus time in the *in situ* NMR polymerization of styrene in the presence of CIDB using AIBN as an initiator, at 70 °C (reaction 1, Table 5.2).

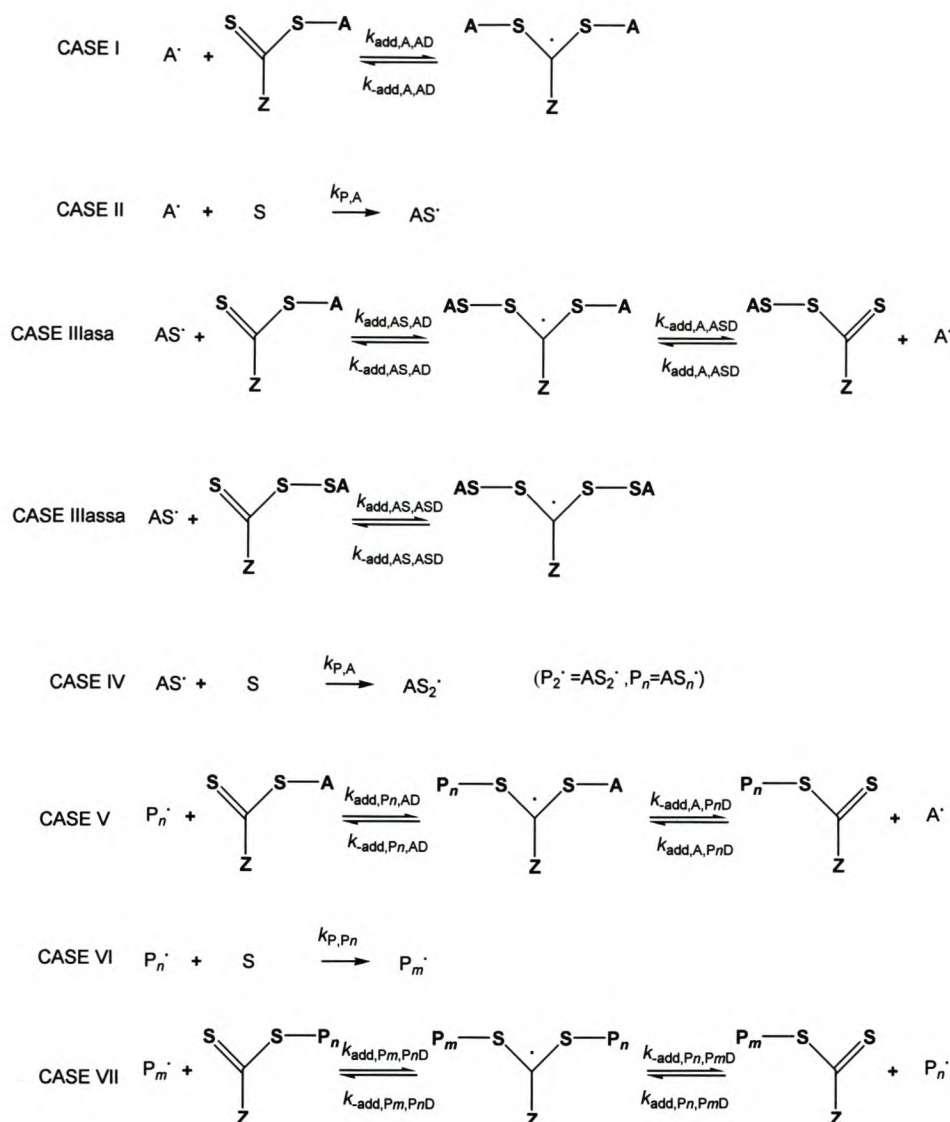
The observed decrease in  $c_Y$  corresponding to the decrease in square root radical flux can be explained by at least two possible rationales. If, after a maximum in  $c_Y$  is reached, and the RAFT system is in equilibrium, the intermediate radical concentration ( $c_Y$ ) and the propagating radical concentration ( $c_P$ ) will be in rapid equilibrium with each other according to the equation:

$$K_{\text{eq}} = \frac{c_Y}{c_P c_{PX}} \quad (5-1)$$

As  $K_{\text{eq}}$  is a constant at equilibrium,<sup>11</sup> and  $c_{PX}$  (the concentration of the chains with RAFT end groups) is constant, the ratio of  $c_Y$  to  $c_P$  must be constant. As  $c_P$  is proportional to the square root of initiator decomposition (assuming classical kinetics), so will  $c_Y$  be. Thus, a decrease in (square root) radical flux will be seen as a decrease in  $c_P$  and thus also a proportional decrease in  $c_Y$ .

A possible second explanation is that the RAFT system has not yet attained equilibrium after a maximum in  $c_Y$  is reached. The decrease in  $c_Y$  will thus correspond to an increase in the average degree of polymerization of the system. The rate of increase of the average degree of polymerization is proportional to the rate of polymerization, which in turn is proportional to the square root of initiator decomposition. Again, a decrease in square root radical flux will be seen as a proportional decrease in  $c_Y$ .

In Scheme 5.2, the proposed reactions occurring during the *in situ* polymerization are represented; termination events are not displayed. The relative probabilities of competing reactions occurring are proportional to their overall rates, which are proportional to the concentrations of reactants and the rate coefficients for the other competing processes. The reagent concentrations for this system are a function of a combination of the addition, fragmentation and propagation rates of the species shown in Scheme 5.2. Throughout the reaction, several different types of intermediate radical species can form, each of which has different stabilities (and thus concentrations) due to different addition rate coefficients for formation and asymmetric fragmentation rate coefficients for decomposition of the intermediate radicals. The large differences in addition and fragmentation rate coefficients for the different intermediate radicals are the key to understanding the behavior of the reaction during the initialization period. As intermediate radical concentrations can be measured from ESR data, and thus also information obtained about the intermediate radical stabilities (which is governed by their respective addition and fragmentation rates), it is therefore essential to view the <sup>1</sup>H NMR spectroscopy data in the light of the corresponding ESR spectroscopy data. The competing processes and fates of each of the important species in this initial period are now described in detail.



**Scheme 5.2** The steps involved in the initialization period of the RAFT reaction of cyanoisopropyl dithiobenzoate, styrene monomer and AIBN initiator.

Cyanoisopropyl radicals ( $A^{\cdot}$ ) generated in the system will undergo one of three main reactions: 1) addition to a RAFT agent, with relative frequency =  $k_{\text{add}}[\text{RAFT}]$  (e.g.  $k_{\text{add,AD}}[\text{AD}]$ ), to form an intermediate radical (these reactions are depicted in cases I, III<sub>asa</sub> and V; note that case I gives a degenerate product after fragmentation of the formed intermediate radical); 2) addition to monomer (propagation, with relative frequency =  $k_{\text{p,A}}[\text{M}]$ , case II), to give radical species  $\text{AS}^{\cdot}$ ; or 3) termination with other radical species.

The radical species  $\text{AS}^{\cdot}$  can partake in reactions that are similar to the reactions undergone by the  $A^{\cdot}$  species. These reactions are firstly, addition (with different addition rate coefficients) to the RAFT agents (cases III<sub>asa</sub>, III<sub>assa</sub>, or VII), secondly, propagation with the relevant propagation rate coefficient, to form radical species  $\text{AS}_2^{\cdot}$  (case IV), or thirdly, termination. The products of these reactions will be described below.

For the RAFT process to be efficient, propagating radicals must display higher addition rates to the RAFT agent than to monomer.<sup>15</sup> This prevents possible rapid propagation to form long chains before the addition-fragmentation process can allow radical exchange (via the intermediate radical species) between growing chains. Depending on the monomer concentration, a portion of initiator-derived radicals adds directly to the RAFT agent (case I). These reactions cannot be distinguished (in this specific reaction) from reactions where an initial RAFT originated leaving group adds to another RAFT agent. When  $A^*$  (from AIBN decomposition or fragmentation of the original RAFT agent) adds to AD, resulting in fragmentation to form  $A^*$  and AD, the overall result is degenerate, and no effect on the NMR spectrum is observed. This degenerate type of interchange will become evident if the initiating radical is different from the initial RAFT leaving group (systems using AIBN as initiator and cumyl dithiobenzoate as RAFT agent). A fraction of the  $A^*$  species will eventually add a styrene monomer, leading to the formation of  $AS^*$  species.

The fragmentation behavior of the formed intermediate radical species is the key to the mechanism during initialization. It is suspected that the fragmentation reaction is generally very asymmetric, with a very strong preference to form the more stable propagating radical. Possible termination reactions of the intermediate radicals can be neglected here since their concentrations during initialization are very small. This will be discussed later.

Usually, secondary radical species are more reactive than tertiary radical species with the same substituents, as the reactivity of radical species is inversely related to their stability.<sup>12</sup> When radical species with varied substituents are compared however, care must be taken when making generalizations. This implies that the tertiary cyanoisopropyl radicals ( $A^*$ ) are better leaving groups and thus more likely to fragment when attached to a RAFT agent, than their respective styryl adducts ( $AS^*$ ). For example, in the case of  $AS-D^*-A$ , the fragmentation rate constant,  $k_{add,ASD,A}$  of the tertiary cyanoisopropyl radicals will be much larger than the fragmentation rate constant,  $k_{add,AD,AS}$  of the secondary  $AS^*$  radical species (case IIIa in Scheme 5.2) due to the higher stabilities of the  $AS^*$  leaving radicals compared to the  $A^*$  leaving radicals. Cyanoisopropyl radicals also have higher addition rate constants to styrene than long chain styryl radicals.<sup>19,20</sup>

It should be noted here that the above-proposed partial RAFT mechanism (Scheme 5.2) implies dissimilarity in the fragmentation rate coefficients of the species present on the same intermediate radical, and possibly also in the addition rate coefficients to the same RAFT agent for the various radicals in the system. According to the proposed mechanism the rate coefficients for fragmentation of the species present in the reaction on the same intermediate radical will thus decrease according to the order  $k_{add,(A^*)} > k_{add,(AS^*)} \geq k_{add,(AS_2^*)} \geq \dots \approx k_{add,(AS_n^*)}$ , until such time when the addition of another monomer unit onto the growing chain will not significantly affect the rate of fragmentation of the chains i.e.  $k_{add,(AS_n^*)} \approx k_{add,(AS_{n+1}^*)}$ . The proposed mechanism also implies a dissimilarity in the addition rate constants to the same RAFT agent for the various radicals in the system, as they would increase in the order  $k_{add,(A^*)} < k_{add,(AS^*)} \leq k_{add,(AS_2^*)} \cdot \dots \approx k_{add,(AS_n^*)}$ . Note, the value of  $n$ , i.e., the number of monomer additions to  $A^*$  before  $k_{add,(AS_n^*)} \approx k_{add,(AS_{n+1}^*)}$  and

$k_{\text{add},(\text{AS}_{n+1}^*)}$ , was estimated for this reaction to be about 2. This will be discussed in more detail in section 5.2.3. Unfortunately, up to this stage it has been impossible to deconvolute the individual changes in  $k_{\text{add}}$  and  $k_{\text{-add}}$  for RAFT mediated systems. However, by means of the equilibrium coefficient ( $K_{\text{eq}}$ , equation 5-1), the relative changes of  $k_{\text{add}} / k_{\text{-add}}$  for a RAFT mediated system can be investigated. This will be discussed in section 5.1.3.

The abovementioned dissimilarity in fragmentation rate coefficients implies that the lifetime of intermediate radicals containing two secondary species will be longer than that of intermediate radicals containing at least one tertiary radical (which will consequently be longer than intermediate radicals containing only tertiary species). The generated  $\text{AS}^*$  radical species will therefore quickly become end-capped as a dithiobenzoate species (ASD), because addition is very fast, and in the process displace tertiary radicals ( $\text{A}^*$  in this case) that are attached to the RAFT agent (case III<sub>asa</sub>). The expelled tertiary radicals can then undergo addition (case I, III<sub>asa</sub>, V) or propagation (case II).

It is unlikely that the tertiary radicals ( $\text{A}^*$ ) will displace the secondary radical species (e.g.  $\text{AS}^*$ ) that are effectively trapped in the dormant state (e.g. case III<sub>asa</sub>), since the rate coefficient for fragmentation to form the secondary species is much lower than that to form the tertiary species. In such a case, they ( $\text{A}^*$ ) will instead begin to behave in a similar fashion to a reversible end-capping reaction such as ATRP or SFRP until such time as they encounter a monomer and propagate (to form  $\text{AS}^*$ ), encounter an AD species to form an intermediate radical, before again fragmenting (resulting in a degenerate end-product), or undergo termination. This process will still maintain control over the polymerization process, but the mechanism by which chains are being activated to allow propagation is different from the reversible addition-fragmentation process.

Almost every cyanoisopropyl dithiobenzoate molecule (AD) in the system is converted to a dormant ASD species before significant concentrations of  $\text{AS}_2^*$  radicals (and therefore  $\text{AS}_2\text{D}$ ) or higher dormant species have the opportunity to form in the system. This selectivity results from a combination of the fast rates of addition of propagating radicals to the RAFT agent, and the extreme asymmetry of the fragmentation step. Accordingly, the formation of  $\text{AS}^*$  radicals (which quickly form the ASD species) becomes the rate-determining step in the consumption of AD to form ASD. It has been mentioned above that the RAFT agent consumption is pseudo-zero order with respect to the RAFT agent concentration. As ASD cannot form until  $\text{AS}^*$  radicals are formed, the rate determining step is the propagation of  $\text{A}^*$  to form  $\text{AS}^*$  (with rate  $k_{p,A}[\text{M}][\text{A}^*]$ ), since this is much slower than the addition of  $\text{AS}^*$  to AD. The result of this propagation step can be seen as the formation of ASD from AD.

As it is unlikely that a secondary radical ( $\text{AS}^*$ ) will be displaced by the addition of a tertiary radical to ASD, the probability of the secondary radical species being reactivated (i.e. case III<sub>asa</sub>) is thus dependent on the concentration of the “free” secondary radical species ( $\text{AS}^*$ ). The concentration of the “free” secondary species in turn depends on both propagation of the cyanoisopropyl radicals, and their consequent addition to

a RAFT agent that already contains a dormant secondary species. This will only occur when there is a *significant* concentration of RAFT agents containing dormant secondary species (ASD), which is not the case during the early stages of the initialization period. In the early stages of this period, the rate of addition of  $AS^*$  to the RAFT agent (this includes the initial RAFT agent (AD) containing tertiary species, and a RAFT agent containing a dormant secondary species (ASD)), is too high to allow significant concentrations of “free”  $AS^*$  to exist. Thus, during the early reaction times, the dominant propagating radical will be  $A^*$ , and the concentration of the secondary radical species (and ASD) will increase until it reaches a maximum at the end of the initialization period (when no AD remains). Once a significant concentration of ASD is formed at the end of the initialization period, and a significant fraction of secondary radicals ( $AS^*$ ) are “free”, can longer chains form in significant concentrations.

Therefore, according to the proposed mechanism, during the initialization period two types of propagating ( $A^*$  and  $AS^*$ ) and three types of intermediate ( $A-D^*-A$ ,  $AS-D^*-A$  and  $AS-D^*-SA$ ) radicals will be present in significant quantities, while after initialization, intermediate radicals of the type  $AS_m-D^*-S_nA$ , where  $m, n = 2, 3, 4, \dots$  etc., will be the dominant radicals present. The contribution of each radical species towards the total radical concentration observed by ESR spectroscopy will be dependent on the concentration of the reactants used and the stability (i.e. lifetime) of the respective intermediate radicals, which in turn is dependent on the relative rates of addition and fragmentation for each propagating radical - RAFT agent combination. During the early stages of the initialization period (0 ~ 20 min), only a very small ESR signal (only detectable through accumulation of multiple ESR scans) originating from propagating and intermediate radicals were observed by ESR spectroscopy, indicating that the formed intermediate radicals must be relatively unstable and thus short-lived. This period corresponds well with the proposed period in which only the less stable  $A-D^*-A$  and  $AS-D^*-A$  intermediate radicals are expected to be present. After approximately 20 min, a sharp increase in intermediate radical concentration ( $c_Y$ ) is observed. This corresponds to the stage in the reaction where the competition for the addition of  $AS^*$  to the initial RAFT agent (AD), rather than to the ASD RAFT agent, breaks down. This can be explained as follows. During the reaction, the initial dominant propagating radical  $A^*$  is continuously converted to its single monomer adduct, species  $AS^*$ . As described above, the  $AS^*$  species can have a number of possible fates: firstly,  $AS^*$  can add to an AD (case III<sub>asa</sub>) or ASD (case III<sub>assa</sub>) RAFT agent; secondly, propagate to form  $AS_2^*$ ; or thirdly, terminate. For the RAFT process to be efficient (as is the case in the reactions under discussion), it is expected that the probability for addition of  $AS^*$  to a RAFT agent will be higher than the probability for propagation or termination. The probability of the addition of  $AS^*$  to an AD species rather than to a ASD species, will be given by the ratio  $k_{add,AS,AD}[AS^*][AD] / k_{add,AS,ASD}[AS^*][ASD]$ , where  $k_{add,AS,AD}$  and  $k_{add,AS,ASD}$  are the coefficients of addition for species  $AS^*$  to the AD and ASD species respectively and  $[AS^*]$ ,  $[AD]$  and  $[ASD]$  the concentrations of the  $AS^*$ , AD and ASD species respectively. Initially  $k_{add,AS,AD}[AD] \gg k_{add,AS,ASD}[ASD]$ , therefore species  $AS^*$  will more than likely add to a AD species to expel a tertiary radical ( $A^*$ ). However, after 20 minutes, the above-mentioned ratio will change to  $k_{add,AS,AD}[AD] \approx k_{add,AS,ASD}[ASD]$  due to the formation of significant concentrations of the ASD species. Thus, a significant concentration of the  $AS^*$  species will now also add to

the ASD species to form an AS-D<sup>•</sup>-SA type intermediate radical. As the secondary radical species (AS<sup>•</sup>) are poorer leaving groups than the tertiary radical species (A<sup>•</sup>), it is expected that the intermediate species AS-D<sup>•</sup>-SA should be more stable than the intermediate radicals with only one or none secondary species, i.e., intermediate species A-D<sup>•</sup>-A and AS-D<sup>•</sup>-A. As more ASD species are formed, the ratio will change to  $k_{\text{add,AS,AD}}[\text{AD}] \ll k_{\text{add,AS,ASD}}[\text{ASD}]$ , leading to the AS-D<sup>•</sup>-SA type intermediate radicals thus becoming the dominating intermediate radicals. These radicals are stable enough to be detected by ESR spectroscopy, and the increase in  $c_Y$  is mainly due to the increase in AS-D<sup>•</sup>-SA species. If this is the case,  $c_Y$  would increase (roughly) in a linearly fashion, since it only depends on the ratio of  $[\text{ASD}] / [\text{AD}]$ . According to the time evolution of  $c_Y$  given in Figure 5.4, this appears to be the case. The maximum in intermediate radical concentration is reached some time after the end of the initialization period as some residual A<sup>•</sup> are converted to AS<sup>•</sup>, which in its turn adds to the dominant ASD species, resulting in the formation of AS-D<sup>•</sup>-SA intermediate radicals. After the initialization period, as the propagating radicals add a second (and later a third) monomer unit, more stable intermediate radicals are formed.

It should be mentioned here that if the above-mentioned condition, i.e., the preference of species AS<sup>•</sup> to add to a RAFT agent rather than to undergo propagation or termination, does not hold or only partly holds, then the increase in  $c_Y$  corresponds to the stage in the reaction where the competition for the addition of AS<sup>•</sup> to the initial RAFT agent (AD), rather than to propagate, to form to AS<sub>2</sub><sup>•</sup>, breaks down. As explained above, stable intermediate radicals of the type AS-D<sup>•</sup>-SA (or AS<sub>n</sub>-D<sup>•</sup>-S<sub>n</sub>A, where  $n = 1, 2 \dots$  etc.) are required to give the increase in observed  $c_Y$ . This requires high concentrations of AS<sup>•</sup> and ASD species to form during the reaction. The probability of the addition of AS<sup>•</sup> to an AD species rather than propagation, will be given by the ratio  $k_{\text{add,AS,AD}}[\text{AS}^{\bullet}][\text{AD}] / k_{\text{p,AS}}[\text{AS}^{\bullet}]$ , where  $k_{\text{add,AS,AD}}$  is the coefficient of addition for species AS<sup>•</sup> to the AD,  $k_{\text{p,AS}}$  the propagation rate coefficient for species AS<sup>•</sup> and  $[\text{AS}^{\bullet}]$  and  $[\text{AD}]$  the concentrations of the AS<sup>•</sup> and AD species respectively. Initially  $k_{\text{add,AS,AD}}[\text{AD}] \gg k_{\text{p,AS}}$ , therefore species AS<sup>•</sup> will more than likely add to an AD species to expel a tertiary radical (A<sup>•</sup>) than to propagate. However, after 20 minutes, the above-mentioned ratio will change to  $k_{\text{add,AS,AD}}[\text{AD}] \approx k_{\text{p,AS}}$  due to the steady decline in concentration of the AD species. Thus, a small concentration of the AS<sup>•</sup> species will now propagate to form AS<sub>2</sub><sup>•</sup>, which can then either add to an AD or ASD species to form a less stable AS<sub>2</sub>-D<sup>•</sup>-A, or a more stable AS<sub>2</sub>-D<sup>•</sup>-SA type intermediate radical. In the first case, an A<sup>•</sup> radical will be expelled rapidly (which in turn will quickly propagate to a AS<sup>•</sup> species) to form an AS<sub>2</sub>D species, while in the second case the AS<sub>2</sub><sup>•</sup> radical will be expelled due to the dissimilarity in the fragmentation rates, ranging in the order  $k_{\text{-add,A}} > k_{\text{-add,AS}} \geq k_{\text{-add,AS}_2} \geq k_{\text{-add,AS}_3} \dots$  etc.,<sup>21</sup> to form an ASD species. The formed AS<sub>2</sub><sup>•</sup> radical can then again undergo a case one or two scenario, as it is expected that the probability of the AS<sub>2</sub><sup>•</sup> radical propagating again, is remote. As at that stage in the reaction, the concentration of species ASD is rapidly increasing, it is expected that the occurrence of the second case will be the mostly likely. However, the occurrence of both cases will lead to the increase in concentration of AS<sup>•</sup> radicals, and thus to the formation of AS-D<sup>•</sup>-SA type intermediate

radicals. It is also likely that the formation of  $AS_2-D^*-SA$  type intermediate radicals might lead to the observed increase seen in  $c_Y$ .

During the initialization period, the dominating propagating radicals will be the  $A^*$  and, to a lesser extent, the  $AS^*$  radicals. This is due to the fact that the less stable  $AS^*$  radicals are quickly converted to ASD species. Normally, the contributions of the propagating radicals towards the observed ESR signals in RAFT systems are relatively small due to their order of magnitude smaller (under these conditions) concentrations and shorter lifetimes compared to the intermediate radicals. However, during the early stages of initialization, the propagating and intermediate radicals' lifetimes are comparable, and signals due to the propagating radicals (mostly  $A^*$ ) could indeed be observed via ESR spectroscopy, together with signals for intermediate radicals  $A-D^*-A$  and  $AS-D^*-A$  when multiple scans (16, instead of a single scan) were accumulated during the initialization period.

The varying coefficients for addition ( $k_{add}$ ) and fragmentation ( $k_{-add}$ ), which control the intermediate radical concentration, is posed to be the reason for the observed time evolution of  $c_Y$  for this reaction. As of yet, it has been impossible to deconvolute the separate changes in  $k_{add}$  and  $k_{-add}$  throughout a reaction, due to the intricacies involved in determining  $k_{add}$  and  $k_{-add}$  individually. However, the ratio of the two rate constants,  $K_{eq}$ , can be calculated through rate and ESR spectroscopy data. A varying  $K_{eq}$  will be indicative of a changing  $k_{add}$  and  $k_{-add}$  during the reaction. It has been generally accepted that  $K_{eq}$  is a constant throughout a RAFT reaction. However, it is expected (based on the initial ESR spectroscopy investigations) for the reactions investigated, that the  $K_{eq}$  will increase during the initialization period to eventually reach a constant value sometime afterwards, as the reaction reaches equilibrium.

The reason for the extremely selective and stepwise behavior of the reactions during initialization are, firstly, that the fragmentation of the formed intermediate radicals is very selective towards radicals that have not yet undergone propagation and, secondly, that addition of propagating radicals of degree of polymerization of at least unity to the RAFT agent is much faster than to monomer. The first of these reasons will usually hold if the initial leaving group on the RAFT agent is a much better leaving group than that formed after one propagation step, as is the case here. The second criterion will hold if  $k_{add}[RAFT] \gg k_{p,1}[M]$  (with the appropriate  $k_{add}$  for the incoming radical, and for all forms of the RAFT agent), which will typically be the case when efficient RAFT agents are used.  $k_{p,1}$  (the propagation rate coefficient for a monomeric radical) is chosen here since  $k_{p,1}$  is typically greater than  $k_p$ . In these systems, most oligomeric radicals will consist of a single monomer unit added to an initiator fragment or RAFT leaving group. If  $k_{add}[RAFT] \ll k_{p,1}[M]$  then the selective and stepwise behavior will probably not occur, since chains of degree of polymerization greater than unity will form before all of the initial RAFT agent has been consumed. Scenarios in which this is likely are when  $k_{add}$  (e.g. a low activity RAFT agent, such as a MADIX agent) is small,  $[RAFT] / [M]$  is small (e.g. a very high molar mass is targeted), or  $k_{p,1}$  is very large (which might occur for some initiators, and/or very active monomers). Note that to achieve very high molar masses, the  $[RAFT] / [M]$  ratio can be kept high during initialization, and further monomer added, to overcome the problem mentioned above.

### 5.2.1 Temperature effects

To investigate the effect of temperature on the reaction mechanism, a duplicate *in situ*  $^1\text{H}$  NMR (reaction 2, Table 5.2) and corresponding *in situ* ESR reaction were carried at 84 °C (Figure 5.6 and Figure 5.7).

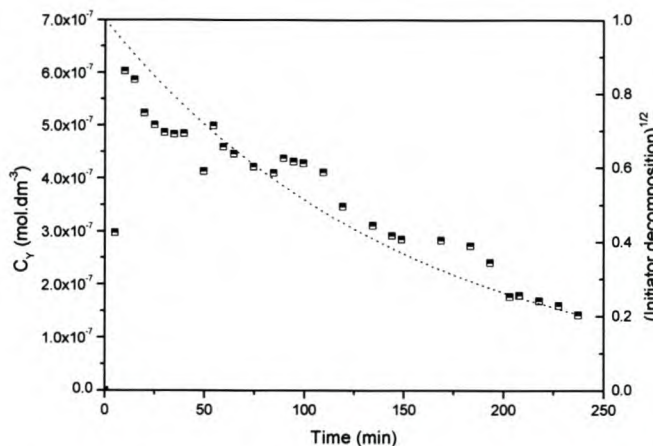


**Figure 5.6** The time evolution of  $c_Y$  (■) and the corresponding rate of initiator decomposition (···) for solution 1, Table 5.1 polymerizes *in situ* at 84 °C.

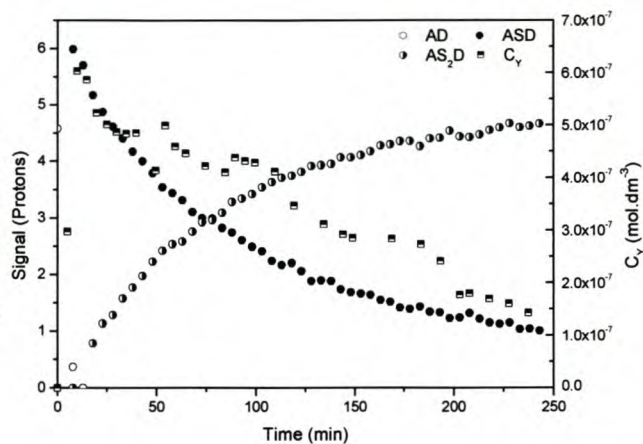


**Figure 5.7** Overlay of  $c_Y$  and the relative concentrations of the methyl protons of dithiobenzoate species versus time in the polymerization of styrene in the presence of CIBD using AIBN as an initiator polymerized *in situ* at 84 °C (solution 2, Table 5.2).

In the corresponding *in situ* ESR reaction (using the same reagent concentrations as in the ESR reaction at 70 °C, solution 1 Table 5.1), the rate was substantially faster than the reaction carried out at 70 °C, presumably due to the higher radical flux due to faster initiator decomposition and higher propagation rate coefficients. In this case, no initial period of little or no intermediate radical concentration was observed in the time evolution of the intermediate radical concentration. After reaching a maximum within the first 10 minutes, the intermediate radical concentration declined rapidly as the radical flux decreased.

The *in situ*  $^1\text{H}$  NMR reaction proceeds so rapidly that most of the cyanoisopropyl dithiobenzoate is consumed prior to the time the first spectrum (8 minutes) was collected. The initialization period for this reaction is therefore only about 10 minutes compared to 50 minutes in the lower temperature reaction. This is presumably due to both the higher radical flux from initiator decomposition, and the higher propagation rate coefficient for the cyanoisopropyl radicals.

Overall, the same characteristics were observed at this higher temperature. The reaction showed similar selectivity, with no significant concentrations of  $\text{AS}_2\text{D}$  or higher dormant species formed until after the end of the initialization period.

## 5.2.2 Monomer Consumption

The fractional conversions for the  $^1\text{H}$  NMR reactions 1 and 2 are compared in the first order kinetic plot in Figure 5.8. The rate of monomer consumption is substantially higher during the initialization period than afterwards.

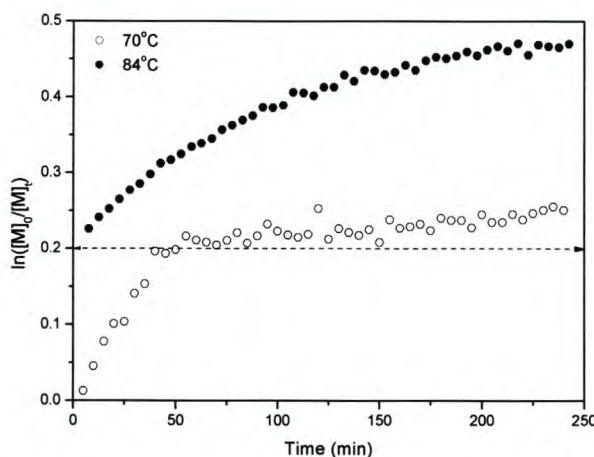


**Figure 5.8** Semi-logarithmic plot of fractional conversion versus time in the reactions of cyanoisopropyl dithiobenzoate with AIBN and styrene in deuterated benzene at 84 and 70 °C. Reactions 1 and 2, Table 5.2. Reaction 1: 6.03 M  $\text{C}_6\text{D}_6$ ,  $1.03 \times 10^{-1}$  M AIBN, 4.06 M styrene,  $8.17 \times 10^{-1}$  M cyanoisopropyl dithiobenzoate. Reaction 2: 6.14 M  $\text{C}_6\text{D}_6$ ,  $1.05 \times 10^{-1}$  M AIBN, 4.06 M styrene,  $7.78 \times 10^{-1}$  M cyanoisopropyl dithiobenzoate. The dashed line (--) is an indication of the end of the initialization period.

The decrease in the rate of reaction after initialization at 70 °C is so extreme that after the initialization period, polymerization appears to almost cease (though it must be noted that it does not, the rate is just so slow that it would not be noticed by most analysis techniques). This is consistent with reports of RAFT mediated systems that show little polymerization at lower temperatures, even though radicals are being generated in the system.<sup>22</sup>

The time derivatives of the monomer consumption can be expressed in terms of the propagation rate ( $k_p$ ) and the propagating radical concentration,  $c_p$ .

$$\frac{d(\ln([M]_0/[M]_t))}{dt} = k_p c_p \quad (5-2)$$

The dominant propagating species in the two periods of the polymerization (i.e. initialization and equilibrium) are quite different, namely  $\text{A}^*$  (cyanoisopropyl radicals) during initialization, and  $\text{AS}_n^*$  (oligostyryl or polystyryl radicals) after initialization. The propagation rate coefficient for the addition of cyanoisopropyl radicals to styrene is  $5200 \text{ M}^{-1} \text{ s}^{-1}$  at 70 °C,<sup>20</sup> and the propagation rate coefficient for addition of polystyryl radicals to styrene is  $480 \text{ M}^{-1} \text{ s}^{-1}$  at 70 °C,<sup>23</sup> possibly higher for short oligomeric radicals. The decrease in rate from initialization to the period after, is by a factor of approximately 20. The difference in propagation rate coefficients alone is therefore unable to account for the huge change in reaction rates. Thus the propagating radical concentration must also have decreased after initialization, leading to rate retardation that was not

present during the initialization period. In these reactions, rate retardation was observed without inhibition being present.

The propagating radical concentration (and thus the reaction rate) is dependent on the overall rates of initiation and termination. In RAFT systems there is an extra radical species (intermediate radicals) whose concentration is potentially very significant.<sup>8,24,25</sup> The propagating radical concentration is given by

$$\frac{dc_P}{dt} = 2fk_d c_I - k_{add} c_P c_{PX} + k_{-add} c_Y - k_t c_P^2 - k'_t c_P c_Y \quad (5-3)$$

where  $k_t$  and  $k'_t$  are the respective termination rate constants for the propagating and intermediate radicals,  $c_I$ ,  $c_{PX}$ ,  $c_P$  and  $c_Y$  the initiator, dormant chains, propagation and intermediate radical concentrations,  $f$  the initiator efficiency,  $k_d$  the rate of initiator decomposition and  $k_{add}$  and  $k_{-add}$  the coefficients for addition and fragmentation.<sup>26</sup> If a steady state in  $c_P$  is assumed ( $\frac{dc_P}{dt} = 0$ ), the resulting quadratic equation solved, and the positive root taken, the expression for  $c_P$  is then

$$c_P = \frac{1}{2k_t} \sqrt{(k_{add} c_{PX} + k'_t c_Y)^2 + 4k_t (2fk_d c_I + k_{-add} c_Y) - k_{add} c_{PX} - k'_t c_Y} \quad (5-4)$$

For the purposes of discussing the reaction rate during the initialization period, as a simplification it is assumed that the concentration of the intermediate radicals is relatively small ( $c_Y \approx 0$ ) and that termination of the intermediate radicals does not significantly change the rate of polymerization ( $k'_t \approx 0$ ) during initialization. This simplification can be justified by the observation that *significant* concentrations of intermediate radicals were only formed after ca. 40 minutes of reaction time for the *in situ* ESR reaction at 70 °C (Figure 5.4). Equation 5-4 then simplifies to

$$c_P = \frac{1}{2k_t} \sqrt{(k_{add} c_{PX})^2 + 8k_t f k_d c_I - k_{add} c_{PX}} \quad (5-5)$$

From Figure 5-4 and 5-5 it can be seen that the change in  $c_P$  from during to after initialization can be due to a variety of factors. These factors include a possible change in intermediate radical concentration, due to a change in the values for the addition and fragmentation rate coefficients, or a possible change in termination kinetics, which includes possible intermediate radical termination, as significant concentrations of intermediate radicals formed after the initialization period.

To illustrate the effect  $k_p$  has on the reaction rates, it is assumed that the intermediate radical lifetime is not so extensive as to cause rate retardation and that the termination and initiation kinetics do not significantly change during the initialization period.

As mentioned earlier, the rate of reaction is significantly faster during initialization than afterwards (when styrene is used as monomer). In contrast, some of the most significant inhibition times that have been reported have been in methyl acrylate (MA) systems.<sup>27</sup> If the methyl acrylate RAFT system using the same RAFT agents used in this study is examined, the following relationship can be derived from literature values:<sup>19,20,28</sup>

$$\frac{k_{p,MA}}{k_{p,A,MA}} \gg 1 \gg \frac{k_{p,St}}{k_{p,A,St}} \quad (5-6)$$

Here  $k_{p,MA}$  and  $k_{p,St}$  refer to the long chain propagation rate coefficients for methyl acrylate (MA) and styrene (St), and  $k_{p,A,MA}$  and  $k_{p,A,St}$  to the rate coefficients for the addition of the cyanoisopropyl radical to MA and St. Assuming, as a first approximation, similar propagating radical concentrations before and after initialization (this is apparently not true here, as the propagating radical concentration will be lower after initialization), the relative reaction rates will primarily depend on the relevant  $k_p$  values. For styrene, this gives a higher rate during initialization than for the period afterwards. For MA, the rate of reaction will be much slower during initialization than afterwards, as  $k_{p,MA}$  at 25 °C is  $13\,100\text{ M}^{-1}\text{ s}^{-1}$ ,<sup>29</sup> and  $k_{p,A,MA}$  is  $367\text{ M}^{-1}\text{ s}^{-1}$  at 42 °C.<sup>20</sup> It should be mentioned here that the above prediction given was confirmed by preliminary experiments done with MA as monomer, using the same reactants and similar reactant concentrations under the same experimental conditions as the reactions given in Table 5.2, utilizing styrene as monomer.

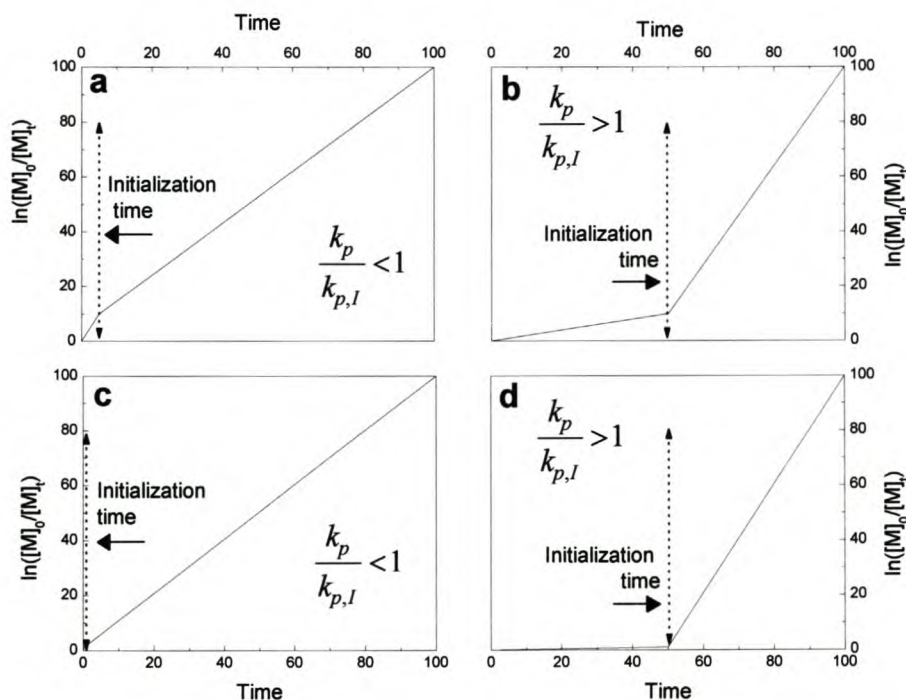


**Figure 5.9** The effect of  $k_p/k_{p,I}$  on the rate of monomer consumption during the two phases of the reaction, is indicated in the figures. Case (a) and (b) has a monomer to RAFT agent molar ratio of 10:1, case (c) and (d) has a monomer to RAFT agent molar ratio of 100:1. The dashed vertical line indicates the end of initialization.

When there is a relatively small amount of RAFT agent present in a reaction (i.e., long chains are targeted), then a very small percentage of the monomer will be consumed during the initialization period. This would be difficult to distinguish from complete inhibition if the target molar mass is high. RAFT agent to monomer concentration ratios that have been used in the literature are commonly very high,<sup>27</sup> often of the order of a thousand to one. Figure 5.9 demonstrates semi-qualitatively the effect on the rate of polymerization during and after initialization when  $k_p/k_{p,i}$  (where  $k_{p,i}$  is the rate constant for addition of the initiating radical to monomer) is greater and less than unity, for different target molar masses.

In Figure 5.9 (a) and (b) molar ratios of 1:10 RAFT agent to monomer and in (c) and (d) molar ratios of 1:100 RAFT agent to monomer were used, assuming constant propagating radical concentrations before and after initialization, in which case the relative reaction rates are proportional to the relevant  $k_p$  values. In experiments with high molar ratios of RAFT agent to monomer (cases a and b), a  $k_p < k_{p,i}$  will lead to a faster rate of polymerization during initialization than afterwards. However, when  $k_p > k_{p,i}$  a longer initialization time will be observed with a consequent slower rate of polymerization during initialization than afterwards. In experiments where high molar mass chains are targeted (cases c and d), the above-mentioned effects will be enhanced. A  $k_p < k_{p,i}$  in this systems will lead to a very short initialization time, whereas a  $k_p > k_{p,i}$  will lead to a longer initialization time with a very low rate of reaction during polymerization.

One of the consequences of the initialization period is that the rate of monomer consumption is governed by the rate of conversion of the starting RAFT agent (AD) into the single monomer adduct analog (ASD). This in turn is governed by the addition rate constants of the RAFT agent leaving group radical (or initiator fragment radical, which is the same in this case) to monomer.<sup>19,20</sup> Here it can be seen that the experimental evidence that has been presented for inhibition in RAFT polymerization<sup>27,30,31</sup> is actually a result of the initialization period (when AIBN is used as initiator). Even for systems in which the monomer to RAFT agent ratio is such as to allow for the addition of two monomer units per transfer (in which the transfer rate constant is still sufficiently greater than the propagation rate constant) approximately one mole of monomer is consumed per mole of RAFT agent during the initialization period. This monomer consumption would be difficult to distinguish from total inhibition as less than 0.1 % conversion would have occurred during this time. Even cases in which e.g. four monomer additions occur prior to transfer, the conversion will be less than 1 % conversion, and therefore also indistinguishable from total inhibition. It is important to note that examples of systems in which there is supposed to be total inhibition are reported to show color change, which is a well-known indication of polymerization in RAFT mediated polymerizations. This is consistent with the suggestion that these systems have an initialization period instead of an inhibition period.<sup>22</sup> Due to the high ratios of reagents used in this study, the initialization period is emphasized.

### 5.2.3 The Apparent Equilibrium “constant”, $K_{eq}$

An equilibrium coefficient ( $K_{eq}$ ) in a RAFT system is usually assumed to be invariable, and thus also an indication of when a steady state reaction equilibrium has been reached, i.e., when the core addition and fragmentation reactions (Scheme 5.1) are in a steady state. According to equation 5-7,  $K_{eq}$  can be

determined by investigating the ratio of  $c_Y$  and  $c_P$ , which in turn can be calculated through analysis of ESR spectra and rate data respectively. According to equation 5-1,  $c_P$  can be calculated from the derivative of the monomer consumption as determined by the *in situ*  $^1\text{H}$  NMR spectroscopy reactions at 70 °C and 84 °C (Figure 5.10), if the corresponding correct value for  $k_p$  (and the type of propagating species) is known. When calculating the time derivative of the monomer consumption, care has to be taken, as differentiating noisy data can introduce a large scatter in the calculated derivatives. A better means of calculating the derivative of the monomer consumption is to fit a mathematical function to the monomer consumption data (when possible), and calculate the derivative of the obtained fit function.

Two distinct regions in the monomer consumption can be observed for the 70 °C reaction, i.e. an approximately linear region of fast monomer consumption during initialization, and a region of slower monomer consumption after initialization. The monomer consumption data was approximated by fitting exponential curves ( $y = 0.1255x^{0.1207}$  and  $y = 0.1143x^{0.2655}$ ) to the 70 °C and 84 °C data respectively. The coefficients for the exponential curves were determined by plotting  $\log(\ln[M]_0/[M]_t)$  vs.  $\log(\text{time})$ , and fitting a straight line (with  $R^2 = 0.6827$  and  $R^2 = 0.9832$ ) to the entire monomer consumption data for the 70 °C and 84 °C reactions. The inability of the fitted curve to represent the data during the initialization period for the 70 °C reaction resulted in the low  $R^2$  value observed. The monomer consumption data during the initialization period for the reaction at 70 °C was thus approximated by fitting a straight line ( $y = 0.00466x$ ) to the data. It can be seen from the residuals given in Figure 5.11 that the above-mentioned calculated straight line and exponential curve for the data of the 70 °C reaction, and only the exponential curve for the 84 °C data, fit the respective monomer consumption data well, with marginal deviations during the early (for the 84 °C data) and late stages (for both data sets) of the reactions. The derivative of the fitted line and curves yield  $k_p c_P$  for the reaction at a specific time ( $k_p$  here is an average if there is more than one propagating species present).

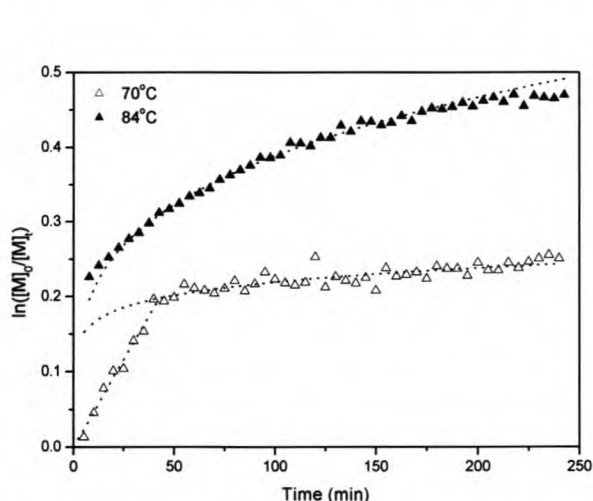


**Figure 5.10** Semi-logarithmic plot of fractional conversion versus time in the reactions of CIBD with AIBN and styrene in deuterated benzene at 70 and 84 °C. The broken lines (---) correspond to the best fit to the data.

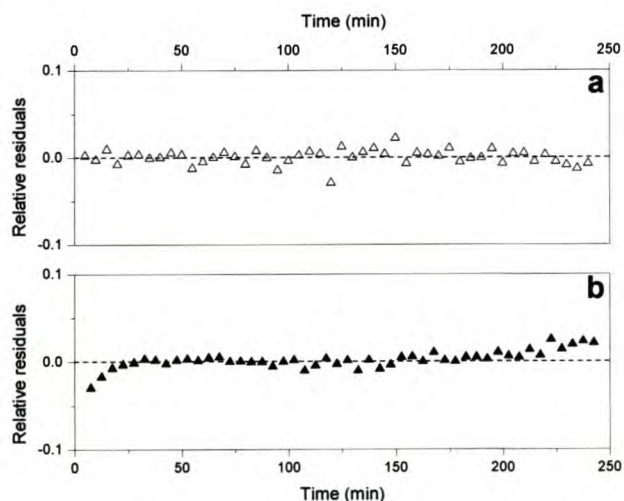


**Figure 5.11** Residuals from the fit of an exponential curve ( $y=0.1255x^{0.1207}$  and  $y=0.1143x^{0.2655}$ ) to the monomer consumption data for the reaction at (a) 70 °C and (b) 84 °C respectively.

To determine the correct value for  $c_P$ , it is essential to know the correct corresponding value for  $k_p$  at a specific time in the reaction. It was determined by  $^1\text{H}$  NMR spectroscopy data that in the majority of cases

only one styrene unit per RAFT agent is added to the growing chains during initialization. Thus,  $k_p$  here is for a cyanoisopropyl radical. It is known that the rate of addition of a cyanoisopropyl radical to a styrene unit and the long chain propagation rate of styrene differs by more than an order of magnitude for the reaction at 70 °C.<sup>19,20</sup> Thus, the average  $k_p$  will change drastically throughout the reactions investigated (especially from during to after the initialization period); therefore assuming a constant value for  $k_p$  throughout the reaction will yield incorrect values for  $c_p$  in some parts.

It was shown earlier that the rate determining step during the initialization period in the systems investigated was the propagation of the cyanoisopropyl radical to form the species  $AS^*$ , which was quickly converted to ASD. After the initialization period, the  $AS^*$  species propagated to form species  $AS_2^*$ , which is seen as the formation of species  $AS_2D$ . Therefore, the value for  $k_p$  during the initialization period (linear region) in the reaction at 70 °C was approximated by the literature value for the addition of a cyanoisopropyl radical to a styrene monomer ( $k_p = 5\,200\text{ M}^{-1}\text{s}^{-1}$ ).<sup>20</sup> For the period after initialization it was assumed that the propagation rate coefficient for species  $AS^*$  would be similar to that of styrene, thus, an average value of  $960\text{ M}^{-1}\text{s}^{-1}$ , corresponding to twice the literature value for the propagation rate coefficient of styrene at 70 °C ( $480\text{ M}^{-1}\text{s}^{-1}$ ), was assumed for  $k_p$ . As the initialization period was over before the first  $^1\text{H}$  NMR scan could be made of the reaction at 84 °C, an average  $k_p$  of  $1\,500\text{ M}^{-1}\text{s}^{-1}$  (corresponding to twice the literature value of  $k_p$ ) was used throughout the reaction period. The choice of  $k_p$  value was based on the observation that mostly monomeric or dimeric species were present during the course of the reaction.

The calculated  $c_p$  values for the 70 and 84 °C reactions are given in Figure 5.12. It should be noted here that the values given for  $c_p$  in Figure 5.12 are not absolute, but based on an assumed value of  $k_p$  for the respective reactions. For both reactions, the calculated  $c_p$  values are at least a magnitude of order smaller than the respective observed  $c_Y$  values at any given time.

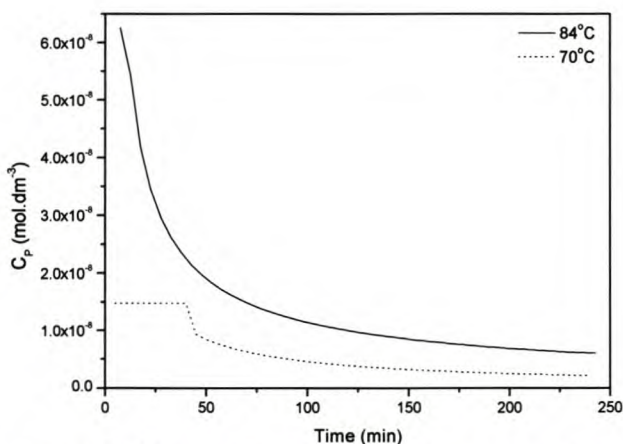


**Figure 5.12** The calculated propagation radical concentration ( $c_p$ ) time evolution for the CIDB mediated reactions with AIBN and styrene in deuterated benzene at 70 °C and 84 °C (reactions 1 and 2, Table 5.2).

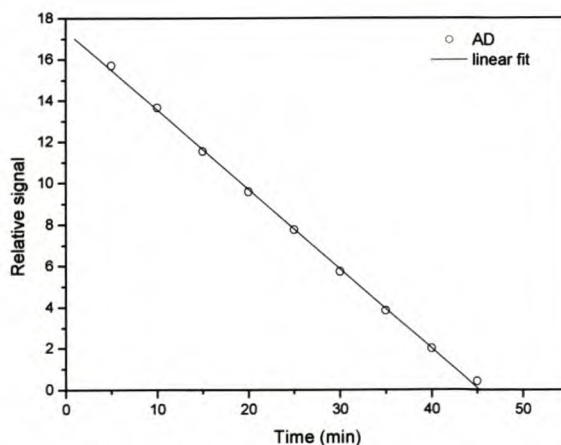


**Figure 5.13** The decrease in concentration of species AD as observed by *in situ*  $^1\text{H}$  NMR spectroscopy at 70 °C (reaction 1, Table 5.2). The solid line (—) represents the best fit to the data.

The  $c_P$  values calculated for the 70 °C data show a discontinuity at approximately 50 minutes, i.e. at the end of the initialization period. This sudden change in calculated  $c_P$  is due to the sharp decrease in monomer consumption after the initialization period for the 70 °C reaction. This discontinuity portrayed in Figure 5.12 is also exacerbated by the assumed large change in  $k_p$  during ( $k_p = 5\,200\text{ M}^{-1}\text{s}^{-1}$ ) and after ( $k_p = 960\text{ M}^{-1}\text{s}^{-1}$ ) the initialization period as well as the sudden increase in  $c_Y$  that is observed to occur during that period. The real change in  $c_P$  from during to after the initialization period is likely to be more gradual. The continuous value of  $c_P$  during the early reaction time for the 84 °C reaction might also be an artifact from the way  $c_P$  is calculated. It is expected that  $c_P$  will show a marked decrease during the early reaction time, as a rapid increase in  $c_Y$  was observed to occur during that period. Varying  $c_P$  and  $c_Y$  values will have a marked effect on the apparent equilibrium of the system.

As mentioned in the introduction of section 5.2, the equilibrium coefficient ( $K_{\text{eq}}$ ) is given by

$$K_{\text{eq}} = \frac{c_Y}{c_P c_{\text{PX}}} = \frac{k_{\text{add}}}{k_{-\text{add}}} \quad (5-6)$$

where  $c_Y$  and  $c_P$  are the intermediate and propagating radical concentrations,  $c_{\text{PX}}$  the concentration of the dormant chains, i.e. chains with dithiobenzoate end groups, and  $k_{\text{add}}$  and  $k_{-\text{add}}$  the addition and fragmentation coefficients for the addition of a propagating radical to a RAFT agent and the fragmentation of a formed intermediate radical. The equilibrium coefficient ( $K_{\text{eq}}$ ) for each reaction was calculated by means of  $c_Y$  values obtained from ESR spectroscopy data and the  $c_P$  values calculated from the monomer consumption data, as discussed above.

If it is assumed that the decrease in concentration of species AD during the initialization period for the reaction at 70 °C corresponds to the formation of dormant chains with dithiobenzoate endgroups, and that there is no significant “loss” in dithiobenzoate endgroups through the formation of intermediate radicals or by possible degradation or termination mechanisms, then the concentration of dormant chains of degree of polymerization  $\geq 1$  with dithiobenzoate endgroups, i.e.  $c_{\text{PX}}$ , can be calculated. For the reaction at 70 °C,  $c_{\text{PX}}$  was calculated by fitting a straight line ( $y = -0.365x + 17.1$  with  $R^2 = 0.991$ ) to the decrease in concentration of species AD as observed by  $^1\text{H}$  NMR spectroscopy, given in Figure 5.13. Using the initial concentration of the cyanoisopropyl dithiobenzoate RAFT agent used ( $8.17 \times 10^{-1}\text{ M}$ ), and estimating a time value for the end of initialization (approximately 46 min), the decrease in concentration of the AD species during the initialization period could be calculated. The calculated  $c_{\text{PX}}$  increases linearly during the initialization period, after which it attains a constant value, taken as  $8.17 \times 10^{-1}\text{ M}$ , the initial cyanoisopropyl dithiobenzoate RAFT agent concentration used in the reaction mixture. Note that the “loss” of dithiobenzoate endgroups through the formation of intermediate radicals can be neglected as their concentrations are low (ca.  $10^{-6} \sim 10^{-8}\text{ M}$ ) compared to the value for  $c_{\text{PX}}$ . The value of  $c_{\text{PX}}$  for the reaction at

84 °C was taken as the initial cyanoisopropyl RAFT agent concentration ( $7.78 \times 10^{-1}$  M) used in the reaction mixture. This approximation was valid since the initialization period was over before the first  $^1\text{H}$  NMR scan could be recorded (at 8 min).

In Figure 5.14, the time evolutions of the equilibrium coefficients for the reactions at 70 °C and 84 °C are given. A large uncertainty in the ESR spectroscopy determined values of  $c_Y$  (which was used in the calculation of  $K_{\text{eq}}$ ), resulted in some scatter of the calculated  $K_{\text{eq}}$  values for both reactions. To reduce the resultant scatter,  $c_Y$  was estimated (for both reactions) by assuming that the decrease in  $c_Y$ , after a maximum was reached, follows the corresponding decrease in square root radical flux in the system due to a rapidly decreasing initiator concentration (see Figure 5.4 and Figure 5.6). Thus, the values for  $c_Y$  after a maximum was reached (at ca. 50 and 10 minutes for the reactions at 70 °C and 84 °C respectively), were approximated by the equations used to describe the decrease in square root initiator decomposition, as shown in Figure 5.4 and Figure 5.6 ( $K\sqrt{e^{-k_d t}}$ , where  $K = 2.9 \times 10^{-7}$  and  $k_d = 3.79 \times 10^{-5} \text{ M}^{-1}\text{s}^{-1}$  for the 70 °C reaction, and  $K = 7 \times 10^{-7}$  and  $k_d = 2.22 \times 10^{-4} \text{ M}^{-1}\text{s}^{-1}$  for the reaction at 84 °C, with  $t$  the time in seconds), as shown in Figure 5.4 and Figure 5.6. It should be noted here that the approximated  $c_Y$  values (determined using the given equations), gave a good representation of the observed decrease in  $c_Y$  for the reaction at 84 °C (see Figure 5.6), but a poor representation of the decrease in  $c_Y$  for the reaction at 70 °C (see Figure 5.4). This might be due to the large uncertainty involved in the determination of the  $c_Y$  values, especially when the determined  $c_Y$  values are low and thus near the detection limits of the ESR spectrometer. It should be remembered that the reason for determining values of  $K_{\text{eq}}$  for the reactions polymerized at 70 °C and 84 °C are not to obtain absolute values, but to give an indication of the changes in the apparent  $K_{\text{eq}}$  with time. Employing the estimated values for  $c_Y$  in the calculation of  $K_{\text{eq}}$  gave a less noisy time evolution profile for the calculated  $K_{\text{eq}}$ .

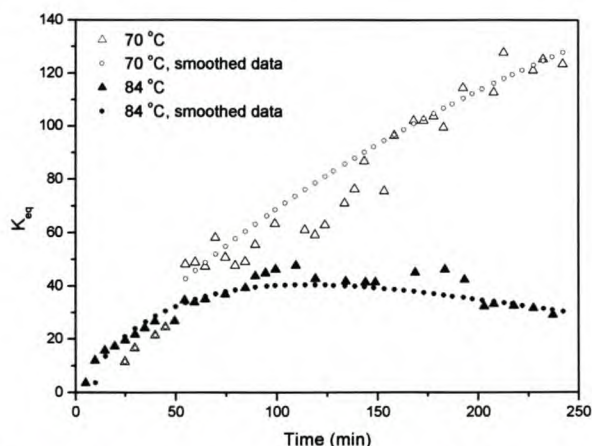


**Figure 5.14** The time evolution for the calculated equilibrium coefficient ( $K_{\text{eq}}$ ) for the CIDB mediated reactions at 70 °C ( $\Delta$ ) and 84 °C ( $\blacktriangle$ ), based on  $c_Y$  and  $c_P$  values obtained from ESR spectroscopy and rate data.  $K_{\text{eq}}$  calculated by estimation of  $c_Y$  for the 70 °C ( $\circ$ ) and 84 °C ( $\bullet$ ) reactions is also given.

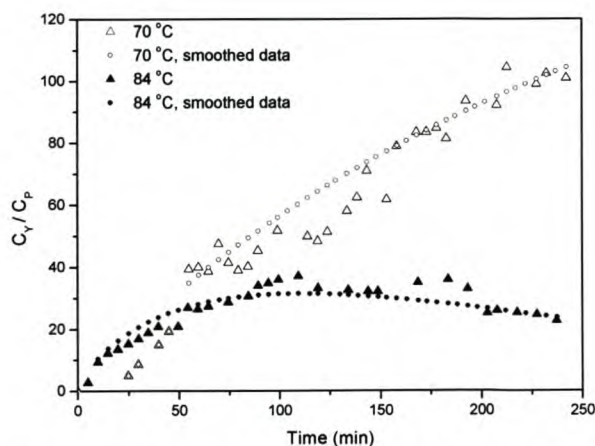


**Figure 5.15** The time evolution for the intermediate to propagating radical concentration ( $c_Y/c_P$ ) for the CIDB mediated reactions at 70 °C ( $\Delta$ ) and 84 °C ( $\blacktriangle$ ), based on  $c_Y$  and  $c_P$  values obtained from ESR spectroscopy and rate data. The  $c_Y/c_P$  ratio represented by  $\circ$  and  $\bullet$  was determined by estimation of  $c_Y$  and calculation of  $c_P$  using rate data.

From Figure 5.15 it can be seen that the observed profiles for the time evolution for  $K_{eq}$  are mostly due to the calculated  $c_Y/c_P$  time profile. As expected for the investigated reaction polymerized at 84 °C,  $K_{eq}$  shows a rapid increase, and then approaches a constant value as the reaction enters an apparent equilibrium (after approximately 100 min). However, an unexpected decrease in  $K_{eq}$  was also observed.  $K_{eq}$  for the reaction polymerized at 70 °C showed a fast increase after an initial induction period, and never reached a constant value during the time of reaction. The implication of this is that, even though the RAFT systems might be in (rapid) dynamic equilibrium, true steady state equilibrium is not reached until at least 3 monomer additions to the growing chains. This has implications on the early mechanism and reaction rate of the RAFT systems investigated. This might however not be true for other RAFT systems in which the RAFT agent to monomer ratio is not as large as the systems investigated in this study, or when a different monomer and/or RAFT agent to the systems investigated here, are used.

According to equation 5-6, the equilibrium coefficient ( $K_{eq}$ ) will give an indication of the changes in  $k_{add} / k_{-add}$ . The proposed (partial) reaction mechanism (Scheme 5.2) for the RAFT process during the early stages of the reaction is based on the principle that  $k_{add}$  will decrease as the selectivity for addition of a propagating radical to a RAFT agent, rather than propagate, is diminished, and that there is a dissimilarity in the fragmentation rate coefficients of the species present in the reaction (of the same intermediate radical), to vary in the order  $k_{add,(A^*)} > k_{add,(AS^*)} \geq k_{add,(AS_2^*)} \geq k_{add,(AS_3^*)}$ , until such a degree of polymerization where the addition of another monomer unit onto the growing chains will not significantly affect the rate of fragmentation of the chains i.e.,  $k_{add,(AS_n^*)} \approx k_{add,(AS_{n+1}^*)}$ . In Figure 5.14, the increase observed in  $K_{eq}$  for the *in situ* reaction run at 70 °C, can be divided into two distinct regions: a fast increase during the first ca. 50 minutes of the reaction (corresponding to the initialization period for the reaction); and a second slower increase of  $K_{eq}$  for the remainder of the reaction. If it is assumed, as a first approximation, that  $k_{add}$  is approximately constant during the reaction, the initial rapid increase in  $K_{eq}$  can be explained by a progressively decreasing  $k_{-add}$ , i.e.,  $k_{add,(A^*)} \gg k_{add,(AS^*)}$ . The second slower increase in  $K_{eq}$  can also be explained by a progressively decreasing  $k_{-add}$ , but the decrease in  $k_{-add}$  during this second period is less than during the first period. This would imply that  $k_{add,(AS^*)} \geq k_{add,(AS_2^*)}$ . This might also be realized if it is assumed that besides  $k_{-add}$  decreasing during the reaction (or that  $k_{-add}$  is approximately constant), that  $k_{add}$  is also continuously decreasing during this period ( $k_{add,(AD)} \gg k_{add,(ASD)} > k_{add,(AS_2D)}$ ). During the second period of the reaction, the decrease in  $k_{-add}$  is less pronounced than the decrease in  $k_{-add}$  during the first period, which will result in a less rapid increase in  $K_{eq}$ .

If the same assumption (an approximately constant  $k_{add}$  for the reaction) is extended for the reaction at 84 °C, the rapid increase in  $K_{eq}$  can also be explained in the light of a rapid decreasing  $k_{-add}$ , i.e.  $k_{add,(AS^*)} \geq k_{add,(AS_2^*)}$ . At approximately 100 min, however, a decrease in  $K_{eq}$  is observed. This would imply (if  $k_{add}$  remains constant) that  $k_{-add}$  is then increasing. This can be explained if the growing chains (attached to an intermediate radical) become progressively better leaving groups. The sudden decrease in  $K_{eq}$  might be possible if it is assumed that besides  $k_{-add}$  decreasing during the reaction, that  $k_{add}$  also decreases (by

varying extents) during the reaction. During the first 100 minutes, the decrease in  $k_{\text{add}}$  is less than the decrease in  $k_{\text{add}}$ , while after 100 minutes the decrease in  $k_{\text{add}}$  will exceed the decrease in  $k_{\text{add}}$ . This will result in a rapid increase in  $K_{\text{eq}}$  up to 100 minutes, after which a decrease in the equilibrium coefficient might be observed. It should be noted here that the calculated decrease in  $K_{\text{eq}}$  seen, might be an artifact resulting from the way the calculations were done. Small dissimilarities between reactant concentrations of solutions used in the NMR and ESR reactions and small temperature variations might cause, for example, the intermediate radical concentration to decrease faster than expected, leading to a decrease in the value of  $K_{\text{eq}}$ . Thus, if  $K_{\text{eq}}$  (for the reaction at 84 °C) indeed reaches and constant value after approximately 100 minutes, it implies that the value of  $n$ , i.e. the number of monomer additions to  $A^*$  before  $k_{\text{add},(\text{ASn}^*)} \approx k_{\text{add},(\text{ASn}+1^*)}$  is approximately 2 for this reaction. The above given results are consistent with the proposed reaction mechanism (Scheme 7.2) of the RAFT process during the early stages of the reaction, for the RAFT mediated polymerization reactions investigated here.

Evidence that RAFT systems do eventually reach a steady state equilibrium was given by Kwak *et al.*<sup>11</sup> who studied, by ESR spectroscopy and dilatometry, the polymerization of styrene mediated by a polystyryl dithiobenzoate RAFT agent ( $\overline{M}_n = 1100$ ,  $\overline{M}_w/\overline{M}_n = 1.08$ ). By using a long chain RAFT agent, the system was effectively at high conversion, i.e. long  $\overline{M}_n$  chains, from the start of the reaction. Thus, the effects of short chains on the RAFT mechanism and kinetics will be reduced. Utilizing their ESR and kinetic data, Kwak *et al.*<sup>11</sup> calculated that the system had a roughly constant  $K_{\text{eq}}$  throughout the time of reaction. This confirms that the system will eventually attain a steady state equilibrium (observed as a constant  $K_{\text{eq}}$ ) after sufficient monomer units have added to the growing chains.

It should be remembered here that the calculated values of  $K_{\text{eq}}$  for the reactions polymerized at 70 and 84 °C are not absolute values, but were calculated to give an indication of the changes in the apparent  $K_{\text{eq}}$  with time. The values calculated for  $K_{\text{eq}}$  for the two systems are thus not directly comparable. The higher observed value of  $K_{\text{eq}}$  for the 70 °C reaction is possibly due to a higher activation energy for fragmentation compared to that for addition. This would imply that the rate coefficient for fragmentation would be more affected by a lowering in temperature compared to the rate coefficient for addition, leading to an effective increase in the value of  $K_{\text{eq}}$ .

Bearing in mind that at lower temperatures the ratio of  $c_Y/c_P$  is higher than at higher temperatures for the same RAFT mediated system, systems at lower temperatures should be more prone to possible intermediate radical termination reactions, due to their relative higher  $c_Y$  value. However, at a lower temperature, the radical flux is significantly lower and thus also the total intermediate radical concentration ( $3 \times 10^{-7}$  M compared to  $6 \times 10^{-7}$  M at the maximum, see Figure 5.4 and Figure 5.6). Thus, even though a relative buildup in intermediate radicals is predicted to occur at lower temperatures compared to a reaction at higher temperatures, the total value of  $c_Y$  is predicted to be still significantly lower at lower reaction temperatures. As spectroscopy techniques only detect total concentrations of species, a reaction at higher temperatures might still yield higher concentrations of possible intermediate radical termination products. This is one of

the rationales behind using a reaction temperature of 84 °C in the *in situ*  $^{13}\text{C}$  NMR detection of products of termination reactions of intermediate radicals utilizing a labeled RAFT agent.

In the light of the above discussion of  $K_{\text{eq}}$ , the values calculated for  $K_{\text{eq}}$  in the reactions in section 3.3.1 were probably incorrect, as no adjustment was made in  $c_{\text{P}}$  for the possibly (rapidly) changing  $k_{\text{p}}$  during the earlier stages of the reactions. Even though a correction for  $k_{\text{p}}$  will change the calculated values for  $K_{\text{eq}}$  to some extent, the fact still remains that  $K_{\text{eq}}$  changes rapidly during the early parts of the reactions investigated.

## 5.2.4 Radical Generation and Termination Products

As mentioned in section 5.1.2, it is suspected that there might be a significant change in the termination (and initiation) kinetics during the polymerization time for the reactions investigated. Initiator (AIBN) decomposition and the formation of the AA (tetramethyl succinonitrile, TMSN) species is compared to that of a conventional free radical (control) reaction (reactions 3 and 4, Table 5.2). The AA product is formed by mutual termination of cyanoisopropyl radicals and from geminate recombination (cage product) due to AIBN decomposition. In Figure 5.16, the concentration-time evolution of AIBN and the formed AA species of reaction 2 and the control (reaction 4, Table 5.2) at 84 °C are presented. The concentration of the AA product in reaction 2 shows a slight increase when compared to the control reaction. The concentration difference appears to be due to different initial values. It is suspected that as the formation of the AA product in reaction 2 is slower than in reaction 4, some event prior to observation caused the different initial concentrations. The higher initial concentration of reaction 2 is probably due to the termination behavior of (mostly) the cyanoisopropyl radicals during the initialization period, which could not be examined at this reaction temperature (84 °C), since initialization was completed before the first scan could be made. The results suggest that the presence of the RAFT agent does not increase the amount of TMSN formation after initialization is complete, i.e., the RAFT agent does not directly promote termination in the system after initialization (although it alters the relative populations of propagating radicals, which can change the termination kinetics). The difference between the formed amounts of AA (TMSN) in the RAFT mediated polymerization and the control lies in the nature and concentration of the radical species during the initialization period, and the length of the initialization period.

Comparison between the RAFT mediated reaction (reaction 2) and the control (reaction 4) at 84 °C (Figure 5.16) also indicates that the presence of a RAFT agent does not increase the rate of AIBN decomposition.

In Figure 5.17, the AIBN and AA product concentrations of reactions 1 and 3, as determined at 70 °C, are compared. The formation of the AA product in reaction 1 occurs at an increased rate throughout the initialization period (lasting approximately 50 min). This confirms the above argument, that the higher initial value of the AA product is produced during initialization. Following the initialization period, the AA product is formed at a similar rate to its corresponding control reaction (reaction 4).

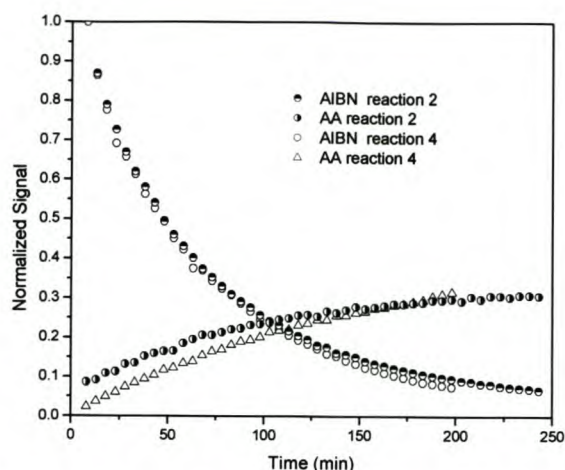


**Figure 5.16** The concentrations of AIBN and AA of reactions 2 and 4 carried out in deuterated benzene at 84 °C. Reaction 2 contains RAFT agent cyanoisopropyl dithiobenzoate and Reaction 4 is a conventional free radical polymerization. (Reaction 2: 6.14 M  $C_6D_6$ ,  $1.05 \times 10^{-1}$  M AIBN, 3.98 M styrene,  $7.78 \times 10^{-1}$  M cyanoisopropyl dithiobenzoate; Reaction 4: 4.85 M  $C_6D_6$ ,  $0.829 \times 10^{-1}$  M AIBN, 4.98 M styrene).

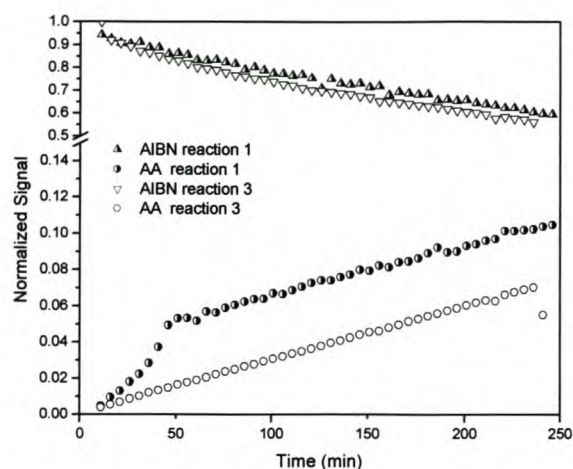


**Figure 5.17** The concentrations of AIBN and AA of reactions 1 and 3 carried out in deuterated benzene at 70 °C. Reaction 1 contains RAFT agent cyanoisopropyl dithiobenzoate and Reaction 3 is a conventional free radical polymerization. (Reaction 1: 6.03 M  $C_6D_6$ ,  $1.03 \times 10^{-1}$  M AIBN, 4.06 M styrene,  $8.17 \times 10^{-1}$  M cyanoisopropyl dithiobenzoate; Reaction 3: 5.46 M  $C_6D_6$ ,  $0.834 \times 10^{-1}$  M AIBN, 4.55 M styrene).

The increased concentrations of the respective termination products in the RAFT mediated polymerizations during initialization are due to an unusual process in which radicals are kept short (Figure 5.18).

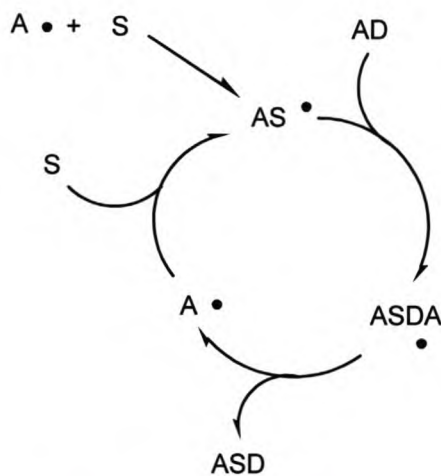


**Figure 5.18:** The cycle by which cyanoisopropyl radicals ( $A^\bullet$ ) are rapidly regenerated by addition-fragmentation through a dithioester mediating species, during the early stages of the cyanoisopropyl dithiobenzoate-mediated polymerization of styrene.

The process starts by the  $A^\bullet$  radicals adding to a monomer unit to form species  $AS^\bullet$ . These species undergo efficient transfer (characteristic of RAFT mediated polymerizations) to expel a short  $A^\bullet$  species. Thus, unlike a conventional radical polymerization, the initialization period replaces the slower terminating  $AS^\bullet$  species with faster terminating  $A^\bullet$  radical species. After initialization the usual geminate recombination process dominates the formation of the AA species. The concentration curves for AA are roughly parallel in Figure 5.17, although in Figure 5.16 there is a deviation at higher temperature. This deviation at higher temperature can be attributed to higher conversions and viscosities in the control reaction, leading to a decrease in initiator efficiency and an increase in the geminate recombination product being produced at longer reaction

times. A weaker increase in viscosity is expected in the corresponding RAFT system since both overall conversion and average chain length (on both of which viscosity depends) are both much lower than in the control system.

Due to the chain length dependence of the termination rate coefficients,<sup>32-36</sup> short species will usually have a higher rate of termination. Therefore the overall termination rate will be higher during initialization than in a corresponding control reaction in which the short chains are quickly converted into longer chains. Reactions with long initialization periods will consequently have a lower propagating radical concentration after initialization (compared to reactions with a short initialization period) due to the higher rate of radical loss through termination during initialization.

### 5.2.5 Beyond Initialization

To minimize the length of the initialization period, it is important that the propagation rate constant of the homolytic leaving group of the original RAFT agent (with respect to the monomer in use), be as high as possible. A caution being that it should remain a better leaving (fragmenting) group than the incoming monomer-adduct radicals. The monomer-adduct radicals must also have high rate coefficients for addition to the original RAFT agent with respect to their propagation rate coefficient, otherwise initialization will break down. The choice of initiator fragments produced by initiator decomposition is also an important consideration, as the initiator fragment or its monomer adduct should be able to displace the initial RAFT agent leaving group, and should thus also have a high rate coefficient for addition to the original RAFT agent with respect to their coefficients for propagation. To minimize rate differences due to propagation rate constant differences between initialization and the equilibrium phase of the reaction, a polymeric RAFT agent of the same monomer can be used. In this case the propagation of the initiator fragment, which is unable to displace the polymeric chain until it has propagated, will result in an immediate increase in the concentration of intermediate radicals, as has been seen by ESR spectroscopy.<sup>37</sup> The experimental implication of using the polymeric agent is that the RAFT equilibrium period should be reached very quickly and initialization is therefore effectively circumvented.

### 5.2.6 Conclusions

*In situ* <sup>1</sup>H NMR spectroscopy showed that the first observed interval of polymerization in the studied systems is an initialization period, which has been defined as the period prior to the complete consumption of the initial RAFT agent. *In situ* ESR and <sup>1</sup>H NMR spectroscopy provided direct evidence for the mechanism during the initialization period of the RAFT process. It was found that the addition-fragmentation process was extremely selective during this period and, because of this, significant quantities of RAFT adducts of degrees of polymerization greater than unity were formed only after complete conversion of the initial RAFT agent to its single monomeric adduct. The critical process in the initialization of a RAFT controlled polymerization was identified to be the formation of a single monomer adduct species and, by implication,

the propagation of the initial leaving group radicals and the initiator derived radicals (which are both the cyanoisopropyl radical here).

The reasons for the selective behavior observed for the RAFT systems are suggested as being dependent on the relative addition and fragmentation rate coefficients of the tertiary radical species and their monomer adducts in the system. This was confirmed by a changing equilibrium coefficient for the reactions investigated, inferred from ESR spectroscopy data.

A more rapid rate of reaction was observed during the initialization period than during the period afterwards. It was shown that the rate of polymerization is a function of the propagation rate coefficients for the initiator and leaving group fragments and of the propagating radical concentration. It was proposed that the observed difference in reaction rates during, to those after initialization, was due to a difference in propagation rate coefficients on the one hand and termination kinetics and partitioning of radicals between the propagating and intermediate forms on the other. According to the RAFT scheme, an increase in intermediate radical concentration will not change the reaction kinetics, i.e., the rate of reaction. However, intermediate radical termination, which is a probable cause of rate retardation, will be enhanced (if it occurs) by the increase in intermediate radical concentration.

The initialization period has largely been mistaken for inhibition in the RAFT literature for homogenous reactions. The lack of previous reports of the rapid rate of reaction during this period is suggested as being due to the long chain lengths targeted in other studies, which means that the initialization period would have been completed before significant conversion had occurred, and thus this period may in many systems have gone unnoticed.

This can be extended to all efficient RAFT systems, even those where multiple radical species are present, and should not be considered as solely an explanation of the cyanoisopropyl dithiobenzoate system. Cases where this behavior might not occur include the use of RAFT agents with low addition rate coefficients, the use of very high initial ratios of  $[M]/[RAFT]$ , or systems in which  $k_{p,1}$  is very large.

The second part of this chapter addresses similar reactions using cumyl dithiobenzoate, where the initiating and leaving groups are different, and illustrates the similarities and differences in observed behavior.<sup>18</sup>

## RAFT Mediated Polymerization with Different Initiating and Leaving Groups.

This section addresses, in a similar manner to the previous section, the early part of the reaction of AIBN-initiated styrene polymerization in the presence of cumyl dithiobenzoate, at 70 and 84 °C, before complete consumption of the initial RAFT agent i.e. initialization, and the period immediately following initialization. *In situ*  $^1\text{H}$  NMR spectroscopy was used to directly observe the concentration of several characteristic species during the course of the reaction, with focus on the early parts of the reaction, i.e. the first monomer addition step(s). The effects of using a system in which there are dissimilar initiator fragments and the initial RAFT agent leaving groups ( $\text{R}^*$ ), on the rate of polymerization and length of the initialization period, and the implications on the RAFT mechanism, are investigated and compared to the case where these groups are the same.

### 5.3 Reactions Mediated by Cumyl Dithiobenzoate

The concentrations and molar ratios of the reaction components used in all reactions are summarized in Table 5.2. A representative selection of peaks that were integrated for this study can be found in Table 5.4. Where two or more peaks are indicated, diastereotopic groups were present.

**Table 5.4**  $^1\text{H}$  NMR chemical shifts of the integrated species relevant to the investigation of cumyl dithiobenzoate mediated reactions.

Methyl protons of R groups $\delta$ (ppm)	Ortho protons of corresponding dithiobenzoate ring $\delta$ (ppm)	Species
Singlet 0.93	N/A	AA
Singlet 1.18	N/A	CC
Two peaks 1.10, 1.08	N/A	AC
Singlet 1.45	Doublet 7.71	AD
Singlet 1.81	Doublet 7.81	CD
Two peaks 1.01, 0.87	Doublet 7.85	ASD
Two peaks 1.25, 1.20	Doublet 7.78	CSD
Two peaks 0.81, 0.65	Doublet 7.90	AS <sub>2</sub> D
Two peaks 0.95, 1.02	Doublet 7.81	CS <sub>2</sub> D

Figure 5.19 shows the chemical structures of the primary species of interest. The following naming convention will be used. Species CD is the initial RAFT agent containing the dithiobenzoate species (D) and the initial cumyl leaving group (C), CSD is the dithiobenzoate species of the single styrene (S) adduct of a cumyl radical (C<sup>\*</sup>), while CS<sub>2</sub>D is the second styrene adduct of the cumyl radicals. The same naming convention applies for derivatives of the RAFT agent cyanoisopropyl dithiobenzoate (AD), with consecutive monomer adducts ASD and AS<sub>2</sub>D. A sample spectrum showing the most important peaks during initialization is shown in Figure 5.20. The CC product is formed by mutual termination of two cumyl radicals.

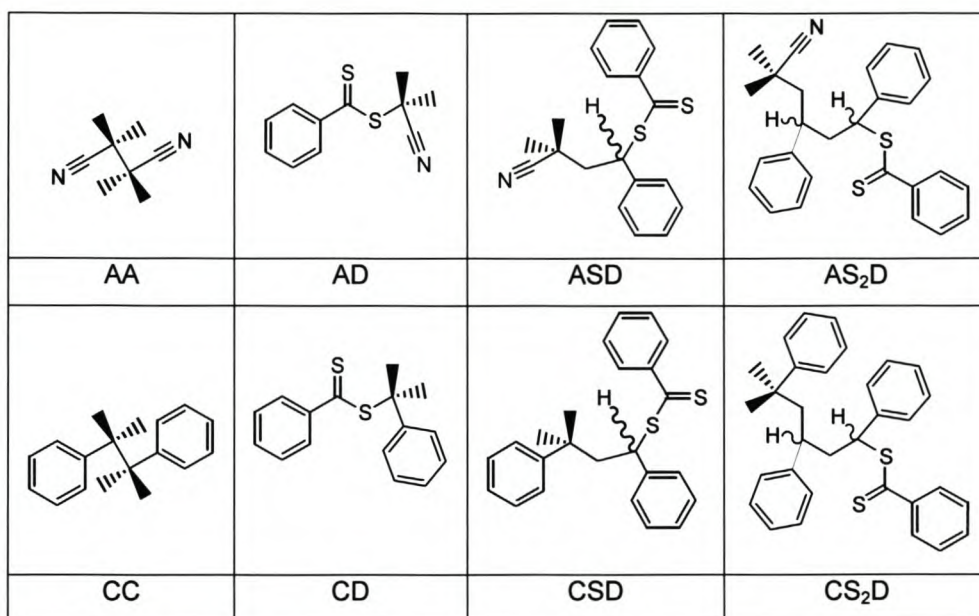


**Figure 5.19** The species of interest for the investigation of initialization in the free radical polymerization of styrene in the presence of cumyl dithiobenzoate, using AIBN as an initiator.

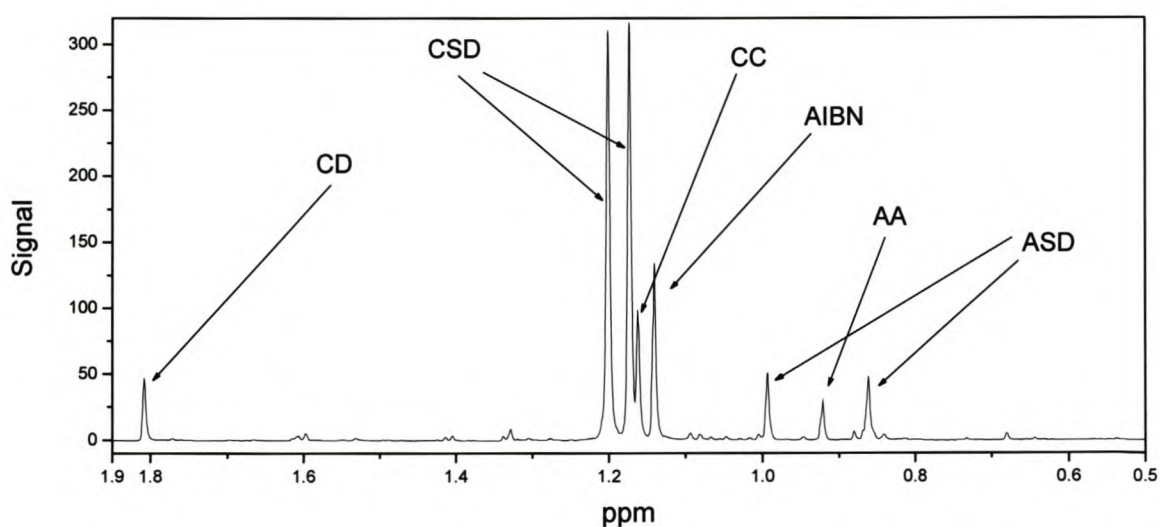


**Figure 5.20** A typical <sup>1</sup>H NMR spectrum between 1.9 and 0.5 ppm taken during initialization, showing the peaks corresponding to several of the important species, for the *in situ* polymerization of solution 5 (Table 5.2) at 70 °C.

The use of cumyl dithiobenzoate as RAFT agent, styrene as monomer and AIBN as initiator, results in a system in which two different tertiary radical species are present. The choice of styrene as monomer results in a vast majority of radicals formed from propagation reactions being secondary radicals.

In a cyanoisopropyl dithiobenzoate mediated polymerization the radical reactivity for only one type of tertiary initiating radical needs to be considered. When a system with two tertiary radical species (cyanoisopropyl and cumyl) is considered, the polymerization becomes substantially more complex.

A solution of cumyl dithiobenzoate ( $6.48 \times 10^{-1}$  M), styrene (4.30 M) and AIBN ( $1.11 \times 10^{-1}$  M) in benzene (5.68 M) (solution 2, Table 5.1) was polymerized *in situ* in an ESR spectrometer at 70 °C. In a similar fashion to the cyanoisopropyl dithiobenzoate mediated reactions, a corresponding *in situ*  $^1\text{H}$  NMR spectroscopy polymerization of a solution containing  $6.67 \times 10^{-1}$  M cumyl dithiobenzoate, 4.55 M styrene and  $1.11 \times 10^{-1}$  M AIBN in 5.40 M deuterated benzene (reaction 5, Table 5.2) was reacted at 70 °C under similar reaction conditions. Figure 5.21 shows the time dependence of the concentrations of the dithiobenzoate species and intermediate radicals within the first 7 hours of the reaction. Initially, a small but significant amount of AD species is formed, due to addition of the initiator-derived cyanoisopropyl radicals to the original RAFT agent (CD), followed by fragmentation to produce cumyl radicals and AD. Simultaneously, there is a decrease in concentration of species CD, and a corresponding increase in concentration of the species CSD and ASD as a single monomer unit is added. This trend continues until the cumyl dithiobenzoate and any formed cyanoisopropyl dithiobenzoate have been completely consumed (after about 240 minutes). At this point the concentrations of species CSD and ASD have reached a maximum. Once the cumyl dithiobenzoate has disappeared from the reaction, the second monomer addition to the radical species begins to increase in frequency (species  $\text{CS}_2\text{D}$  and  $\text{AS}_2\text{D}$ ). The implication of this behavior is that the formation of the CSD and ASD (i.e. propagation of  $\text{A}^*$  and  $\text{C}^*$  to form  $\text{AS}^*$  and  $\text{CS}^*$ ) species or the consumption of the starting RAFT agent is the rate-determining step in the process. This behavior is the same as was previously described when the initiating and leaving groups were the same, and is expected, since the rate-determining step is similar in both cases.

The time evolution of the intermediate radical concentration ( $c_Y$ ) given in Figure 5.21 for the reaction shows similar trends to the corresponding time evolution of  $c_Y$  observed in the cyanoisopropyl dithiobenzoate mediated reactions. In this case, there was an initial period (approximately 310 minutes) during which very little intermediate radicals were observed, followed by a rapid increase in  $c_Y$ . It should be mentioned here that upon re-examination of the initial reaction period with different ESR spectroscopy parameters (16 scans were accumulated for every ESR spectrum with a 2 G modulation amplitude, compared to the usual single scans for every ESR spectrum with a 1 G modulation amplitude), in an attempt to increase the signal to noise ratio of the ESR spectra, a relatively large concentration of propagating radicals and a small concentration of intermediate radicals could be detected. During the reaction time, no maximum in  $c_Y$  was observed, but it is suspected that  $c_Y$  will eventually reach a maximum after which it will decrease according

to the decrease in square root radical flux in the system, as observed in the cyanoisopropyl dithiobenzoate mediated reactions at 70 and 84 °C.

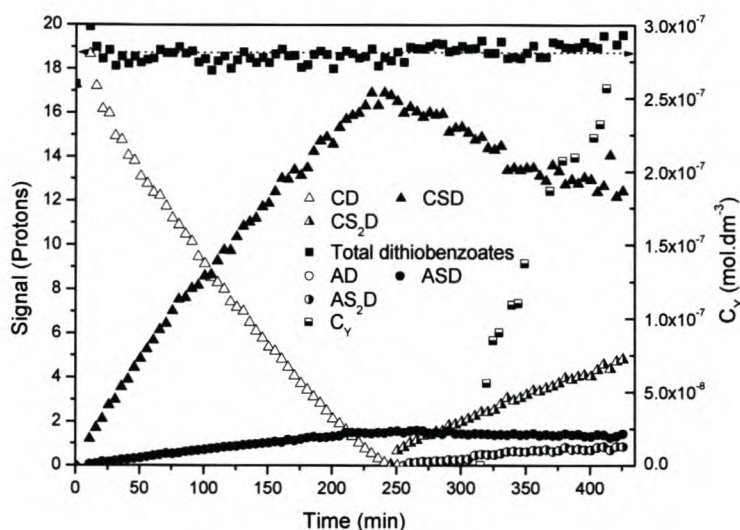
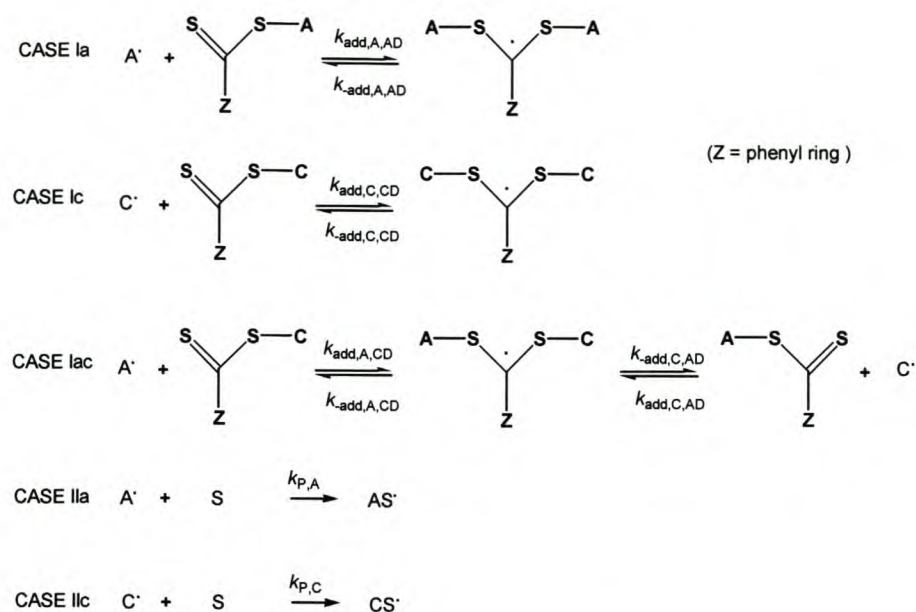


**Figure 5.21** Relative concentrations of the methyl protons of dithiobenzoate species versus time, overlaid with the intermediate radical concentration evolution in the free radical polymerization of styrene in the presence of cumyl dithiobenzoate using AIBN as an initiator polymerized *in situ* at 70 °C (solution 2, Table 5.1 and reaction 5, Table 5.2).

The reaction scheme is now substantially more intricate than, although quite similar to, the scheme proposed previously (Scheme 5.2) for the cyanoisopropyl dithiobenzoate mediated reactions. Scheme 5.3 shows the types of reactions that can occur at the beginning of the reaction (i.e. prior to total consumption of the initial RAFT agent). Reactions labeled with subscripts **c** and **a** denote the reactions that are specific to cumyl or cyanoisopropyl radical species respectively, and **as** and **cs** denote those referring to the single monomer adducts of the cumyl and cyanoisopropyl radical species. Termination reactions are not shown.

For convenience, the reaction scheme *during* initialization has been divided into two parts. The first part, as shown in Scheme 5.3, describes the main processes occurring at the start of the reaction before propagation has occurred, and the second part (Scheme 5.4), the remaining reactions in the initialization period. The species involved in the first scheme include RAFT agents that have not added monomer units, radicals that have not yet undergone propagation, and intermediate radicals formed from the reaction of the aforementioned species. Note that the reactions depicted in Scheme 5.3 can still occur throughout the initialization period, until such time as all the initial RAFT agent has been consumed. According to Scheme 5.3, the cyanoisopropyl radicals generated by initiator decomposition can undergo one of three main reactions: firstly, addition to a RAFT agent (case Ia or Iac); or secondly, addition to monomer (propagation), to give radical species AS\* (case IIa); or thirdly, termination. Cumyl radicals generated by case Iac (and other cases as will be seen in Scheme 5.4) will either undergo addition to a RAFT agent (case Ic or Iac) or addition to monomer (propagation) to produce species CS\* (case IIc), or terminate.

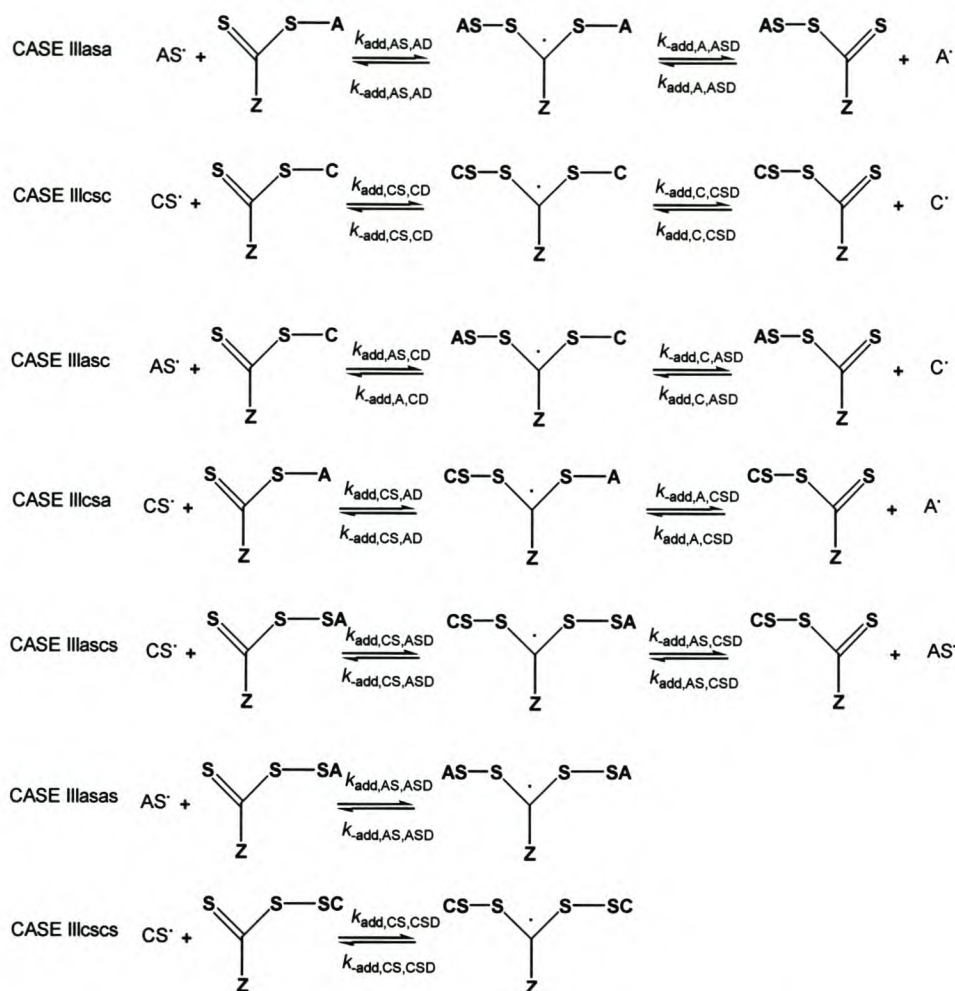


**Scheme 5.3** The main steps involved in the early part of the initialization period of the RAFT reaction of cumyl dithiobenzoate, styrene monomer and AIBN initiator at the beginning of initialization.

The remaining important reactions during the initialization period are shown in Scheme 5.4. The additional reactions are as follows: the cyanoisopropyl and cumyl radicals can undergo two other reactions, namely addition to either cyanoisopropyl-styryl or cumyl-styryl dithiobenzoate (shown on the right hand sides of either cases IIIasa or IIIcsc (for  $A^\cdot$ ), or cases IIIasc or IIIcsc (for  $C^\cdot$ )) to form the corresponding intermediate radicals. Similarly, species  $AS^\cdot$  and  $CS^\cdot$  can add to a RAFT agent, i.e., cases IIIasa, IIIasc, IIIcsas, IIIasas and cases IIIcsc, IIIcsc, IIIcsas and IIIcscs, respectively.

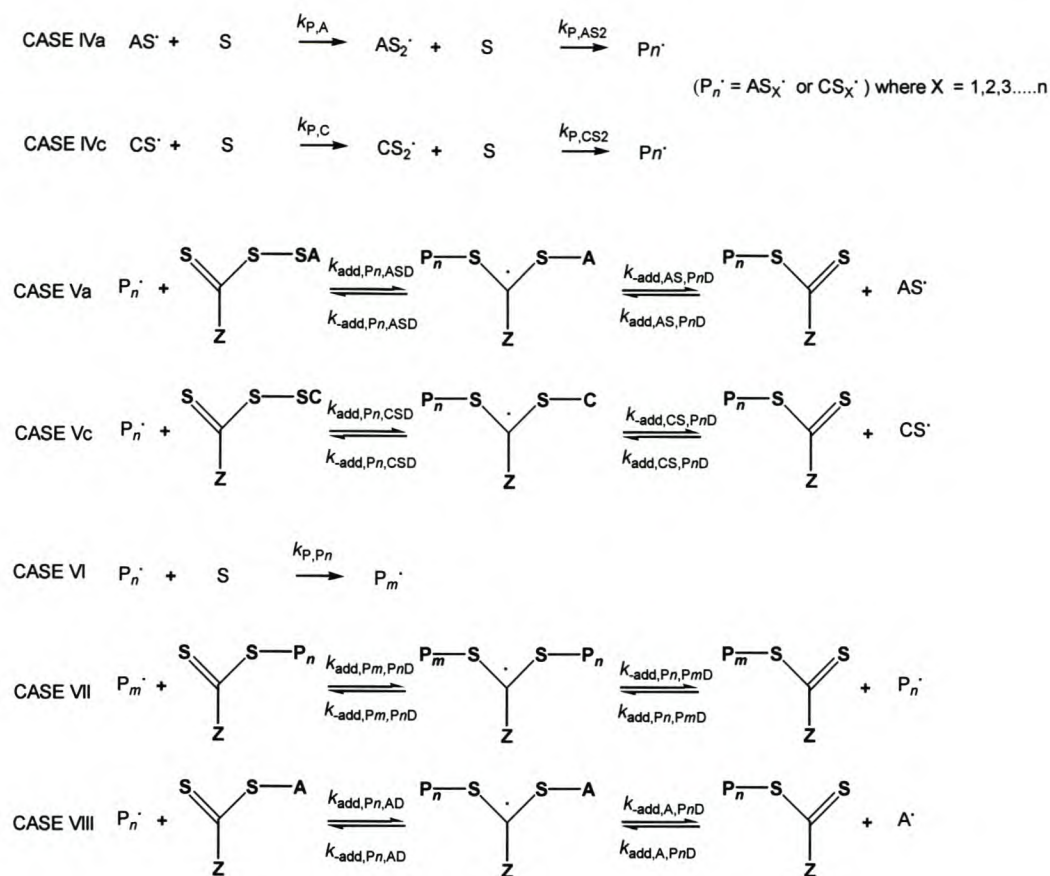
Note that in this cumyl dithiobenzoate mediated reaction, where the initiating and leaving radicals are different, there are now ten distinct types of intermediate radicals that can form during the initialization period, whereas there are only three such types of intermediates when the two radicals are the same (Scheme 5.2). This can potentially change the kinetics of the system, and makes accurate modeling of the kinetics extremely problematic, since there are then 32 potentially different rate coefficients (all of which are currently unknown) for the addition-fragmentation equilibrium in just the initialization period. However, based on the previously described cyanoisopropyl dithiobenzoate system, it appears that again the most important factors that determine the length of the initialization period are the propagation rates of the cyanoisopropyl and cumyl radicals. This is again based on the observation that almost every cumyl and formed cyanoisopropyl dithiobenzoate species (CD and AD) in the system are converted to a dormant CSD or ASD species before significant concentrations of  $CS_2^\cdot$  and  $AS_2^\cdot$  radicals (and therefore  $CS_2D$  and  $AS_2D$  species) have the opportunity to form in the system. The formation of  $CS_2^\cdot$  and  $AS_2^\cdot$  radicals (which quickly form the CSD and ASD species) and thus the propagation of  $C^\cdot$  and  $A^\cdot$  becomes the rate-determining step (with rates  $k_{\text{P,C}}[M][C^\cdot]$  and  $k_{\text{P,A}}[M][A^\cdot]$ ), in the consumption of CD (and AD) to form CSD (and ASD). The contribution of each type of radical towards the total reaction rate is dependent, amongst other factors, on the cumyl and cyanoisopropyl radical concentrations in the system. The contribution of each type of radical towards the

total reaction rate and the implication thereof will be discussed in section 5.31, after a reaction mechanism for the *in situ* polymerization reaction has been proposed.



**Scheme 5.4** The additional steps involved in the initialization period of the RAFT reaction of cumyl dithiobenzoate, styrene monomer and AIBN initiator during initialization.

At the end of the initialization process, the reactions shown in Scheme 5.5 begin to dominate. Species  $AS^{\bullet}$  and  $CS^{\bullet}$  formed can propagate further (cases IVa or IVc respectively). Alternatively, species  $AS^{\bullet}$  and  $CS^{\bullet}$  can add to a RAFT agent (cases Va and Vc). It is expected that after initialization no  $C^{\bullet}$  radicals (seen as species CD) will remain in the reaction mixture. If, however, any CD species remain after initialization, they will be quickly converted (within 100 s) to CSD species through the formation of an intermediate radical with  $C^{\bullet}$  as one adduct, with a lifetime of less than 100 s (according to the fragmentation rate of Barner-Kowollik *et al.*<sup>5</sup>), to expel a  $C^{\bullet}$  radical which will be converted to  $CS^{\bullet}$  (seen as CSD). Once equilibrium has been reached, long chain propagation can occur, i.e., case VI.  $A^{\bullet}$  radicals formed by initiator decomposition throughout the reaction will be unable to displace the longer chains that are attached to RAFT agents, i.e. case VIII, but will instead propagate to a length to which it can effectively participate in the equilibrium reversible addition fragmentation process (case VII).



**Scheme 5.5** The additional steps involved at the end of initialization in the RAFT reaction of cumyl dithiobenzoate, styrene monomer and AIBN initiator.

### 5.3.1 ESR Observations and Implications on the RAFT Mechanism

It has been shown in section 5.2 that the  $c_Y$  profile observed in the investigated cyanoisopropyl dithiobenzoate RAFT systems is probably due to a change in intermediate radical stabilities as a result of different addition and fragmentation rates of the species present in the reaction, especially during the first few monomer addition steps. In reactions mediated by cumyl dithiobenzoate, a similar  $c_Y$  evolution with reaction time is observed. It is suspected that this is again due to differences in the changes of the addition and fragmentation rates coefficients of the various radicals present in the reaction mixture with the degree of polymerization, which contributes to a variation in the stabilities of the various intermediate radicals that form during the course of reaction. However, due to the fact that two different types of radicals play a role in the cumyl dithiobenzoate reactions, i.e., cyanoisopropyl and cumyl radicals, resulting in (at least) fourteen possible different types of intermediate radicals (see Schemes 5.3, 5.4 and 5.5), elucidating the contribution of each type of intermediate radical towards the observed ESR signal is not elementary.

During the cumyl dithiobenzoate mediated *in situ* ESR polymerization reaction at 70 °C, using “normal” ESR spectroscopy parameters (single scans with 1 G modulation amplitude and a sweep width of 200 G) for detection of intermediate radicals, a period during which only a small ESR signal for intermediate radicals

could be observed (310 minutes), occurred. The same observation was made for the reaction at 84 °C, when the same stock solution, under similar reaction conditions, was polymerized *in situ*. This reaction will be discussed in section 5.3.1. When, during this period, the number of scans accumulated for each ESR spectrum was increased to 16 and a modulation amplitude of 2 G was used, an ESR signal corresponding to mostly the propagating and partly due to the intermediate radicals, could be observed (Figure 5.22). From the spectra displayed in Figure 5.22 it can be seen that the lineshape and intensity of the ESR signals change during the course of the reaction. By inspection it could be estimated that the biggest contribution towards the observed ESR spectrum during the early parts of the initialization period are due to propagating radicals. This was based on the observation of only very small ESR signals due to intermediate radicals, and comparative big ESR signals due to propagating radicals. This will be discussed later. As the reaction proceeds, the contribution of the propagating radicals decreases and that of the intermediate radicals increases.

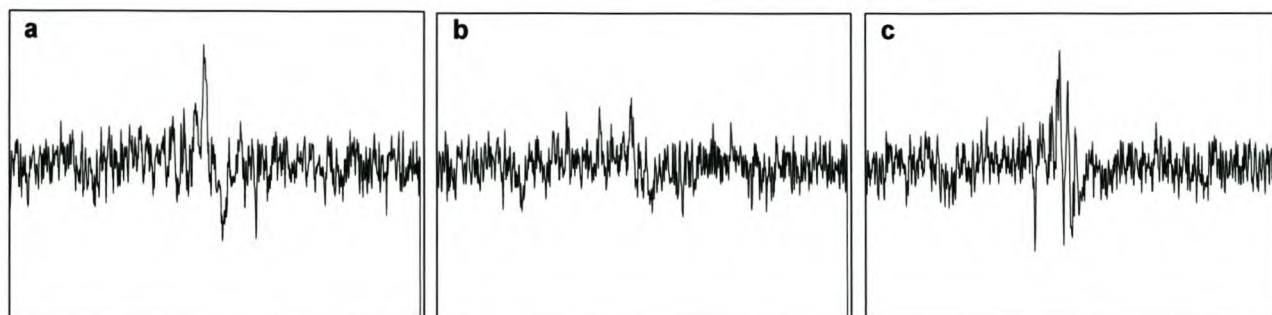


**Figure 5.22** The observed ESR signals at (a) 4, (b) 113 and (c) 240 minutes for the *in situ* ESR polymerization reaction at 70 °C. Each spectrum was recorded by accumulating 16 spectra by employing a modulation amplitude of 2 G and a sweep width of 200 G.

A similar change in ESR signal intensity and lineshape was observed when the reaction temperature was increased to 84 °C and 4 spectra accumulated (to increase the signal to noise ratio) for every observed ESR spectrum (Figure 5.23).

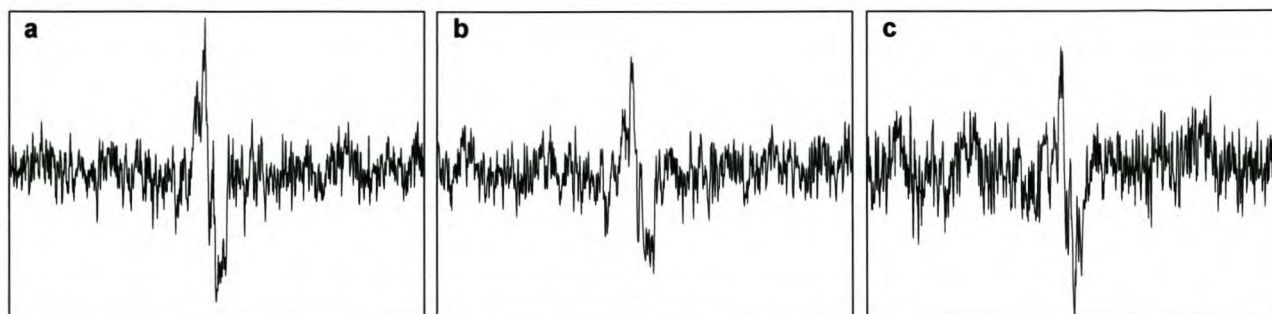
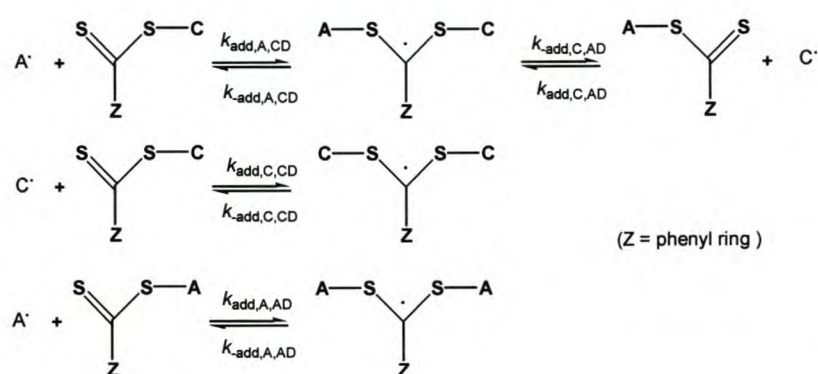


**Figure 5.23** The observed ESR signals at (a) 9, (b) 37 and (c) 65 minutes for the *in situ* ESR polymerization reaction at 84 °C. Each spectrum was recorded by accumulating 4 spectra by employing a modulation amplitude of 2 G and a sweep width of 200 G.

This observation of a change in ESR signals was expected, as according to the  $^1\text{H}$  NMR data during initialization, the predominant propagating radicals will be the  $\text{C}^{\bullet}$  and  $\text{A}^{\bullet}$  and to a lesser extent, the  $\text{CS}^{\bullet}$  and

AS\* radicals, as they will be quickly converted to CSD and ASD species. Normally, the contributions of propagating radicals towards the observed ESR signal in RAFT systems are relatively small due to their order of magnitude smaller concentrations and shorter lifetimes compared to the formed intermediate radicals under these conditions. However, during the initialization period, the propagating and intermediate radicals' lifetimes and/or concentrations are comparable, as ESR signals due to propagating radicals can be observed together with (small) signals for intermediate radicals (Figures 5.22 and 5.23). According to the proposed reaction scheme for the cumyl dithiobenzoate mediated *in situ* polymerization reaction, the predominant intermediate radicals during the early initialization period will be the C-D\*-C and CS-D\*-C intermediate radicals and to a lesser extent the A-D\*-A, AS-D\*-A and C-D\*-A, CS-D\*-A and C-D\*-SA intermediate radicals, according to the relative concentrations of the CD, CSD, AD and ASD species in the reaction mixture, as determined by <sup>1</sup>H NMR spectroscopy. This order is based on the fact that the predominant propagating radical during the initialization period is the C\* radical, therefore it is expected that intermediate radicals consisting of C\* radicals will form in higher concentrations. As increasing concentrations of CS\* and AS\* form during (later stages of) the initialization period (seen as the formation of significant concentrations of CSD and ASD species), significant concentrations of intermediate radicals CS-D\*-SC, CS-D\*-SA and AS-D\*-SA will also form. As only a small ESR signal due to intermediate radicals could be detected during the initialization period, it can be concluded that the abovementioned intermediate radicals must either be relatively unstable and therefore short-lived, or that they are only present in very small concentrations.

In Figure 5.24 the observed ESR signal during the *in situ* ESR spectroscopy reaction at 84 °C of a solution containing  $6.45 \times 10^{-1}$  M cumyl dithiobenzoate and  $5.28 \times 10^{-1}$  M AIBN in 11.2 M benzene (solution 4, Table 5.1) is given. It is instructive to note that no monomer was present in this reaction. The reactions given in Scheme 5.6 are envisaged to occur during the polymerization process.



**Scheme 5.6** The possible reaction steps involved in the *in situ* reaction of cumyl dithiobenzoate with AIBN initiator in benzene at 84 °C.

From Scheme 5.6 it can be seen that the propagating radicals present in this cumyl dithiobenzoate/AIBN system will be the cumyl and cyanoisopropyl propagating radicals, together with 3 possible intermediate radicals. This will be reflected in the observed ESR spectrum for this reaction, as it will be a summation of

the signals from the above-mentioned radicals. The observed ESR signal for this reaction (Figure 5.24 (a)) consisted of signals due to cyanoisopropyl radicals (Figure 5.24 (b)), intermediate radicals (Figure 5.24 (c)) and cumyl radicals (Figure 5.24 (d)). This was proven to be the case by preliminary ESR spectral simulations done by Tonge.<sup>38</sup> The ESR spectrum for the cyanoisopropyl radicals was obtained by *in situ* polymerization of  $5.31 \times 10^{-1}$  M AIBN in 11.2 M benzene (solution 3, Table 5.1) at 84 °C, the intermediate radical signal was taken as an example from the cumyl dithiobenzoate mediated polymerizations, and the cumyl radical spectrum was simulated by Tonge using an ESR spectra simulator program (Winsim Public EPR Software Tools (PEST), using the parameters given by Hawthorne *et al.*<sup>24</sup> A brief summary of the theory and parameters used is given in the Appendix. As the reaction progressed, the observed ESR spectrum changed, as the contributions of the cyanoisopropyl, cumyl and intermediate radicals towards the observed ESR spectrum changed (not shown). It was deduced from inspection of the observed ESR spectra that the contribution of the cumyl radicals towards the observed ESR spectrum was greater than that of the cyanoisopropyl propagating radicals. This means that the cumyl propagating radicals are probably the predominant propagating radicals during this reaction.

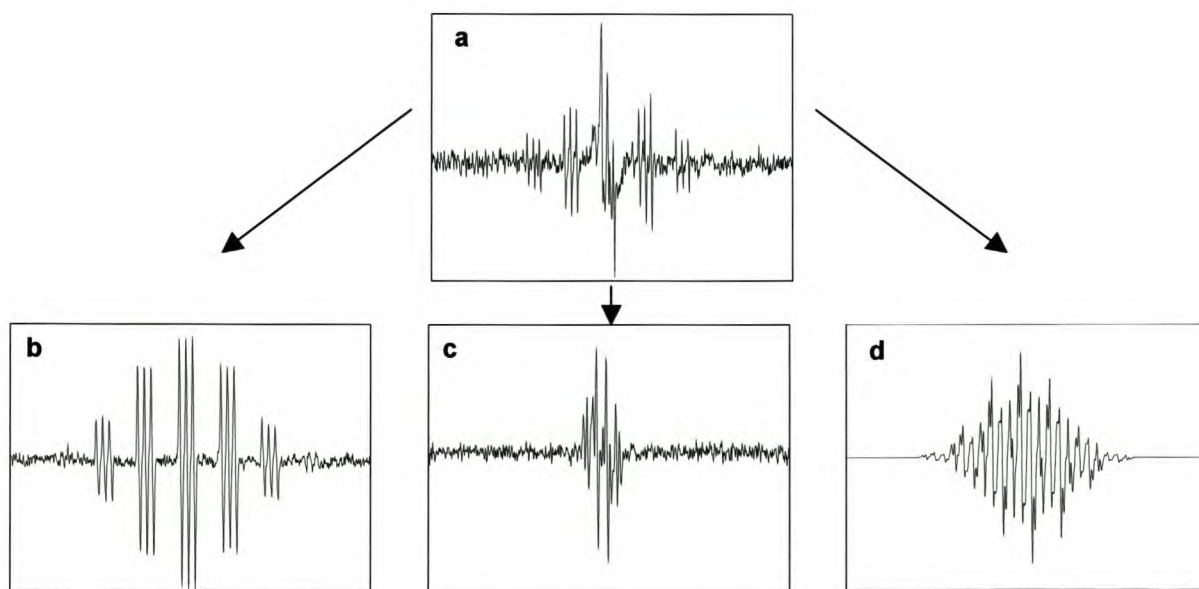


**Figure 5.24** (a) The ESR signal detected when 8 scans were accumulated for an ESR spectrum during the reaction of cumyl dithiobenzoate and AIBN in benzene at 84 °C. The detected signal consisted of the signals due to (b) cyanoisopropyl radicals, (c) intermediate radicals and (d) cumyl radicals (spectrum simulated).

The reactions occurring in this cumyl dithiobenzoate/AIBN system (Scheme 5.6) are similar to those occurring in the initial situation (portrayed in Scheme 5.3) during the *in situ* polymerization of the cumyl dithiobenzoate/styrene/AIBN system. Thus, ESR simulations could be done in a similar fashion to those simulating the cumyl dithiobenzoate/AIBN system, in an attempt to deconvolute the ESR spectra observed during the early stages of the *in situ* polymerization of the cumyl dithiobenzoate/styrene/AIBN system (solution 2, Table 5.1). From preliminary ESR simulations done by Tonge, it could be determined that the cumyl propagating radicals are probably the predominant propagating radicals during the (initial stages of the) initialization period in the *in situ* polymerized cumyl dithiobenzoate/styrene/AIBN system and that any

intermediate radicals formed during that period will be short-lived. This is consistent with the observation of a large amount of cumyl-cumyl radical termination and little cyanoisopropyl-cyanoisopropyl radical termination during initialization (Section 5.3.5). This has vast implications for the behavior and kinetics of the cumyl dithiobenzoate mediated system compared to the cyanoisopropyl mediated system. The differences between the two systems (specifically, the rate of monomer consumption) are thus probably due to the various different properties ( $k_p$ , addition rate coefficient, leaving group ability *etc.*) and inferred kinetics of the cumyl radical compared to the cyanoisopropyl radical. An important point to note here was that the ESR signal due to cyanoisopropyl radicals could barely be seen when styrene is added to the reaction mixture, as is the case for the cumyl dithiobenzoate/styrene/AIBN system. This is presumably because of fast propagation of the cyanoisopropyl radicals to form  $AS^*$  species, which will then (preferentially) add to a CD species, to displace the (shorter) cumyl group (better leaving group).

As shown in Figure 5.5, the increase of the intermediate radical concentration during the initialization period in the cyanoisopropyl dithiobenzoate mediated systems reactions shows an almost direct correlation to the increase in concentration of species ASD. As discussed in section 5.2, this is probably due to the formation of significant concentrations of stable intermediate radicals, i.e., intermediate species containing 2 secondary species ( $AS-D^*-SA$ ) during the reaction. There are two important factors to take note of in the cumyl dithiobenzoate system when comparing the intermediate radical concentration profiles of the cumyl and cyanoisopropyl dithiobenzoate mediated systems. Firstly, the rapid increase in  $c_Y$  for the cumyl dithiobenzoate mediated reaction is only observed to occur after initialization; secondly, the increase in  $c_Y$  for the cumyl dithiobenzoate mediated reaction shows a correlation to the formation of species  $CS_2D$  and  $AS_2D$  (and not CSD or ASD as in the cyanoisopropyl dithiobenzoate case). This immediately implies that the intermediate radicals produced during initialization, i.e.,  $C-D^*-C$ ,  $CS-D^*-C$ ,  $CS-D^*-SC$ ,  $A-D^*-A$ ,  $AS-D^*-A$ ,  $AS-D^*-SA$ ,  $C-D^*-A$ ,  $CS-D^*-A$ ,  $C-D^*-SA$  and  $CS-D^*-SA$ , are not stable enough (or if they are, as is the case for the  $AS-D^*-SA$  type intermediate radical, their concentrations are too low) to be observed via ESR spectroscopy using single scans and 1 G modulation amplitude. Thus, the increase in  $c_Y$  is probably due to the formation of significant concentrations of  $CS_2-D^*-S_2C$  and  $AS_2-D^*-S_2A$ .

This observation is unexpected, as the observed  $c_Y$  in the cyanoisopropyl dithiobenzoate systems showed a sharp increase when significant concentrations of  $AS-D^*-SA$  type intermediate radicals were formed. The implication of this is that even though intermediate radicals of the type  $AS-D^*-SA$  form during initialization in the cumyl dithiobenzoate systems, their concentrations are not high enough to cause a large increase in the observed  $c_Y$ . This also implies that the intermediate radicals of the type  $CS-D^*-SC$  are not stable enough to cause an increase in  $c_Y$ . From the  $^1H$  NMR data, it can be seen that significant concentrations of the CSD species are formed during initialization, and therefore significant concentrations of the  $CS-D^*-SC$  type intermediate radicals must also be present during initialization. Thus, as no large increase in  $c_Y$  is observed during initialization, it can be deduced that the  $CS-D^*-SC$  type intermediate radical must be too short-lived to be detected by ESR spectroscopy (when normal ESR operating conditions are used). This confirms the

above deduction that the intermediate radicals present during initialization will either be too unstable or not present in high enough concentrations to be detected via ESR spectroscopy. These conclusions indicate that the cumyl and cyanoisopropyl radicals (and their single monomer adducts) have vastly different fragmentation and, most likely, addition rate coefficients. It also indicates that the presence of a cumyl or cyanoisopropyl moiety as a penultimate unit in a species (for instance species  $CS^*$  or  $AS^*$ ) still has an overriding effect on the properties and behavior of the species. Thus, the character ( $k_p$ , rate of addition, leaving group ability) of species  $CS^*$  for example, will be closer to that of a cumyl radical than a styrene radical. This again implies that the behavior and kinetics of the cumyl dithiobenzoate mediated system is mostly governed by the reactions and properties of the cumyl radical.

After initialization, as a second monomer addition occurs to the growing chain, i.e., resulting in the formation of  $AS_2^*$  and  $CS_2^*$  radicals (seen at the formation of species  $AS_2D$  and  $CS_2D$ ), will the stable intermediate radicals,  $CS_2-D^*-S_2C$  and  $AS_2-D^*-S_2A$  form. The maximum in intermediate radical concentration is reached some time after the end of the initialization period.

### 5.3.2 Temperature effects

Duplicate (to the *in situ* reactions carried out at 70 °C)  $^1H$  NMR (5.40 M deuterated benzene,  $1.11 \times 10^{-1}$  M AIBN, 4.55 M styrene and  $6.67 \times 10^{-1}$  M CDB, reaction 6, Table 5.2) and ESR spectroscopy reactions (5.68 M benzene,  $1.10 \times 10^{-1}$  M AIBN, 4.30 M styrene and  $6.48 \times 10^{-1}$  M CDB, solution 2, Table 5.1) were carried out at 84 °C for comparative purposes. The time dependences of the concentrations of important species and of the intermediate radical concentration are shown in Figure 5.25. The initialization period in this case (about 50 min) was shorter than that of the reaction at 70 °C (about 240 min). The increase in intermediate radical concentration again corresponds to the formation of significant concentrations of species  $CS_2D$  and  $AS_2D$ , after which it follows a decrease according to a decrease in square root radical flux. The radical flux from the initiator clearly plays a very important role in the length of the initialization period. It is interesting to note that species AD, which is not an original component of the reaction mixture, reaches a maximum concentration prior to the commencement of spectral data collection at 8 minutes. This is shown in Figure 5.26.

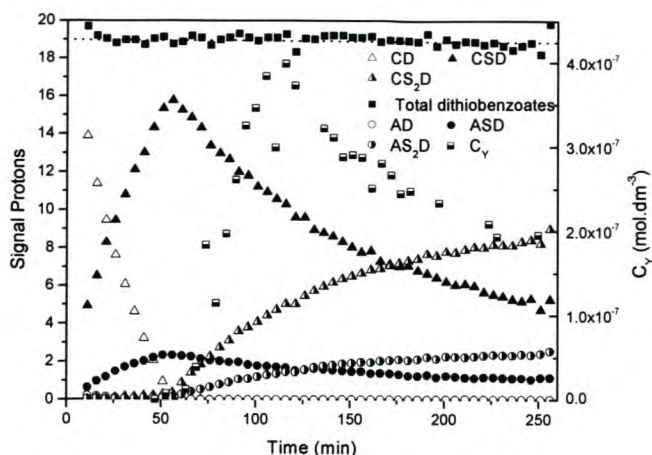


**Figure 5.25** Relative concentrations of the methyl protons of the dithiobenzoate species versus time in the polymerization of styrene in the presence of cumyl dithiobenzoate using AIBN as an initiator polymerized *in situ* at 84 °C (reaction 6, Table 5.2). The corresponding time evolution of  $c_\gamma$  is also given.

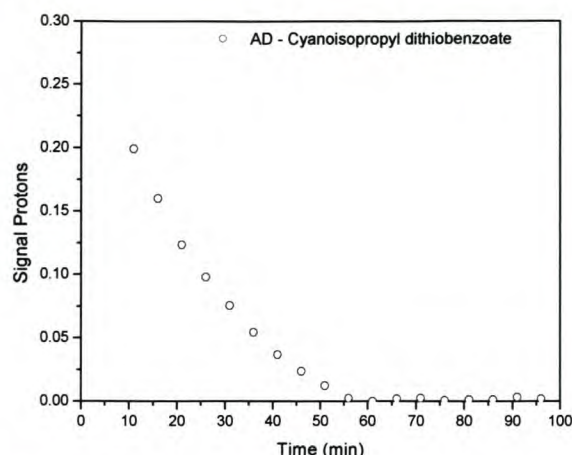


**Figure 5.26** The consumption of the AD species in the reaction at 84 °C (reaction 6, Table 5.2) is enlarged for clarity.

It has been shown in section 5.2 that the initialization time is temperature dependent in reactions mediated by cyanoisopropyl dithiobenzoate. This is again true for the case where cumyl dithiobenzoate is used as RAFT agent. This suggests that the same initialization behavior is followed for both RAFT systems. In the initial cyanoisopropyl dithiobenzoate experiments, the initialization time was determined by the rate of addition of a single styrene unit to the cyanoisopropyl radicals ( $A^*$ ) to form species  $AS^*$ , which then added to the initial RAFT agent to form species  $ASD$ . In the cumyl dithiobenzoate experiments, the duration of the initialization period is directly dependent on the rate of addition of a single styrene unit to the cumyl and (to a lesser extent) the cyanoisopropyl radicals. The length of the initialization period is much greater for the cumyl dithiobenzoate systems than for the cyanoisopropyl dithiobenzoate systems polymerized under similar reaction conditions, thus either the average termination rates are much higher in the cumyl dithiobenzoate mediated systems (leading to a lower propagating radical concentration), and/or the average propagation rate coefficient is lower in the current system. Since both of these are directly related to monomer conversion, they are discussed below.

### 5.3.3 Monomer Consumption

In RAFT polymerizations in which initiator-derived initiating radicals and initial leaving group radicals are different, the number of different propagating (and intermediate) radicals during the early stages in the reaction is increased. Specifically, here  $C^*$  and (to a lesser extent)  $A^*$  radicals are present in significant quantities, whereas before only  $A^*$  radicals were present in significant quantities. In these cases the rate of monomer consumption in the initialization period becomes a composite term to compensate for the fractions of the two types of radicals active in the system. This will substantially increase the difficulty in resolving different influences on the propagating radical concentration.

If the monomer consumption of the cumyl dithiobenzoate reactions at 70 and 84 °C, given in Figure 5.27, is examined, it can be seen that the monomer consumption is faster during the initialization period for both reactions than after this period has ended. Unlike in the cyanoisopropyl dithiobenzoate mediated systems, where an abrupt change in monomer consumption from during to after the initialization period was observed, the change in the rate of monomer consumption for the cumyl dithiobenzoate systems are far more gradual. This difference will be discussed later. This change in monomer consumption, and thus also in the reaction rate, is due to either a change in propagation and/or termination kinetics or a difference in partitioning of radicals between the intermediate and propagating forms. All of these are consistent of a system not yet having reached equilibrium.

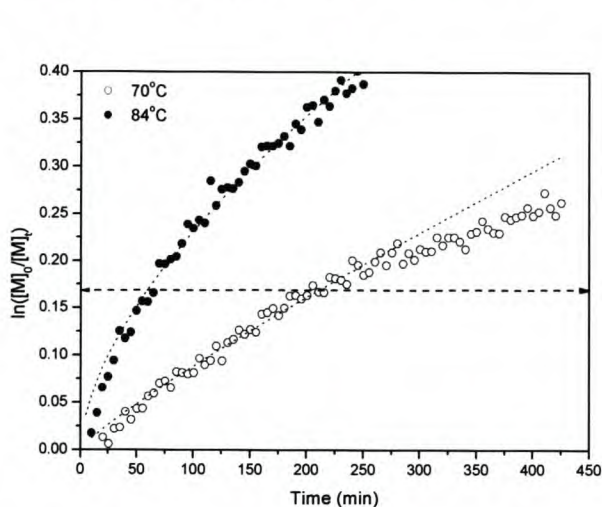


**Figure 5.27** Semi-logarithmic plot of fractional conversion versus time in the reactions of cumyl dithiobenzoate with AIBN and styrene in deuterated benzene at 84 and 70 °C (reactions 6 and 5, Table 5.2). The dotted lines (—) represent the best fit to the data. The dashed line (---) is an indication of the end of the initialization period.

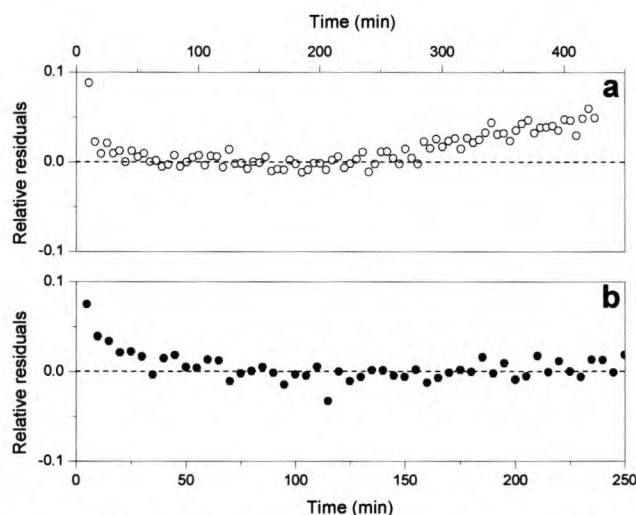


**Figure 5.28** Residuals from the fit of an exponential curve ( $y=0.001595x^{0.8713}$  and  $y=0.1379x^{0.6124}$ ) to the monomer consumption data for the reaction at (a) 70 °C and (b) 84 °C respectively.

To investigate the cause of the decrease in rate of monomer consumption observed after the initialization period, the monomer consumption data was approximated by fitting exponential curves ( $y = 0.001595x^{0.8713}$  and  $y = 0.1379x^{0.6124}$ ) to the monomer consumption data for the 70 °C and 84 °C reactions respectively. The coefficients for the exponential curves were determined by plotting the monomer consumption data in a log ( $\ln [M]_0/[M]_t$ ) vs. log (time) form, and fitting a straight line (with  $R^2 = 0.9789$  and  $R^2 = 0.9828$ ) to the 70 °C and 84 °C data respectively. It can be seen from Figure 5.28 that the above-mentioned calculated exponential curves fit the respective monomer consumption data well, with marginal deviations from the data during the early (for both data sets) and later stages (for the 70 °C data set) of the reactions.

According to equation 5-2, the time derivative of the monomer consumption data (and thus the fitted curves) yields  $k_p c_p$ , where  $k_p$  is the coefficient of propagation and  $c_p$  the propagating radical concentration, for the reaction at a specific time. Different from the term calculated in the cyanoisopropyl dithiobenzoate mediated systems,  $k_p c_p$  calculated for the cumyl dithiobenzoate systems here (during initialization) is a composite term

consisting of the coefficient for propagation of a cyanoisopropyl ( $k_{p,A}$ ) and a cumyl radical ( $k_{p,C}$ ) and the cyanoisopropyl ( $[A^*]$ ) and cumyl ( $[C^*]$ ) radical concentrations, according to equation 5-7.

$$\frac{d(\ln([M]_0/[M]_t))}{dt} = k_p c_P = k_{p,C} [C^*] + k_{p,A} [A^*] \quad (5-7)$$

Due to the selectivity inferred from the  $^1\text{H}$  NMR data, equation 5-7 is expected to be a good first approximation to the systems as it is expected that very few  $AS^*$  and  $CS^*$  species will be active in the system during initialization. After initialization, as all  $A^*$  and  $C^*$  radicals are converted to  $ASD$  and  $CSD$  species (during initialization), which fragment to form  $AS^*$  and  $CS^*$  species, equation 5-7 changes to

$$\frac{d(\ln([M]_0/[M]_t))}{dt} = k_{p,CS} [CS^*] + k_{p,AS} [AS^*] + k_{p,A} [A^*] \quad (5-8)$$

where  $k_{p,AS}$  and  $k_{p,CS}$  are the coefficients for propagation of cyanoisopropyl-styryl and cumyl-styryl radicals and  $[AS^*]$  and  $[CS^*]$  the cyanoisopropyl-styryl and cumyl-styryl radical concentrations. It should be noted here that some  $A^*$  radicals will form after initialization (due to initiator decomposition), but their concentrations are likely to be small. Due to the selectivity of the RAFT process for this system, these initiator-derived  $A^*$  radicals will propagate until they reach a degree of polymerization at which they are able to displace other fragments in the reaction mixture, before partaking in the transfer processes.

The time evolution of  $k_p c_P$ , calculated by taking the time derivative of the monomer consumption of the cumyl dithiobenzoate reaction at 70 and at 84 °C, is given in Figure 5.29. Here  $k_p$  is an average propagation rate coefficient that encompasses  $k_{p,A}$  and  $k_{p,C}$  during the initialization period and  $k_{p,A}$ ,  $k_{p,AS}$  and  $k_{p,CS}$  after initialization. The  $c_P$  here is the total propagating radical concentration for the reaction mixture. From the data presented in Figure 5.29 it can be seen that the rate of monomer consumption changes significantly from during the initialization period to the period after initialization. This change in rate is by approximately a factor of 1.5 for the 70 °C reaction and by approximately 2 for the 84 °C reaction. As mentioned above, this observed decrease in rate of monomer consumption (and thus also in rate of reaction) can either be due to a changing  $k_p$  as the  $A^*$  and  $C^*$  species are converted to their respective monomer adducts ( $AS^*$  and  $CS^*$ ), and/or due to a rapid changing  $c_P$ , which implies that either the initiation kinetics, termination kinetics or the partitioning of radicals between the propagating and intermediate forms are changing (and thus also the amount of possible intermediate radical termination). The possible change in  $k_p$  will be discussed first.

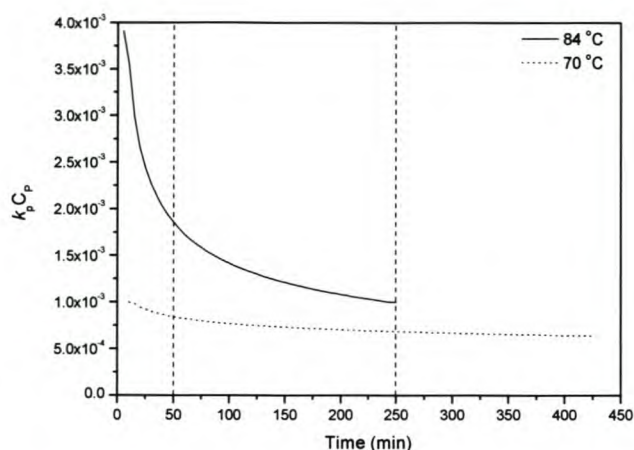


**Figure 5.29** The calculated  $k_p C_p$  time evolution for the cumyl dithiobenzoate mediated reactions with AIBN and styrene in deuterated benzene at 70 °C and 84 °C. The vertical dashed lines (--) indicate the end of the initialization periods at ± 50 min and 250 min for the 70 °C and 84 °C reactions respectively.

It is suspected that, similar to the cyanoisopropyl dithiobenzoate systems, that the decrease in reaction rate is partly due to a rapid changing (average)  $k_p$  and partly due to a change in termination kinetics for both reactions. To differentiate between the effects that  $k_p$  and the termination kinetics have on the reaction rate is extremely complex. Not only is  $k_p$  a composite term where the change in  $k_{p,A}$  to  $k_{p,AS}$  (from during to after the initialization period) is up to by more than a factor of 5 (5 200 to 960  $M^{-1}s^{-1}$  during the 70 °C reaction and 7461 to 1500  $M^{-1}s^{-1}$  during the 84 °C reaction), but the change in  $k_{p,C}$  to  $k_{p,CS}$  is also by more than a factor of 6 (6380 to 960  $M^{-1}s^{-1}$  during the 70 °C reaction and 9836 to 1500  $M^{-1}s^{-1}$  during the 84 °C reaction).<sup>19,20</sup> It should be mentioned here that the values given for the coefficient for propagation of the cumyl radicals above, were calculated based on the Arrhenius parameters for a benzyl radical, provided by Herberger *et al.*<sup>20</sup> and Walbinder *et al.*<sup>19</sup> Thus, the change in  $k_p$  for the cumyl and cyanoisopropyl radicals can explain the change observed in the monomer consumption during and after the initialization period for the cumyl dithiobenzoate mediated reactions. This result is unexpected, as the change in  $k_p$  (for the cumyl dithiobenzoate systems) predicts that the change in reaction rate should be more pronounced than the change observed in the cyanoisopropyl dithiobenzoate mediated systems. However, a gradual change in reaction rates was observed for the cumyl dithiobenzoate systems. Possible explanations for this behavior will be given when comparisons are made between the cyanoisopropyl and cumyl dithiobenzoate mediated systems.

It is also suspected that the termination kinetics of the cumyl dithiobenzoate systems, similar to the cyanoisopropyl dithiobenzoate mediated reactions, will change drastically from during to after the initialization period, and that this might contribute to the observed change in rate of monomer consumption. This will be discussed in section 5.3.5. Another factor to take into consideration is the observed formation of significant concentrations of intermediate radicals after initialization for the cumyl dithiobenzoate systems. These formed intermediate radicals can potentially undergo termination reactions (see Chapter 4). The formation of even small concentrations of terminated intermediate radicals could potentially have an enormous effect on the propagating radical concentration, as 2 propagating radicals are required to form one terminated intermediate radical species. Thus, it is expected that the sudden increase in intermediate radical

concentration after the initialization period would have a detrimental effect on the rate of monomer consumption. Any intermediate radical termination that may occur will further reduce the reaction rate.

For the purpose of discussing the difference in the reaction rates during the initialization period for the reactions at 70 and 84 °C it is assumed, as a simplification, that classical kinetics applies to the RAFT system during the initialization period. This assumption is viable as the concentration of the intermediate radicals is very small ( $c_Y \approx 0$ ) during most of the initialization period (Figure 5.21 and Figure 5.25) and therefore possible termination of the intermediate radicals during this period will not significantly change the rate of polymerization (see Chapter 4). Thus, if it is assumed that classical kinetics apply to the RAFT system during initialization, then  $c_P$  is given by

$$\frac{dc_P}{dt} = 2fk_d c_I - \langle k_t \rangle c_P^2 \quad (5-9)$$

where  $\langle k_t \rangle$  is the average termination rate constant,  $c_I$  and  $c_P$  the initiator and total propagating radical concentrations,  $f$  the initiator efficiency and  $k_d$  the rate coefficient for initiator decomposition. If a steady state in  $c_P$  is assumed ( $\frac{dc_P}{dt} = 0$ ), the resulting quadratic equation solved, and the positive root taken, the expression for  $c_P$  is then

$$c_P = \sqrt{\frac{2fk_d c_I}{\langle k_t \rangle}} \quad (5-10)$$

If  $k_p c_P$  is now corrected for the rate of initiation by dividing it by the square root of radical flux in the system ( $\sqrt{2fk_d c_I}$ ), the effects of a variable (average)  $k_p$  and possible changing termination kinetics on the reaction rate can be seen (Figure 5.30).

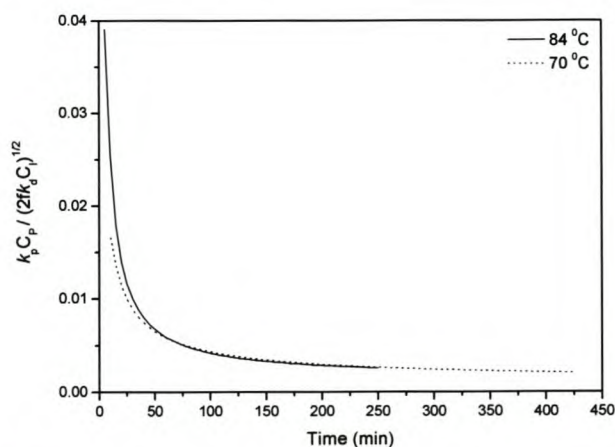


**Figure 5.30** The calculated  $k_p c_P$  (corrected for the square root of radical flux) time evolution for the cumyl dithiobenzoate mediated reactions with AIBN and styrene in deuterated benzene at 70 and 84 °C.

From Figure 5.30 it can be seen that there is an initial difference in the rate of decrease of  $k_p c_P$  for the 70 and 84 °C reactions. This initial difference can be explained in the light of different propagation rate coefficients and propagating radical concentrations for the various radicals present in the reaction (equation 5-7). It should be taken into consideration that the two systems are not directly comparable, as at a specific time interval their respective degrees of polymerization of the polymer chains present and concentrations of the various species in the reaction mixture will be significantly different. Three possible reasons might be envisaged to cause this initial difference in rate of decrease in  $k_p c_P$ . Firstly, at a higher temperature, the rate of initiator decomposition will be higher. Thus, initially, a higher concentration of  $A^*$  species will be present in the reaction mixture at 84 °C than in the reaction mixture at 70 °C, due to faster initiator decomposition. Thus the situation might be created where, in the reaction at 70 °C, the  $A^*$  species does not significantly influence the reaction kinetics and thus the reaction rates, but when the reaction temperature is increased to 84 °C, the higher concentrations of  $A^*$  radicals present might then significantly influence the reaction kinetics and rates. Secondly, an increase in temperature might (and probably does) affect the activation energies for propagation for the cyanoisopropyl and cumyl radicals ( $E_{a,A}$  and  $E_{a,C}$ ), and thus the  $k_{p,A}$  and  $k_{p,C}$  values, to different extents. Thirdly, the temperature also probably affects the termination kinetics of the cumyl and cyanoisopropyl radicals (and their monomer adducts) differently (see section 5.3.5).

Apart from an initial difference in reaction rate (up to approximately 50 min) for the reactions at 70 and 84 °C presented in Figure 5.30, both reactions show remarkably similar rates of reaction. It was seen in Figure 5.25 that the concentration of intermediate type radicals starts increasing (rapidly) after approximately 50 minutes in the 84 °C reaction, and that intermediate radical termination occurs to a detectable extent after approximately 70 minutes (Figure 4.1, Chapter 4). However, intermediate radicals are only formed in significant quantities after 310 min in the reaction at 70 °C. As the rate of reaction is similar in both the 70 and 84 °C reactions after approximately 50 minutes, it can be concluded that the partitioning of radicals between the propagating and intermediate forms (and thus also intermediate radical termination) have little effect on the rate of polymerization. Another explanation for the similar reaction rates for both reactions might be a cancellation of differences, where the change in  $k_p c_P$  (due to a change in  $k_p$  and termination kinetics) for the reaction at 70 °C closely corresponds to the change in  $k_p c_P$  (due to a change in  $k_p$ , termination kinetics and the occurrence of possible intermediate radical termination), in the reaction at 84 °C.

#### Monomer consumption of cyanoisopropyl and cumyl dithiobenzoate mediated systems compared

When comparisons are made between the monomer consumption of the cumyl and cyanoisopropyl dithiobenzoate reactions (Figure 5.31), it is clear that the rate of monomer consumption during the initialization period of the cumyl dithiobenzoate reaction is significantly slower than in the case of cyanoisopropyl dithiobenzoate. This is also reflected in Figure 5.32 where the rate of monomer consumption, corrected for the square root of radical flux, is given for the various cumyl and cyanoisopropyl mediated reactions. For the comparison in Figure 5.32 it is assumed that the initiation efficiency is the same

in all cases and that the coefficient for initiator decomposition (at a specific temperature) is the same for both systems. Since the length of the initialization period is dependent on the rate of monomer consumption under these conditions, the following explanations for the difference in rates of monomer consumption also apply to the length of the initialization periods.

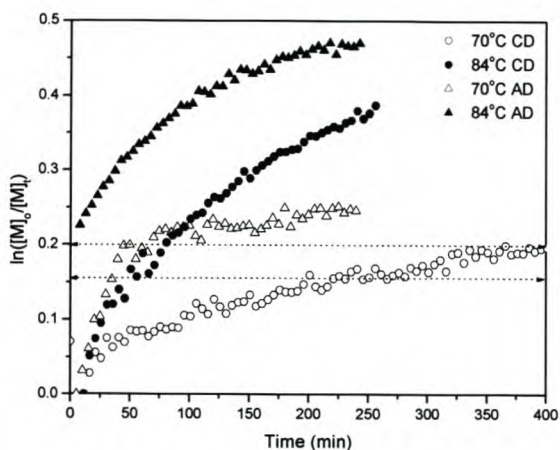


**Figure 5.31** Semi-logarithmic plot of fractional conversion versus time in the reactions of cumyl dithiobenzoate (CD) and cyanoisopropyl dithiobenzoate (AD) with AIBN and styrene in deuterated benzene at 84 and 70 °C respectively. The dotted lines indicate the end of the respective initialization periods.

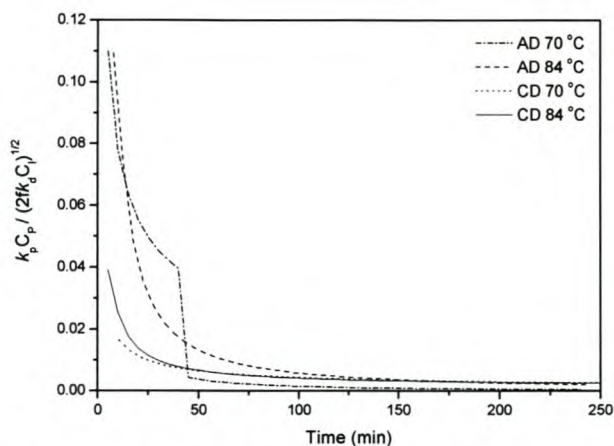


**Figure 5.32** The calculated  $k_p C_p$  (corrected for the square root of radical flux) time evolution for the cyanoisopropyl (AD) and cumyl (CD) dithiobenzoate mediated reactions with AIBN and styrene in deuterated benzene at 70 and 84 °C.

The extended initialization period (bottom dotted line given in Figure 5.31) and slower rate of monomer consumption observed in the cumyl dithiobenzoate mediated reactions when compared to the that for cyanoisopropyl dithiobenzoate mediated reactions, are probably due to different propagation and/or termination kinetics or a difference in partitioning of radicals between either the intermediate or propagating form during that period. (Note: In the ESR studies it has been observed that significant amounts of intermediate radicals form during the latter parts of initialization for the cyanoisopropyl dithiobenzoate reactions but not in the cumyl dithiobenzoate reactions). As mentioned above, the difference in the initialization time might be due to differences in propagation kinetics, in particular, the type (and corresponding propagation rate coefficient) of the predominant propagating radical in the reaction. During initialization, the rate of monomer consumption in the reactions using cyanoisopropyl and cumyl dithiobenzoate as RAFT agents, is given by

$$\frac{d(\ln([M]_0/[M]_t))}{dt} = k_{p,A} [A^*]_a \quad (5-11)$$

and

$$\frac{d(\ln([M]_0/[M]_t))}{dt} = k_{p,C} [C^*] + k_{p,A} [A^*]_c \quad (5-12)$$

where  $k_{p,A}$  and  $k_{p,C}$  are the coefficients for propagation of cyanoisopropyl and cumyl radicals with styrene monomer, and  $[A^*]$  and  $[C^*]$  the respective cyanoisopropyl and cumyl radical concentrations in the system. The subscripts **a** and **c** denote the cyanoisopropyl and cumyl dithiobenzoate reactions respectively. It should be noted that in the cumyl dithiobenzoate system there are two main types of propagating radical species present during the initialization period, i.e.,  $C^*$  and  $A^*$ . Due to the complexity of the cumyl dithiobenzoate mediated system, it was not possible to deconvolute the effect that every variable has on the rate of monomer consumption. Thus, as a simplification, it is assumed that the rate of monomer consumption is governed by the properties and kinetics of the cumyl radical and its monomer adducts. This is based on three observations: Firstly, it was observed in the recorded ESR spectra for the cumyl dithiobenzoate mediated reactions that the cumyl radical, and therefore also its monomer adducts, was the predominant propagating radical during initialization. Secondly, the  $^1H$  NMR data indicates that the concentration of the dithiobenzoate species with cumyl endgroups were higher by a factor of 8 than the concentration of the species with cyanoisopropyl endgroups. Thirdly, significantly greater amounts of cumyl-cumyl termination products were seen during initialization than any other termination-originated products (section 5.3.5). The discussion following will thus focus on the changing properties and inferred kinetics of the cumyl radical in order to explain the observed data compared to the cyanoisopropyl dithiobenzoate mediated system.

Thus, as a first approximation equation 5-12 can be re-written as

$$\frac{d(\ln([M]_0/[M]_t))}{dt} \approx k_{p,C} [C^*] \quad (5-13)$$

Based on equations 5-11 and 5-13, the differences in monomer consumption for the cyanoisopropyl and cumyl dithiobenzoate reactions during initialization could be due to either a difference in  $k_{p,A}$  and  $k_{p,C}$  on the one hand, and/or due to a difference in  $[A^*]$  and  $[C^*]$  on the other. It was discussed in section 5.2 that, in the cyanoisopropyl dithiobenzoate systems, the rate determining step during initialization (and also the reaction that determines the length of the initialization time) is the propagation of the cyanoisopropyl radicals. In the cumyl dithiobenzoate systems, the rate determining step during initialization is the propagation of the cumyl and the cyanoisopropyl radicals in the system. As a first approximation, it will be assumed that the concentration of the cyanoisopropyl radicals is small, thus the rate determining step during initialization will become the propagation of the cumyl radicals. As  $k_{p,A}$  is  $5\,200\text{ M}^{-1}\text{s}^{-1}$  and the calculated value for  $k_{p,C}$  (based on the Arrhenius parameters of a benzyl radical) is  $6\,380\text{ M}^{-1}\text{s}^{-1}$  at  $70\text{ }^\circ\text{C}$  during initialization, it is expected (based on the  $k_p$  values given above and assuming all else is equal in both systems) that the cumyl systems will exhibit a faster rate of monomer consumption during initialization and therefore a shorter initialization time than the cyanoisopropyl systems. This was however not observed.

Given the values for  $k_{p,A}$  and  $k_{p,C}$  and the significantly higher values of  $k_{p,C}$  for the cyanoisopropyl compared to the cumyl dithiobenzoate systems (given in Figure 5.32), it can be concluded that the total propagating radical concentration ( $[A^*]$ ) in the cyanoisopropyl dithiobenzoate systems must be significantly higher than

the total propagating radical concentration (approximated by  $[C^*]$ ) in the cumyl dithiobenzoate systems during initialization. As all values for  $k_p c_p$  given in Figure 5.32 are corrected for the square root of initiator decomposition, the difference in propagating radical concentrations for the two systems must be due to a difference in termination kinetics, with the cumyl dithiobenzoate system having the higher rate coefficient for termination. It is also important to recall that an increase in intermediate radical termination was observed *during* initialization for the cyanoisopropyl dithiobenzoate system at 70 °C, whereas significant concentrations of intermediate radicals only formed *after* initialization in the corresponding cumyl dithiobenzoate system. This would imply that the propagating radical concentration for the cyanoisopropyl dithiobenzoate system would be further diminished due to the increased partitioning of radicals to an intermediate radical form, where the formed intermediate radicals may still undergo possible termination reactions. Based on the observation given above, one would expect that the cyanoisopropyl dithiobenzoate systems would have a lower rate of reaction than the cumyl dithiobenzoate systems. This was however not the case. Thus, bearing all this observations in mind, the cumyl dithiobenzoate systems are predicted to have significant higher rate coefficients for termination than the corresponding cyanoisopropyl systems investigated.

From Figure 5.31 it can also be seen that the change in monomer consumption from during the initialization period compared to after initialization is far more pronounced in the cyanoisopropyl systems, than in the cumyl dithiobenzoate systems. Furthermore, the change in  $k_{p,A}$  to  $k_{p,AS}$  is up to a factor of 5 for both reaction temperatures, while  $k_{p,C}$  to  $k_{p,CS}$  also changes by up to a factor of 6 in both reactions.<sup>19,20</sup> It can also be seen from Figure 5.32 that the reaction rates for the two systems are similar at longer reaction times. As the changes in  $k_p$  (from during to after the initialization period) for the cyanoisopropyl and cumyl dithiobenzoate systems (at both temperatures) are similar, the differences in the change of monomer consumption during to after initialization must lie in the difference of the rate of monomer consumption from during initialization, which in turn is dependent on the amount of termination occurring during initialization. Thus, a higher rate of termination in the cumyl dithiobenzoate system will not only account for the observed slower rate of monomer consumption during the initialization period, but also for the lesser change in monomer consumption seen from during to after initialization.

#### 5.3.4 The Apparent Equilibrium “constant”, $K_{eq}$

In the same manner as mentioned in section 5.2.3,  $K_{eq}$  was again calculated by determination of the ratio  $c_Y$  to  $c_p$ , which was calculated through ESR spectroscopy and rate data respectively. The value for  $c_p$  was again calculated from the monomer consumption (as determined during the *in situ* NMR spectroscopy reactions) for the reactions at 70 and 84 °C.

From the  $^1H$  NMR data and ESR observations it was determined that the cumyl radical was the predominant radical present during initialization. It was stated earlier that the rate determining step during the initialization period in the cumyl dithiobenzoate systems investigated, was the propagation of the cumyl radicals to form

the species  $CS^*$ , which was quickly converted to CSD. After the initialization period, the  $CS^*$  species propagate to form species  $CS_2^*$ , which is seen as the formation of species  $CS_2D$ . Therefore, the value for  $k_p$  during the initialization period in the reaction at 70 °C was approximated by the calculated value for the addition of a benzyl radical to a styrene monomer ( $k_p = 6\,380\text{ M}^{-1}\text{s}^{-1}$ ) based on the Arrhenius parameters for a benzyl radical, provided by Herberger *et al.*<sup>20</sup> and Walbiner *et al.*<sup>19</sup> For the period after initialization it was assumed that the propagation rate coefficient for species  $CS^*$  will be slightly larger to that of styrene, thus, an average value of  $960\text{ M}^{-1}\text{s}^{-1}$ , corresponding to twice the literature value for the propagation rate coefficient of styrene at 70 °C ( $480\text{ M}^{-1}\text{s}^{-1}$ ), was assumed for  $k_p$ . The value for  $k_p$  during the initialization period in the reaction at 84 °C was approximated by the calculated value of  $9\,836\text{ M}^{-1}\text{s}^{-1}$ , and for the period after initialization, an average  $k_p$  of  $1\,500\text{ M}^{-1}\text{s}^{-1}$  (corresponding to twice the literature value of  $k_p = 750\text{ M}^{-1}\text{s}^{-1}$ ) was used.

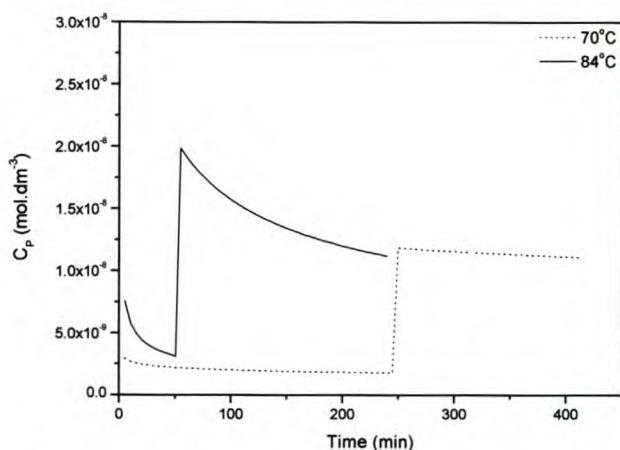


**Figure 5.33** The calculated propagating radical concentration ( $c_p$ ) time evolution for the CDB mediated reactions with AIBN and styrene in deuterated benzene at 70 °C and 84 °C (reactions 5 and 6, Table 5.2).

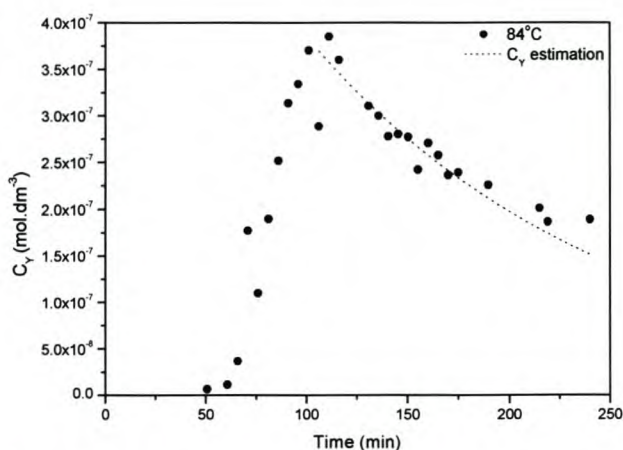


**Figure 5.34** The determined and estimated intermediate radical concentration ( $c_Y$ ) time evolution for the CDB mediated reactions with AIBN and styrene in deuterated benzene at 84 °C (solution 2, Table 5.1).

The calculated  $c_p$  values for the 70 and 84 °C reactions are given in Figure 5.33. It should be noted here that the values given for  $c_p$  in Figure 5.33 are not absolute, but based on an assumed value of  $k_p$  for the respective reactions. It can be seen for both reactions that a discontinuity in  $c_p$  exists at a time corresponding to the end of the initialization period. This is due to the large difference in  $k_p$  assumed for the reactions during, compared to after initialization. As the reason for calculating  $c_p$  was to determine  $K_{eq}$  for the reactions, the only  $c_p$  values of interest are those after initialization, when significant concentrations of intermediate radicals are formed. Thus, although a discontinuity exists, it will not influence the values calculated for  $K_{eq}$ .

A large uncertainty in the ESR spectroscopy determined values of  $c_Y$  (which is used in the calculation of  $K_{eq}$ ), resulted in some scatter of the values for  $c_Y$  in the reaction at 84 °C. To reduce the scatter,  $c_Y$  was estimated by assuming that the decrease in  $c_Y$  after a maximum was reached, follows the corresponding

decrease of square root radical flux in the system due to a rapidly decreasing initiator concentration (see Figure 5.34). Thus, the value for  $c_Y$  after a maximum was reached (at ca. 110 minutes), was approximated by the equations used to describe the decrease in square root initiator decomposition, as shown in Figure 5.34 ( $K\sqrt{e^{-k_d t}}$ , where  $K = 7.5 \times 10^{-7}$  is a constant and  $k_d = 2.22 \times 10^{-4} \text{ M}^{-1}\text{s}^{-1}$ , with  $t$  the time in seconds). Employing the estimated values for  $c_Y$  in the calculation of  $K_{\text{eq}}$  gave a less noisy time evolution profile for the calculated  $K_{\text{eq}}$ .

If it is assumed that the decrease in concentration of species CD during the initialization period for the reaction at 70 °C and 84 °C is correspondent to the formation of dormant chains with dithiobenzoate endgroups, and that there is no significant “loss” in dithiobenzoate endgroups through the formation of intermediate radicals or by possible degradation or termination mechanisms, the concentration of dormant chains of degree of polymerization  $\geq 1$  with dithiobenzoate endgroups, i.e.,  $c_{\text{PX}}$ , can be calculated. For the both reactions,  $c_{\text{PX}}$  was calculated by fitting an exponential curve of  $y = 1.29 \times 10^{-4}x^2 + 1.08 \times 10^{-1}x + 18.7$  with  $R^2 = 0.998$  for the reaction at 70 °C, and  $y = 3.33 \times 10^{-3}x^2 + 5.24 \times 10^{-1}x + 19.1$  with  $R^2 = 0.999$  for the reaction at 84 °C, to the decrease in concentration of species CD as observed by  $^1\text{H}$  NMR spectroscopy, given in Figure 5.35. Using the initial concentration of the cumyl dithiobenzoate RAFT agent used ( $6.67 \times 10^{-1} \text{ M}$ ), the decrease in concentration of the CD species during the initialization period for both reactions could be calculated. The calculated  $c_{\text{PX}}$  increases during the initialization period, after which it attains a constant value, taken as  $6.67 \times 10^{-1} \text{ M}$ , the initial cumyl dithiobenzoate RAFT agent concentration used in both the reaction mixtures. Note that the “loss” of dithiobenzoate endgroups through the formation of intermediate radicals can be neglected as their concentrations are low (ca.  $10^{-8} \text{ M}$ ) compared to the value for  $c_{\text{PX}}$ .

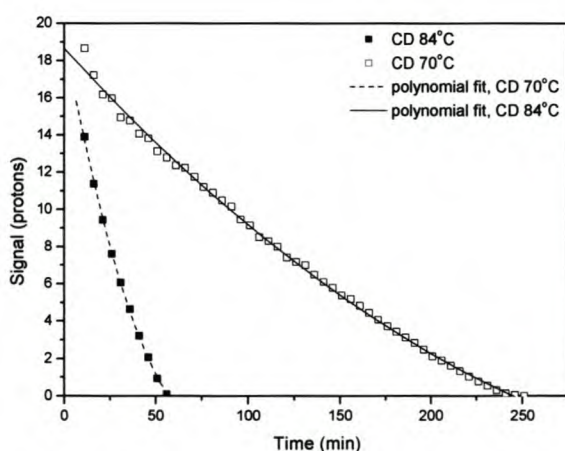


**Figure 5.35** The decrease in concentration of species CD as observed by *in situ*  $^1\text{H}$  NMR spectroscopy at 70 °C and 84 °C (reaction 5 and 6, Table 5.2). The dashed (---) and solid (—) lines represent the respective best fit to the data.

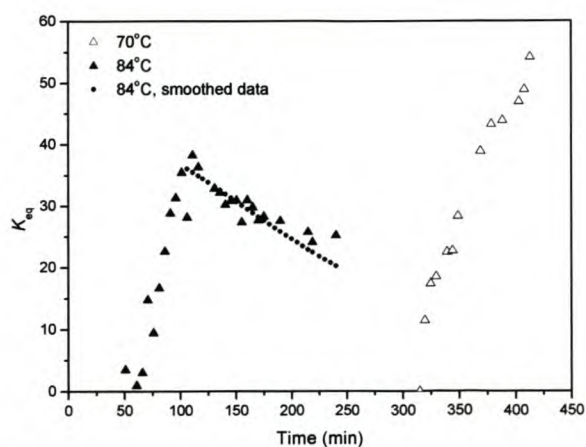


**Figure 5.36** The time evolution for the calculated equilibrium coefficient ( $K_{\text{eq}}$ ) for the CDB mediated reactions at 70 (△) and 84 °C (▲), based on  $c_Y$  and  $c_P$  values obtained from ESR spectroscopy and rate data.  $K_{\text{eq}}$  calculated by estimation of  $c_Y$  for the 84 °C (●) reaction is also given.

In Figure 5.36 the time evolution of the equilibrium coefficient for the reactions at 70 and 84 °C are given.  $K_{eq}$  for the reaction polymerized at 84 °C shows a rapid increase, and then approaches a constant value as the reaction enters an apparent equilibrium (after approximately 110 min). However, in a similar fashion to the cyanoisopropyl mediated reaction at 84 °C, an unexpected decrease in  $K_{eq}$  was also observed.  $K_{eq}$  for the reaction polymerized at 70 °C showed a fast increase after an initial induction period, and never reached a constant value during the time of reaction.

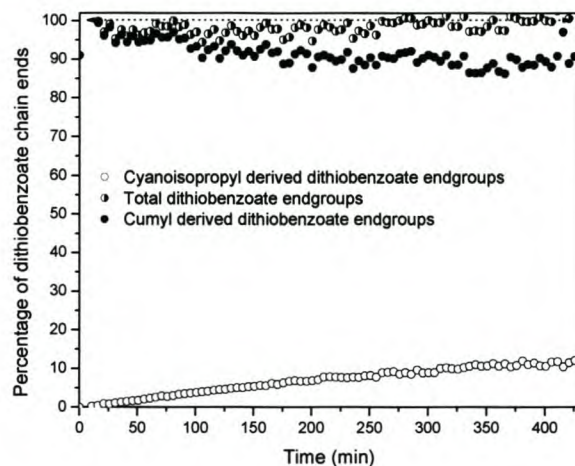
According to equation 5-6, the equilibrium coefficient ( $K_{eq}$ ) will give an indication of the changes in  $k_{add} / k_{add}$ . The proposed (partial) reaction mechanism for the cumyl dithiobenzoate mediated RAFT process during the early stages of the reaction is based on the principle that  $k_{add}$  will decrease, and that the fragmentation rate coefficients of the species present in the reaction (of the same intermediate radical) will decrease in the order  $k_{add,(C^*)} > k_{add,(CS^*)} \geq k_{add,(CS_2^*)} \geq k_{add,(CS_3^*)}$ , until such a degree of polymerization where the addition of another monomer unit onto the growing chains will not significantly affect the rate of fragmentation of the chains, i.e.  $k_{add,(CSn^*)} \approx k_{add,(CSn+1^*)}$ . If it is assumed, as a first approximation, that  $k_{add}$  is approximately constant during the reaction, the rapid increase in  $K_{eq}$  for the 70 °C reaction given in Figure 5.36, can be explained by a progressively decreasing  $k_{add}$ , i.e.  $k_{add,(CS^*)} > k_{add,(CS_2^*)}$ . Note,  $k_{add,(CS^*)}$  and  $k_{add,(CS_2^*)}$  is used here as the reaction has already passed through initialization.

If the same assumption (an approximately constant  $k_{add}$  for the reaction) is made for the reaction at 84 °C, the rapid increase in  $K_{eq}$  can also be explained in the light of a rapidly decreasing  $k_{add}$ , i.e.  $k_{add,(CS^*)} \geq k_{add,(CS_2^*)}$ . At approximately 110 min, however, a decrease in  $K_{eq}$  is observed. This would imply (if  $k_{add}$  remains constant) that  $k_{add}$  is then increasing. The sudden decrease in  $K_{eq}$  might be possible if it is assumed that  $k_{add}$  also decreases (by varying extents) during the reaction. During the first 110 minutes, the decrease in  $k_{add}$  is less than the decrease in  $k_{add}$ , resulting in a rapid increase in  $K_{eq}$ , while after 110 minutes the decrease in  $k_{add}$  will exceed the decrease in  $k_{add}$ , resulting in a decrease in the equilibrium coefficient. It should be noted here that the calculated decrease in  $K_{eq}$  might be an artifact resulting from the way the calculations were done. Small dissimilarities between reactant concentrations of solutions used in the NMR and ESR reactions and small temperature variations might cause, for example, the intermediate radical concentration to decrease faster than expected, leading to a decrease in the value of  $K_{eq}$ .

It should be remembered here that the calculated values of  $K_{eq}$  for the reactions polymerized at 70 and 84 °C are not absolute values, but were calculated to give an indication of the changes in  $K_{eq}$  with time. The values calculated for  $K_{eq}$  for the two systems are thus not directly comparable. The higher observed value of  $K_{eq}$  for the 70 °C reaction is, similarly to the cyanoisopropyl dithiobenzoate mediated reactions, possibly due to a higher activation energy for fragmentation compared to that for addition. This would imply that the rate coefficient for fragmentation would be more affected by a lowering in temperature compared to the rate coefficient for addition, leading to an effective increase in the value of  $K_{eq}$ .

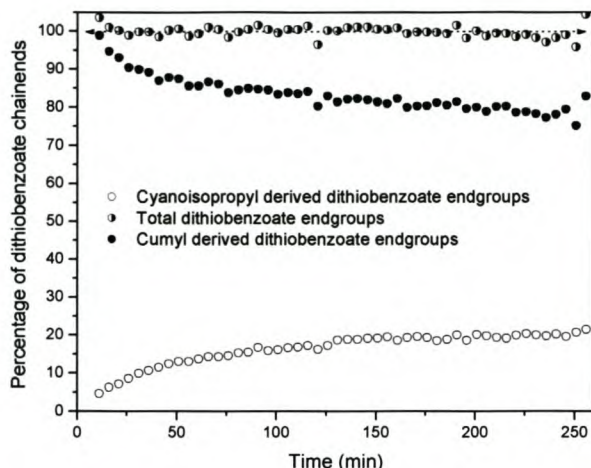
### 5.3.5 Radical Generation and Termination Products

Examining the terminated species gives insight into the reactions that govern the RAFT mechanism during the earlier stages of the polymerization process. This can be done in two ways: firstly by examining the relative concentrations of all of the (living) dithiobenzoate species with cumyl and cyanoisopropyl end-groups and secondly, by examining the formed terminated species directly.



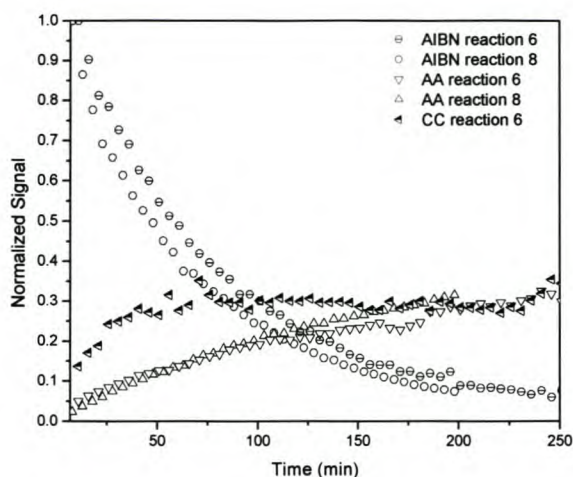
**Figure 5.37** Plot of the cumulative integrated end-groups of the dithiobenzoate species, in the polymerization of 4.55 M styrene, in the presence of  $6.67 \times 10^{-1}$  M cumyl dithiobenzoate, using  $1.11 \times 10^{-1}$  M AIBN as an initiator in 5.40 M deuterated benzene at 70 °C (solution 5, Table 5.2).

Figure 5.37 shows the time dependence of the relative concentrations of all dithiobenzoate species with cumyl (CD, CSD, CS<sub>2</sub>D), and cyanoisopropyl (AD, ASD, AS<sub>2</sub>D) endgroups in reaction 5 (reaction at 70 °C). There is a gradual displacement of the cumyl endgroups from the living polymer, with a corresponding increase in species with cyanoisopropyl endgroups, and no observable overall loss of dithiobenzoate species. Termination of cumyl and cumylstyryl radicals is responsible for the decrease in species with cumyl endgroups. It can be seen that approximately 10% of the total chains with cumyl endgroups are displaced, which indicates that approximately 10% of chains with cumyl endgroups are lost to termination during the reaction, under the conditions used. The concentration of dithiobenzoate chains with cyanoisopropyl endgroups increase throughout the reaction as more initiator decomposes. The number of living chains with a cyanoisopropyl endgroup increases with time due to two 2 factors: (1) “transfer” is efficient, therefore species CD will be displaced with species AD, allowing termination of expelled C\*, (2) there is a limited supply of cumyl groups, whereas A\* are continually supplied. Under such conditions, the total number of chains with cyanoisopropyl endgroups must therefore increase. A constant concentration of chains with dithiobenzoate endgroups throughout the reaction indicates that very little (below the detection limit of the NMR equipment) loss of these types of chains occurs (due to intermediate radical termination or degradation) throughout the duration of the reaction.



**Figure 5.38** A plot of the cumulative integrated end-groups of the dithiobenzoate species, in the polymerization of 4.55 M styrene mediated by  $6.67 \times 10^{-1}$  M cumyl dithiobenzoate, using  $1.11 \times 10^{-1}$  M AIBN as an initiator in 5.404 M deuterated benzene at 84 °C (reaction 6, Table 5.2).

Figure 5.38 shows the time dependence of the relative concentrations of all dithiobenzoate species with cumyl and cyanoisopropyl end-groups within the first 3 hours of reaction 6 (reaction at 84 °C). This shows a gradual increase of cyanoisopropyl end-groups during the reaction – the rate of which is at a maximum early in the reaction. This is to be expected, as the number of cyanoisopropyl radicals generated by AIBN decomposition is highest early in the reaction. As all of the dithiobenzoate species with cumyl endgroups are present at the beginning of the reaction, a maximum is expected at the beginning of the reaction and a gradual decrease in the concentration of the dithiobenzoate species with cumyl endgroups, as some of the cumyl groups (or cumyl adducts) are involved in termination. This was observed. It is also interesting to note that the highest rate of decrease is during the earlier part of the reaction, i.e. during the initialization period (approximately 50 minutes). This is evidenced by the high level of cumyl-cumyl (CC) termination seen during the initialization period (Figure 5.39). Compared to reaction 5, the higher temperature used in reaction 6 increased the radical flux in the system, leading to a higher rate of cumyl endgroup displacement from the dithiobenzoate species. The net result was approximately 20% of cumyl endgroup displacement occurred by the end of the reaction. The interchange of endgroups is especially important for applications in which specific endgroups are required.



**Figure 5.39** The concentration evolution of the termination products formed and initiator decomposition in the reaction of styrene and AIBN with and without cumyl dithiobenzoate (reaction 6 and 8, Table 5.2) in deuterated benzene at 84 °C. Reaction 6: 4.55 M styrene,  $6.67 \times 10^{-1}$  M cumyl dithiobenzoate,  $1.11 \times 10^{-1}$  M AIBN and 5.40 M deuterated benzene. Reaction 8: 4.85 M styrene,  $0.829 \times 10^{-1}$  M AIBN and 4.98 M deuterated benzene.

By directly following the concentration of the termination products formed during reaction 6, it is seen (Figure 5.39) that there are significantly more cumyl-cumyl (CC) termination products than other termination products. Other termination reactions occur (i.e. giving products AC and CSC) but due to their lack of symmetry in structure (leading to fine structure and broad peaks) and small concentrations, these termination products were too small to be integrated accurately and are therefore not shown in Figure 5.39. If it is assumed that the rate coefficients for termination for the short chain radicals present in the reaction at this stage are similar, then this implies that the transfer process is very efficient, leading to a predominance of cumyl radicals in the system during the early stages of the polymerization. This is due to displacement of cumyl radicals by  $AS^*$ ,  $CS^*$  and  $A^*$  ( $A^*$  are the next most common propagating species) radicals, although the concentration of the generated species AD is low relative to that of the CD species. When this is examined in the context of the monomer consumption data (Figure 5.27) it can be seen that the concentration of propagating species is at a maximum during the early part of the reaction; consequently termination will also be at a maximum. We observe a high rate of CC termination products forming during the early parts of the reaction, implying that the cumyl radical will be the most abundant radical during the early reaction (this was also confirmed by ESR spectroscopy observations). The other termination product that may be expected in the initialization period, species AC, is present only in very low concentrations with respect to CC species in the reaction. This would suggest that very low concentrations of  $A^*$  species are present in the reaction in relation to the  $C^*$  species.

The formation of the AA species in reaction 6 can be examined in comparison with the AA termination that would occur in a conventional free radical polymerization (Figure 5.39). The concentration of the AA (tetramethyl succinonitrile) termination product is almost identical to that found in a control reaction (reaction 8, Table 5.2) at early reaction times suggesting that the AA termination product is predominantly a geminate recombination product as in the case of the control reaction.

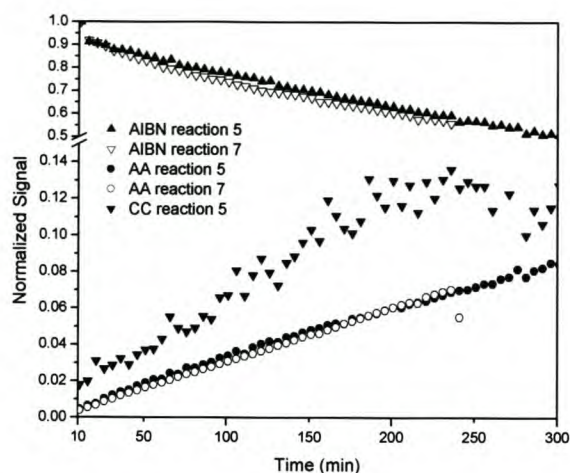


**Figure 5.40** The concentration evolution of the termination products formed in the reaction of styrene and AIBN with and without cumyl dithiobenzoate (reaction 5 and 7) in deuterated benzene at 70 °C. (Reaction 5: 4.55 M styrene,  $6.67 \times 10^{-1}$  M cumyl dithiobenzoate,  $1.11 \times 10^{-1}$  M AIBN and 5.40 M deuterated benzene. Reaction 7: 4.55 M styrene,  $0.834 \times 10^{-1}$  M AIBN and 5.40 M deuterated benzene)

In Figure 5.40 the termination products for reaction 5 at 70 °C are shown. The very small amounts of termination products formed at the lower temperature complicated analysis but similar trends were observed as in the reaction at higher temperature. The CC termination product formation is dominant until the end of initialization (approximately 250 min) at which time the termination of the CC radicals ceases. This is due to all cumyl radicals being converted to their single monomer analogues during the initialization period. Thus, no cumyl radicals are expected to remain in the reaction mixture after the initialization period.

Due to the unique process occurring during the initialization period which active chains are kept short, increased concentrations of termination products are observed to form in RAFT mediated polymerizations during this time. During the initialization period the  $A^*$  or  $C^*$  will add to a monomer unit to form  $AS^*$  and  $CS^*$ . When these species undergo efficient transfer, a short  $A^*$  or  $C^*$  will be expelled. This means that unlike a conventional radical polymerization, during the initialization period the slower terminating  $AS^*$  and  $CS^*$  species will be replaced with faster terminating  $A^*$  and  $C^*$  radical species. There are significantly higher concentrations of these short chain termination products compared with a control reaction because of this replacement during the initialization period. After the initialization period the geminate recombination process dominates the formation of the AA species as shown in Figure 5.37 and Figure 5.38. The chain length dependence of the termination rate coefficients means that short species will have a higher rate of termination, thus the overall termination rate will be higher in RAFT mediated reactions than that of a control reaction in which the short chains are quickly converted into longer chains.<sup>32,33</sup> The higher rate of radical loss through termination implies that RAFT mediated reactions will require significantly higher radical fluxes to allow reactions to proceed at the same reaction rates as conventional reactions. As most termination occurs during the initialization period, reactions with pronounced initialization periods will consequently have a lower propagating radical concentration after the initialization period, leading to a slower rate of reaction after the initialization period. This behavior would be a contributing factor to reported increased retardation in cases where cumyl dithiobenzoate has been used as a RAFT agent.<sup>39</sup>

### 5.3.6 Beyond Initialization

In the hypothetical case of an initiator that provides radicals that are unable to displace initial R groups from the initial RAFT agent, the process of initialization will be begun by the propagation of the initiator-derived radicals prior to exchange. In the reactions of cumyl dithiobenzoate with AIBN as initiator, the relative leaving abilities of the radicals are such that some displacement of the cumyl group (by the cyanoisopropyl radical) can occur before the first propagation step, as has been seen by the formation of small concentrations of AD species in reactions. The small concentrations of AD produced however made very little difference to the system.

On the other hand, the use of very active radical initiator species should be carefully monitored. As this active initiator radical species can easily displace the R group of the initial RAFT agent, it may be possible to create a situation in which the incoming polymer chain (formed through propagation of the initial R group) is unable to displace the initiator fragment from the RAFT agent, preventing or retarding the RAFT process leading to a potential increase in polydispersity.

### 5.3.7 Conclusions

This study has provided more direct evidence for details of the mechanism of the initialization period of the RAFT process. It was found that the addition-fragmentation process was extremely selective during this period and, because of this, significant quantities of RAFT adducts of degrees of polymerization greater than one were formed only after complete conversion of the initial RAFT agent to its monomeric adducts. The critical process in the initialization of a RAFT controlled polymerization was found to be the formation of the single monomer adduct dithiobenzoate species and, by implication, the propagation of the initial leaving and initiator-derived radical groups.

*In situ*  $^1\text{H}$  NMR spectroscopy showed that the first interval of polymerization that could be observed in the studied systems is an initialization period, which we have defined as the period prior to the consumption of the initial RAFT agent. In the case of styrene this initialization period shows a more rapid rate of reaction than afterwards. *In situ* ESR spectroscopy showed that the intermediate radicals formed during this period were short lived and/or present in small concentrations. The cumyl radical was identified to be the predominant propagating radical during initialization.

The cumyl dithiobenzoate system investigated showed, similar to the cyanoisopropyl dithiobenzoate system, a decrease in reaction rate after initialization. This retardation was attributed to a change in termination kinetics or the formation of terminated intermediate radical products. The cumyl dithiobenzoate systems investigated also exhibited an overall slower rate of reaction during and after the initialization period, compared to the corresponding cyanoisopropyl dithiobenzoate systems. This was mainly attributed to higher termination rates in the cumyl dithiobenzoate system, thereby causing rate retardation.

It was seen in the calculation of the equilibrium coefficient that there is a marked change in  $c_p$  from during to after the initialization period. This was attributed to a change in the rate of termination of the system, and/or the occurrence of intermediate radical termination, as the intermediate radical concentration increased rapidly during this time.

The termination product of two cumyl radicals was observed to occur only during initialization, and was identified to be significantly higher in concentration than the formed TMSN termination product. This enhanced the indication that the cumyl radicals are the predominant propagating radicals during initialization.

In the system studied, the poorest leaving group was the styryl radical ( $AS^*$  and  $CS^*$ ), although the "long chain" value of addition, propagation, and fragmentation rate coefficients needs to be achieved before the system is at equilibrium. This could be two or more monomer units for propagation.

The reasons for the behavior observed for the RAFT system are suggested as again being dependent on the relative reactivities and radical stabilities, and therefore the related addition and fragmentation rate coefficients of the tertiary radical species in the systems and their monomer adducts. This can be extended to all efficient RAFT systems where multiple radical species are present and should not be considered as solely an explanation of the cumyl dithiobenzoate system.

## 5.4 Overall Conclusions

It was shown that for the RAFT mediated reactions investigated, an initialization period occurred, which was defined as the period prior to complete consumption of the initial RAFT agent. During this period, the RAFT reactions showed extreme selectivity in addition of a single monomer unit to the growing chains before the addition of another monomer unit. By implication, the rate determining step during the initialization period is the propagation of the initial RAFT leaving groups.

This extreme selectivity was attributed to dissimilar addition and fragmentation rate coefficients of the species present in the reaction mixtures. Calculations of the equilibrium coefficient were consistent with a continuous decrease in the addition and fragmentation rate coefficients of the species in the reactions.

Analysis of ESR spectra indicated that propagating radicals were the predominant radicals present during the initialization period in the reactions investigated. Intermediate radicals present during the initialization period were either unstable or present in low concentrations. This instability and/or low concentrations of the intermediate radicals was attributed to the fast fragmentation rate coefficients of the initial RAFT agent leaving group (R), compared to its single monomer adduct (RM).

A decrease in reaction rate was observed to occur after initialization. However, the magnitude of this decrease was highly system (RAFT agent) dependant. This change in reaction rate was attributed to a

change in termination kinetics, propagation rate coefficients and/or the formation of terminated intermediate radical products. Analysis of the termination products formed during and after initialization, indicated that termination is a more frequent event during the initialization period than afterwards.

The results given in this chapter indicate that the early time reactions defining the RAFT mechanism are not as elementary as first believed. Propagation, termination, addition and fragmentation rate coefficients all change significantly during this period. Assumptions of constant values for these rate coefficients will thus yield incorrect values and might lead to incorrect conclusions. It also indicates that intermediate radical termination can lead to possible rate retardation, and should therefore be included in the reactions defining the RAFT mechanism.

## References

1. Barner-Kowollik, C.; Heuts, J. P. A.; Davis, T. P. *J. Polym. Sci., Part A: Polym. Chem.* **2001**, *39*, 656.
2. Haddleton, D. M.; Perrier, S.; Bon, S. A. F. *Macromolecules* **2000**, *33*, 8246.
3. Aguilar, M. R.; Gallardo, A.; Fernandez, M. D. M.; Roman, J. S. *Macromolecules* **2002**, *35*, 2036.
4. Goto, A.; Sato, K.; Tsujii, Y.; Fukuda, T.; Moad, G.; Rizzardo, E.; Thang, S. H. *Macromolecules* **2001**, *34*, 402.
5. Barner-Kowollik, C.; Quinn, J. F.; Morsley, D. R.; Davis, T. P. *J. Polym. Sci., Part A: Polym. Chem.* **2001**, *39*, 1353.
6. Coote, M. L.; Radom, L. *J. Am. Chem. Soc.* **2003**, *125*, 1490.
7. Barner-Kowollik, C.; Coote, M. L.; Davis, T. P.; Radom, L.; Vana, P. *J. Polym. Sci., Part A: Polym. Chem.* **2003**, *41*, 2828.
8. Monteiro, M. J.; de Brouwer, H. *Macromolecules* **2001**, *34*, 349.
9. Wang, A. R.; Zhu, S.; Kwak, Y.; Goto, A.; Fukuda, T.; Monteiro, M. J. *J. Polym. Sci., Part A: Polym. Chem.* **2003**, *41*, 2833.
10. Wang, A. R.; Zhu, S. *J. Polym. Sci., Part A: Polym. Chem.* **2003**, *41*, 1553.
11. Kwak, Y.; Goto, A.; Tsujii, Y.; Murata, Y.; Komatsu, K.; Fukuda, T. *Macromolecules* **2002**, *35*, 3026.
12. Moad, G.; Solomon, D. H. *The Chemistry of Free Radical Polymerization*; First ed.; Elsevier Science Ltd, **1995**.
13. Huang, D. M.; Monteiro, M. J.; Gilbert, R. G. *Macromolecules* **1998**, *31*, 5175.
14. Heuts, J. P. A.; Gilbert, R. G.; Radom, L. *Macromolecules* **1995**, *28*, 8771.
15. Le, T. P.; Moad, G.; Rizzardo, E.; Thang, S. H., *PCT Int Appl*, **1998**, wo98/01478.
16. Van Geet, A. L. *Anal. Chem.* **1968**, *40*, 2227.
17. Tonge, M. P.; Kajiwara, A.; Kamachi, M.; Gilbert, R. G. *Polymer* **1998**, *39*, 2305.
18. McLeary, J. B.; Calitz, F. M.; McKenzie, J. M.; Tonge, M. P.; Sanderson, R. D.; Klumperman, B. *Macromolecules*, Submitted.
19. Walbiner, M.; Wu, J. Q.; Fischer, H. *Helvetica chimica acta* **1995**, *78*, 910.
20. Herberger, K.; Fischer, H. *International Journal of Chemical Kinetics* **1993**, *25*, 249.
21. Chong, Y. K. B.; Krstina, J.; Le, T. P. T.; Moad, G.; Postma, A.; Rizzardo, E.; Thang, S. H. *Macromolecules* **2003**, *36*, 2256.
22. Barner-Kowollik, C.; Vana, P.; Quinn, J. F.; Davis, T. P. *J. Polym. Sci., Part A: Polym. Chem.* **2002**, *40*, 1058.
23. Buback, M.; Gilbert, R. G.; Hutchinson, R. A.; Klumperman, B.; Kuchta, F.-D.; Manders, B. G.; O'Driscoll, K. F.; Russell, G. T.; Schweer, J. *Macromol. Chem. Phys.* **1995**, *196*, 3267.
24. Hawthorne, D. G.; Moad, G.; Rizzardo, E.; Thang, S. H. *Macromolecules* **1999**, *32*, 5457.
25. Calitz, F. M.; Tonge, M. P.; Sanderson, R. D. *Macromolecules* **2003**, *36*, 5.
26. Kwak, Y.; Goto, A.; Fukuda, T. *Macomolecules* **2003**, Submitted.
27. Perrier, S.; Barner-Kowollik, C.; Quinn, J. F.; Vana, P.; Davis, T. P. *Macromolecules* **2002**, *35*, 8300.
28. Brandrup, J.; Immergut, E. H.; Grulke, E. A. *Polymer Handbook*; John Wiley and Sons, Inc, **1999**.
29. Manders, B. G., **1997**, Thesis, Eindhoven University of Technology.

30. Barner, L.; Quinn, J. F.; Barner-Kowollik, C.; Vana, P.; Davis, T. P. *Eur. Polym. J.* **2003**, *39*, 449.
31. Vana, P.; Davis, T. P.; Barner-Kowollik, C. *Macromolecular theory and simulations* **2002**, *11*, 823.
32. Heuts, J. P. A.; Davis, T. P.; Russell, G. T. *Macromolecules* **1999**, *32*, 6019.
33. Buback, M.; Egorovc, M.; Gilbert, R. G.; Kaminsky, V.; Olaj, O. F.; Russel, G. T.; Vana, P. *Macromol. Chem. Phys.* **2002**, *203*, 2570.
34. Scheren, P. A. G. M.; Russell, G. T.; Sangster, D. F.; Gilbert, R. G.; German, A. L. *Macromolecules* **1995**, *28*, 3637.
35. Russell, G. T.; Gilbert, R. G.; Napper, D. H. *Macromolecules* **1992**, *25*, 2459.
36. Russell, G. T.; Gilbert, R. G.; Napper, D. H. *Macromolecules* **1993**, *26*, 3538.
37. Calitz, F. M.; Tonge, M. P.; Sanderson, R. D. *Manuscript in preparation*.
38. Tonge, M. P., Personal Communication
39. Moad, G.; Chiefari, J.; Chong, Y. K.; Krstina, J.; Mayadunne, R. T. A.; Postma, A.; Rizzardo, E.; Thang, S. H. *Polym. Int.* **2000**, *49*, 993.

# Chapter 6

## Epilogue

### Summary

*This chapter is a summary of the experiments, results and discoveries that lead us to discover some of the secrets of the RAFT mechanism. Unusual ESR results (Chapter 3) and the observation of some unexpected behaviour of the RAFT systems investigated prompted the search for possible terminated intermediate RAFT radicals, which was deemed a probable explanation for the anomalous behaviour seen. In situ  $^{13}\text{C}$  NMR spectroscopy, with a  $^{13}\text{C}$  labeled RAFT agent (Chapter 4), provided the first experimental evidence for possible terminated intermediate radical species. In situ  $^1\text{H}$  NMR spectroscopy was also found to be an excellent way to follow the time evolution of the species involved in the RAFT reactions (Chapter 5). The in situ  $^1\text{H}$  NMR spectroscopy together with follow-up ESR investigations (Chapter 5) provided some of the last missing pieces to the RAFT mechanism puzzle and some answers to anomalies observed in some RAFT systems. Finally, recommendations are given for future research to further unravel the mysteries surrounding the RAFT mechanism.*

## 6.1 Conclusions

The investigations in this thesis were aimed at gaining a more thorough understanding of the RAFT mechanism and the important reactions therein. Experiments done were specifically designed to investigate the probable causes for inhibition and rate retardation observed in some RAFT mediated polymerization systems.

In Chapter 3, the type of radicals and the concentration of radicals present in a RAFT system were examined by employing electron spin resonance (ESR) spectroscopy. *In situ* ESR reactions were performed to determine the time evolution of the intermediate radical concentration ( $c_Y$ ). In all styrene/CDB reactions,  $c_Y$  was initially too low for direct observation in the ESR spectra, but increased (to observable concentrations) with time to a maximum, followed by a very slow decrease. The equilibrium coefficient for the reactions ( $K_{eq}$ ) was determined by combining ESR and rate data. This calculated value for  $K_{eq}$  always started very low, and increased with time (showing initial correlations with  $\overline{M}_n$ ). It appeared to be dependent on the reaction temperature and the concentration of the RAFT agent used. The variation in  $K_{eq}$  with time and/or  $\overline{M}_n$  is inconsistent with the standard RAFT model.<sup>1</sup> A simple explanation was proposed for this which included that both  $k_{add}$  and  $k_{add}$  are chain-length dependent. Other possibilities for a varying  $K_{eq}$  include reactions that consume intermediate radicals, such as reversible or irreversible termination reactions involving the intermediate. Although the idea of intermediate radical termination was not a new concept,<sup>2</sup> it was thought that it might be a probable explanation for the observed behavior.

Unusual behavior of certain RAFT systems was also observed, a summary of which is given below.

- The observed intermediate radical concentrations were not consistent with the predictions based on existing literature models.<sup>2-4</sup>
- The time dependence of the intermediate radical concentration varied significantly with the type of RAFT agent.
- Intermediate radicals were detected at very long reaction times in the virtual absence of initiator.
- An extra radical (non-propagating or intermediate) species was observed to form during the reaction; its concentration increased with time.
- The RAFT process (for CDB) was not particularly sensitive to oxygen.

As mentioned above, it was suspected that some "other" process must be in operation to decrease the intermediate radicals present in the system. It was proposed by some authors that termination of intermediate radicals was possible.<sup>2,4</sup>  $^{13}\text{C}$  NMR spectroscopy (Chapter 4) was therefore used to find these proposed intermediate radical termination products.

In Chapter 4, the spectra of an *in situ*  $^{13}\text{C}$  NMR reaction of styrene and AIBN in deuterated benzene at 84 °C, mediated by a  $^{13}\text{C}$  enriched (at the dithioester carbon) cumyl dithiobenzoate, are given. A  $^{13}\text{C}$  labeled RAFT agent was used to increase the signal-to-noise ratio, as it was expected that only minute quantities of the

terminated intermediate RAFT radicals would form. To increase the occurrence of possible side reactions (it was believed that intermediate radicals are most likely to be terminated by short species at early reaction times), high RAFT agent and initiator concentrations were used to target low molecular weight chains at full conversion. Initial analysis of the  $^{13}\text{C}$  spectra revealed the formation of peaks corresponding to possible intermediate radical terminated species. Upon comparison with corresponding DEPT spectra, these peaks were identified to be due to quaternary carbons. The chemical shifts of these peaks (74 - 78ppm) corresponded well to chemical shift predictions for possible terminated intermediate radical species predicted to form. In a similar *in situ*  $^{13}\text{C}$  NMR reaction, mediated by a non-labeled RAFT agent, no such peaks were observed to form. It was also discovered through analysis of the  $^{13}\text{C}$  spectra that the RAFT reaction is extremely selective during the early stages of the reaction. As a result, stable intermediate radicals only formed after longer polymerization times. Consequently, the peaks corresponding to possible termination products were seen to only form at longer reaction times when significant intermediate radical concentrations existed.

During  $^{13}\text{C}$  NMR analysis it was discovered that the RAFT reactions could probably be followed via *in situ*  $^1\text{H}$  NMR spectroscopy. Chapter 5 describes the *in situ*  $^1\text{H}$  NMR reactions done in deuterated benzene with cyanoisopropyl or cumyl dithiobenzoate as RAFT agent, styrene as monomer and AIBN as initiator at 70 °C and 84 °C. High RAFT agent and initiator concentrations (similar to those used in the *in situ*  $^{13}\text{C}$  reactions) were again used.

The concentration evolution for the dithiobenzoate species in the reaction mixture could be followed with time. It was discovered that all of the reactions go through an "initialization period", the term being defined as the period before consumption of all of the initial RAFT agent. It was found that the length of the initialization period was governed by the reaction temperature, the type of R group on the initial RAFT agent and the initiator fragments produced. Based on these observations, a mechanism was proposed for the RAFT process during the early stages of the reaction. This proposed mechanism indicated extreme selectivity of the RAFT process, i.e., no chains with a degree of polymerization greater than unity formed before the end of the initialization period. The proposed mechanism was based on the assumption of asymmetric fragmentation rate coefficients of the formed intermediate radicals and varying addition rate coefficients of propagating radicals to RAFT agents. It was also found via *in situ* ESR experiments, conducted on similar solutions to those used in the *in situ* NMR experiments, that during this initialization period the intermediate radical concentrations were extremely low, but increased to a maximum as significant concentrations of chains with two (or more) monomer units formed.

A significant decrease in monomer consumption from during to after the initialization period was seen to occur when cyanoisopropyl dithiobenzoate was used as RAFT agent. This was ascribed to a rapidly changing value for  $k_p$ , a change in the partitioning of radicals between intermediate and propagating forms due to the formation of significant concentrations of relative stable intermediate radicals (which in turn is might be subjected to possible intermediate radical termination reactions), and a change in termination kinetics during to after the initialization period. A similar, but less pronounced, decrease in monomer

consumption was seen for the reactions mediated by cumyl dithiobenzoate. This behavior was again ascribed to a rapidly changing  $k_p$  and a possible change in termination kinetics during to after the initialization period. As an increase in intermediate radical concentration was only seen to occur after initialization for the cumyl dithiobenzoate case, it was concluded that more styrene units need to add to the growing chains (compared to the cyanoisopropyl dithiobenzoate case), before stable intermediate radicals could form. The different behavior of the two systems is attributed to the different properties of the cumyl compared to the cyanoisopropyl radicals, and the influence their respective properties have on the kinetics of the polymerization systems.

The equilibrium coefficients ( $K_{eq} = k_{add} / k_{-add}$ ) for the reactions were calculated through monomer consumption and ESR data. For all reactions,  $K_{eq}$  initially started out low, but increased rapidly with time.  $K_{eq}$ , for the reactions polymerized at 84 °C, increased to a maximum, after which a decrease in  $K_{eq}$  was seen. In the reaction polymerized at 70 °C,  $K_{eq}$  showed only a rapid increase but never reached a maximum. This was explained in the light of  $k_{add}$  and  $k_{-add}$  being chain length dependent.

Radical generation and termination reactions occurring during and after initialization were compared for both cyanoisopropyl and cumyl dithiobenzoate systems. It was found that termination was a more frequent event during initialization (than afterwards) due to the unusual process by which chains are kept short during that period. The rate of initiator decomposition for the RAFT systems was compared to respective control reactions (without added RAFT agents). Results indicated that the addition of a RAFT agent to a system does not influence the rate of initiator decomposition.

## 6.2 Recommendations

Although some of the mysteries surrounding the RAFT mechanism have been revealed through this study, there are still plenty of unanswered questions. Some of these questions will be given below together with possible ways of determining answers to these questions.

In Chapter 3 it was seen that the observed intermediate radical concentration time profile was partly due to the short chain lengths targeted in the reactions. Will the intermediate radical concentration have a similar time-profile when different monomer to RAFT agent and RAFT agents to initiator concentration are used? As different lineshapes for the ESR signals were observed when different RAFT agent were used as mediating agents in styrene reactions, it might be possible to determine the stability, and thus the rate of fragmentation of the intermediate radicals from these changes in lineshapes. Identification of the extra radical species observed to form during some reactions, and the possible effects these species have on the reaction kinetics, is also an interesting subject for future investigations. By utilizing a photo-initiator during an *in situ* ESR RAFT mediated polymerization, with a UV light as initiating source, focused on the ESR tube, it might be possible to record the decay of the intermediate radicals with time when the initiating source is

switched off. From the decay data it might be possible to calculate the rate of termination for a specific RAFT system.

In Chapter 4 it was established that intermediate radical termination does indeed occur, although quantitative determination of the amount of terminated intermediate radical products could not be completed. A possible next step would be to design reactions specifically to attain a qualitative analysis of the terminated intermediate products. This can be done in a variety of ways. If the length of the initialization period and the time at which a maximum in intermediate radical concentration occurs, is known, more initiator could be added to the reaction, to increase the formation of terminated intermediate radical products. By using peak integration of the obtained  $^{13}\text{C}$  NMR spectra, an estimate of the concentration of termination products formed may be determined. If a sufficient concentration of terminated intermediate radicals is formed, 2-D NMR spectroscopy could be used to correlate the peaks appearing in the  $^{13}\text{C}$  spectra, due to terminated intermediate radical products, to peaks appearing in a corresponding  $^1\text{H}$  NMR spectra. These  $^1\text{H}$  NMR peaks can then be used (together with a suitable internal standard) to accurately determine the concentrations of the terminated intermediate radical products formed.

If butyl or methyl acrylate is used as monomer instead of styrene, the polymer resulting from the above-mentioned reaction can be analyzed via ES-MS spectroscopy. It should be possible to thus determine the nature of the formed terminated intermediate radical products. HPLC coupled to an ES-MS or alternatively to a NMR spectrometer, can also be used to first separate, and then to analyze the formed terminated intermediate radical products.

Decoupling of the ESR spectra recorded during the initialization period is another subject for future research. Through simulations, it should be possible to determine the types and concentrations of all the different radicals present in the reaction mixture during the initialization period. Another interesting aspect for future investigation is the effect of various monomers, initiator concentrations and different types of RAFT agents on the length of the initialization period and also on the change in rate of polymerization from during to after initialization. As mentioned in chapter 5, it is predicted on the basis of the change in propagation rate coefficient for the addition of a MA monomer unit to a cyanoisopropyl radical, that the rate should increase after initialization, rather than decrease, as seen when styrene was used as monomer.

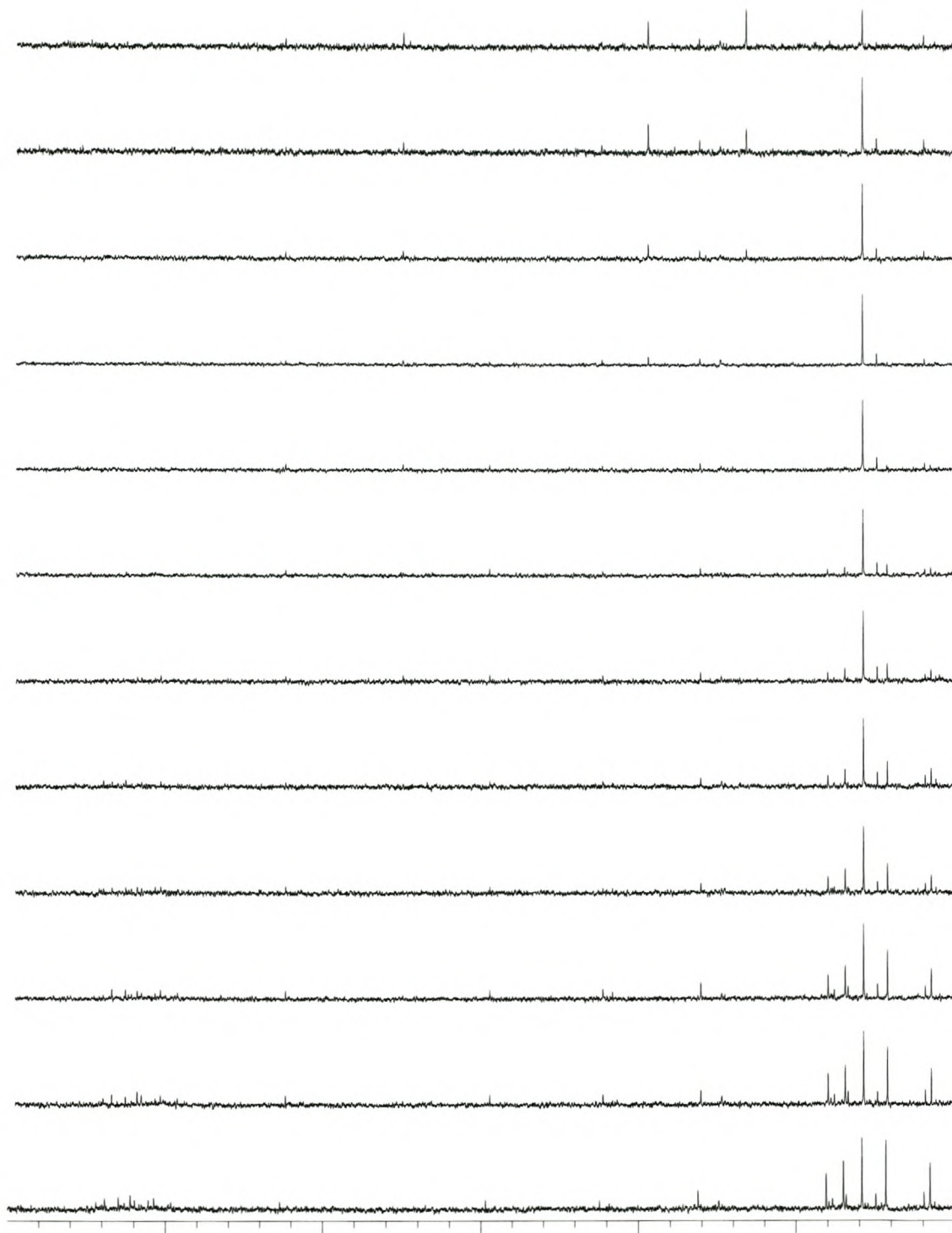
Calculations done for the equilibrium coefficient in Chapter 5 indicated a variable  $K_{\text{eq}}$  for the reactions investigated due to a possible variation in the values of  $k_{\text{add}}$  and  $k_{-\text{add}}$ . Obtaining exact values for these variables would not only aid in the determination of more accurate values for the equilibrium constants, but will also aid in resolving the current dispute on the fate of the intermediate radicals.

## References

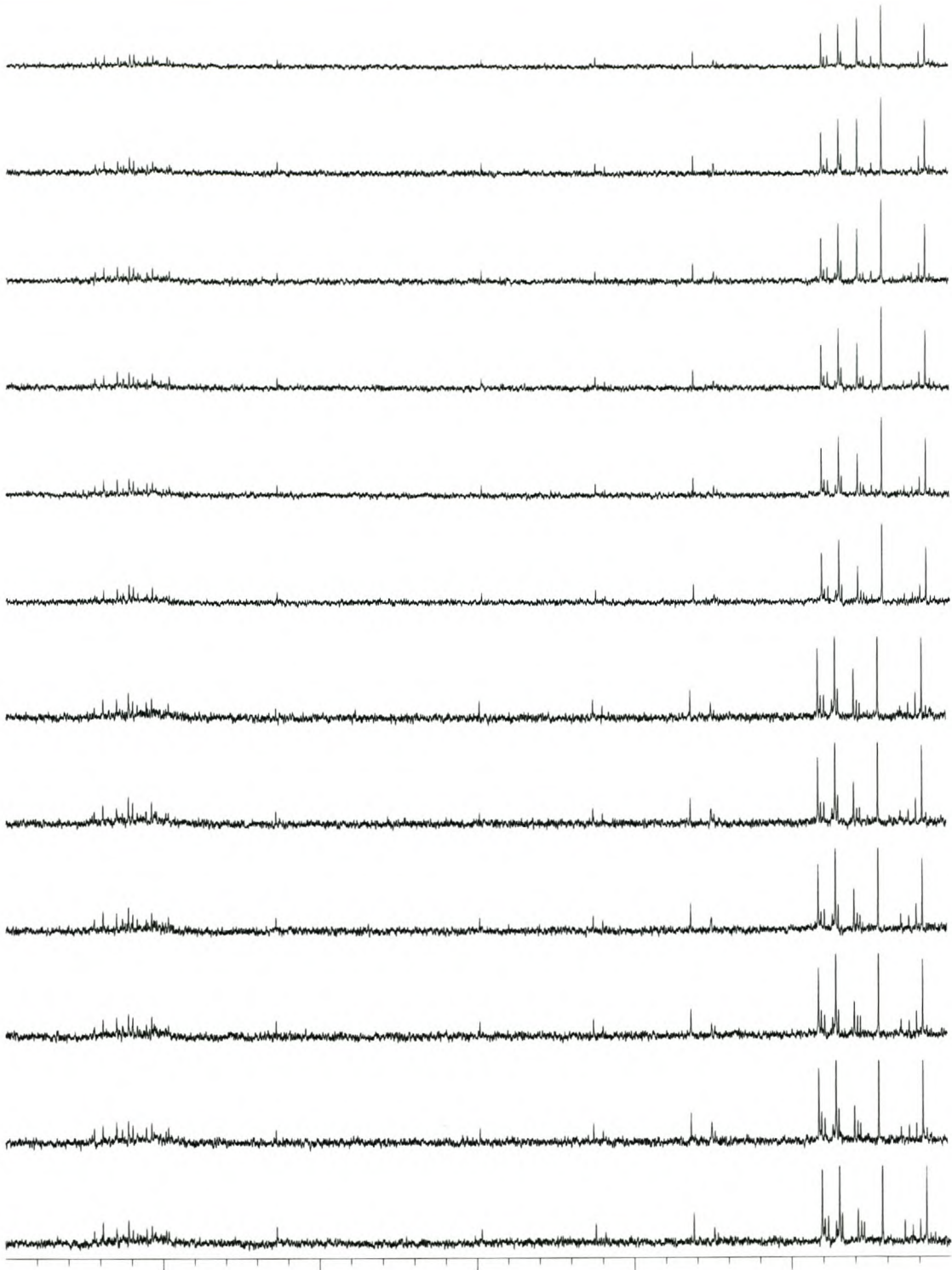
1. Le, T. P.; Moad, G.; Rizzardo, E.; Thang, S. H., *PCT Int Appl*, **1998**, wo98/01478.
2. Monteiro, M. J.; de Brouwer, H. *Macromolecules* **2001**, *34*, 349.
3. Barner-Kowollik, C.; Quinn, J. F.; Nguyen, T. L. U.; Heuts, J. P. A.; Davis, T. P. *Macromolecules* **2001**, *34*, 7849.
4. Kwak, Y.; Goto, A.; Tsujii, Y.; Murata, Y.; Komatsu, K.; Fukuda, T. *Macromolecules* **2002**, *35*, 3026.

# Appendix

## A.1 Additional $^{13}\text{C}$ NMR Spectra

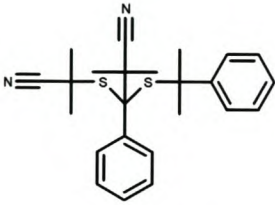
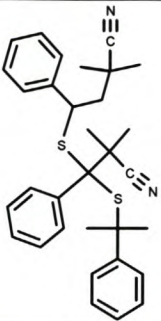
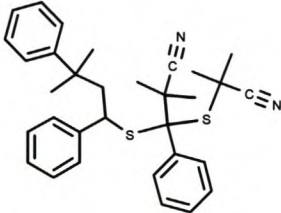
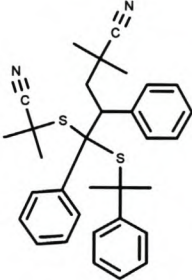
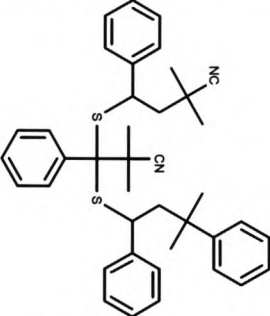
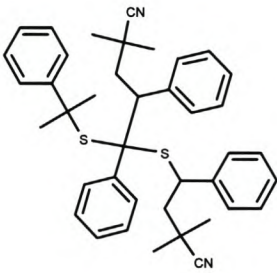
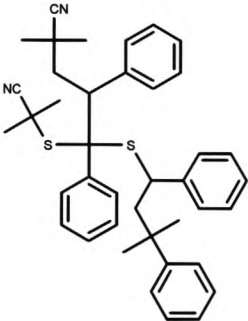
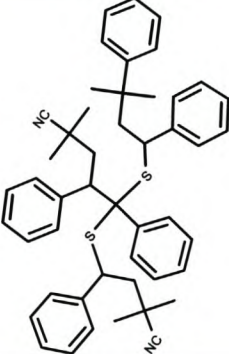
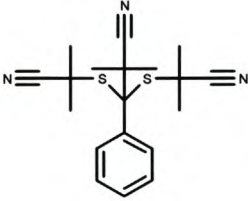
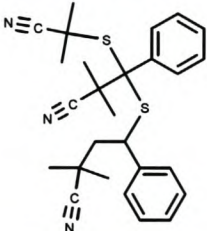
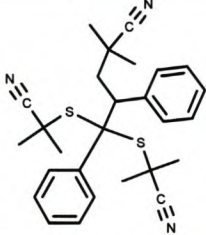
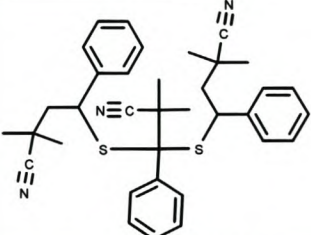
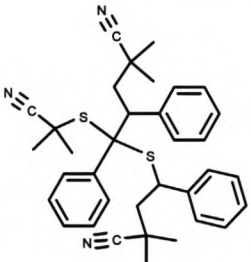
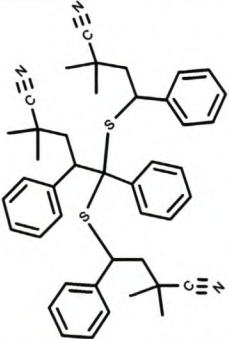
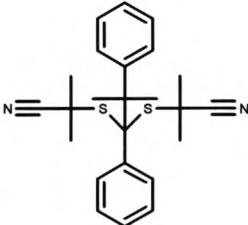


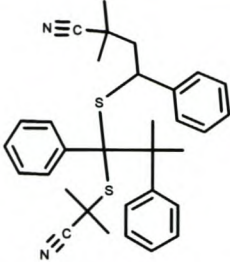
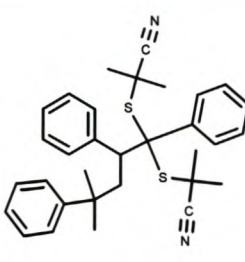
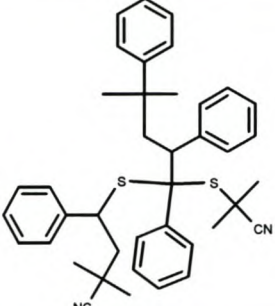
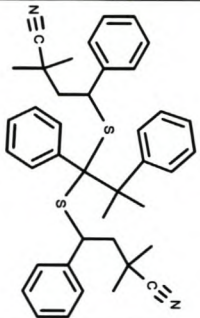
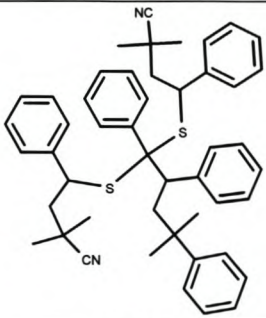
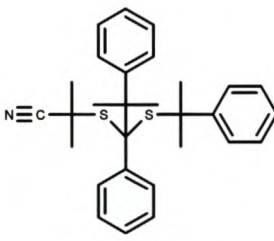
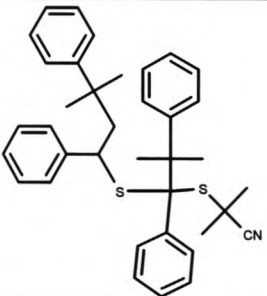
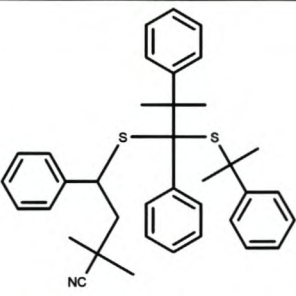
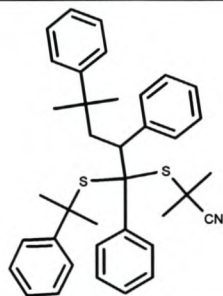
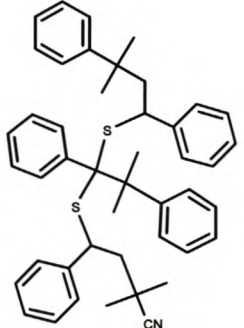
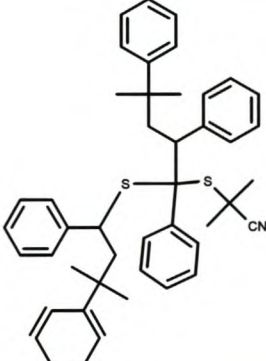
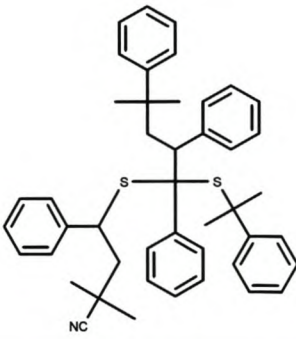
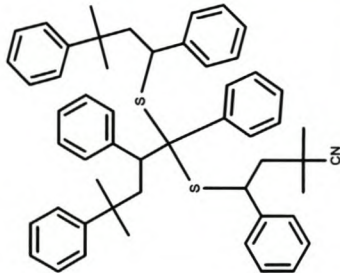
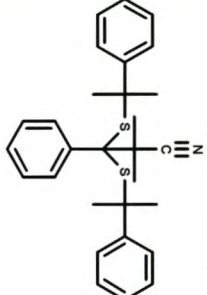
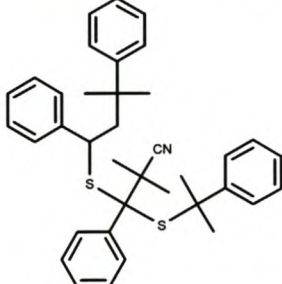
**Figure A.1**  $^{13}\text{C}$  NMR spectra in the 50 – 80 ppm region of the solution (50 wt% in  $\text{C}_6\text{D}_6$ ) polymerization of styrene in the presence of  $\text{CDB-}^{13}\text{C}$  at 84 °C, using AIBN as initiator. Spectra given were recorded in 10 minute time intervals up to 136 minutes.



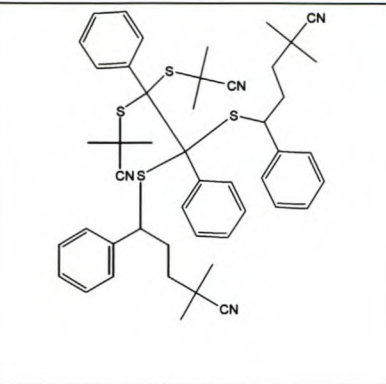
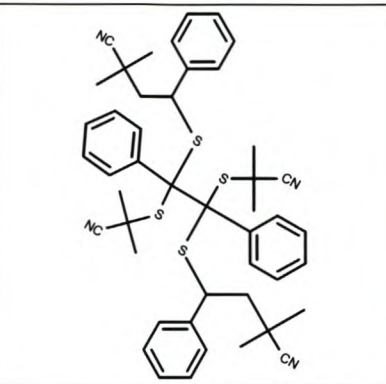
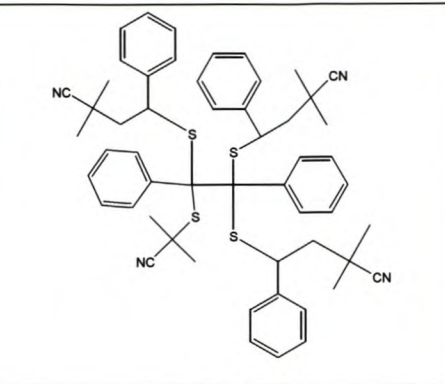
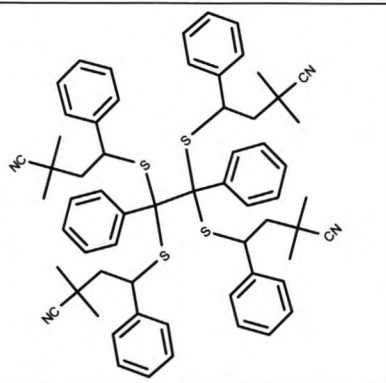
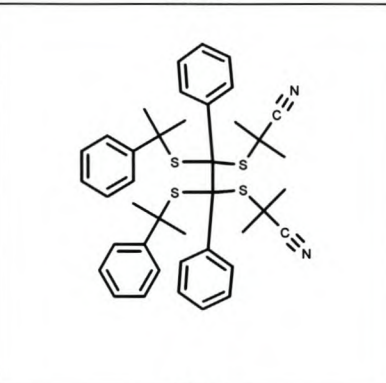
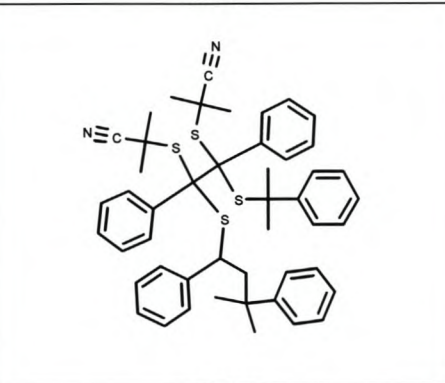
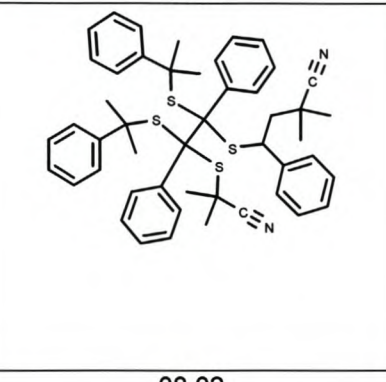
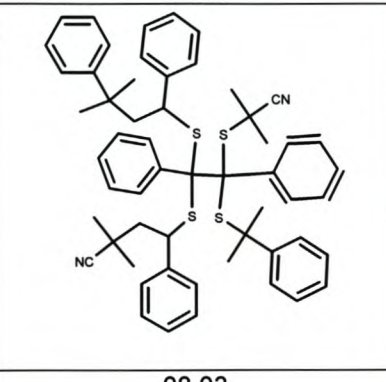
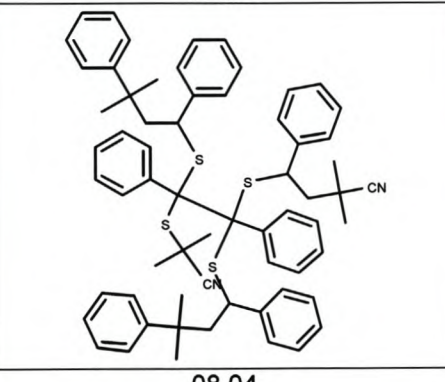
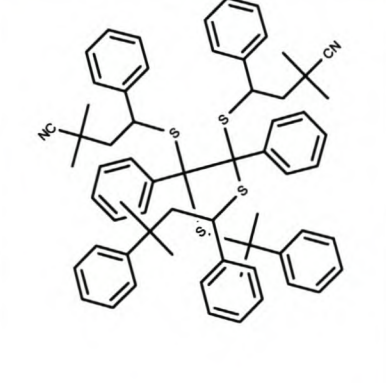
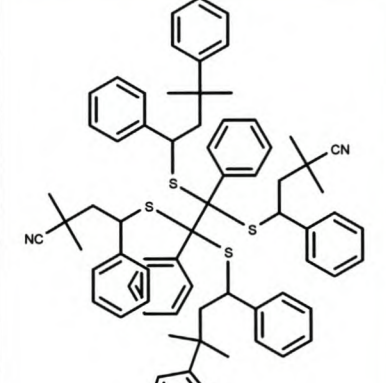
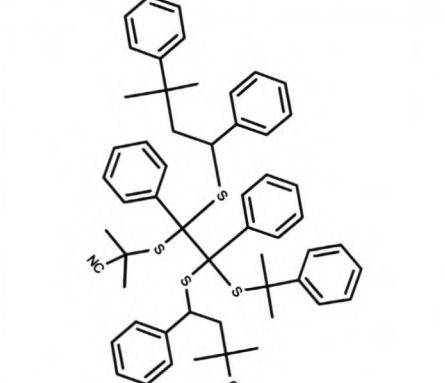
**Figure A.2**  $^{13}\text{C}$  NMR spectra in the 50 – 80 ppm region of the solution (50 wt% in  $\text{C}_6\text{D}_6$ ) polymerization of styrene in the presence of  $\text{CDB-}^{13}\text{C}$  at 84 °C, using AIBN as initiator. Spectra given were recorded in 15 minute time intervals up to 331 minutes.

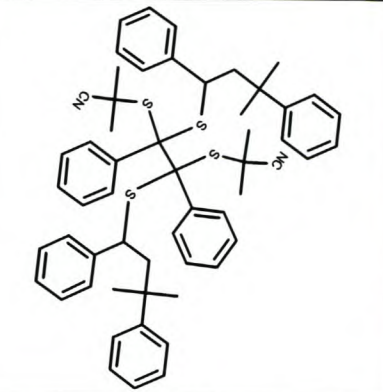
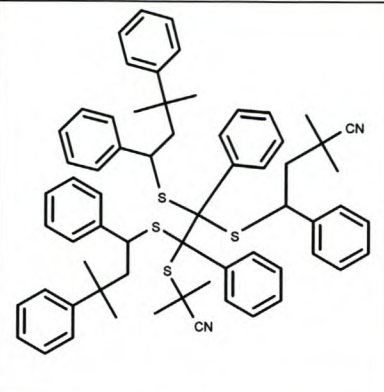
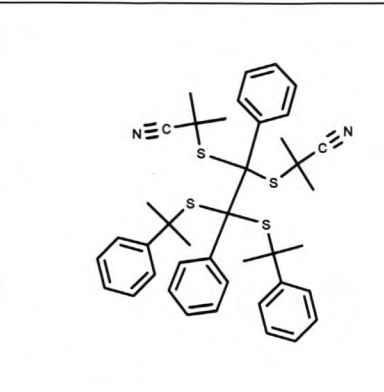
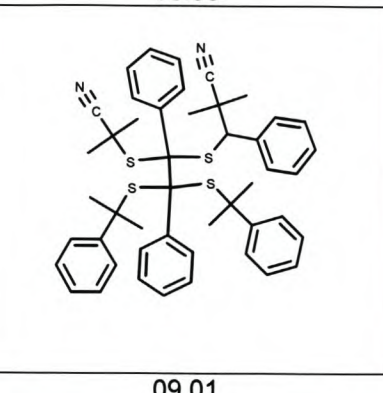
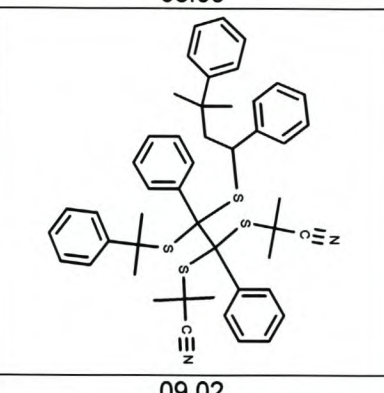
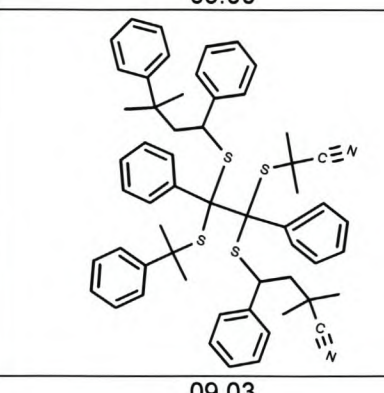
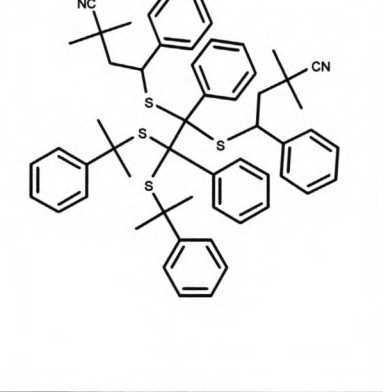
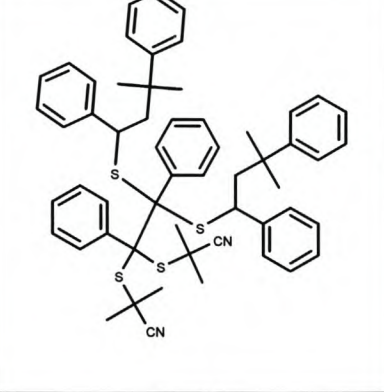
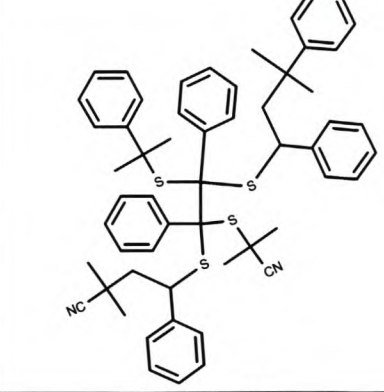
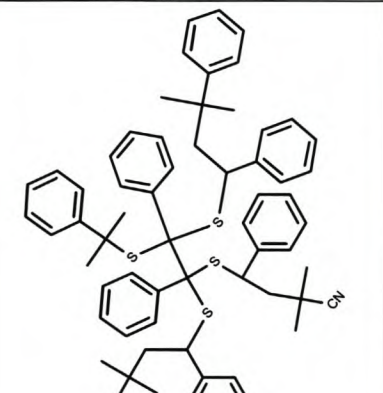
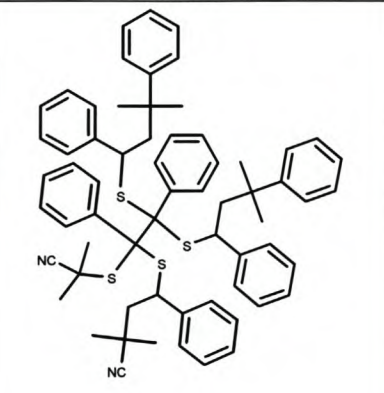
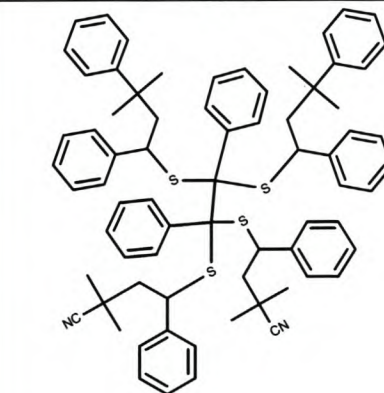
**A.2 Possible Intermediate Radical Termination Products**

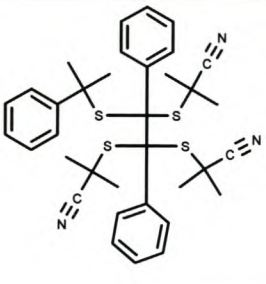
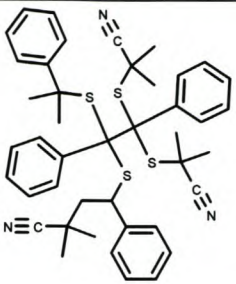
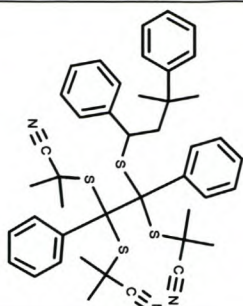
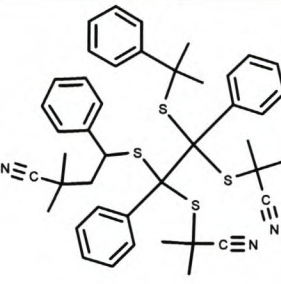
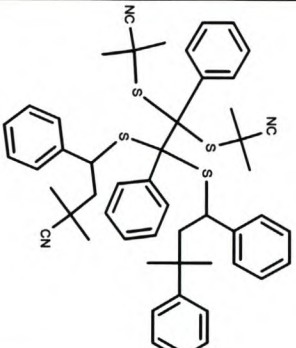
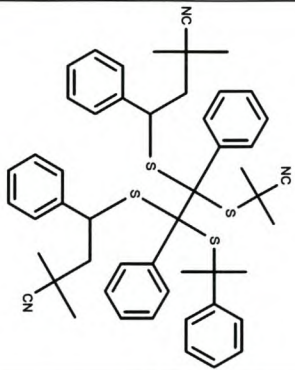
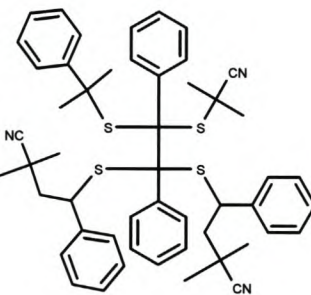
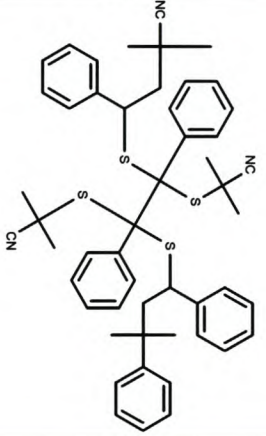
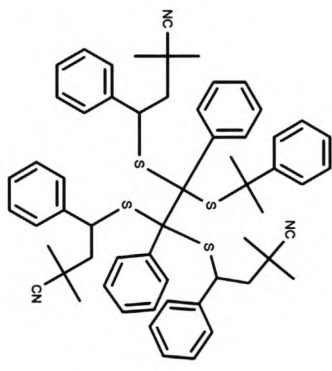
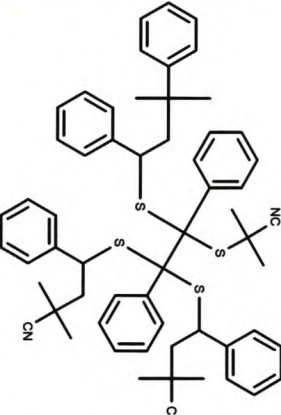
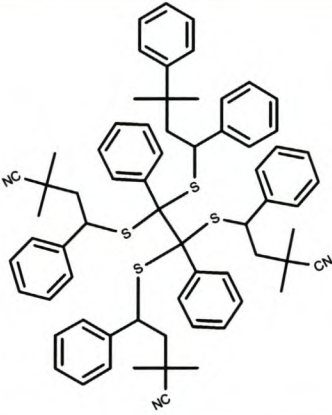
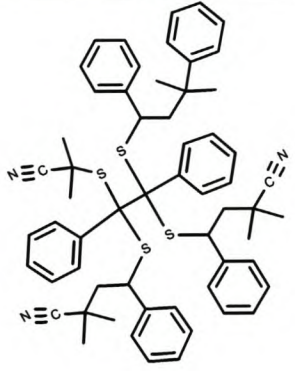
		
01.00	01.01	01.02
		
01.03	01.04	01.05
		
01.06	01.07	02.00
		
02.01	02.02	02.03
		

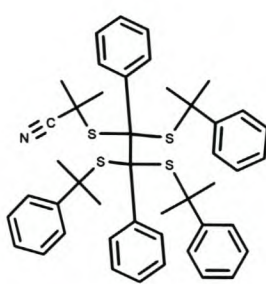
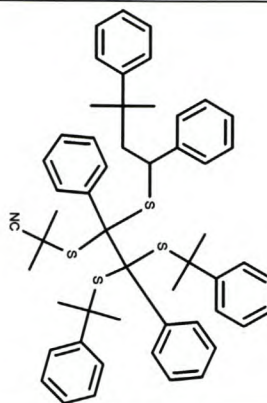
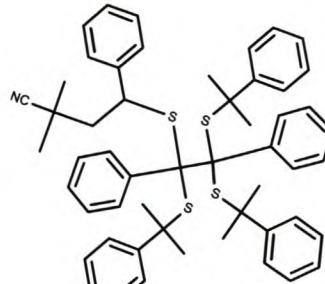
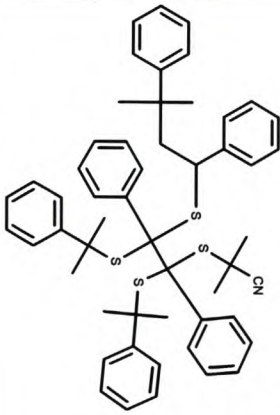
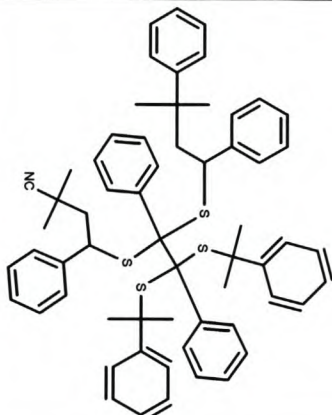
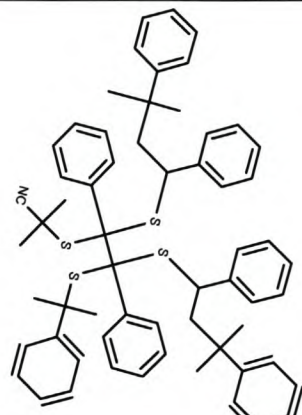
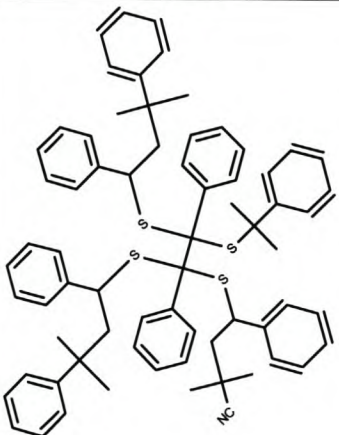
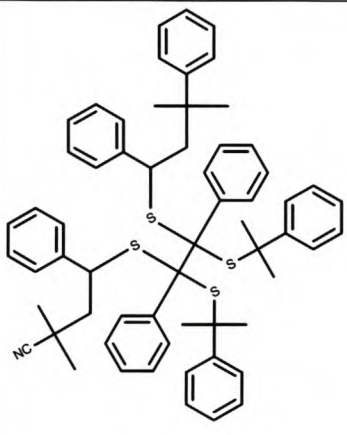
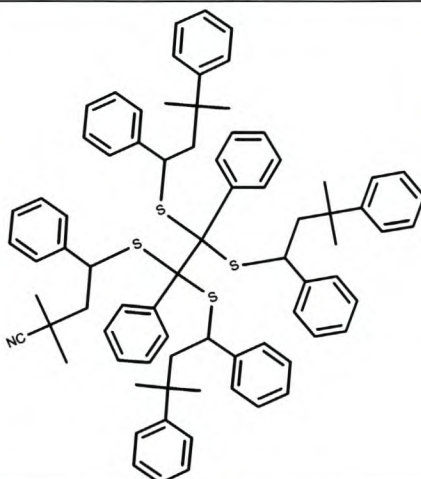
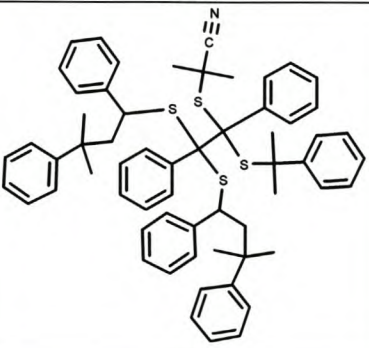
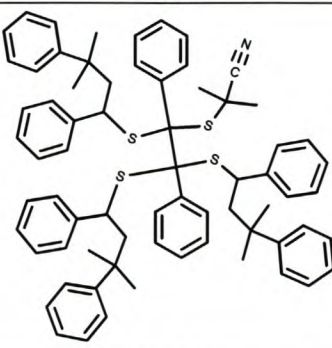
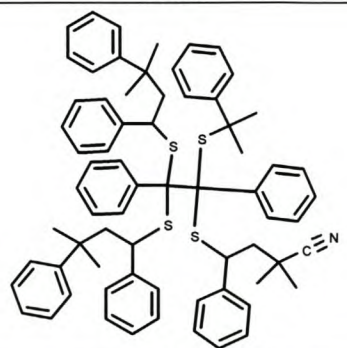
<p>02.04</p> 	<p>02.05</p> 	<p>03.00</p> 
<p>03.01</p> 	<p>03.02</p> 	<p>03.03</p> 
<p>03.04</p> 	<p>03.05</p> 	<p>04.00</p> 
<p>04.01</p> 	<p>04.02</p> 	<p>04.03</p> 
<p>04.04</p> 	<p>04.05</p> 	<p>04.06</p> 

04.07	05.00	05.01
05.02	05.03	05.04
05.06	06.00	06.01
06.02	06.03	06.04
06.05	07.00	07.01

		
07.02	07.03	07.04
		
07.05	08.00	08.01
		
08.02	08.03	08.04
		
08.05	08.06	08.07

		
08.08	08.09	09.00
		
09.01	09.02	09.03
		
09.04	09.05	09.06
		
09.07	09.08	09.09

		
10.00	10.01	10.02
		
10.03	10.04	10.05
		
10.06	10.07	10.08
		
10.09	10.10	10.11

		
11.00	11.01	11.02
		
22.03	11.04	11.05
		
11.06	11.07	11.08
		
11.09	11.10	11.11

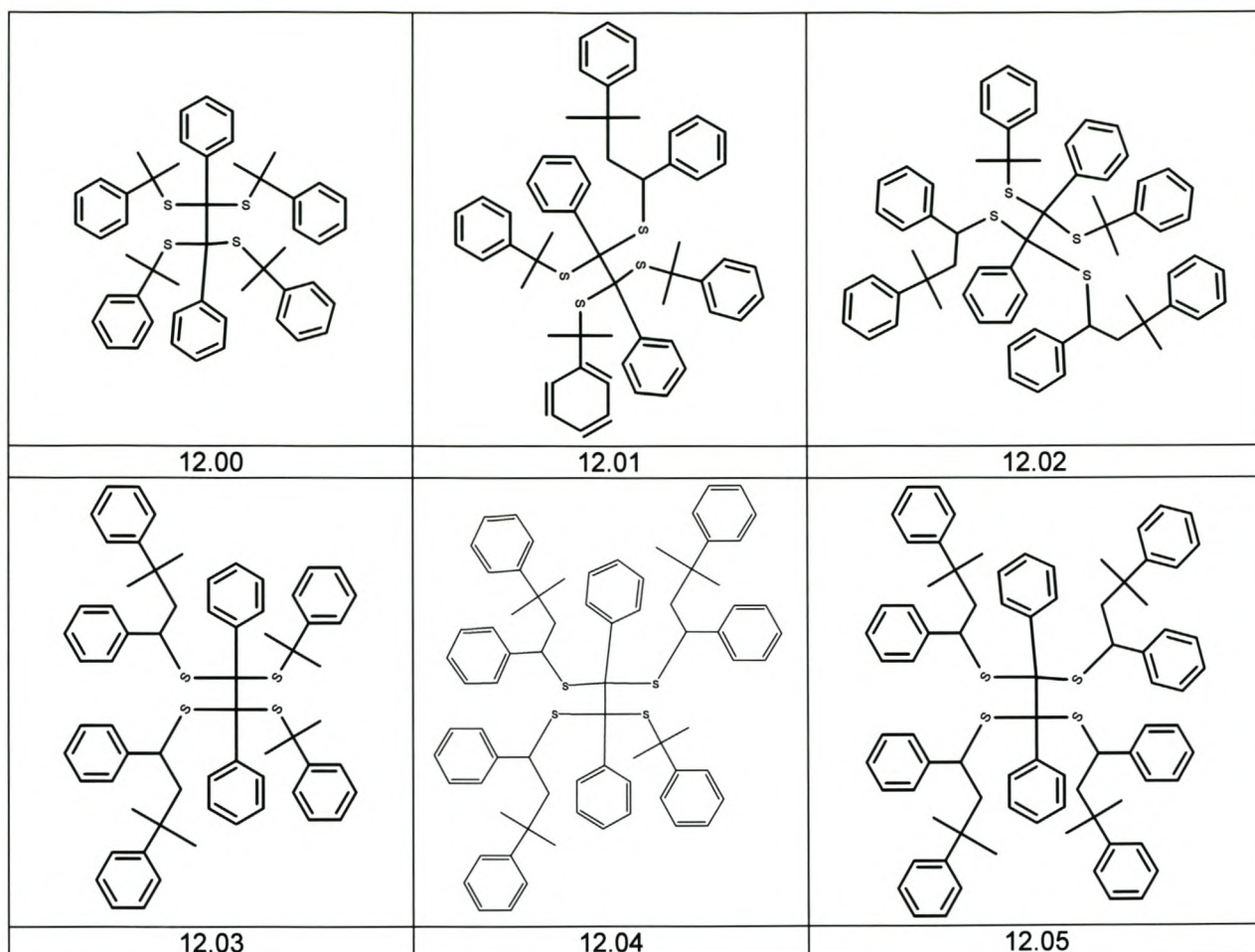


**Figure A.3** Potential terminated intermediate radical species. The structure number of each species is also given.

A.3  $^{13}\text{C}$  NMR Shift PredictionsTable A.1  $^{13}\text{C}$  NMR shift predictions of the possible terminated intermediate radical species.

Prediction (ppm)		Structure number	Prediction (ppm)		Structure number
First carbon	Second carbon		First carbon	Second carbon	
51.1	62.7	3.00	65.4	62.4	10.02
51.9	63.4	4.00	65.9		7.03
52.7	64.1	6.00	65.9	65.9	8.08
53.4		2.02	65.9	65.9	10.07
54.1		1.03	66.1	63.2	10.01
54.2		3.02	66.2		3.01
54.8		5.02	66.2		4.01
54.9		4.03	66.2	63.1	8.01
55.6		6.02	66.4	69.4	8.09
55.8		2.00	66.4	69.4	9.08
56.5		1.00	66.4	69.4	10.09
56.9		1.06	66.4	69.4	11.10
56.9		2.04	66.6	66.7	10.05
57.2		5.00	66.7	66.6	8.07
57.6		1.05	66.7	66.6	9.03
57.6		5.04	66.7	66.6	9.06
57.7		3.03	66.7	66.6	11.05
57.7		4.05	66.9		4.02
58.4		4.06	66.9		6.01
58.4		6.03	66.9	63.9	8.02
59.3		1.02	67	63.8	9.01
59.3		2.01	67	63.8	11.01
60		1.01	67.1	70.2	10.08
60		5.01	67.1	70.2	11.11
60.4		1.07	67.4	67.4	11.07
60.4		2.05	67.4	67.4	12.03
60.4		5.05	67.7	64.6	11.02
61.2		3.05	67.7	64.6	12.01
61.2		4.07	69.4	66.4	7.04
61.2		6.04	69.4	66.4	8.04
61.9		7.00	69.4	66.4	10.11
62.6	62.7	10.00	69.7		3.04
62.8		1.04	69.7		4.04
62.8		2.03	69.7		6.05
62.8		5.03	69.7	63.6	8.03
62.9	68.9	7.02	69.9	69.9	7.05
62.9	68.9	9.05	69.9	69.9	8.06
62.9	68.9	10.04	69.9	69.9	9.09
63.1	66.2	10.03	69.9	69.9	10.10
63.2	66.1	9.02	69.9	69.9	11.08
63.4		8.00	69.9	69.9	12.05
63.5	63.3	9.00	70.2	67.1	8.05
63.6	69.7	10.06	70.2	67.1	9.07
63.6	69.7	11.09	70.2	67.1	11.06
64	67.7	11.03	70.2	67.1	12.04
64.2	64.1	11.00	70.5	64.3	9.04
64.9		12.00	70.5	64.3	11.04
65.4	62.4	7.01	70.5	64.3	12.02

#### A.4 ESR simulations: Theory and parameters

The computer software used for the ESR simulations was a PEST Winsim 0.96. The PEST Winsim parameters used to simulate the spectra for the cumyl radical were: a Gaussian lineshape (width = 0.1 G), with a modulation amplitude of 1 G, a g-value of 2.0026, and hyperfine coupling constants ( $\alpha_H$ ): 16.6 G (6H, methyl protons on cumyl group) leading to a wide septet basic structure, 4.7 G (2H, ortho protons on benzyl ring), 1.6 G (2H, meta protons on benzyl ring), 5.5 G (1H, para protons on benzyl ring).<sup>1</sup> Using these parameters leads to a fairly complex cumyl radical spectrum, which is clearly different from those of the intermediate and cyanoisopropyl radicals.

The parameters used to simulate the intermediate radical spectrum were: a Gaussian lineshape (width = 0.1 G), with a modulation amplitude of 1 G, a g-value of 2.0043, and hyperfine coupling constants ( $\alpha_H$ ): 1.32 G (2H, ortho protons), 1.32 G (2H, meta protons), 4.40 G (1H, para protons), 0.28 G (2H,  $\chi$  protons).<sup>1</sup>

The parameters used to simulate the cyanoisopropyl radical spectrum were: a Gaussian lineshape (width = 0.1 G), with a modulation amplitude of 1 G, a g-value of 2.0030, and hyperfine coupling constants ( $\alpha_H$ ): 20.65 G (6H, methyl protons) a septet of triplets, 3.36 G (N, equal triplet, since  $S = 1$  for N).<sup>2</sup>

## References

1. Hawthorne, D. G.; Moad, G.; Rizzardo, E.; Thang, S. H. *Macromolecules* **1999**, *32*, 5457.
2. Savitsky, A. N.; Paul, H.; Shusin, A. I. *J. Phys. Chem. A* **2000**, *104*, 9091.